Oxifuncionalización selectiva de compuestos alifáticos por peroxigenasas fúngicas

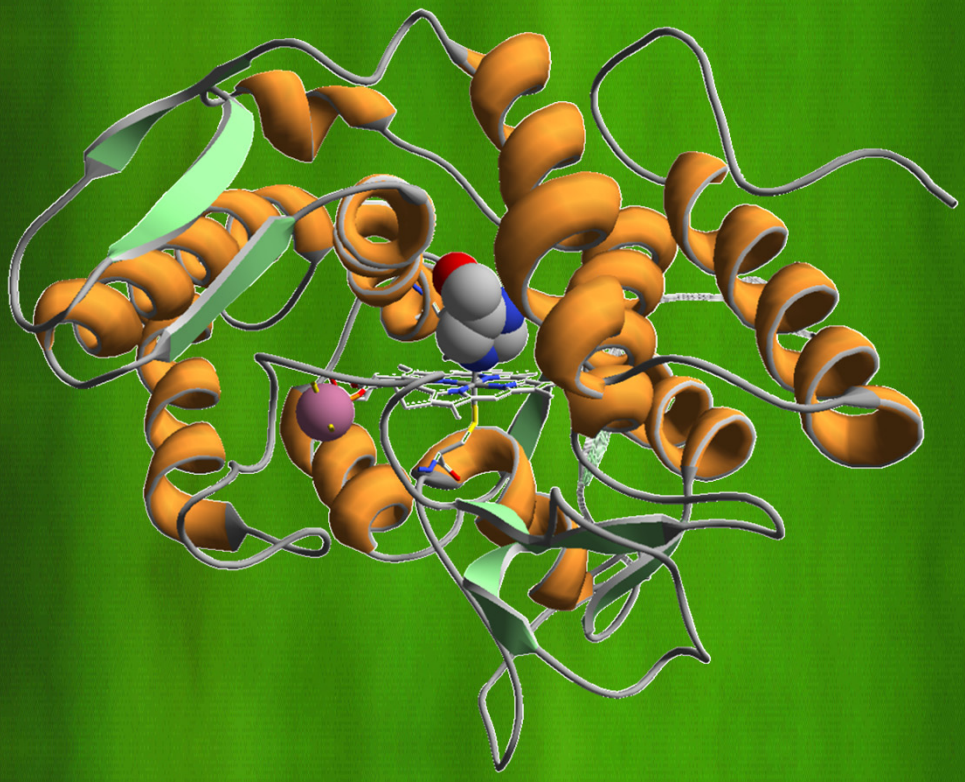

Esteban Daniel Babot

Sevilla, 2016

OXIFUNCIONALIZACIÓN SELECTIVA DE COMPUESTOS ALIFÁTICOS POR PEROXIGENASAS FÚNGICAS

Memoria que presenta:

Esteban Daniel Babot

para optar al título de Doctor en Ciencias Químicas por la Universidad de Sevilla.

Oxifuncionalización selectiva de compuestos alifáticos por peroxigenasas fúngicas

Visado en Sevilla, a 16 de junio de 2016

LOS DIRECTORES

Dra. Dña. Ana Gutiérrez Suárez
Investigador Científico del CSIC
IRNAS-CSIC

Dr. D. José C. del Río Andrade
Profesor de Investigación del CSIC
IRNAS-CSIC

EL TUTOR

Dr. D. Fernando de Pablos Pons
Catedrático de la Universidad de Sevilla

Memoria que presenta:

Esteban Daniel Babot

Para optar al grado de Doctor en Ciencias Químicas por la Universidad de Sevilla.

DOCTOR D. JOSÉ ENRIQUE FERNÁNDEZ LUQUE, DIRECTOR DEL INSTITUTO DE RECURSOS NATURALES Y AGROBIOLOGÍA DE SEVILLA DEL CONSEJO SUPERIOR DE INVESTIGACIONES CIENTÍFICAS.

CERTIFICA: Que la presente Memoria de Investigación titulada "Oxifuncionalización selectiva de compuestos alifáticos por peroxigenasas fúngicas", presentada por Esteban Daniel Babot para optar al grado de Doctor en Ciencias Químicas, ha sido realizada en el Departamento de Biotecnología Vegetal, bajo la dirección de los Drs. Dña. Ana Gutiérrez Suárez y D. José C. del Río Andrade, reuniendo todas las condiciones exigidas a los trabajos de Tesis Doctorales.

En Sevilla, a 16 de junio de 2016

AGRADECIMIENTOS

Este trabajo se ha llevado a cabo en el Instituto de Recursos Naturales y Agrobiología de Sevilla (IRNAS) del Consejo Superior de Investigaciones Científicas (CSIC). Ha sido financiado por una beca JAE-Predoc del CSIC y por los proyectos europeos "Novel and more robust fungal peroxidases as industrial biocatalyst" (PEROXICATS, KBBE-2010-4-265397) e "Industrial oxidoreductases" (INDOX, GA-KBBE-2013-7-613549).

Quiero expresar mi sincero agradecimiento a las personas que tanto directa como indirectamente me han acompañado durante el transcurso de esta Tesis:

A los ***Dres. Ana Gutiérrez*** y ***José Carlos del Río***, directores de esta Tesis, por haberme dado la oportunidad de realizar este trabajo de investigación en su laboratorio, por todo lo que me han aportado tanto a nivel científico como a nivel personal y por la confianza en su trato personal.

Al ***Prof. Ángel Martínez***, del Centro de Investigaciones Biológicas (CIB-CSIC), por ofrecerme la posibilidad de realizar una estancia en su laboratorio, aportándome numerosos y valiosos conocimientos, y por haber seguido el desarrollo de esta Tesis.

Al ***Prof. Fernando de Pablos Pons***, Catedrático de la Universidad de Sevilla, tutor de esta Tesis, por la ayuda en la parte burocrática.

A los ***Dres. Henrik Lund*** y ***Lisbeth Kalum***, de la empresa Novozymes (Bagsvaerd, Dinamarca), por suministrarnos la peroxigenasa recombinante de *Coprinopsis cinerea*.

Al ***Prof. Martin Hofrichter*** y al ***Dr. Rene Ullrich***, de la Universidad de Zittau-Dresden (Zittau-Alemania), por suministrarnos la peroxigenasa de *Agrocybe aegerita*.

A los ***Dres. Katrin Scheibner*** y ***Glenn Gröbe***, de la empresa JenaBios (Jena, Alemania), por suministrarnos la peroxigenasa de *Marasmius rotula*.

A los ***Dres. Victor Guallar*** y ***Fátima Lucas*** y a los doctorandos ***Marina Cañellas*** y ***Ferrán Sancho***, por la realización e interpretación de los estudios computacionales presentados en esta Tesis.

Al ***Dr. Manuel Angulo***, del servicio de Resonancia Magnética Nuclear del CITIUS (Sevilla, España), por la realización e interpretación de los espectros de RMN de la Vitamina D.

Al grupo del CIB, ***Javi***, ***Marta***, ***Susana***, ***Aitor***, ***Vero***, ***Lola***, ***Isa***, por su apoyo durante mi estancia en el CIB y por los buenos momentos brindados. Quiero agradecer especialmente al ***Dr. Javier Ruiz-Dueñas*** por su apoyo en los experimentos realizados durante la estancia y al ***Dr. Aitor Hernández Ortega*** por su apoyo personal y su amistad.

A mis compañeros de laboratorio, ***Jorge***, ***Alejandro***, ***Pepijn***, ***Antonio*** y ***Andrés***, por todo su apoyo durante la realización de esta Tesis y a las nuevas integrantes del grupo, ***Carmen A.*** y ***Carmen F.***, por todo su apoyo y aguante durante la etapa final de esta Tesis. Quiero agradecer especialmente al futuro médico ***Antonio Pereira*** por su amistad y múltiples charlas confidentes.

A mi compañera y amiga, la ***Dra. Gisela Marquez Silva***, por haberme brindado su amistad y por enseñarme todo lo que aprendí al inicio de esta Tesis. Por todos los buenos y malos momentos compartidos.

A mis compañeros de desayuno, ***Álvaro***, ***Oliver*** y ***José***, por los buenos momentos compartidos. Quiero agradecer especialmente a ***Álvaro*** por su amistad incondicional y por acompañarme durante estos años.

A mi familia, ***madre***, ***hermanos***, ***esposa*** e ***hijas***, por apoyarme en todas mis locas decisiones. Quiero agradecer especialmente a ***Yolanda*** por aguantarme cada minuto del día y por su paciencia y por compartir conmigo esas dos personitas tan maravillosas que la vida nos dio, ***Lucía*** e ***Indiana***. A mi ***padre*** y ***abuelos*** que a pesar de que ya no están entre nosotros me enseñaron muchos valores.

Al resto de la familia, ***tíos*** y ***primos***, por estar siempre presentes. A mi ***suegro*** (que en paz descanse), ***cuñado*** y ***sobrino*** por haberme abierto sus brazos y permitirme ser parte de su familia. A ***Pili***, ***Juan***, ***Ángeles*** y ***Juanma*** por su cariño y aguante.

A la familia ***Huerta***, que ha sido un pilar firme en mi vida y que a pesar de la distancia siguen apoyándome en mis decisiones.

A mis amigos españoles, ***Sonia***, ***José Carlos*** y ***Mayte*** y a mis sobrinitos del corazón ***Rodrigo***, ***José Carlos*** y ***Cristina*** por todo su cariño y apoyo y por haberme dado un lugar en sus corazones.

Finalmente, a todos mis amigos argentinos, ***Silvia*** y ***Gerardo***, ***Leo*** y ***Nati***, ***Jessi***, ***Fran***, ***Gabi*** y ***Tere***, ***Nena***, ***Silvio***, y todos aquellos que de una forma u otra formaron parte de mi vida y compartimos innumerables momentos.

ABREVIATURAS

ε	Coeficiente de extinción molar
δ_c	Desplazamiento químico del carbono
^{13}C-NMR	Resonancia Magnética Nuclear de carbono 13 (*Carbon-13 Nuclear Magnetic Resonance*)
^{1}H-NMR	Resonancia Magnética Nuclear de protones (*Proton Nuclear Magnetic Resonance*)
Å	Ångström
***Aae*UPO**	Peroxigenasa inespecífica de *Agrocybe aegerita*
ABTS	2,2'-azinobis(3-etilbenzotiazolin-6-sulfonato)
***Aau*DyP**	Peroxidasa decolorante del tinte del hongo *Auricularia auricula- judae*
APO	Peroxigenasa de compuestos aromáticos (*aromatic peroxygenase*)
BSTFA	*N,O*-bis-(trimetilsilil)-trifluoroacetamida
***Cfu*CPO**	Cloroperoxidasa de *Caldariomyces fumago*
CYP153A1	Citocromo P450 bacteriano de *Acinetobacter* sp
CYP27A1	Esterol-27-hidroxilasa
EC	Comisión de Nomenclatura de las Enzimas (*"Enzyme Commission"*)
EMBOSS	*The European Molecular Biology Open Software Suite*
ER	Retículo endoplásmico
FAD	Flavín adenín dinucleótido
FMN	Flavín mononucleótido
Fd	Ferredoxina
FdR	Ferredoxina reductasa
GC	Cromatografía de Gases (*Gas Chromatography*)
GC-MS	Cromatografía de Gases acoplada a Espectrometría de

	Masas (*Gas Chromatography-Mass Spectrometry*)
$H_2{}^{18}O_2$	Peróxido de hidrógeno marcado con oxígeno 18
HSQC	Heteronuclear single quantum coherence spectroscopy
HTP	Hemo-tiolato peroxidasa
JGI	Joint Genome Intitute
K_m	Constante cinética de Michaelis-Menten
LiP	Lignina peroxidasa
MnP	Manganeso peroxidasa
***Mro*UPO**	Peroxigenasa inespecífica de *Marasmius rotula*
MTBE	Metil *tert*-butil éter (*methyl tert-butyl ether*)
NADH	Nicotinamida adenina dinucleótido
NADPH	Nicotinamida adenina dinucleótido fosfato
NC-IUBMB	Comité de Nomenclatura de la Unión Internacional de Bioquímica y Biología Molecular (*Nomenclature Committee of the International Union of Biochemistry and Molecular Biology*)
NMR	Espectroscopía de Resonancia Magnética Nuclear (*Nuclear Magnetic Resonance*)
P450	Citocromo P450
P450BM3	Citocromo P450 monooxigenasa de *Bacillu megaterium*
PBD	Base de datos de proteínas (*Protein Data Bank*)
PELE	Programa *Protein Energy Landscape Exploration*
PQQ	Pirroloquinolina quinona
r*Cci*UPO	Peroxigenasa inespecífica recombinante de *Coprinopsis cinerea*
rpm	Revoluciones por minuto
SDS-PAGE	Electroforesis en gel de poliacrilamida con dodecilsulfato sódico (sodium dodecyl sulfate polyacrylamide gel electrophoresis)

TMS	Trimetilsililo
U	Unidad de actividad enzimática
UPO	Peroxigenasa inespecífica (*unspecific peroxygenase*)
UV-Vis	Espectroscopía de ultravioleta-visible
VP	Peroxigenasa versátil (*Versatile peroxidase*)

ÍNDICE

RESUMEN

La presente Tesis aborda el estudio de la oxifuncionalización enzimática de diferentes compuestos alifáticos lineales (ácidos grasos, alcoholes grasos y alcanos/alquenos) y cíclicos (esteroides y secosteroides), catalizada por diferentes peroxigenasas fúngicas (en presencia de H_2O_2 como co-sustrato) incluyendo las peroxigenasas salvajes de *Agrocybe aegerita* (*Aae*UPO) y *Marasmius rotula* (*Mro*UPO) y la peroxigenasa recombinante de *Coprinopsis cinerea* (r*Cci*UPO). La evaluación de la conversión de los distintos sustratos así como la identificación de los productos de reacción se llevó a cabo mediante Cromatografía de Gases acoplada a Espectrometría de Masas (GC-MS) y en algunos casos Resonancia Magnética Nuclear (RMN). Por otro lado, el mecanismo de reacción de dichas oxifuncionalizaciones enzimáticas se estudió utilizando $H_2{}^{18}O_2$ como co-sustrato. Finalmente, con el objeto de investigar diferentes aspectos de las relaciones estructura-función de las peroxigenasas se realizaron estudios computacionales utilizando el programa PELE (Protein Energy Landscape Exploration).

En términos generales, las peroxigenasas fúngicas *Aae*UPO y r*Cci*UPO catalizaron la oxifuncionalización selectiva de los diferentes compuestos alifáticos lineales estudiados. Se observó que r*Cci*UPO resultó ser más eficiente que *Aae*UPO hidroxilando los diferentes ácidos grasos (saturados e insaturados) ya que consiguió mayor grado de conversión de los sustratos (en las mismas condiciones de reacción) aunque con ambas enzimas se observó que dicho grado de conversión dependía de la longitud de la cadena del ácido graso. Por otro lado, ambas enzimas dieron lugar a los mismos productos de reacción que fueron principalmente derivados monohidroxilados (en las posiciones ω-1 y ω-2) de los ácidos grasos, tanto saturados como insaturados. Sin embargo, con el ácido miristoleico, se observó una estricta regioselectividad en las reacciones de ambas enzimas formándose exclusivamente el isómero monohidroxilado en la posición ω-2. Se estudiaron además, las reacciones de varios ésteres de ácidos grasos con las enzimas *Aae*UPO y r*Cci*UPO observándose también la formación de derivados monohidroxilados en las posiciones ω-1 y ω-2. En cuanto a los alcoholes grasos, ambas enzimas fueron capaces de transformar estos compuestos en igual medida. Como productos principales de la reacción se obtuvieron los ácidos grasos correspondientes, así como derivados hidroxilados en las posiciones ω-1 y ω-2 de los alcoholes y de los ácidos. En las reacciones enzimáticas

realizadas con los alcanos se obtuvieron diferentes productos monohidroxilados en las posiciones ω-1 y ω-2, y dihidroxilados en las posiciones 2,(ω-1); 2,(ω-2) y 3,(ω-2). Se observó que la predominancia de los derivados mono- o dihidroxilados está relacionada con la concentración de acetona presente en el medio de reacción. Cabe mencionar que la obtención enzimática de dioles a partir de alcanos reviste gran interés industrial y se depositó una patente internacional (WO 2013/004639 A2) que se ha incluido en la Tesis.

Por otro lado, también se estudió la oxifuncionalización selectiva de diferentes compuestos esteroidales (esteroles libres y esterificados, y cetonas e hidrocarburos esteroidales) por las peroxigenasas r*Cci*UPO, *Aae*UPO y *Mro*UPO. En general se observó una mayor reactividad de la r*Cci*UPO (seguida de *Aae*UPO) que de la *Mro*UPO frente la mayoría de estos compuestos esteroidales, excepto con el pregnano (que sólo fue hidroxilado por la *Mro*UPO). La hidroxilación catalizada por estas peroxigenasas tuvo lugar en la cadena lateral (principalmente en la posición C-25) en la mayoría de los compuestos estudiados. Sólo se observó hidroxilación en el anillo (además de en la cadena lateral) en los compuestos esteroidales con dobles enlaces conjugados en C-3 y C-5 (además de en el pregnano).

En esta Tesis se ha demostrado la hidroxilación regioselectiva de la vitamina D (vitamina D_3 y D_2) por las peroxigenasas r*Cci*UPO y *Aae*UPO, en la posición C-25. La hidroxilación de estos secosteroides reviste gran interés industrial ya que además de que la reacción trascurre con una alta regioselectividad en todos los casos (100% con r*Cci*UPO) la 25-hidroxitamina D se considera mejor agente terapéutico para diferentes enfermedades que la propia vitamina D y también tiene aplicación en alimentación animal.

Con el fin de estudiar el mecanismo de la oxifuncionalización enzimática de los diferentes compuestos alifáticos mencionados, se llevaron a cabo reacciones de los mismos en presencia de $H_2{}^{18}O_2$, y se observó que el átomo de oxígeno introducido por las enzimas en los diferentes sustratos proviene del H_2O_2 (y no del O_2) demostrándose la actividad peroxigenasa de las enzimas en estas reacciones de hidroxilación.

Finalmente, un enfoque combinado mediante estudios experimentales y computacionales permitió demostrar que no existe un único factor que determine el perfil de hidroxilación del sustrato por la enzima, sino que es el resultado de la suma de muchos factores estructurales, tanto sobre la molécula

del sustrato como del sitio activo de la enzima. En el caso particular de los esteroides (que fueron los compuestos estudiados en mayor profundidad) estos factores incluyen el carácter polar/apolar de los grupos sustituyentes en las posiciones C-3/C-7 del anillo, la presencia/ausencia de dobles enlaces en el anillo esteroidal, y la longitud y características de la cadena lateral que afectan a la entrada del sustrato en el sitio activo de la enzima por C-25.

En conclusión, las peroxigenasas estudiadas en esta Tesis (r*Cci*UPO, *Aae*UPO y *Mro*UPO) representan una alternativa sostenible a la síntesis química ya que catalizan la oxifuncionalización selectiva de diferentes compuestos alifáticos (tanto lineales como cíclicos) de interés en la industria química y farmacéutica, en presencia de H_2O_2 como único co-sustrato.

1. Introducción

Agrocybe aegerita

1. INTRODUCCIÓN

1.1 Reacciones de oxifuncionalización

Las reacciones de oxidación constituyen uno de los medios más poderosos para la síntesis de compuestos químicos de interés industrial y se encuentran entre las reacciones más deseadas de la síntesis orgánica convencional (Ullrich and Hofrichter, 2005; Torres Pazmiño et al., 2010). Como ejemplo de estas reacciones de oxidación podemos destacar la hidroxilación de compuestos aromáticos utilizados como precursores y productos en la industria farmacéutica, y para la producción de herbicidas en la industria química; la oxidación de alcanos para la síntesis de alcoholes; la oxidación de terpenos para la síntesis de aromas, fragancias, insecticidas, solventes y compuestos de interés farmacéutico; la oxidación de ciclohexano para la producción de ciclohexanona en la síntesis del Nylon y el Perlón; la producción de epóxidos y alcoholes secundarios ópticamente activos para la síntesis de compuestos aromáticos, productos de química fina y moléculas bioactivas como productos farmacéuticos y antibióticos, etc. El problema principal de estas reacciones consiste en que requieren oxidantes fuertes, reactivos químicos muy agresivos, catalizadores específicos y altas temperaturas y presiones, y además pueden conducir a la formación de subproductos tóxicos e indeseables. Por otro lado, estas reacciones de oxidación requieren también de varios pasos para la obtención de compuestos químicos y suelen conllevar bajos rendimientos y altos costes de producción (Ullrich and Hofrichter, 2007; Kinne et al., 2008; Kinne et al., 2009; Bordeaux et al., 2012; Kluge et al., 2012; Peter et al., 2013; Fuchs and Schwab, 2013; Peter et al., 2014). Por lo tanto, la oxifuncionalización catalizada por enzimas es una de las áreas más interesantes tanto en la química orgánica como en la enzimología (Bormann et al., 2015).

La utilización de células o enzimas demostró su eficacia en la síntesis de fármacos, herbicidas, insecticidas y otros productos químicos; en la producción de biocombustibles alternativos al petróleo y en la industria textil y de detergentes, entre otros muchos ejemplos. La utilización de estas enzimas representa una alternativa más eficiente y a la vez más ecológica a la química sintética tradicional, ya que los procesos que catalizan transcurren a través de reacciones en medios más respetuosos con el medio ambiente y bajo condiciones de pH, presión y temperatura suaves, obteniéndose mayores rendimientos y con menor coste económico (Hollmann et al., 2011). Por tal motivo, es de gran

interés entender los mecanismos de acción de las enzimas que catalizan estas biotransformaciones y aplicar esta biocatálisis como herramienta para la síntesis orgánica. Las reacciones de oxidación enzimática son catalizadas generalmente por oxidorreductasas (oxidasas, oxigenasas, deshidrogenasas y peroxidasas), siendo éstas los biocatalizadores más empleados en la industria química y farmacéutica para la oxifuncionalización de diferentes sustratos orgánicos (Fuchs and Schwab, 2013). En la **Figura 1** se puede observar un panorama representativo de los diferentes tipos de reacciones de oxidación biocatalítica llevadas a cabo en la industria (Hollmann et al., 2011).

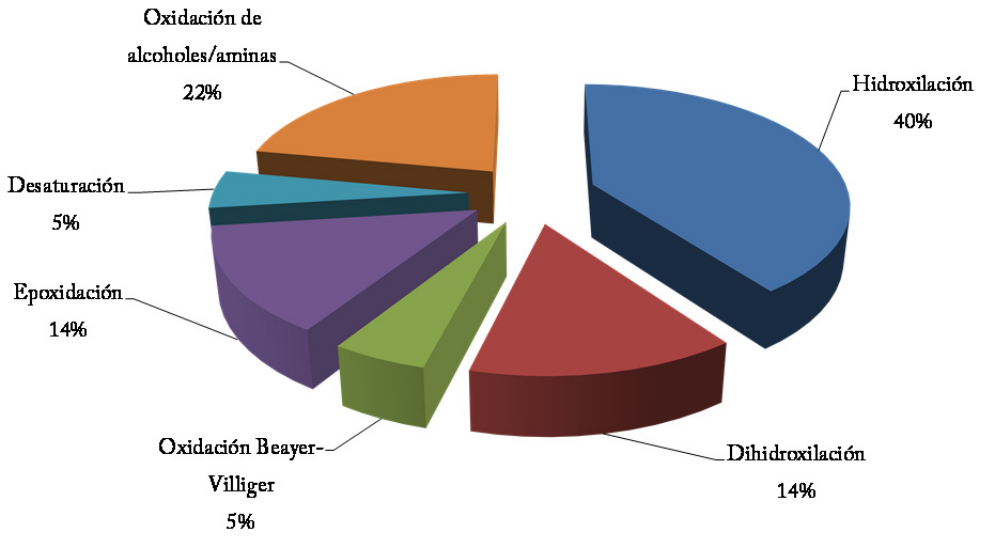

Fig. 1. Tipos de reacciones de oxidación biocatalítica llevadas a cabo en la industria (adaptado de Hollmann et al., 2011).

1.2 Oxidorreductasas

1.2.1 Clasificación

Las oxidorreductasas comprenden un gran número de enzimas que catalizan reacciones biológicas de oxidación/reducción y que se encuentran ampliamente distribuidas entre los organismos microbianos, vegetales y animales. Estas

enzimas catalizan la transferencia de electrones o equivalentes redox entre moléculas dadoras y aceptoras de electrones en reacciones que involucran la transferencia de un electrón, abstracción de un protón, extracción de un hidrógeno, transferencia de hidruro o inserción de oxígeno. En general, esta transferencia se lleva a cabo mediante dos reacciones, una oxidativa y otra reductora, y al menos dos sustratos (uno reducido y otro oxidado) son activados y/o transformados (Feng Xu, 2005). Con el objeto de asignar a las diferentes enzimas un identificador numérico específico, el Comité de Nomenclatura de la Unión Internacional de Bioquímica y Biología Molecular (NC-IUBMB), enumera a las mismas con el número EC que clasifica a las enzimas en términos de la reacción catalítica particular en la que está involucrada (www.chem.qmul.ac.uk/iubmb/enzyme). Las oxidorreductasas están clasificadas con el número EC 1 en el sistema de clasificación NC-IUBMB. Además, según el tipo de reacción que catalizan se dividen en 24 subclases EC (EC 1.1 - EC 1.23 y EC 1.97). Por otro lado, para ejercer su actividad, la mayoría de las oxidorreductasas requieren de cofactores como flavinas, iones metálicos, grupos hemo y pirroloquinolina quinona (PQQ), los cuales por lo general se pueden unir estrechamente a la enzima, con afinidades en el rango de los nanómetros, o covalentemente en el caso de algunas oxidorreductasas. Cuando los cofactores se encuentran estrecha o covalentemente unidos a la enzima, pueden ser considerados como grupos prostéticos, es decir, que forman parte permanente de la estructura de la enzima. Por otro lado, hay cofactores que se unen con baja afinidad y que pueden ser considerados como sustratos, como por ejemplo el NADH o coenzima A, a los cuales se les denomina coenzimas (Torres Pazmiño et al., 2010). Según el tipo de reacción que catalizan y/o su dependencia a una coenzima, las oxidorreductasas se clasificaron de forma general en cuatro subgrupos (Feng Xu, 2005): **(i)** oxidasas, **(ii)** deshidrogenasas/reductasas, **(iii)** oxigenasas/hidroxilasas y **(iv)** peroxidasas (**Tabla 1**).

En cuanto a las aplicaciones de estas enzimas, podemos mencionar la oxifuncionalización asimétrica de esteroides y otros productos de interés farmacéutico, síntesis y modificación de polímeros, degradación oxidativa de contaminantes, oxifuncionalización de hidrocarburos, oxidación de alcoholes, compuestos insaturados y cetonas, la reducción de cetonas y la construcción de biosensores para una variedad de aplicaciones analíticas y clínicas comercializadas para la industria textil y alimentaria, entre otras (May, 1999; Straathof et al., 2002; Xu, 2005; Hudlick and Reed, 2009; Kluge et al., 2012).

Tabla 1

Clasificación de las diferentes oxidorreductasas según la reacción que catalizan y su dependencia de coenzimas (Feng Xu, 2005).

Oxidasas	**Centro activo**
Oxidasas libres de cofactor	Thr-Lys
Tiol oxidasas	Fe, Cu, o Cys + FAD
Oxidasas que contienen Cu	Cu
Oxidasas que contienen flavina	FMN o FAD
Oxidasas con centros multi-redox	Cu, Tyr, flavina, hemo
Deshidrogenasas/reductasas (dependientes de NAD[P])	
Deshidrogenasas que contienen flavina	FMN o FAD
Deshidrogenasas que contienen quinona	PQQ
Deshidrogenasas que contienen Zn	Aminoácido + Zn
Deshidrogenasas con centro multi-redox	Flavina, PQQ, hemo, Fe-S, Mo
Aldo-ceto reductasas	Tyr-His-Asp-Lys
Reductasas que contienen Cu	Cu
Reductasas que contienen flavina	FMN o FAD
Oxigenasas/hidroxilasas	
Oxigenasas libres de cofactor	Aminoácidos
Oxigenasas/hidroxilasas que contienen Fe	Fe o hemo
Oxigenasas/hidroxilasas que contienen Cu	Cu
Oxigenasas/hidroxilasas que contienen flavina	FMN o FAD
Oxigenasas/hidroxilasas multicentro	Fe, Mo, pterin, flavina, Fe-S
Peroxidasas	
Hemo peroxidasas	Hemo
Catalasas	Hemo
Haloperoxidasas	Ser-His-Asp, hemo, o Val
Otras peroxidasas	Cys o Ser-Cys

1.2.1.1 Oxidasas

Las oxidasas, como la alcohol oxidasa, glucosa oxidasa y lacasa, entre otras, son enzimas que catalizan reacciones de oxidación o reducción utilizando simplemente como cofactor el oxígeno molecular (O_2) que actúa como aceptor final de electrones. En estas reacciones el oxígeno molecular se reduce a agua (H_2O) o a peróxido de hidrógeno (H_2O_2). Las lacasas, junto con la ascorbato oxidasa y bilirrubina oxidasa, son enzimas que contienen cuatro átomos de cobre en el sitio activo, y catalizan la oxidación (con transferencia de un electrón) de diferentes sustratos fenólicos y aminas aromáticas mientras que transfieren el electrón abstraído al O_2, que es reducido a H_2O (Hofrichter and Ullrich, 2010; Hollmann et al., 2011).

1.2.1.2 Deshidrogenasas

Las deshidrogenasas son enzimas que catalizan la oxidación o reducción de un sustrato por sustracción de átomos de hidrógeno (deshidrogenación), los cuales son recibidos por coenzimas en su estado oxidado tales como NAD^+, $NADP^+$, FAD y FMN, que son reducidas a NADH, NADPH, $FADH_2$ y $FMNH_2$, respectivamente. Las deshidrogenasas catalizan la oxidación reversible de alcoholes y aminas. La alcohol deshidrogenasa, por ejemplo, es el catalizador más utilizado para la oxidación de alcoholes (Hollmann et al., 2011).

1.2.1.3 Oxigenasas/hidroxilasas

Las oxigenasas e hidroxilasas son enzimas capaces de introducir un átomo de oxígeno en sustratos orgánicos con enlaces C-H y C=C desactivados y en heteroátomos, utilizando O_2 y H_2O_2 como dadores de oxígeno. Las reacciones en que los compuestos orgánicos son oxigenados o hidroxilados son de gran valor para la síntesis orgánica. Sin embargo, como se ha mencionado anteriormente la oxifuncionalización selectiva de estos compuestos puede ser un problema en la síntesis química de compuestos orgánicos ya que a menudo se realizan con agentes oxidantes fuertes y ocurren con una baja quimio, enantio y regioselectividad (Torres Pazmiño et al., 2010; Holtmann et al., 2014). Por el contrario, estas enzimas son capaces de introducir un átomo de oxígeno en compuestos orgánicos como ácidos grasos, alcoholes, alcanos, esteroides y compuestos aromáticos, entre otros, incrementando la reactividad de la molécula

inicial y dando lugar a la síntesis de metabolitos específicos como hormonas, antibióticos, fitoalexinas, etc., bajo condiciones medioambientalmente favorables (ej.: pH y temperaturas moderadas, solventes acuosos, etc.) (Ullrich and Hofrichter, 2007; Torres Pazmiño et al., 2010). Por otro lado, estos procesos de oxifuncionalización son de particular importancia para la iniciación de vías de degradación específicas de descontaminación. De este modo, contaminantes medioambientales como benceno, tolueno e hidrocarburos policíclicos aromáticos, por estar sujetos a la epoxidación e hidroxilación enzimática, son transformados en metabolitos asimilables (en el caso de bacterias y hongos) o en productos solubles en agua que pueden ser excretados (en el caso de animales) (Anh et al., 2007). Existen numerosas oxigenasas provenientes de diferentes organismos, que son capaces de catalizar la inserción de uno (monooxigenasas) o dos átomos de oxígeno (dioxigenasas) en moléculas orgánicas, como la tolueno monooxigenasa, el citocromo P450 monooxigenasa (P450) y la naftaleno dioxigenasa (Anh et al., 2007). La mayoría de las oxigenasas naturales utilizan como fuente el O_2, pero hay también enzimas, presentes en plantas y hongos, que pueden actuar como peroxidasas/peroxigenasas transfiriendo oxígeno a partir del H_2O_2 o de peróxidos orgánicos (**Fig. 2**). La mayoría de estas reacciones, cuando son catalizadas por las mono- y dioxigenasas, suceden intracelularmente mientras que las reacciones catalizadas por las peroxidasas/peroxigenasas son extracelulares (Ullrich and Hofrichter, 2007).

1.2.1.4 Peroxidasas

Las peroxidasas son enzimas secretadas, microsomales o citosólicas, que se encuentran en todos los dominios de la vida, y que catalizan reacciones de transferencia de oxígeno similares a las oxigenasas, utilizando H_2O_2 o hidroperóxidos orgánicos (ROOH) como co-sustratos aceptores de electrones (Hofrichter and Ullrich, 2010). Estas enzimas están involucradas en la degradación de polímeros aromáticos recalcitrantes (lignina y sustancias húmicas) y en la descontaminación oxidativa de componentes vegetales y contaminantes orgánicos.

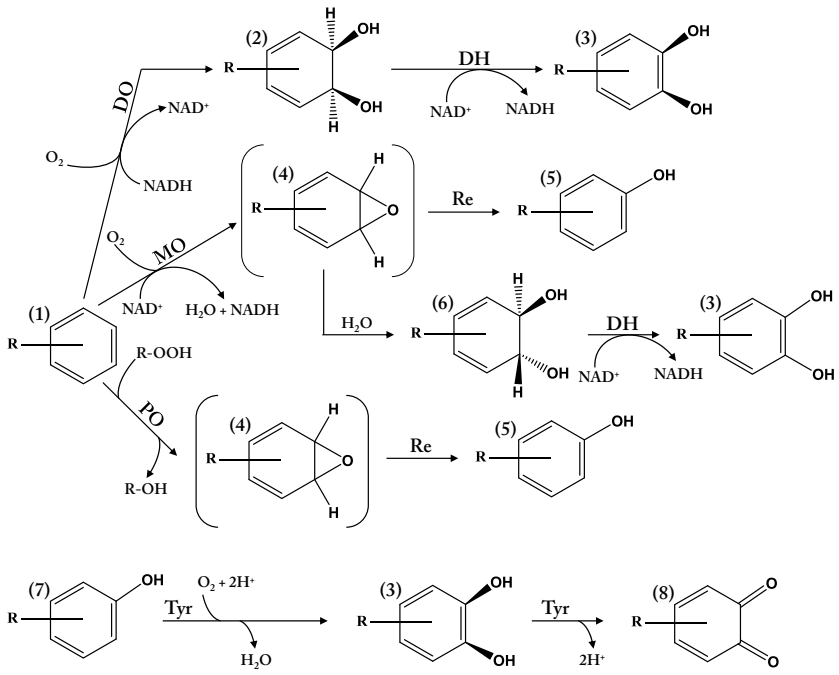

Fig. 2. Rutas básicas de hidroxilaciones enzimáticas de compuestos aromáticos. **DO:** dioxigenasa, **MO**: monooxigenasa, **PO**: peroxidasa/peroxigenasa, **Tyr**: Tirosinasa, **DH**: deshidrogenasa, **Re**: reordenamiento. **(1)** Sustrato aromático, **(2)** *cis*-dihidrodiol, **(3)** Producto catecólico, **(4)** Epóxido intermediario, **(5)** Producto fenólico, **(6)** *cis*,*trans*-dihidrodiol, **(7)** Sustrato fenólico, **(8)** Producto benzoquinona. (Adaptado de Ullrich and Hofrichter, 2007).

Además, las peroxidasas son capaces de oxidar moléculas aromáticas recalcitrantes por la abstracción de un electrón, resultando en la formación de radicales inestables, que tienden a desintegrarse espontáneamente. Por tanto, debido a su versatilidad y estabilidad, las peroxidasas son de particular interés para las biooxidaciones industriales (Ullrich et al., 2004; Hofrichter et al., 2010). Según la reacción que catalizan, las peroxidasas están agrupadas bajo el número EC 1.11.1.x (peróxido de hidrógeno oxidorreductasas) en el sistema de clasificación NC-IUBMB. Actualmente se registraron 23 números EC diferentes para las peroxidasas, que comprenden desde el EC 1.11.1.1 hasta el EC 1.11.1.23, donde el número EC 1.11.1.4 se reclasificó como EC 1.13.11.11 en el grupo de las dioxigenasas (Passardi et al., 2007; Hofrichter et al., 2010) (**Tabla 2**).

Tabla 2

Clasificación de las peroxidasas bajo los números EC 1.11.1.1 al EC 1.11.1.23 (peróxido de hidrógeno oxidorreductasas) en el sistema de clasificación y nomenclatura de enzimas del Comité de Nomenclatura de la Unión Internacional de Bioquímica y Biología Molecular (NC-IUBMB). (www.chem.qmul.ac.uk/iubmb/enzyme)

Número EC	**Nombre recomendado**	**Organismo**
EC 1.11.1.1	NADH peroxidasa	*Clostridium acetobutylicum*
EC 1.11.1.2	NADPH peroxidasa	*Desulfovibrio desulfuricans*
EC 1.11.1.3	Ácido graso peroxidasa	*Arachis hypogaea*
EC 1.11.1.4	EC 1.13.11.11, Triptófano 2,3 dioxigenasa	*Pseudomonas putida*
EC 1.11.1.5	Citocromo c peroxidasa	*Saccharomyces cerevisiae*
EC 1.11.1.6	Catalasa	*Mycobacterium tuberculosis*
EC 1.11.1.7	Peroxidasa	*Armoracia rusticana*
EC 1.11.1.8	Yoduro peroxidasa	*Ascophyllum nodosum*
EC 1.11.1.9	Glutatión peroxidasa	*Mammalia*
EC 1.11.1.10	Cloro peroxidasa	*Caldariomyces fumago*
EC 1.11.1.11	L-Ascorbato peroxidasa	*Pisum sativum*
EC 1.11.1.12	Fosfolípido hidroperóxido glutatión peroxidasa	*Sus scrofa*
EC 1.11.1.13	Manganeso peroxidasa	*Phanerochaete chrysosporium*
EC 1.11.1.14	Lignina peroxidasa	*Phanerochaete chrysosporium*
EC 1.11.1.15	Peroxirredoxina	*Haemophilus influenzae*
EC 1.11.1.16	Peroxidasa versátil	*Pleurotus eryngii*
EC 1.11.1.17	Glutatión peroxidasa dependiente de amida	*Marichromatium gracile*
EC 1.11.1.18	Bromuro peroxidasa	*Corallina pilulifera*
EC 1.11.1.19	Peroxidasa decolorante	*Geotrichum candidum*
EC 1.11.1.20	Prostamida/prostaglandina F2 alfa sintasa	*Mus musculus*
EC 1.11.1.21	Catalasa-peroxidasa	*Mycobacterium tuberculosis*
EC 1.11.1.22	Hidroperóxido ácido graso reductasa	*Synechocystis* PCC6803
EC 1.11.1.23	Ácido (S)-2-hidroxipropilfosfónico epoxidasa	*Streptomyces wedmorensis*

La mayoría de las peroxidasas son hemoproteínas (hemoperoxidasas) que llevan a cabo una variedad de funciones biosintéticas y degradativas actuando sobre un amplio espectro de sustratos que incluyen compuestos orgánicos e inorgánicos. El grupo prostético hemo que poseen las hemoperoxidasas, tiene un grupo protoporfirina IX donde en la parte central se encuentra el átomo de hierro (Fe) que puede formar hasta seis enlaces, de los cuales cuatro están unidos al anillo de porfirina (**Fig. 3**). El quinto enlace es un enlace coordinado con el nitrógeno de un residuo de histidina, la histidina distal, que sirve como catalizador ácido-base en la reacción entre el H_2O_2 y la enzima (Yarman et al., 2012; Bordeaux et al., 2012). El sexto enlace está ocupado por una molécula de agua fácilmente intercambiable que es desplazada por el sustrato cuando éste se une al sitio activo de la enzima (Hrycay and Bandiera, 2015).

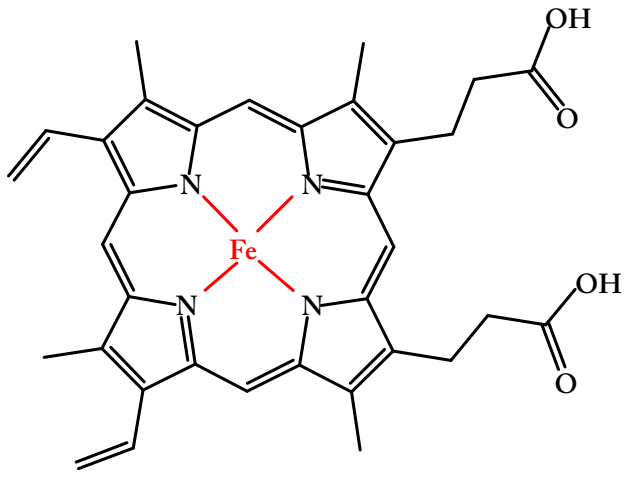

Fig. 3. Complejo Protoporfirina IX con Hierro (Fe).

Aunque las hemoperoxidasas muestran diferentes especificaciones para los sustratos oxidables como indoles, fenoles, aminas aromáticas, lignina, iones Mn^{2+} e iones haluro, entre otros, todas ellas tienen el mismo ciclo catalítico que el P450, basado en tres etapas redox consecutivas (**Fig. 4**). En la primer etapa la enzima reacciona con una molécula de H_2O_2 en un proceso de

oxidación/reducción de dos electrones, donde el H_2O_2 se reduce a H_2O y a su vez la enzima se oxida al compuesto I, que contiene un centro oxiferrilo [Fe(IV)=O] y un catión radical orgánico localizado en el grupo hemo (catión radical porfirina π). Posteriormente, el catión radical sufre una reducción de un electrón, oxidando una molécula de AH_2 y dando lugar a la formación del compuesto II, el cual mantiene el centro oxiferrilo. Finalmente, el compuesto II es reducido volviendo la enzima al estado férrico inicial de reposo con la concominante oxidación de una segunda molécula de sustrato, en un proceso que es la etapa determinante de la velocidad (Ullrich and Hofrichter, 2007; Battistuzzi et al., 2010; Ortiz et al., 2010).

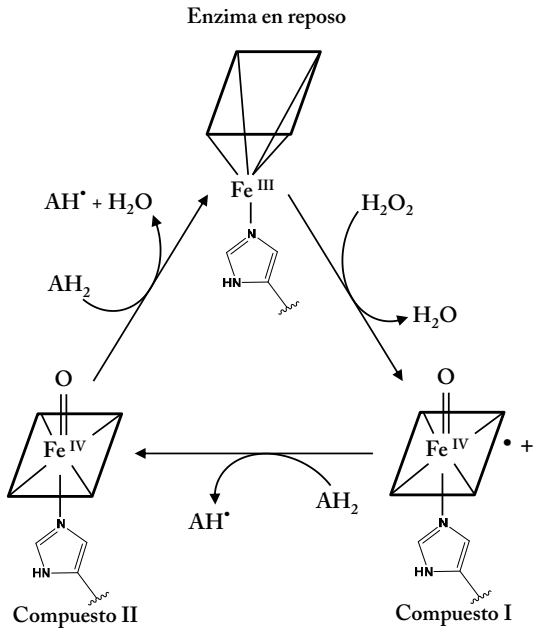

Fig. 4. Ciclo catalítico de las hemoperoxidasas (adaptado de Battistuzzi et al., 2010).

En base a sus propiedades estructurales, las hemoperoxidasas están clasificadas en dos superfamilias: **a)** la peroxidasa-ciclooxigenasa (anteriormente denominada animal o mamífero peroxidasa) y **b**) la peroxidasa no animal o peroxidasa vegetal. De esta manera, dependiendo de la secuencia, el organismo hospedador y la función fisiológica, la superfamilia de la peroxidasa no animal comprende tres clases principales: la *Clase I*, que incluye las peroxidasas intracelulares bacterianas y eucariotas localizadas en orgánulos (mitocondrias, cloroplastos, peroxisomas); la *Clase II*, donde se encuentran las hemoperoxidasas extracelulares fúngicas como la lignina peroxidasa (LiP), manganeso peroxidasa (MnP) y la peroxidasa versátil (VP); y finalmente la *Clase III*, donde están las hemoperoxidasas extracelulares vegetales que están involucradas en la síntesis de lignina. Además, existe un nuevo grupo de peroxidasas que contienen el grupo hemo y que no se encuentran incluidas en las dos superfamilias mencionadas anteriormente, las llamadas hemo-tiolato peroxidasas (HTP), que comprenden la peroxidasa clásica de *Caldariomyces fumago* cloroperoxidasa (*Cfu*CPO) y las peroxigenasas de *Agrocybe aegerita*, *Coprinopsis cinerea* y *Marasmius rotula*, y las peroxidasas decolorantes del tinte, del hongo *Auricularia auricula-judae* (*Aau*DyP) (Hofrichter et al., 2010).

Las HTPs son enzimas pertenecientes a la superfamilia de las peroxidasas que, igual que éstas, poseen un grupo protoporfirina IX con la parte central unida a un átomo de Fe formando seis enlaces (**Fig. 3**), cuatro unidos al anillo porfirina y el sexto enlace unido a una molécula de H_2O. A diferencia de las hemoperoxidasas, las HTPs tienen el quinto enlace unido al nitrógeno de un residuo de cisteína (Cys), como en los P450s (Ullrich and Hofrichter, 2007). Por otro lado, al contrario que el P450, las HTPs son enzimas extracelulares y por tanto más estables (Hofrichter and Ullrich, 2014).

La *Cfu*CPO (EC 1.11.1.10) fue la primera HTP aislada (1960) y fue la enzima de elección para las oxidaciones realizadas con peróxido y para la oxifuncionalización química (Hollmann et al., 2011; Hofrichter and Ullrich, 2014).

El siguiente apartado se centra en las reacciones enzimáticas llevadas a cabo por las peroxigenasas fúngicas (objeto de esta Tesis), comparándolas con las reacciones enzimáticas realizadas por los P450s.

1.2.2 Reacciones enzimáticas de Citocromo P450 y Peroxigenasas

1.2.2.1 Citocromo P450 monooxigenasas (EC 1.14.x.x)

El citocromo P450 es una monooxigenasa que cataliza la inserción de un átomo de oxígeno en un sustrato orgánico (R-H) dando como producto final el correspondiente compuesto orgánico hidroxilado (R-OH):

$$R\text{-}H + \mathbf{O}_2 + 2H^+ + 2e^- \rightarrow R\text{-}\mathbf{O}H + H_2O$$

El P450 representa una enorme y diversa superfamilia de hemoproteínas presentes en bacterias, arquaeas y eucariotas siendo la enzima hidroxilante más versátil. Su nombre viene dado porque al combinarse en su estado reducido con el monóxido de carbono (CO), forma un complejo ion Fe^{2+}-CO que exhibe un máximo de absorción a 450 nm (Hrycay and Bandiera, 2015). Estas enzimas actúan sobre un amplio rango de compuestos exógenos como drogas, pesticidas, procarcinógenos, anestésicos y solventes orgánicos, y endógenos como esteroides, eicosanoides, ácidos grasos, hidroperóxidos lipídicos y retinoides, y además están involucradas en diferentes procesos bioquímicos intracelulares como el metabolismo de drogas, la detoxificación de pesticidas y xenobióticos, la modificación de ácidos grasos y la biosíntesis de esteroides y alcaloides (Orellana and Guajardo, 2004; Ullrich and Hofrichter, 2005; Ortiz et al., 2010; Brill et al., 2014; Shoji and Watanabe, 2014). En la actualidad, el interés industrial de los P450s se debe principalmente a la industria farmacéutica para la generación de metabolitos secundarios y la producción de precursores farmacéuticos activos, como los esteroides (Holtmann et al., 2014). Además, los P450s catalizan una amplia variedad de reacciones que incluyen epoxidación de insaturaciones C=C, N-alquilación, O-desalquilación, S- y N-oxidación, oxidación de aldehídos y alcoholes, deshalogenación, desnitración e hidroxilación de compuestos aromáticos y alifáticos y, dependiendo de la disponibilidad de oxígeno en el tejido, reacciones de reducción (Orellana and Guajardo, 2004; Ulracher and Eiben, 2006; Ullrich and Hofrichter, 2007).

El ciclo catalítico de P450 (**Fig. 5a**) fue objeto de estudio durante décadas usando como modelo los citocromos P450CAM y P450BM3. Al iniciar el ciclo, el grupo hemo de la enzima está en su estado oxidado (Fe^{3+}) de reposo (**Fig. 5b**).

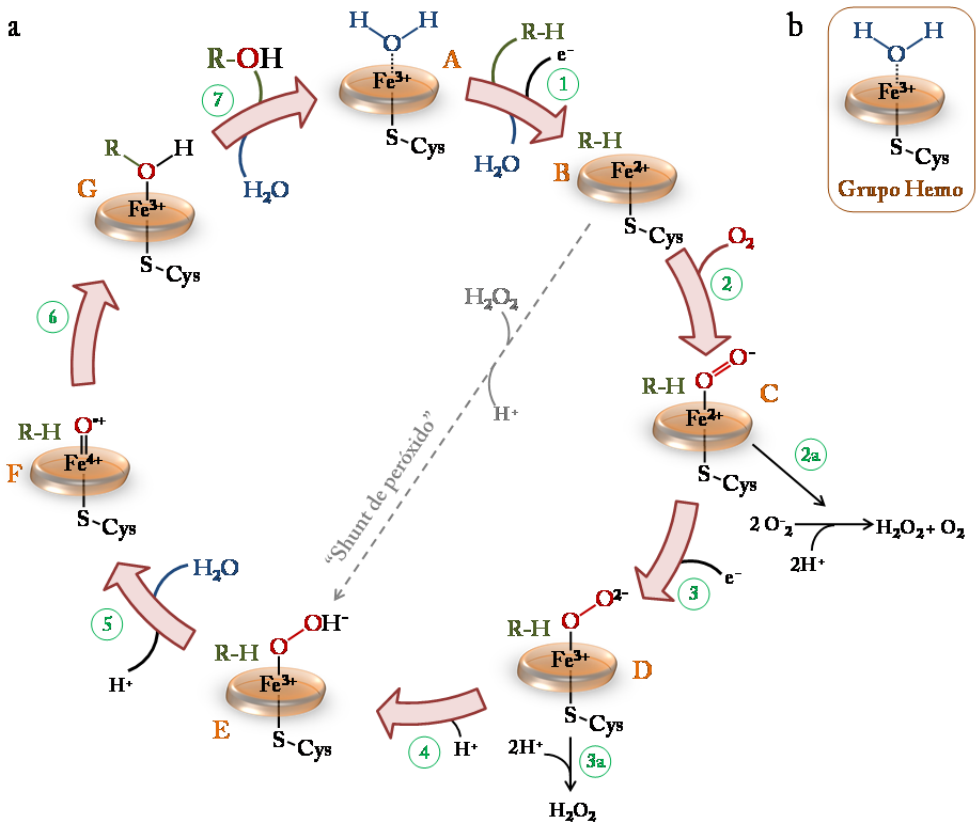

Fig. 5. (a) Ciclo catalítico del citocromo P450. Los pasos secuenciales mediante los cuales el P450 cataliza la oxidación de un sustrato (R-H) al producto monooxigenado (R-OH), son ilustrados numéricamente entre los pasos 1-7: **1)** El *paso 1* involucra la unión de R-H a la enzima (A), seguido de la pérdida de una molécula de H_2O y luego, por la transferencia de un electrón (e^-), se genera la reducción del Fe^{3+} presente en el grupo hemo a Fe^{2+} formando un complejo P450-RH (B). **2)** En el *paso 2* el O_2 se une al grupo hemo-Fe^{2+} para producir un complejo relativamente estable, complejo anión superóxido-ferroso [Cys-S-Fe^{2+}-O_2^-] (C). **3)** En el *paso 3*, mediante la transferencia de un e^-, se genera un intermediario cargado di-negativamente, el peróxido-férrico [Cys-S-Fe^{3+}-O_2^-]$^-$ (D). **4)** En el *paso 4*, este último complejo se protona en el oxígeno distal para generar un complejo hidroperóxido-férrico [Cys-S-Fe^{3+}-OOH]$^-$ (E). **5)** En el *paso 5*, un segundo protón (H^+), produce la ruptura heterolítica del enlace O-O produciendo una molécula de H_2O y el compuesto I (Cpd I) (F). **6)** En el *paso 6*, el Cpd I transfiere su átomo de oxígeno ferrilo a R-H (G), generando R-OH y volviendo la enzima a su estado oxidado inicial (A) (*paso 7*). En el *paso 2A*, [Cys-S-Fe^{2+}-O_2^-] puede disociarse liberando el ion Fe^{2+} y $O_2^{\bullet-}$ y, $O_2^{\bullet-}$, se disocia posteriormente en H_2O_2. En el *paso 3A*, [Cys-S-Fe^{3+}-OO_2^-]$^-$ se disocia con una protonación generando H_2O_2. (b) El grupo hemo de la enzima en su estado oxidado (Fe^{3+}) de reposo. (Adaptado de Torres Pazmiño et al., 2010; Whitehouse et al., 2012; Krest et al., 2013; Hrycay and Bandiera, 2015).

En este ciclo catalítico, a través de una serie de pasos, se forma el compuesto I (Cpd I) que es el responsable de transferir su átomo de oxígeno al R-H, generando el sustrato monooxigenado (R-OH) (**Fig. 5a**) (Urlacher et al., 2004; Ullrich and Hofrichter, 2007; Torres Pazmiño et al., 2010; Whitehouse et al., 2012; Krest et al., 2013; Holtmann et al., 2014; Hrycay and Bandiera, 2015). Los P450s son capaces de formar el compuesto 0 $[Cys\text{-}S\text{-}Fe^{2+}\text{-}OOH]^-$ a partir del complejo P450-RH, usando H_2O_2 como cosustrato a través del "Shunt de peróxido" (**Fig. 5a**). Sin embargo, usualmente la eficiencia de esta vía con H_2O_2 es relativamente baja por la inactivación oxidativa del grupo hemo-prostético (Holtmann et al., 2014)

Dependiendo del sistema de transporte de electrones que tengan, los P450s se pueden clasificar en cuatro clases diferentes. Los P450s de la Clase I se encuentran en las membranas mitocondriales de bacterias y eucariotas. Están compuestos de tres componentes separados, el dominio hemo, una ferredoxina (Fd) NADH dependiente, y una ferredoxina reductasa (FdR) que contiene FAD. Estas enzimas reciben los electrones de la ferredoxina (Fd) que se reduce gracias a la acción de la FdR. Son las encargadas de catalizar diferentes pasos en la biosíntesis de hormonas esteroidales y la vitamina D_3 en mamíferos. Los P450s de la Clase II son los más comunes en eucariotas. Estas enzimas se encuentran ancladas a la cara externa del retículo endoplásmico (RE) por los residuos amino terminales. Reciben los electrones directamente del NADH dependiente de P450 reductasa, que es una diflavoproteína FAD/FMN. Los P450s de la Clase III contienen los mismos componentes que los del sistema de transporte de la Clase II pero no requieren de un donador de electrones, son autosuficientes. Esta característica facilita el transporte de electrones e incrementa considerablemente las velocidades de reacción de los P450s de la Clase III. Estos sistemas pueden ser solubles o estar unidos a membranas, y se encuentran tanto en procariotas como en eucariotas. Estas enzimas catalizan las reacciones de deshidratación de alquil-hidroperóxidos y alquil-peróxidos inicialmente generados por dioxigenasas. Los P450s de la Clase IV reciben los electrones directamente del NADH y de los mismos componentes que los P450s de la Clase I, pero los dominios están fusionados en una cadena polipeptídica simple como en los P450s de la Clase III (Torres Pazmiño et al., 2010). Las enzimas de las clases I y II de todos los organismos participan en la detoxificación, o en algunos casos activación, de xenobióticos. Las clases III y IV

pueden considerarse como los restos más ancestrales de las formas de los P450 involucradas en la detoxificación de especies de oxígeno activo.

Bacillus megaterium es una bacteria principalmente aeróbica Gram (+) que produce en su interior una hemoproteína P450 monooxigenasa (P450BM3). Esta enzima autosuficiente perteneciente a la clase II requiere de una flavoproteína para la transferencia de electrones a partir del NADPH que se encuentra fusionada a la hemoproteína (Capdevila et al., 1996; Ortiz de Montellano, 2010; Brill et al., 2014). Esta hemoproteína es capaz de catalizar la hidroxilación de ácidos grasos de cadena larga en las posiciones ω-1, ω-2 y ω-3 debido a su actividad hidroxilante extremadamente alta (Whitehoue et al., 2012; Shoji and Watanabe, 2015). En condiciones limitantes de sustrato, P450BM3 es capaz de oxidar los metabolitos iniciales en productos que incluyen dioles y cetoalcoholes (Capdevila et al., 1996). Además, P450BM3 es capaz de hidroxilar otros compuestos como naftaleno y ácido 12-*p*-nitrodecanoico (Hofrichter and Ullrich, 2014). Por otro lado, existen otras enzimas P450 bacterianas capaces de hidroxilar hidrocarburos de cadena larga como es el caso de CYP153A1, que fue el primer P450 bacteriano asociado específicamente con esta actividad, e identificado en 2001 en *Acinetobacter* sp (Beilen et al., 2006; Johnston et al., 2011). La esterol 27-hidroxilasa (CYP27A1) por su parte, es la encargada de hidroxilar el C-27 en la cadena lateral de los esteroles y de la biosíntesis de los ácidos biliares a partir de la oxidación del colesterol (Johnston et al., 2011).

Debido a su versatilidad catalítica, los P450s cumplirían perfectamente con los requisitos esenciales para ser el biocatalizador de elección de un gran número de reacciones de interés, pero desafortunadamente presentan una serie de desventajas como su baja estabilidad ya que son enzimas intracelulares, su difícil aislamiento y purificación y además necesitan de cofactores complejos para su funcionamiento (Hofrichter and Ullrich, 2014)

1.2.2.2 Peroxigenasas (EC 1.11.2.x)

Las peroxigenasas son HTPs extracelulares que presentan prácticamente la misma versatilidad catalítica que los P450s pero sin la necesidad de usar cofactores complejos. Estas peroxigenasas son capaces de realizar reacciones de transferencia de oxígeno mediante dos vías diferentes, la vía peroxigenasa y la vía peroxidasa, a través de las cuales transfieren un átomo de oxígeno a partir del H_2O_2 a una gran variedad de sustratos (Yarman et al., 2012, Holtmann et al.,

2014; Hofrichter et al., 2015). En este sentido, mediante la vía peroxigenasa, estas enzimas realizan la abstracción de un átomo de H a partir de Cpd I dando lugar a una rápida formación del sustrato oxidado dentro del sitio activo de la enzima. De este modo la peroxigenasa puede ejercer control sobre la selectividad de la reacción (**Fig. 6a**). Por el contrario, mediante la vía peroxidasa, las peroxigenasas necesitan de dos reacciones sucesivas para la abstracción de dos átomos de H que producen especies reactivas (radicales) y que en su mayoría reaccionan fuera de los sitios activos de las enzimas (**Fig. 6b**). En este sentido, la selectividad de las reacciones generalmente depende de la reactividad química de los sustratos y de los materiales de partida (Bormann et al., 2015, Hofrichter et al., 2015).

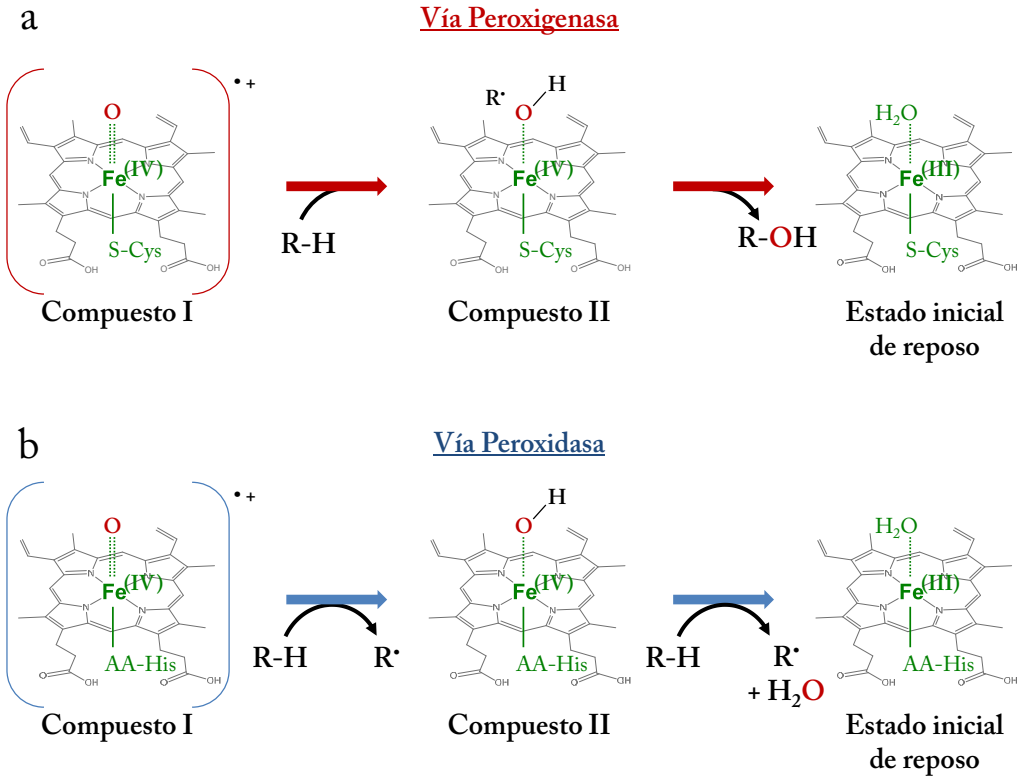

Fig. 6. Reacciones del compuesto I por la vía peroxigenasa (a) y por la vía peroxidasa (b). (Adaptado de Bormann et al., 2015).

Actualmente las peroxigenasas están clasificadas en 5 números EC diferentes en el sistema de clasificación NC-IUBMB, desde EC 1.11.2.1 hasta EC 1.11.2.5 (**Tabla 3**). www.chem.qmul.ac.uk/iubmb/enzyme.

Tabla 3

Clasificación de las peroxigenasas bajo los números EC 1.11.2.1 al EC1.11.2.5 (peróxido de hidrógeno oxidorreductasas) en el sistema de clasificación y nomenclatura de enzimas del Comité de Nomenclatura de la Unión Internacional de Bioquímica y Biología Molecular (NC-IUBMB). (www.chem.qmul.ac.uk/iubmb/enzyme)

Número EC	Nombre recomendado	Organismo
EC 1.11.2.1	Peroxigenasa inespecífica	*Agrocybe aegerita*
EC 1.11.2.2	Mieloperoxidasa	*Mus musculus*
EC 1.11.2.3	Peroxigenasa de semillas	*Arabidopsis thaliana; Avena sativa*
EC 1.11.2.4	Ácido graso peroxigenasa	*Bacillus subtilis; Sphingomonas paucimobilis*
EC 1.11.2.5	3-Metil-L-tirosina peroxigenasa	*Streptomyces lavendulae*

En el año 2004, se describió la primera peroxigenasa fúngica del hongo basidiomiceto *A. aegerita* (Ullrich et al., 2004), que crece sobre troncos de chopos, álamo, olmos, sauces, higueras y plátanos, y a menudo en estrecho contacto con el suelo.

Esta peroxigenasa fúngica, recientemente cristalizada (Piontek et al., 2013) (**Fig. 7**), es una proteína de 45 kD fuertemente glicosilada (20-40% de carbohidratos), que tiene un grupo hemo tipo B unido no covalentemente con la cisteína como ligando al hierro proximal, y que comparte algunas secuencias homólogas y propiedades catalíticas con la *Cfu*CPO y P450 respectivamente y además, cataliza la hidroxilación/epoxidación dependiente de H_2O_2 de diversos compuestos orgánicos (Hofrichter and Ullrich, 2014).

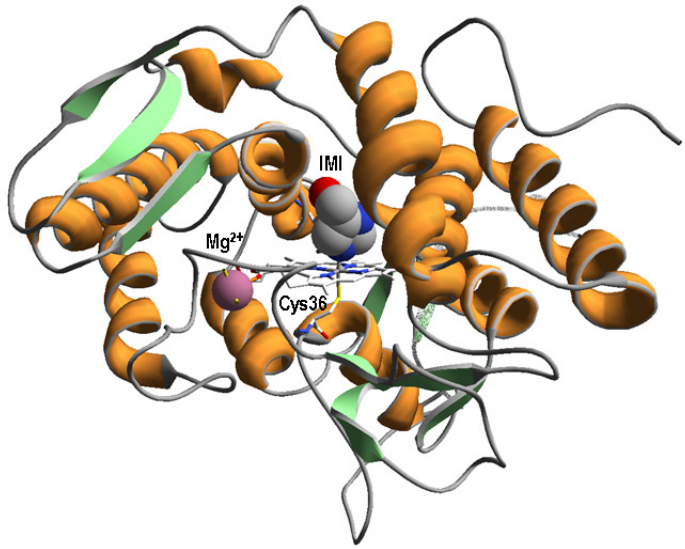

Fig. 7. Estructura molecular de la peroxigenasa de *Agrocybe aegerita* (hélices en naranja y láminas β en verde) incluyendo el cofactor hemo en el centro y su ligando Cys36 (ambos como palos CPK-coloreados), un molécula de sustrato, (IMI, 2/5-hydroxymetilimidazol, como esferas CPK-coloreadas), y un ion Mg^{2+} (esfera rosa). Obtenido de PDB 2YOR.

Al contrario que el P450 que es una enzima intracelular, la peroxigenasa de *A. aegerita* es una enzima extracelular y por tanto más estable, que sólo requiere H_2O_2 para su funcionamiento y que no necesita de cofactores complejos como el NAD(P)H (**Fig. 8**), ni de una flavina reductasa auxiliar para la transferencia de electrones al O_2 (Ullrich and Hofrichter, 2005).

La peroxigenasa de *A. aegerita* fue introducida primeramente en el sistema de clasificación del NC-IUBMB con el número EC 1.11.1.x como una haloperoxidasa (Hofrichter et al., 2010). Sin embargo, debido a que esta enzima es capaz de transferir eficientemente el oxígeno desde el H_2O_2 a diferentes compuestos, resultó ser una verdadera peroxigenasa y además, debido a su habilidad de epoxidar e hidroxilar compuestos aromáticos y su baja actividad halogenasa, fue también clasificada como una peroxigenasa aromática capaz de catalizar reacciones asignadas anteriormente al P450.

Posteriormente, el nombre de "peroxigenasa aromática" (APO) fue sustituido por el de "peroxigenasa inespecífica" (UPO) debido a que no sólo es

capaz de hidroxilar compuestos aromáticos sino que también, como revelaron los resultados obtenidos en esta Tesis (Gutiérrez et al., 2011), es capaz de actuar sobre diferentes compuestos alifáticos como ácidos grasos, alcoholes grasos, alcanos y esteroides, entre otros. Por lo tanto, su correspondiente entrada en el sistema de clasificación NC-IUBMB (EC 1.11.1.x) se cambió por el número EC 1.11.2.1 y aceptada en la nomenclatura de enzimas NC-IUBMB, siendo así la primera entrada en la nueva subclase de oxidorreductasas dependientes de H_2O_2 (**Tabla 3**).

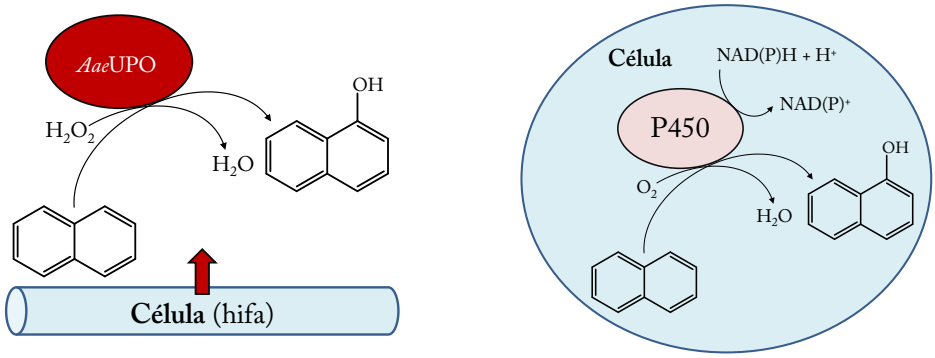

Fig. 8. Esquema de la reacción de hidroxilación del naftaleno por la peroxigenasa de *Agrocybe aegerita* (*Aae*UPO, izquierda) y la monooxigenasa intracelular del citocromo P450 (derecha). (Adaptado de Ullrich and Hofrichter, 2005).

Existe un ciclo catalítico hipotético de *Aae*UPO (**Fig. 9**) que combina elementos de las hemo peroxidasas con rutas de peroxidación derivadas del P450, es decir que *Aae*UPO puede ser considerada como un híbrido funcional de ambos tipos de enzimas. Este ciclo catalítico comienza cuando *Aae*UPO entra en contacto con el H_2O_2 formando un complejo *Aae*UPO-Peróxido, que luego por la pérdida de una molécula de H_2O (por ruptura heterolítica) forma el intermediario UPO-Cpd I. A partir de este paso, el ciclo catalítico puede continuar por dos vías diferentes, una mediante acción peroxigenasa y la otra por acción peroxidasa (Ullrich and Hofrichter, 2007; Yarman et al., 2011, Hofrichter et al., 2015).

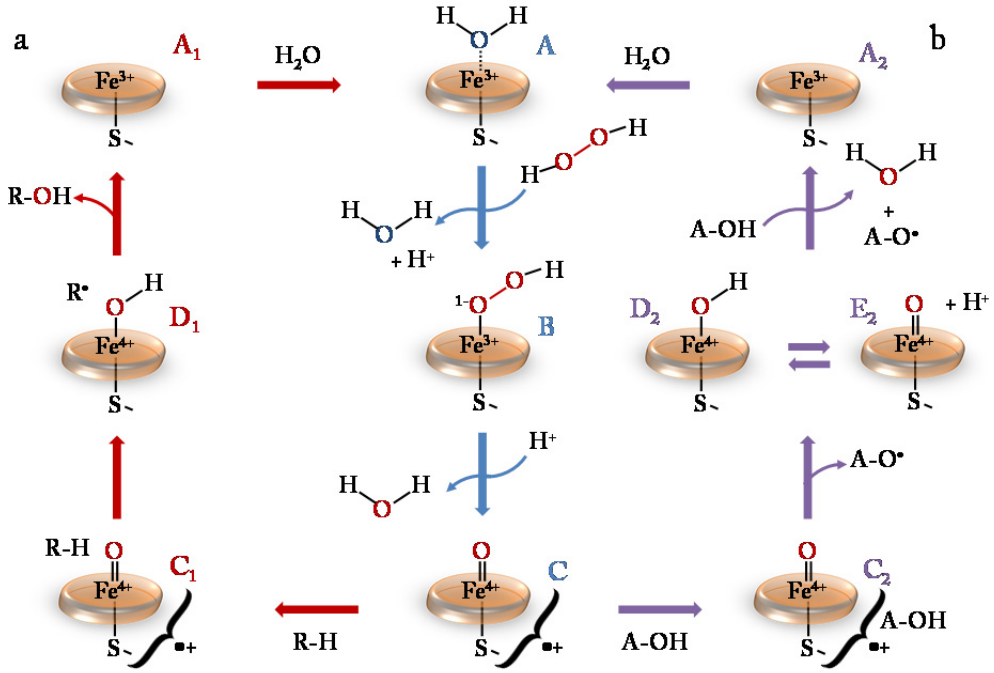

Fig. 9. Ciclo catalítico hipotético de *Aae*UPO. El ciclo catalítico comienza cuando la enzima nativa *Aae*UPO (A) entra en contacto con el H_2O_2 formando un complejo *Aae*UPO-Peróxido ([UPO-Cpd 0]$^-$) (B) que luego por la pérdida de una molécula de H_2O forma el intermediario radical oxo-ferrilo (UPO-Cpd I) (C) (flechas en azul). A partir de este paso, el ciclo catalítico puede continuar por dos vías diferentes, una mediante acción peroxigenasa (flechas en rojo), en la cual el intermediario UPO-Cpd I abstrae un e^- y un H^+ a partir del R-H dando un Cpd II protonado (C_1), el complejo ferril hidróxido y un sustrato radical ($R^•$) localizado cerca del sitio activo de *Aae*UPO, que rápidamente se convierte en un producto hidroxilado (R-OH). Posteriormente, el producto R-OH se disocia de la enzima y una molécula de agua se une al grupo hemo de la UPO dando lugar al comienzo de un nuevo ciclo catalítico. En la segunda vía, por acción peroxidasa (flechas en morado), se puede encontrar el típico ciclo hemo-peroxidasa donde ambos, Cpd I (C) y Cpd II (C_2), abstraen un electrón cada uno a partir de dos moléculas de sustrato (A-OH), los cuales se liberan como radicales libres ($A\text{-}O^•$) y que pueden someterse a reacciones de acoplamiento. Finalmente, la oxidación del segundo A-OH da lugar a que UPO retorne a estado inicial para comenzar con un nuevo ciclo catalítico. (Adaptado de Hofrichter et al., 2015).

En la vía peroxigenasa (**Fig. 9a**), UPO-Cpd I abstrae un e^- y un H^+ a partir del R-H dando un Cpd II protonado, un sustrato radical ($R^{\bullet}$) localizado cerca del sitio activo de *Aae*UPO, que rápidamente se convierte en un producto hidroxilado (R-OH) dando lugar al comienzo de un nuevo ciclo catalítico. En la vía peroxidasa (**Fig. 9b**) ambos, Cpd I y Cpd II, abstraen un electrón cada uno a partir de dos moléculas de sustrato (A-OH), los cuales se liberan como radicales libres ($A\text{-}O^{\bullet}$) que pueden someterse a reacciones de acoplamiento. Posteriormente la oxidación del segundo A-OH da lugar a que UPO retorne a su estado inicial para comenzar con un nuevo ciclo catalítico.

De este modo se puede ver que la vía peroxidasa procede por la transferencia de electrones a través de la superficie del grupo hemo, mientras que en la vía peroxigenasa, se requiere del contacto directo del sustrato con el sitio activo del grupo hemo (Hofrichter and Ullrich, 2006; Ullrich and Hofrichter, 2007; Hofrichter and Ullrich, 2010; Yarman et al., 2011; Hofrichter et al, 2015). Por otro lado, *Aae*UPO presenta una gran ventaja con respecto a P450, catalizando las mismas reacciones, ya que el Cpd I en el ciclo catalítico de *Aae*UPO tan sólo necesita de peróxido para ser activado, y además cataliza la oxidación de dos electrones del sustrato durante la transferencia del átomo de oxígeno (**Fig. 9**). Por el contrario, en el ciclo catalítico de P450, el Cpd I necesita una segunda flavoproteína, y un agente reductor como el NAD[P]H, para ser activado por el oxígeno molecular (Martínez et al., 2014) (**Fig. 5**).

*Aae*UPO cataliza un alto número de reacciones de oxidación interesantes, incluyendo entre otras, la epoxidación/hidroxilación regioselectiva del naftaleno, la sulfoxidación del dibenzotiofeno, la N-oxidación de derivados de piridina, la O-desalquilación de alquil-aril éteres, la oxidación bencílica de derivados del tolueno, la oxidación de aril-alcoholes y aldehídos, la bromación del fenol y la oxidación de cicloalcanos (**Fig. 10**) (Ullrich and Hofrichter, 2007; Aranda et al., 2009; Peter et al., 2011, Poraj-Kobielska et al., 2012; Peter et al., 2013; Karich et al., 2013; Peter et al., 2014; Martínez et al., 2014; Kluge et al., 2014). Además, tal como se describe a lo largo de esta Tesis, *Aae*UPO también cataliza la oxidación/oxigenación de ácidos grasos, alcoholes grasos, alcanos/alquenos, esteroides y secosteroides.

Muchas de estas oxidaciones selectivas representan reacciones difíciles de catalizar por la química orgánica convencional. En este contexto, *Aae*UPO tiene un enorme potencial biotecnológico ya que las reacciones de oxifuncionalización

selectiva que cataliza la convierten en una herramienta biocatalítica versátil para la producción de nuevos compuestos químicos de interés industrial (Hofrichter et al., 2010).

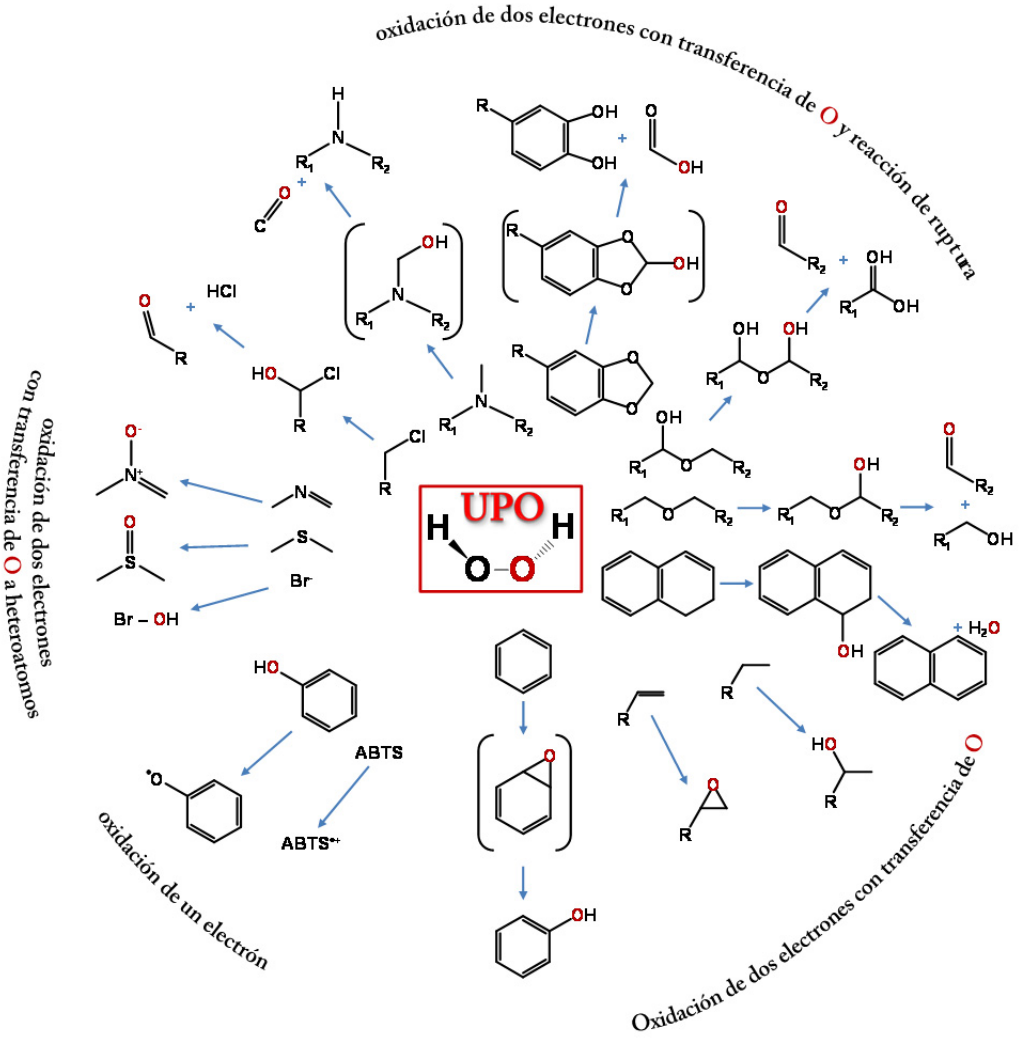

Fig. 10. Resumen general de las diferentes reacciones catalizadas por *Aae*UPO (adaptado de Hofrichter et al., 2015).

Después de la primera peroxigenasa descrita en el basidiomiceto *A. aegerita* (Ullrich et al., 2004), se encontraron otras peroxigenasas en hongos relacionados tales como *Coprinellus radians* y *Marasmius rotula*, siendo este hallazgo indicador de la presencia generalizada de estas enzimas en el reino fúngico (Anh et al., 2007; Hofrichter et al., 2010; Gröbe et al., 2011). La investigación realizada en bases de datos con el gen de *Aae*UPO como sonda, permitó detectar la presencia de genes de peroxigenasas en diversos hongos (Pecyna et al., 2009), como *Coprinopsis cinerea* (sinónimo: *Coprinus cinereus*). *C. cinerea* es un basidiomiceto multicelular que habita en el estiércol, y fue secuenciado por el Broad Institute (http://www.broadinstitute.org) en el marco del proyecto Fungal Genome Initiative (http://www.broadinstitute.org/science/projects/fungal-genome-initiative), cuyo genoma se encuentra disponible para la búsqueda de genes en el Joint Genome Institute (JGI; www.jgi.doe.gov).

Muy recientemente se identificaron más de cien genes de tipo peroxigenasa, codificados por enzimas de la superfamilia de las HTP, durante el análisis de 24 genomas de basidiomicetos (Floudas et al., 2012). La peroxigenasa salvaje de *C. cinerea* aún no fue aislada y caracterizada, pero uno de los genes peroxigenasa de su genoma (JGI modelo CC1G_08427T0) se expresó de forma heteróloga por la empresa Novozymes A/S (Bagsvaerd, Dinamarca) lo que dio lugar a la publicación de una patente internacional (WO/2008/119780). Esta primera peroxigenasa recombinante (r*Cci*UPO) puede ser una herramienta poderosa para aplicaciones sintéticas debido a los niveles altos de expresión que se pueden conseguir, y a la posibilidad de modificar a medida sus propiedades catalíticas y operacionales utilizando herramientas de ingeniería de proteínas.

En al año 2011 se consiguió producir en gran cantidad una nueva HTP sintetizada por el hongo *M. rotula* (Gröbe et al., 2011). Este bacidiomiceto, es una especie saprófita y como tal obtiene sus nutrientes de la materia orgánica muerta en descomposición. Crece en grupos o racimos sobre la madera muerta, en restos de maderas como ramas o palos, y ocasionalmente sobre hojas caducas o podridas. La peroxigenasa de *M. rotula* (*Mro*UPO) presenta una estructura más pequeña que *Aae*UPO y r*Cci*UPO, sin embargo, *Mro*UPO es capaz de oxidar sustratos más voluminosos debido a que la entrada al sitio activo de la enzima es más plana y más amplia que la de *Aae*UPO y r*Cci*UPO (Poraj-Kobielska, 2013).

Además de las tres peroxigenasas mensionadas anteriormente, existen otras especies de hongos que secretan UPOs pero la purificación o caracterización de estas enzimas no se realizó aún (Hofrichter et al., 2015).

En la presente Tesis se describe por primera vez la actividad catalítica de las peroxigenasas *Aae*UPO, r*Cci*UPO y *Mro*UPO sobre compuestos alifáticos incluyendo ácidos grasos, alcanos, alcoholes grasos y ésteres de ácidos grasos, así como esteroides y secosteroides, entre otros.

2. Objetivos

Coprinopsis cinerea

2. OBJETIVOS

La presente Tesis tiene como objetivo principal el estudio de la oxifuncionalización enzimática de diferentes compuestos alifáticos, lineales (ácidos grasos, alcoholes grasos, alcanos/alquenos) y cíclicos (esteroides y secosteroides) por diferentes peroxigenasas fúngicas incluyendo las peroxigenasas salvajes de *Agrocybe aegerita* (*Aae*UPO) y *Marasmius rotula* (*Mro*UPO) así como la peroxigenasa recombinante de *Coprinopsis cinerea* (r*Cci*UPO).

Los objetivos específicos de esta Tesis son los siguientes:

- Estudiar la oxifuncionalización selectiva de diversos compuestos alifáticos lineales como ácidos grasos libres y esterificados, alcoholes grasos y alcanos, y cíclicos como esteroides (esteroles libres y esterificados, hidrocarburos y cetonas) y secosteroides, mediante la acción enzimática de diversas peroxigenasas fúngicas, incluyendo r*Cci*UPO, *Aae*UPO y *Mro*UPO, en presencia de H_2O_2 como único co-sustrato.

- Estudiar los mecanismos de las reacciones de hidroxilación de dichos compuestos alifáticos por las peroxigenasas r*Cci*UPO, *Aae*UPO y *Mro*UPO (utilizando $H_2{}^{18}O_2$ como co-sustrato).

- Investigar diferentes aspectos de las relaciones estructura-función de las peroxigenasas en las reacciones de hidroxilación de compuestos alifáticos mediante estudios computacionales.

3. Materiales y Métodos

Marasmius rotula

3. MATERIALES Y MÉTODOS

3.1 Enzimas

En la presente Tesis se estudia la oxifuncionalización enzimática de diferentes compuestos alifáticos mediante el uso de peroxigenasas de los hongos *Agrocybe aegerita*, *Marasmius rotula* y *Coprinopsis cinerea* (**Fig. 11)**, siendo esta última recombinante.

Fig. 11. Imágenes de los hongos: **a)** *Agrocybe aegerita*, **b)** *Marasmius rotula* y **c)** *Coprinopsis cinerea*.

3.1.1 Peroxigenasa de *Agrocybe aegerita* (*Aae*UPO)

La peroxigenasa extracelular de *A. aegerita* (isoenzima II, 45 kDa) se aisló y purificó en el grupo del Prof. Martin Hofrichter (Zittau, Alemania) (Ullrich et. al., 2004). Los hongos precultivados durante dos semanas en placas de agar con un 2% de extracto de malta, se homogeneizaron en una solución estéril de NaCl. La suspensión micelial resultante se inoculó en cultivo líquido (en matraces de 500 mL) y con agitación (100 rpm) a 24 ºC, en oscuridad durante 14 días. La purificación de la enzima se realizó mediante varios pasos de cromatografía de intercambio iónico utilizando una combinación de columnas de Q-Sefarosa, SP-Sefarosa y Mono S. El peso molecular de la proteína se determinó mediante electroforesis en gel de poliacrilamida con dodecil sulfato de sodio (SDS-PAGE). Su actividad específica es 117 $U \cdot mg^{-1}$, donde 1 unidad de actividad enzimática representa la oxidación de 1 μmol de alcohol veratrílico a vetraldehído (ε_{310} 9300 $M^{-1} \cdot cm^{-1}$) en 1 minuto a 23 ºC y pH 7, en presencia de

2.5 mM de H_2O_2. La velocidad de conversión de la enzima purificada sobre el alcohol veratrílico fue estimada como 85 s^{-1} (con una constante K_m de Michaelis-Menten de 2.4 mM).

3.1.2 Peroxigenasa recombinante de *Coprinopsis cinerea* (r*Cci*UPO)

La peroxigenasa recombinante utilizada en esta Tesis se produjo y purificó en Novozymes (Bagsvaerd, Dinamarca). Esta enzima, corresponde al modelo de gen CC1G_08427T0 proveniente del genoma secuenciado de *C. cinerea* disponible en el *Joint Genome Institute* (JGI) (www.jgi.doe.gov). La proteína correspondiente (genoma ID 7429 de *C. cinerea*) se sintetizó por expresión heteróloga usando como sistema hospedador industrial el hongo *Aspergillus oryzae* (patente WO/2008/119780) y purificó mediante cromatografía de intercambio iónico utilizando columnas de S-Sefarosa y SP-Sefarosa. La peroxigenasa recombinante resultante, es una glicoproteína cromatográficamente homogénea con una masa molecular de alrededor de 44 kDa y una actividad específica de aproximadamente 100 $U \cdot mg^{-1}$.

3.1.3 Peroxigenasa de *Marasmius rotula* (*Mro*UPO)

La peroxigenasa extracelular de *M. rotula* (32 kDa) se aisló y purificó en JenaBios (Jena, Alemania) (Gröbe et. al., 2011). Para ello, los hongos previamente cultivados en agar con un 2% de extracto de malta a 24 ºC se homogeneizaron en una solución estéril de NaCl. La suspensión micelial resultante se inoculó en cultivos líquidos (en matraces de 500 mL) con agitación de 120 rpm a 24 ºC durante 3 a 4 semanas.

La purificación de la enzima se realizó mediante cinco pasos de cromatografía utilizando un sistema FPLC e intercambiadores aniónicos fuertes (Q-Sefarosa FF, Mono Q 10/100, Source 15Q y Mono Q 5/50) así como con un tamizado molecular. Por otro lado, el peso molecular de la proteína se determinó por electroforesis en gel de SDS-PAGE. La actividad específica de la enzima glicosilada es de 77 $U \cdot mg^{-1}$, donde 1 unidad de actividad enzimática representa la oxidación de 1 µmol de alcohol veratrílico a vetraldehído (ε_{310} 9300 $M^{-1} \cdot cm^{-1}$) en 1 minuto a 23 ºC y pH 5.5, en presencia de 4 mM de H_2O_2. La velocidad de conversión de la enzima purificada sobre el alcohol veratrílico se estimó como 49 s^{-1} (con una constante K_m de Michaelis-Menten de 0.279 mM).

3.2 Sustratos

Las reacciones enzimáticas se llevaron a cabo utilizando como sustratos diversos compuestos alifáticos, incluyendo compuestos lineales (**Fig. 12**): **i)** ácidos grasos saturados tales como los ácidos láurico (dodecanoico, C_{12}), mirístico (tetradecanoico, C_{14}), palmítico (hexadecanoico, C_{16}), esteárico (octadecanoico, C_{18}) y araquídico (eicosanoico, C_{20}); **ii)** ácidos grasos insaturados tales como los ácidos *cis*-5-dodecenoico ($C_{12:1}$), miristoleico (*cis*-9-tetradecenoico, $C_{14:1}$), palmitoleico (*cis*-9-hexadecenoico, $C_{16:1}$), oleico (*cis*-9-octadecenoico, $C_{18:1}$), linoleico (*cis*,*cis*-9,12-octadecadienoico, $C_{18:2}$) y gondoico (*cis*-11-eicosenoico, $C_{20:1}$); **iii)** alcoholes grasos como el 1-tetradecanol y 1-hexadecanol; **iv)** alcanos como el dodecano, tetradecano, hexadecano y octadecano; **v)** alquenos como el 1-tetradeceno y *trans*-7-tetradeceno; **vi)** ésteres de ácidos grasos tales como miristato de metilo, octanoato de octilo, miristato de miristilo, monomiristina (glicerol-1-miristato), dimiristina (glicerol-1,2-dimiristato) y trimiristina; y compuestos cíclicos (**Fig. 13**): **i)** esteroles libres como el colesterol, campesterol, ergosterol, sitosterol y estigmasterol; **ii)** cetonas esteroidales como la 5α-colestan-3-ona, 4-colesten-3-ona, testosterona y colesta-3,5-dien-7-ona; **iii)** hidrocarburos esteroidales tales como el 5α-colestano, colesta-3,5-dieno y 5α-pregnano; **iv)** ésteres de esteroles como colesteril acetato, colesteril butirato y colesteril caprilato, y **v)** secosteroides como colecalciferol (vitamina D_3) y ergocalciferol (vitamina D_2). Todos los compuestos se obtuvieron de Sigma-Aldrich excepto el sitosterol que fue suministrado por Calbiochem.

3.3 Reacciones enzimáticas

Las reacciones enzimáticas de los diversos compuestos alifáticos lineales (0,1 mM de sustrato) y cíclicos (0,05 mM de sustrato) con las peroxigenasas fúngicas (1 U) se llevaron a cabo en tampón $NaH_2PO_4.H_2O$ 50 mM (pH 5,5 para *Mro*UPO o pH 7 para *Aae*UPO y r*Cci*UPO) en 5 mL de reacción en presencia de H_2O_2 (0,5 mM en las reacciones con r*Cci*UPO y 2,5 mM en las de *Aae*UPO y *Mro*UPO). En algunos casos y con la finalidad de aumentar la solubilidad de algunos compuestos en el medio de reacción, las reacciones se realizaron en presencia de acetona (20-60%). Se estudiaron distintos tiempos de reacción (30, 60 y 120 minutos) y temperatura (25 ºC y 40 ºC) según la solubilidad del sustrato y con una agitación de 170 rpm.

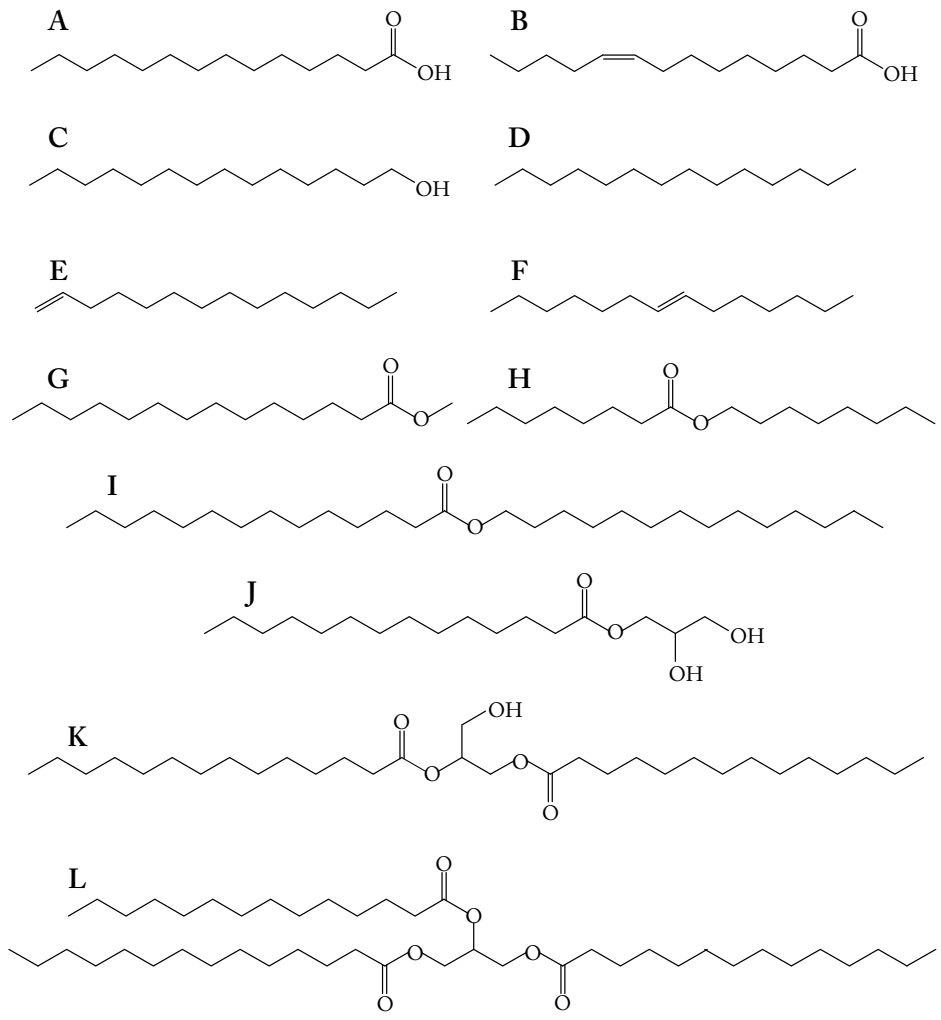

Fig. 12. Estructuras químicas representativas de los diferentes compuestos alifáticos lineales utilizados en las reacciones enzimáticas: **A**) ácidos grasos saturados (C_{12} a C_{20}), **B**) ácidos grasos insaturados (C_{12} a C_{20}), **C**) alcoholes grasos (C_{14} a C_{16}), **D**) alcanos (C_{12} a C_{18}), **E**) *cis*-1-tetradeceno, **F**) *trans*-7-tetradeceno, **G**) miristato de metilo, **H**) octanoato de octilo, **I**) miristato de miristilo, **J**) monomiristina, **K**) dimiristina, **L**) trimiristina.

Los experimentos control se llevaron a cabo bajo las mismas condiciones mencionadas anteriormente pero en ausencia de enzima. Las reacciones enzimáticas llevadas a cabo con $H_2{}^{18}O_2$ (90% de ^{18}O, Sigma-Aldrich) también se realizaron en las mismas condiciones descritas anteriormente.

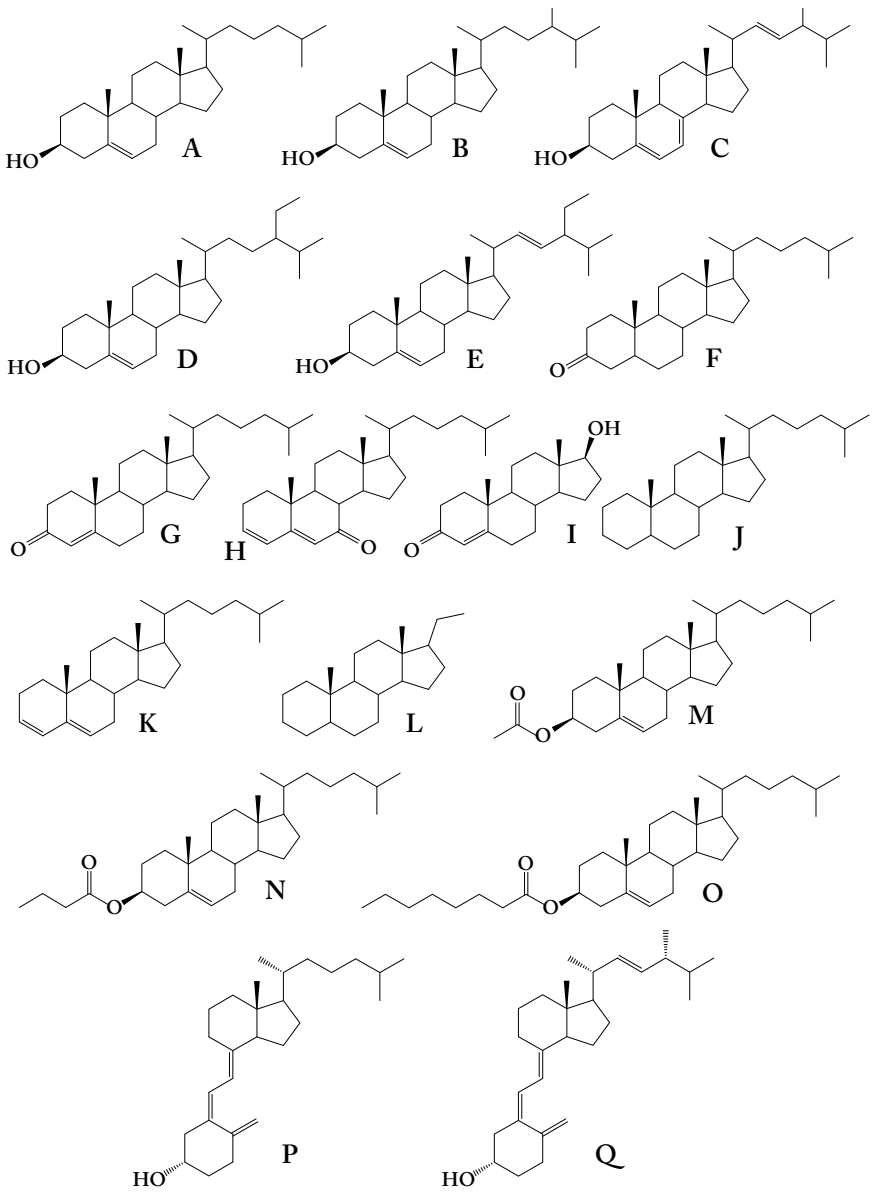

Fig. 13. Estructuras químicas de los diferentes compuestos alifáticos cíclicos utilizados en las reacciones enzimáticas: (**A**) colesterol, (**B**) campesterol, (**C**) ergosterol, (**D**) sitosterol, (**E**) estigmasterol, (**F**) colestan-3-ona, (**G**) 4-colesten-3-ona, (**H**) colesta-3,5-dien-7-ona, (**I**) testosterona, (**J**) colestano, (**K**) colesta-3,5-dieno, (**L**) pregnano, (**M**) colesteril acetato, (**N**) colesteril butirato, (**O**) colesteril caprilato, (**P**) colecalciferol y (**Q**) ergocalciferol.

3.4 Recuperación de los productos de reacción

Una vez finalizadas las reacciones enzimáticas, los productos se recuperaron mediante extracción líquido-líquido con metil *tert*-butil éter (MTBE) (Merck). Después de una agitación vigorosa, se separó la fase orgánica (fase superior) de la fase acuosa (fase inferior) en un matraz Erlenmeyer (**Fig. 14**). Con la fase acuosa resultante, se repitió dos veces más el mismo procedimiento de extracción. En la fase orgánica recuperada, que contiene el sustrato remanente y los productos formados, se agregó Na_2SO_4 anhidro (Panreac) con el objeto de eliminar restos de humedad en la muestra. Finalmente, el material previamente evaporado con N_2, se resuspendió en cloroformo para su posterior análisis mediante cromatografía de gases acoplada a espectrometría de masas (GC-MS). Para ello, las muestras se derivatizaron previamente utilizando Bis-(trimetilsilil)trifluoroacetamida (Supelco) en presencia de piridina (90 minutos, 80 ºC).

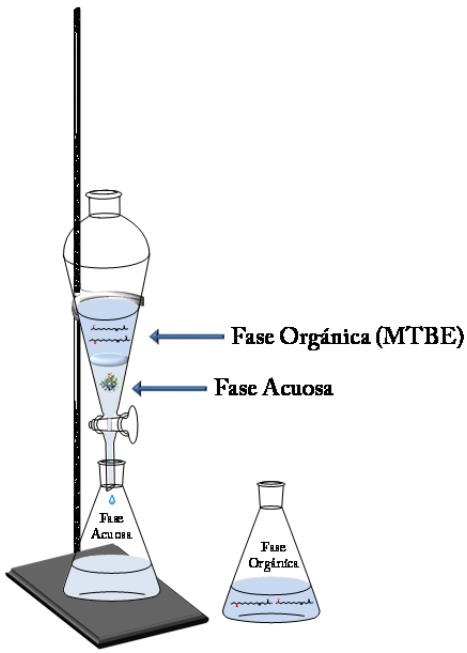

Fig. 14. Representación esquemática de la extracción líquido-líquido. Metil *tert*-butil éter (MTBE).

3.5 Análisis mediante GC-MS

Los análisis de los productos de la reacción mediante GC-MS se llevaron a cabo en un cromatógrafo Varian 3800 acoplado a un detector de trampa de iones (Varian 4000) utilizando una columna capilar de sílice fundida DB-5HT (12 m x 0.25 mm de diámetro interno, con un espesor de película de 0.1 μm) de J&W Scientific. También se utilizó un equipo de GC-MS Shimadzu QP2010 Ultra, con una columna capilar de sílice fundida DB-5HT (30 m x 0.25 mm de diámetro interno, con un espesor de película de 0.1 μm).

Se utilizaron distintos programas de temperatura para los distintos compuestos estudiados, como se describe a continuación:

3.5.1 Alcanos y alquenos

El programa de temperatura se inició de 50 ºC (2 min) a 80 ºC (6 min) a 30 ºC·min^{-1}, posteriormente a 250 ºC (2 min) a 8 ºC·min^{-1}. La temperatura del inyector se mantuvo a 250 ºC durante todo el análisis. La línea de transferencia se mantuvo a 300 ºC y el gas portador utilizado fue Helio (2 mL·min^{-1}).

3.5.2 Ácidos grasos y ésteres (≤ C_{14})

El programa de temperatura se inició desde 50 ºC a 90 ºC (2 min) a 30 ºC·min^{-1}, posteriormente a 250 ºC (2 min) a 8 ºC·min^{-1}. La temperatura del inyector se mantuvo a 250 ºC durante todo el análisis. La línea de transferencia se mantuvo a 300 ºC y el gas portador utilizado fue Helio (2 mL·min^{-1}).

3.5.3 Ácidos grasos y ésteres (≥C_{14}), esteroides y secosteroides

El programa de temperatura se inició de 120 ºC (1 min) a 300 ºC (15 min) a 10 ºC.min^{-1} (5 ºC. min^{-1} en el Shimadzu). El inyector se programó de 60 ºC (0.1 min) a 300 ºC (28 min) a 200 ºC·min^{-1}. La línea de transferencia se mantuvo a 300 ºC y el gas portador utilizado fue el Helio (2 mL·min^{-1}) en ambos equipos.

3.5.4 Identificación y cuantificación de los productos de reacción

Los compuestos se identificaron por espectrometría de masas comparando sus espectros de masas con los espectros existentes en las librerías Wiley y NIST y con estándares. La cuantificación se realizó a partir del área del pico total de iones, utilizando los factores de respuesta de los mismos compuestos o compuestos similares. Los perfiles cromatográficos de un solo ion se utilizaron para estimar la abundancia de un compuesto cuando dos picos se encontraban parcialmente solapados.

3.6 Análisis mediante Resonancia Magnética Nuclear (NMR)

La estructura química de algunos productos de reacción, como el 25-hidroxicolecalciferol y 25-hidroxiergocalciferol (obtenidos en las reacciones realizadas con la Vitamina D), se confirmó por espectroscopía de Resonancia Magnética Nuclear (NMR) monodimensional (^{1}H, ^{13}C) y bidimensional (HSQC). Para ello se utilizó un equipo Bruker Biospin AVANCE de 500 MHz acoplado a una criosonda 5 mm TCI, utilizando secuencias estándar de pulsos.

3.7 Análisis computacional (PELE)

Con el fin de comprender la interacción entre el centro activo de la enzima y los diferentes compuestos alifáticos se realizaron estudios computacionales utilizando el programa *Protein Energy Landscape Exploration* (PELE) en el Barcelona Supercomputing Center (grupo del Dr. Victor Guallar). En estos estudios se utilizaron como estructuras de partida para las simulaciones PELE la estructura cristalina de *Aae*UPO (PDB entry 2YOR) y un modelo homólogo para la estructura de r*Cci*UPO obtenida a partir de 2YOR. Además, se utilizaron como compuestos alifáticos ocho esteroides representativos (colesterol, sitosterol, colestan-3-ona, colesta-3,5-dien-7-ona, colestano, colesta-3,5-dieno, colesteril acetato y colesteril butirato) y dos secosteroides (colecalciferol y ergocalciferol). El criterio que se utilizó para las simulaciones fue el de reducir la distancia entre el átomo de oxígeno del Cpd I de la HTP y el centro de masa del ligando. A partir de los resultados obtenidos se calcularon las fracciones del ligando que entraron al centro activo de la enzima por el extremo C-25 y las fracciones que entraron por el extremo C-3.

4. Resultados Generales y Discusión

Agrocybe aegerita

4. RESULTADOS GENERALES Y DISCUSIÓN

4.1 Oxifuncionalización selectiva de compuestos alifáticos con peroxigenasas fúngicas

En la presente Tesis se ha estudiado la oxifuncionalización enzimática de diferentes compuestos alifáticos lineales (ácidos grasos, alcoholes grasos, y alcanos/alquenos), y cíclicos (esteroides y secosteroides), catalizadas por diferentes peroxigenasas fúngicas incluyendo las peroxigenasas salvajes de *A. aegerita* (*Aae*UPO) y *M. rotula* (*Mro*UPO) y la peroxigenasa recombinante de *C. cinerea* (r*Cci*UPO). Por otro lado, también se ha estudiado el mecanismo de las reacciones de oxifuncionalización enzimática (utilizando $H_2{}^{18}O_2$), y se han realizado estudios computacionales con el objeto de investigar diferentes aspectos de las relaciones estructura-función de las peroxigenasas. Los principales resultados obtenidos, así como la discusión de los mismos, se incluyen a continuación.

4.1.1 Reacciones de oxifuncionalización de compuestos alifáticos lineales

4.1.1.1 Ácidos grasos

Se estudiaron diferentes ácidos grasos saturados (C_{12} a C_{18}), como sustratos de *Aae*UPO y r*Cci*UPO. Ambas enzimas transforman estos sustratos, obteniéndose los mejores resultados con r*Cci*UPO (**Tabla 4**). Como productos de reacción se obtuvieron derivados monohidroxilados, preferentemente en las posiciones ω-1 y ω-2 (**Fig. 15**). Además de los derivados monohidroxilados, también se identificaron ceto-derivados en estas mismas posiciones. Por otro lado, los resultados mostraron que la distribución porcentual de los regioisómeros ω-1 y ω-2 obtenidos en las reacciones con r*Cci*UPO depende de la longitud de la cadena del ácido graso, mientras que con *Aae*UPO se mantiene la misma regioselectividad independientemente de la longitud de la cadena del ácido graso. La hidroxilación de ácidos grasos por el citocromo P450 en las posiciones ω, ω-1 y ω-2, se ha estudiado extensamente (Miura and Fulco, 1975; Narhi and Fulco, 1986; Muerhoff et al, 1989; Boddupalli et al., 1992; Truan et al., 1999; Johnston et al., 2011), observándose similitudes y diferencias con las reacciones de las peroxigenasas fúngicas estudiadas en la presente Tesis.

Tabla 4

Conversión de diferentes compuestos alifáticos lineales por las peroxigenasas de *C. cinerea* (r*Cci*UPO) y *A. aegerita* (*Aae*UPO) (% de sustrato transformado).

	Conversión de sustrato (%)	
Sustrato	**r*Cci*UPO**	***Aae*UPO**
Ácidos grasos		
Ácido láurico (C_{12})	45	25
Ácido mirístico (C_{14})	98	41
Ácido palmítico (C_{16})	93	40
Ácido esteárico (C_{18})	72	31
Ácido miristoleico ($C_{14:1}$)	53	43
Ácido oleico ($C_{18:1}$)	68	60
Ésteres de ácidos grasos		
Miristato de metilo	94	50
Miristato de miristilo	0	0
Octanoato de octilo	40	36
Monomiristina	47	18
Dimiristina	0	0
Trimiristina	0	0
Alcoholes grasos		
1-Tetradecanol	72	72
Alcanos y alquenos		
Tetradecano	52	24
1-Tetradeceno	1	0
trans-7-Tetradeceno	81	13

Estos estudios muestran que el citocromo P450 de *Bacillus megaterium* (P450BM3) es capaz de convertir los ácidos láurico, mirístico y palmítico en sus derivados monohidroxilados ω-1 y ω-2, pero a diferencia de *Aae*UPO y r*Cci*UPO, P450BM3 cataliza también la monohidroxilación en la posición ω-3 (Boddupalli et al., 1992).

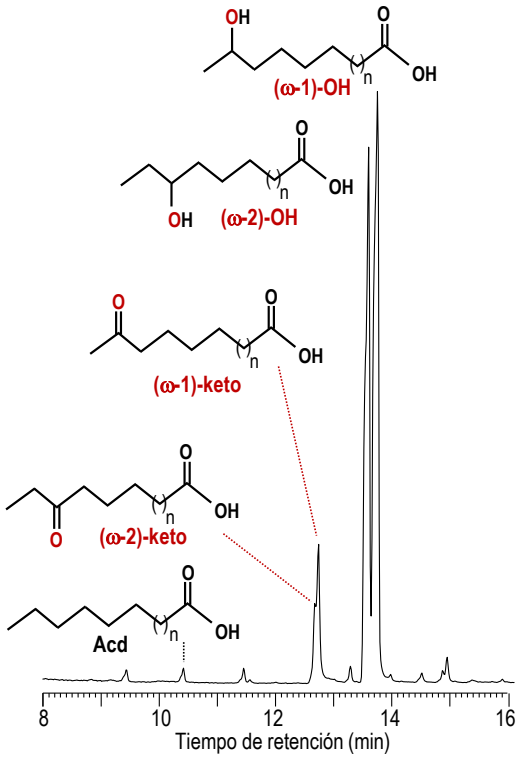

Fig. 15. GC-MS de la reacción de oxifuncionalización del ácido mirístico con r*Cci*UPO.

Además de las reacciones con ácidos grasos saturados, también se estudiaron las reacciones con ácidos grasos insaturados como los ácidos miristoleico y oleico con *Aae*UPO y r*Cci*UPO. Los resultados obtenidos con el ácido oleico mostraron un patrón similar al de los ácidos grasos saturados obteniéndose los derivados monohidroxilados en las posiciones ω-1 y ω-2. La conversión de este compuesto fue similar en las reacciones con las dos enzimas. Por otro lado, se observó una estricta regioselectividad con el ácido miristoleico por las dos peroxigenasas siendo éste monohidroxilado tan sólo en la posición ω-2 y no en la posición ω-1. Al igual que la oxifuncionalización selectiva observada para el ácido miristoleico en las reacciones catalizadas con las peroxigenasas fúngicas *Aae*UPO y r*Cci*UPO, los estudios realizados con P450BM3 utilizando el ácido araquidónico poliinsaturado como sustrato, mostraron que el 99% del producto obtenido correspondía a la hidroxilación en ω-2 (Capdevila et al., 1996) debido

a que la molécula del ácido araquidónico presenta requerimientos estéricos adicionales, resultando de este modo en una hidroxilación altamente selectiva por P450BM3.

Con el objetivo de saber si es necesario que el grupo carboxilo de los ácidos grasos esté libre para la actividad peroxigenasa, se estudiaron las reacciones de varios ésteres de ácidos grasos como miristato de metilo, miristato de miristilo, octanoato de octilo y mono-, di-, y trimiristina con *Aae*UPO y r*Cci*UPO. Los resultados mostraron que estas enzimas fueron capaces de catalizar la transformación, aunque en diferente medida, de algunos de estos ésteres en derivados monohidroxilados (**Tabla 4**). Al igual que el ácido mirístico, el miristato de metilo fue transformado casi por completo por r*Cci*UPO (en 30 minutos de reacción) dando como productos principales los derivados monohidroxilados en las posiciones ω-1 y ω-2, siendo esta última posición preferente. A pesar de que en las reacciones catalizadas con *Aae*UPO también se obtuvieron los mismos derivados monohidroxilados, el grado de conversión del miristato de metilo fue del 50%. En las reacciones del octanoato de octilo, se observaron como productos (después de 30 minutos de reacción) derivados monohidroxilados en las posiciones ω-1 y ω-2 en proporciones similares. Además se observó que estas peroxigenasas son capaces de hidroxilar este compuesto por ambos lados de la molécula, es decir, que los derivados monohidroxilados se forman tanto en las posiciones ω-1 y ω-2 de la cadena del ácido cómo en las posiciones ω-1 y ω-2 de la cadena alcohólica. En cuanto a los productos obtenidos en las reacciones enzimáticas utilizando la monomiristina como sustrato, se observó también la presencia de derivados monohidroxilados en las posiciones ω-1 y ω-2 siendo esta última posición preferente. En este sentido, se observó un mayor grado de conversión por r*Cci*UPO con respecto a *Aae*UPO (**Tabla 4**). Por el contrario, otros autores observaron que el citocromo P450BM3 es incapaz de hidroxilar ésteres metilados de ácidos grasos (Miura y Fulco, 1975). Al igual que P450BM3, las peroxigenasas r*Cci*UPO y *Aae*UPO no fueron capaces de catalizar la hidroxilación del miristato de miristilo y la di- y trimiristina.

4.1.1.2 Alcoholes grasos

Se estudió el 1-tetradecanol como sustrato de r*Cci*UPO y *Aae*UPO. Se observó que ambas enzimas fueron capaces de transformar en igual medida el

sustrato (**Tabla 4**), obteniéndose varios productos de reacción. Se identificó como producto principal el ácido mirístico. Además, se identificaron hidroxiderivados en las posiciones ω-1 y ω-2 del alcohol (1,13- y 1,12-tetradecanediol, respectivamente), junto con los ω-1 y ω-2 hidroxiácidos (ácidos 13- y 12-hidroximirístico, respectivamente) (**Fig 16**). A diferencia de los productos obtenidos en las reacciones de r*Cci*UPO y *Aae*UPO con el tetradecanol, en las reacciones con P450BM3 y 1-hexadecanol, los isómeros del hexadecanodiol fueron los únicos productos identificados, sin observarse la formación del ácido graso correspondiente (Miura and Fulco, 1975).

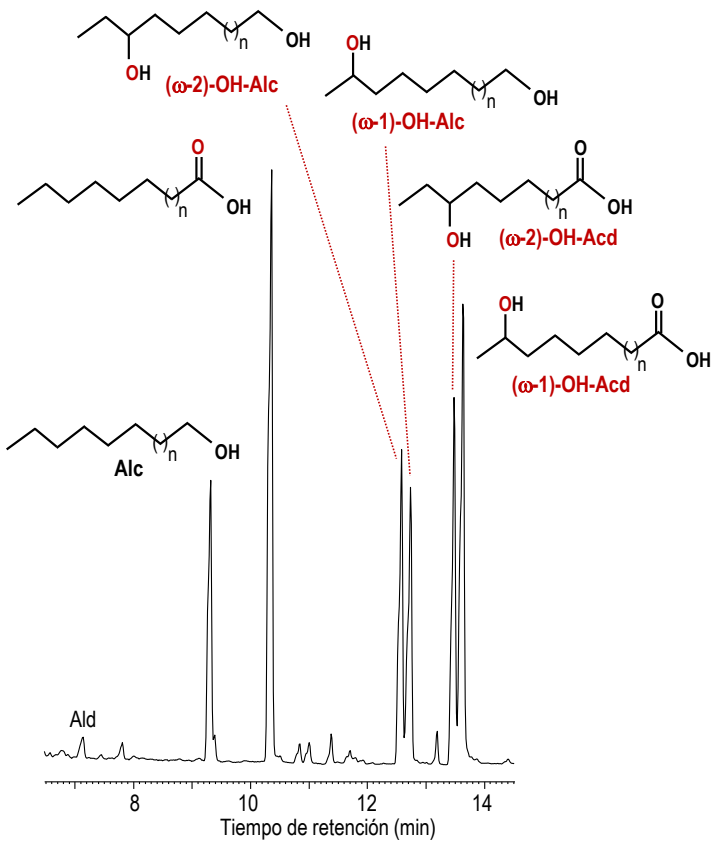

Fig. 16. GC-MS de la reacción de oxifuncionalización del tetradecanol con r*Cci*UPO.

4.1.1.3 Alcanos y alquenos

La oxifuncionalización selectiva de hidrocarburos sigue siendo uno de los grandes retos para la química orgánica contemporánea debido a que el enlace C-H de los alcanos lineales es notoriamente inerte y los catalizadores químicos necesarios para la oxifuncionalización de estos compuestos se caracterizan por ser muy reactivos y por tener bajos rendimientos y poca selectividad (Glieder et al., 2002; Peters et al., 2003; Peter et al., 2013). Además, la naturaleza altamente hidrofóbica de los alcanos hace que sean compuestos difíciles de solubilizar en condiciones acuosas convirtiéndolos en sustratos poco reactivos. En este sentido, la oxifuncionalización enzimática de diferentes hidrocarburos lineales tiene importancia industrial ya que puede ser empleada para la síntesis de una gran variedad de productos químicos.

En la presente Tesis se estudió la oxifuncionalización selectiva del tetradecano por las enzimas r*Cci*UPO y *Aae*UPO (**Tabla 4**). Como productos de reacción se identificaron varios compuestos, incluyendo derivados monohidroxilados en posiciones C-2 o C-3, derivados dihidroxilados en posiciones C-2 o C-3 en ambos extremos de la molécula (ej.: 2 ω-1/ω-2, o 3 y ω-1/ω-2) y varias combinaciones de ceto- e hidroxiderivados (**Fig 17**). Cabe señalar que la producción enzimática de derivados dihidroxilados (dioles), de gran interés industrial, ha dado lugar a la realización de una patente de invención (WO2013/004639 A2) incluida en la presente Tesis. Con el objeto de solventar los problemas de solubilidad de este sustrato, las reacciones enzimáticas se realizaron con tres concentraciones diferentes de acetona (20%, 40% y 60%). En las reacciones con un 20% de acetona se observó una conversión del 52% con r*Cci*UPO y del 24% con *Aae*UPO después de 30 minutos de reacción. En estas condiciones de reacción se observó una mayor cantidad de dihidroxi- y cetohidroxiderivados con respecto a los monohidroxiderivados, que se encontraron en muy pequeña cantidad. En un 40% de acetona se consiguió incrementar el grado de conversión después de 30 minutos de reacción desde el 52% al 64% con r*Cci*UPO y del 24% al 45% con *Aae*UPO. En estas condiciones de reacción se observaron mayoritariamente derivados monohidroxilados en las posiciones C-2 o C-3. Sin embargo, también se observó la formación de una gran cantidad de derivados dihidroxilados. Por el contrario, al aumentar la concentración de acetona a un 60% tan sólo se observó la formación de derivados monohidroxilados en las reacciones con r*Cci*UPO y *Aae*UPO. En este sentido, otros autores han obtenido resultados similares en reacciones de alcanos de

cadena corta con un 60% de acetona y *Aae*UPO (Peter et al., 2011). La capacidad de hidroxilar alcanos no se describió en el P450BM3 (Miura and Fulco, 1975) aunque se han obtenido variantes mediante mutagénesis dirigida capaces de hidroxilar alcanos de cadenas cortas y medianas (Glieder et al., 2002; Peters et al., 2012).

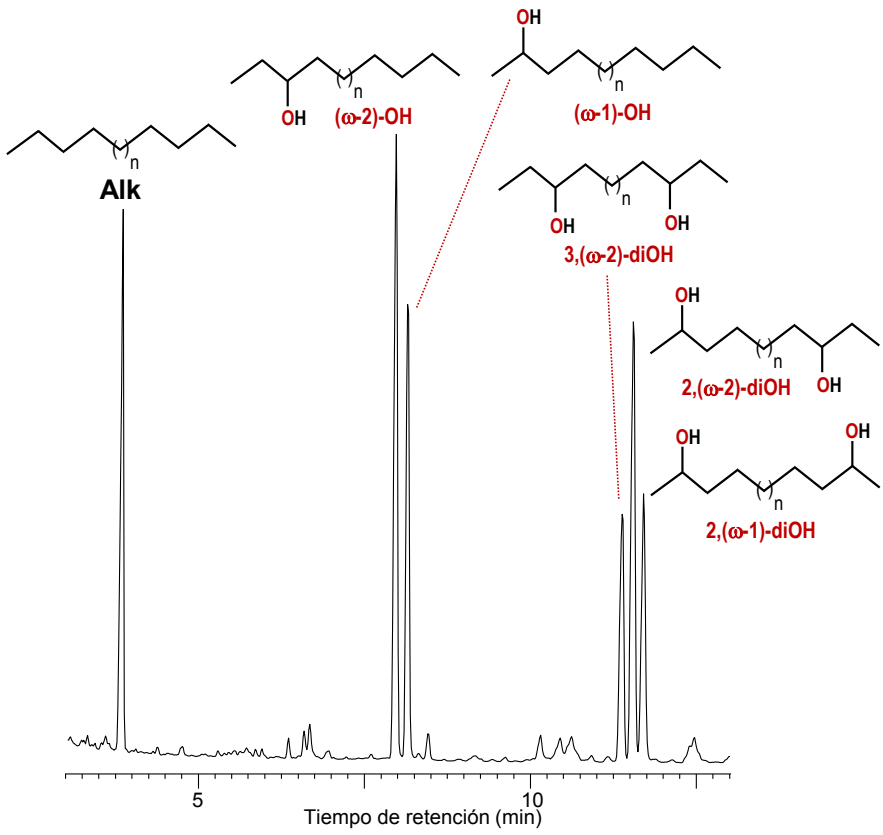

Fig. 17. GC-MS de la reacción de oxifuncionalización del tetradecano con r*Cci*UPO.

Además del tetradecano, se estudiaron dos alquenos (1-tetradeceno y *trans*-7-tetradeceno) (**Tabla 4**) y se observó que las peroxigenasas de *C. cinerea* y *A. aegerita* no fueron capaces de hidroxilar el 1-tetradeceno. Por el contrario, en la reacción con el *trans*-7-tetradeceno, se observó un alto grado de conversión con

r*Cci*UPO (81%) obteniéndose principalmente derivados monohidroxilados en las posiciones C-2 y C-3, y en menor grado derivados dihidroxilados. Por otro lado, con *Aae*UPO se observó tan sólo una conversión del 13% identificándose principalmente los derivados monohidroxilados en las posiciones C-2 y C-3. La falta de actividad de las peroxigenasas con alquenos terminales puede estar relacionada con la alquilación del grupo hemo por los 1-alquenos, que resulta en la inactivación de la enzima (Peter et al., 2013). En dicho estudio se midió la actividad residual de *Aae*UPO después de la conversión del 1-hexeno y *n*-hexano bajo las mismas condiciones. Mientras que en el último caso la actividad se mantuvo, la presencia de 1-hexeno provocó la pérdida completa de la actividad de la enzima.

4.1.2 Reacciones de oxifuncionalización de compuestos alifáticos cíclicos

4.1.2.1 Esteroides

Los esteroides son compuestos orgánicos derivados del núcleo del ciclopentanoperhidrofenantreno o esterano formando cuatro anillos fusionados, tres con seis átomos y uno con cinco. En los esteroides esta estructura básica se modifica por adición de diversos grupos funcionales, como carbonilos e hidroxilos o cadenas hidrocarbonadas (**Fig. 18a**). Los esteroides representan una clase importante de compuestos naturales que tienen una multitud de propiedades farmacológicas. La actividad fisiológica de estos compuestos depende de su estructura, el estado de oxidación de los anillos y del tipo, número y posición de los grupos funcionales presentes en la molécula (Donova and Egorova, 2012). En este sentido, pequeños cambios generados en la estructura molecular de los esteroides pueden afectar su actividad biológica, por lo que se han realizado innumerables estudios basados en la modificación estructural de los esteroides de origen natural con el objeto de encontrar nuevos compuestos con mayor actividad biológica (Beneventi et al., 2009). La hidroxilación es una de las modificaciones estructurales más importantes en la oxifuncionalización de los esteroides. En la presente Tesis se estudiaron reacciones de oxifuncionalización enzimática de varios esteroides incluyendo: (i) esteroles libres, (ii) cetonas esteroidales, (iii) hidrocarburos esteroidales y (iv) ésteres de esteroles, utilizando las peroxigenasas fúngicas r*Cci*UPO, *Aae*UPO y *Mro*UPO.

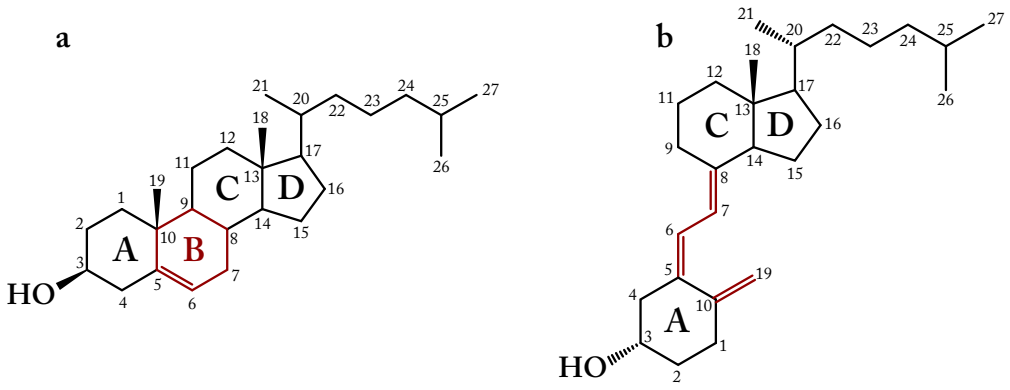

Fig. 18. Estructura química de un esteroide (colesterol) **a)** y un secosteroide (colecalciferol) **b)**.

(i) Esteroles libres

Se llevaron a cabo reacciones enzimáticas de cinco esteroles libres (colesterol, campesterol, ergosterol, sitosterol y estigmasterol), siendo el colesterol el sustrato con el que se obtuvo un mayor grado de conversión con respecto a los demás esteroles libres (**Tabla 5**). En este sentido, entre las enzimas estudiadas, r*Cci*UPO fue la única capaz de transformar por completo el colesterol (**Fig. 19**). En cuanto a los productos de reacción, se obtuvieron derivados monohidroxilados principalmente en la posición C-25 y, en algunos casos, aunque en menor proporción, en las posiciones C-24, C-26 (o C-27) y C-28. En el caso de r*Cci*UPO, se obtuvo el 25-hidroxicolesterol como único derivado monohidroxilado (**Tabla 5**).

Por otro lado, *Aae*UPO presentó una mayor actividad con el campesterol (47%), ergosterol (10%) y sitosterol (13%) frente a las otras dos enzimas. Finalmente, el estigmasterol fue transformado en mayor medida por *Mro*UPO (5%) (**Tabla 5**).

Tabla 5

Conversión de diferentes compuestos alifáticos cíclicos por las peroxigenasas de *C. cinerea*, *A. aegerita* y *M. rotula* (% de sustrato transformado).

	Conversión de sustrato (%)		
Sustrato	**r*Cci*UPO**	***Aae*UPO**	***Mro*UPO**
Esteroides			
Esteroles libres			
Colesterol	100	64	23
Campesterol	30	47	10
Ergosterol	6	10	7
Sitosterol	6	13	4
Estigmasterol	2	2	5
Cetonas esteroidales			
5-Colestan-3-ona	54	42	12
4-Colesten-3-ona	100	67	14
Colesta-3,5-dien-7-ona	97	57	39
Testosterona	0	0	0
Hidrocarburos esteroidales			
5-Colestano	14	3	1
Colesta-3,5-dieno	27	18	23
Pregnano	0	0	37
Ésteres de esteroles			
Colesteril acetato	34	16	5
Colesteril butirato	7	1	1
Colesteril caprilato	0	0	0
Secosteroides			
Colecalciferol (Vit. D_3)	100	90	---
Ergocalciferol (Vit. D_2)	90	81	---

La presencia de un grupo metilo o etilo en el C-24, no presente en el colesterol, parece dificultar la hidroxilación en el campesterol y sitosterol,

respectivamente. De igual forma, el doble enlace en el C-22, además del grupo metilo o etilo en el C-24 en el ergosterol y estigmasterol, respectivamente, parece ser el responsable de la baja conversión de estos compuestos por las tres peroxigenasas, en comparación con el colesterol.

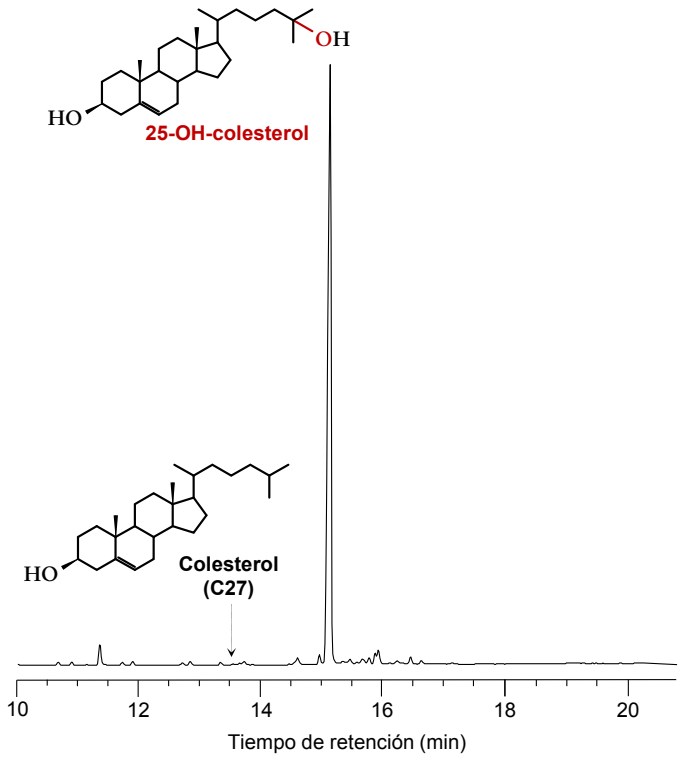

Fig. 19. GC-MS de la reacción de oxifuncionalización del colesterol con r*Cci*UPO.

(ii) Cetonas esteroidales

En las reacciones enzimáticas realizadas con las cetonas esteroidales (colestan-3-ona, 4-colesten-3-ona, colesta-3,5-dien-7-ona y testosterona), se observó que r*Cci*UPO fue la enzima más eficiente en transformar estos compuestos, a excepción de la testosterona que no fue modificada por ninguna

de las tres peroxigenasas estudiadas (**Tabla 5**). En cuanto a los productos obtenidos, se observó en todos los casos la hidroxilación preferente en la posición C-25 de la cadena lateral. Por otro lado, en las reacciones de la colesta-3,5-dien-7-ona como sustrato, se observó además que *Aae*UPO fue la única enzima capaz de monohidroxilar esta molécula también en la posición C-26 (o C-27) y que la hidroxilación en el anillo esteroidal fue catalizada por *Mro*UPO, y en menor medida por r*Cci*UPO y *Aae*UPO.

(iii) Hidrocarburos esteroidales

En las reacciones enzimáticas realizadas con los hidrocarburos esteroidales (colestano, colesta-3,5-dieno y pregnano), se observó que r*Cci*UPO fue la enzima más eficiente en transformar estos compuestos a excepción del pregnano que tan sólo fue modificado por *Mro*UPO (**Tabla 5**).

En cuanto a los productos obtenidos con el colesta-3,5-dieno como sustrato se observó que, además de los derivados monohidroxilados en la posición C-25 de la cadena lateral, r*Cci*UPO, *Aae*UPO y *Mro*UPO fueron capaces de hidroxilar este compuesto en el anillo esteroidal dando como productos derivados dihidroxilados (3α,4α-dihidroxicolest-5-eno; 3α,6α- y 3β,6β-dihidroxicolest-4-eno y x,25-dihidroxicolest-3,5-dieno) y trihidroxilados (3,6,25-trihidroxicolest-4-eno). Finalmente, el pregnano fue modificado tan sólo por *Mro*UPO dando lugar a la formación de varios isómeros monohidroxilados en el anillo esteroidal y un derivado oxidado, el 3-cetopregnano. La posición de los grupos hidroxilo no pudo ser determinada.

(iv) Ésteres de esteroles

Se estudiaron tres ésteres del colesterol (colesteril acetato, colesteril butirato y colesteril caprilato) como sustratos de las reacciones enzimáticas. Los mejores resultados se obtuvieron con r*Cci*UPO y el colesteril acetato (**Tabla 5**), siendo el 25-hidroxiderivado el único producto identificado. No se observó hidroxilación en el grupo acilo. Los resultados revelaron que la presencia de un grupo esterificado dificulta la conversión de sustrato, y que este efecto está directamente relacionado con el aumento de la longitud de la cadena de los ácidos grasos.

4.1.2.2 Secosteroides

Los secosteroides son terpenoides que pertenecen a una subclase de los esteroides, similares en estructura pero que se diferencian en que el anillo B está abierto (**Fig. 18b**). La vitamina D pertenece a un grupo de secosteroides liposolubes que son esenciales en la homeostasis del calcio y fosfato en mamíferos. La deficiencia de la vitamina D puede causar raquitismo en los niños, osteomalacia en adultos, aumentar el riesgo de fracturas óseas en personas mayores y aumentar el riesgo de cánceres, enfermedades cardiovasculares, inmunodeficiencia, y diabetes (Holick, 2007, Bikle, 2014). La vitamina D_3 (colecalciferol) se produce en la piel humana por irradiación de rayos UV provenientes de la luz del sol. Posteriormente, ésta es monohidroxilada en el hígado y dihidroxilada en los riñones dando lugar a la 25-hidroxivitamina D_3 (25-hidroxicolecalciferol) y a la 1α,25-dihidroxivitamina D_3 (1α,25-dihidroxicolecalciferol), respectivamente. La vitamina D_2 (ergocalciferol), sigue unos pasos de activación análogos a los de la vitamina D_3 para dar la 25-hidroxivitamina D_2 (25-hidroxiergocalciferol) y 1α,25-dihidroxivitamina D_2 (1α,25-dihidroxiergocalciferol). Se ha demostrado que los metabolitos 25-hidroxilados de la vitamina D, incluyendo 25-hidroxicolecalciferol (25-hidroxivitamina D_3) y 25-hidroxiergocalciferol (25-hidroxivitamina D_2), son considerablemente mejores agentes terapéuticos para diferentes enfermedades que la propia vitamina D, debido a su actividad biológica directa y su mejor absorción intestinal en algunos casos (Sitrin and Bengoa, 1987; Leichtmann et al., 1991; Jean et al., 2008).

El reconocimiento de que la administración de ambas formas de la 25-hidroxivitamina D exhibe varias ventajas frente a la vitamina D, ha generado un gran interés en la síntesis química de estos compuestos (Blunt and Deluca, 1969; Batcho et al., 1982; Kyler and Watt, 1983; Adrews et al., 1986; Manchand et al., 1995; Fritts and Waldroup, 2003). Sin embargo, estas reacciones requieren a menudo agentes oxidantes fuertes que incluyen varios pasos, son costosas, y tienen lugar con una baja regioselectividad en los pasos de hidroxilación. Además del interés fisiológico de la 25-hidroxivitamina D en la salud humana, este compuesto también es de interés para la alimentación de aves de corral y otros animales de granja (Fritts and Waldroup, 2003; Simoes-Nunes and Weber, 2004; Michalczuk et al., 2010; Käppeli et al., 2011; Hernández, 2013).

Con el objeto de sintetizar los hidroxiderivados de la vitamina D (vitamina D_3 y vitamina D_2), se estudiaron las reacciones enzimáticas de las peroxigenasas fúngicas *Aae*UPO y r*Cci*UPO con vitamina D y se observó que son capaces de catalizar la oxifuncionalización selectiva de estos secosteroides en los derivados monohidroxilados 25-hidroxivitamina D_3 y 25-hidroxivitamina D_2. En este sentido, se observó que el colecalciferol fue completamente transformado por r*Cci*UPO (100%) y en un 90% por *Aae*UPO. El grado de conversión del ergocalciferol fue similar para las peroxigenasas *Aae*UPO (81%) y r*Cci*UPO (85%) (**Tabla 5**). Por otro lado, la peroxigenasa r*Cci*UPO resultó ser altamente regioselectiva con el colecalciferol y el ergocalciferol observándose exclusivamente la formación del 25-hidroxicolecalciferol (**Fig. 20**) y el 25-hidroxiergocalciferol, respectivamente. En el caso de la peroxigenasa *Aae*UPO, se observó una alta regioselectividad para el ergocalciferol dando como único producto el 25-hidroxiergocalciferol, mientras que en el caso del colecalciferol, además del 25-hidroxiderivado, se observó en menor proporción el 24- y el 26/27-hidroxicolecalciferol.

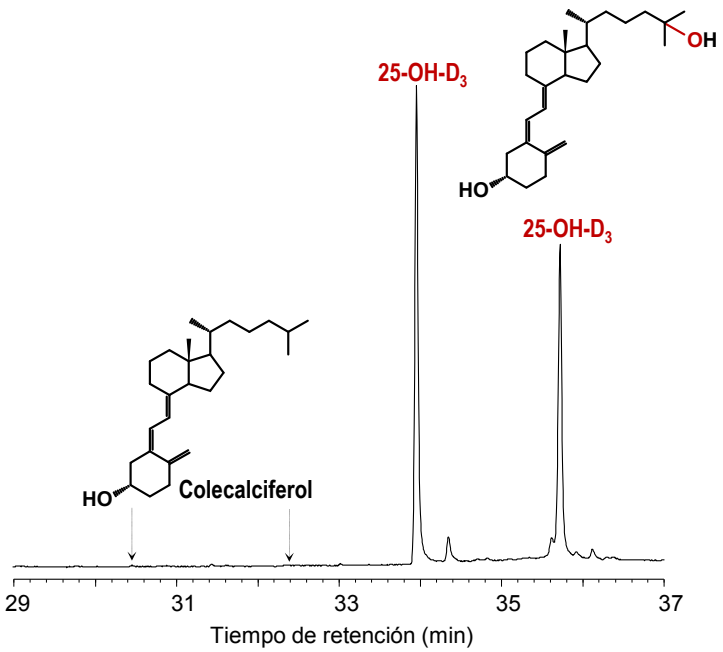

Fig. 20. GC-MS de la reacción de oxifuncionalización del colecalciferol con r*Cci*UPO.

4.2 Mecanismo de oxigenación/oxidación de los compuestos alifáticos con peroxigenasas

Con el fin de estudiar el origen del oxígeno incorporado durante la oxigenación de los diferentes compuestos alifáticos y demostrar la actividad peroxigenasa de estas enzimas, se estudiaron las reacciones enzimáticas de las peroxigenasas *Aae*UPO, *Mro*UPO y r*Cci*UPO en presencia de $H_2{}^{18}O_2$ como co-sustrato. En estos estudios se utilizaron como compuestos representativos el ácido mirístico y el tetradecanol. Las reacciones enzimáticas realizadas con $H_2{}^{18}O_2$ demostraron que el oxígeno introducido en la hidroxilación de los ácidos grasos en las posiciones ω-1 y ω-2 proviene del H_2O_2 y no del O_2, a diferencia de lo que ocurre en reacciones similares catalizadas por P450BM3 (Munro et al., 2002). Por otro lado, se observó que el oxígeno incorporado en el grupo carboxílico durante la oxidación del 1-tetradecanol a ácido mirístico, y sus derivados hidroxilados ω-1 y ω-2, también proviene del H_2O_2 (**Fig. 21**), demostrando así la actividad peroxigenasa de estas enzimas en estas reacciones.

En este sentido, el primer producto que se formaría en la oxidación del alcohol por las peroxigenasas sería un *gem*-diol debido a la hidroxilación del C-1 (**Fig. 21A**), el cual posteriormente podría ser por un lado directamente hidroxilado produciendo un *gem*-triol que se deshidrataría irreversiblemente dando el grupo ácido (**Fig. 21B**), o bien primero deshidratado en el aldehído correspondiente y posteriormente hidroxilado para dar el ácido (**Fig. 21C**).

4.3 Estudios computacionales

Con el objeto de investigar diferentes aspectos de las relaciones estructura-función de las peroxigenasas se realizaron estudios computacionales utilizando el programa *Protein Energy Landscape Exploration* (PELE).

En estos estudios la estructura de partida para las simulaciones PELE fue la estructura cristalográfica de *Aae*UPO (PDB entry 2YOR). Se utilizaron como compuestos alifáticos ocho esteroides y dos secosteroides. El criterio que se tuvo para las simulaciones fue el de reducir la distancia entre el átomo de oxígeno del Cpd I de la HTP y el centro de masa del ligando. A partir de los resultados se calcularon las fracciones del ligando que entraron al centro activo de la enzima por el extremo C-25 y las fracciones que entraron por el extremo C-3.

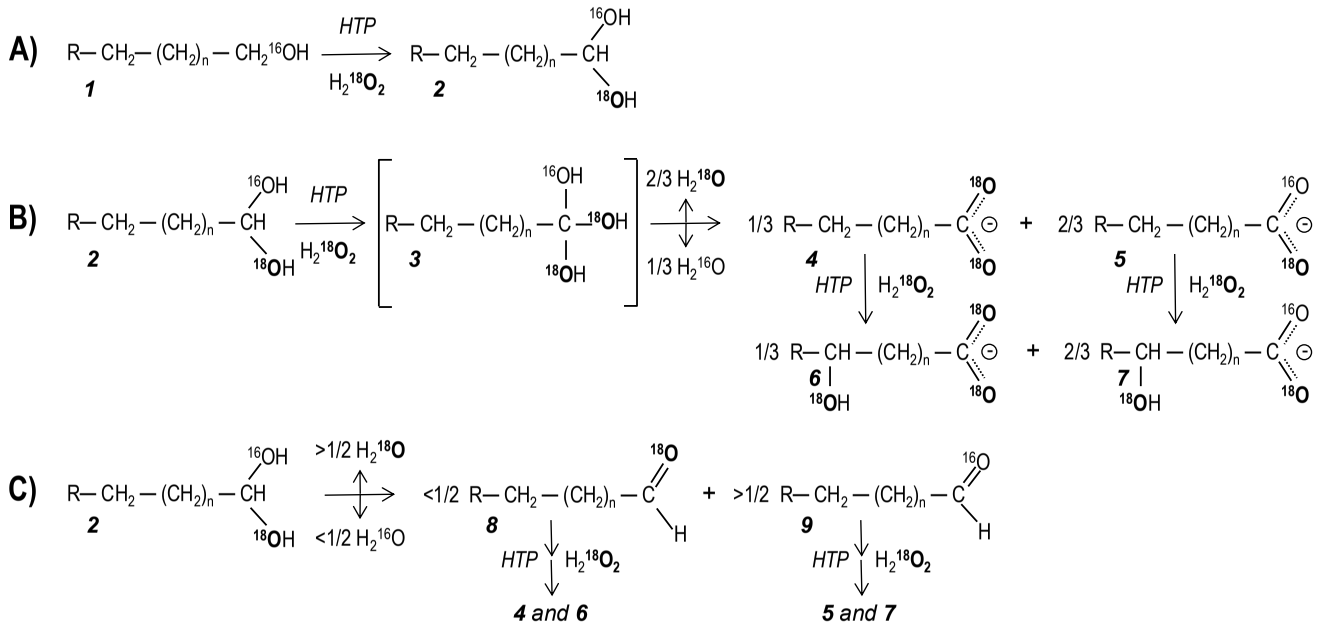

Fig. 21. Posible mecanismo de oxidación de alcoholes grasos, por la hemo-tiolato peroxidasa de *A. aegerita*, mediante el cual se producen los ácidos grasos correspondientes. Los estudios realizados con $H_2{}^{18}O_2$ incluyen: **A**) La hidroxilación del alcohol (***1***) a un *gem*-diol con ^{18}O marcado (***2***); **B**) La oxidación directa del *gem*-diol a un *gem*-triol intermedio (***3***) que por deshidratación irreversible produce ácidos grasos (***4*** y ***5***) con uno o dos ^{18}O marcados, que posteriormente son enzimáticamente hidroxilados (en la posición ω-1 en el esquema) produciendo los correspondientes hidroxiácidos (***6*** y ***7***); y **C**) La deshidratación del *gem*-diol produce el aldehido, con ^{18}O marcado (***8***) y ^{16}O no marcado (***9***), que puede experimentar un intercambio variable de hidroxilo con el solvente resultando en la reducción del ^{18}O marcado, antes de ser hidroxilado sucesivamente por la enzima produciendo los mismos ácidos grasos (***4*** y ***5***) e hidroxiácidos (***6*** y ***7***) que en el paso **B**.

Los resultados permitieron establecer una correlación directa entre el porcentaje de conversión del sustrato (**Tabla 5**) y el porcentaje de entrada del sustrato por C-25 (**Fig. 22**).

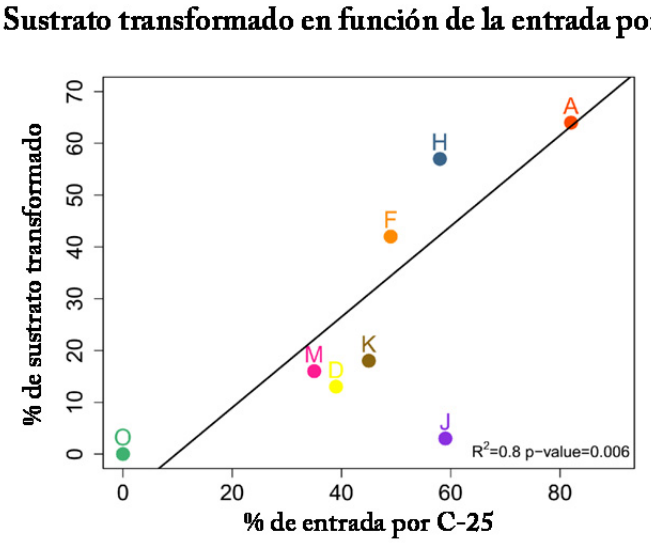

Fig. 22. Gráfica de correlación entre el porcentaje de conversión del sustrato y la entrada del sustrato por C-25 (cadena lateral) en el sitio activo de la enzima. **A**: colesterol, **D**: sitosterol, **F**: colestan-3-ona, **H**: colesta-3,5-dien-7-ona, **J**: colestano, **K**: colesta-3,5-dieno, **M**: colesteril acetato, **O**: colesteril caprilato.

4.3.1 Esteroides

Teniendo en cuenta los criterios mencionados anteriormente, se utilizaron como esteroides representativos el colesterol, sitosterol, colestan-3-ona, colesta-3,5-dien-7-ona, colestano, colesta-3,5-dieno, colesteril acetato y colesteril caprilato. De estos esteroides, el colesterol fue el compuesto de mejor trayectoria de entrada al sitio activo de la enzima por el C-25 (82 %) (**Fig. 22**), debido a que el canal de acceso al hemo hidrófobo de la peroxigenasa de *Aae*UPO favorece la entrada de este compuesto por el lado apolar de la molécula. Además, una vez que la molécula se encuentra posicionada en el sitio activo de la enzima, ésta se

estabiliza adicionalmente por un puente hidrógeno con un residuo de Glu245 en la superficie de la proteína (**Fig. 23a**). Por otro lado, el sitosterol tiene un grupo etilo adicional en C-24 que dificulta la entrada de este compuesto al sitio activo de la enzima (39 %) (**Fig. 22)**. A pesar de esto, la peroxigenasa es capaz de hidroxilar en el C-28 debido a la cercanía que hay entre el grupo hemo y este carbono secundario (**Fig. 23b**).

En cuanto a las cetonas esteroidales, la colesta-3-ona no es capaz de entrar al sitio activo de la enzima con la misma facilidad que el colesterol, en primer lugar debido a que la fracción de entrada por el lado C-25 es menor (del 82 % al 49 %) (**Fig. 22)**, y en segundo lugar debido a que la distancia entre el hidrógeno reactivo y el átomo de oxígeno en la colesta-3-ona es ligeramente más largo (2,5 Å en el colesterol y 2,8 Å en la colesta-3-ona). Por otro lado, la interacción del ligando en el sitio activo de la enzima es menor que el colesterol debido a que la colesta-3-ona es incapaz de formar puentes de hidrógeno con el residuo de Glu245. Sin embargo, en la colesta-3,5-dien-7-ona, al presentar una actividad similar al colesterol (**Tabla 5**), la entrada por el C-25 es menos reducida (58 %) que en la colesta-3-ona (**Fig. 22**) debido a la naturaleza apolar del anillo esteroidal en el lado externo (C-3).

Por otro lado, en el caso de los hidrocarburos esteroidales, el colestano presenta un aumento en la fracción de entrada por el anillo esteroidal debido a que carece del grupo OH polar en C-3 pero la pérdida de planaridad, debido a la presencia de enlaces saturados en C-5 y C-6 más voluminosos, impide que la molécula se sitúe adecuadamente en el sitio activo de la enzima cuando entra por C-25, lo cual explica la baja reactividad de este compuesto. Sin embargo, el colesta-3,5-dieno presenta una mayor reactividad debido a la presencia de dos dobles enlaces en C-3 y C-5, pero la falta de un grupo polar en C-3 conduce a una entrada menos favorable por C-25 (45 %) (**Fig. 22**).

Finalmente, en el caso de los ésteres de esteroles, la entrada del colesteril acetato por C-25 se ve menos favorecida que la del colesterol (82% para el colesterol y 35% para el colesteril acetato) (**Fig. 22**) debido a la presencia de un grupo éster en lugar de un grupo OH en el C-3 de la molécula (**Fig. 23c**). En este sentido, la cadena alquílica hidrofóbica más larga en el grupo éster del colesteril caprilato, genera una fuerte estructura de mínima energía que impide la correcta colocación de la molécula, por ambos extremos, en el sitio activo de la enzima.

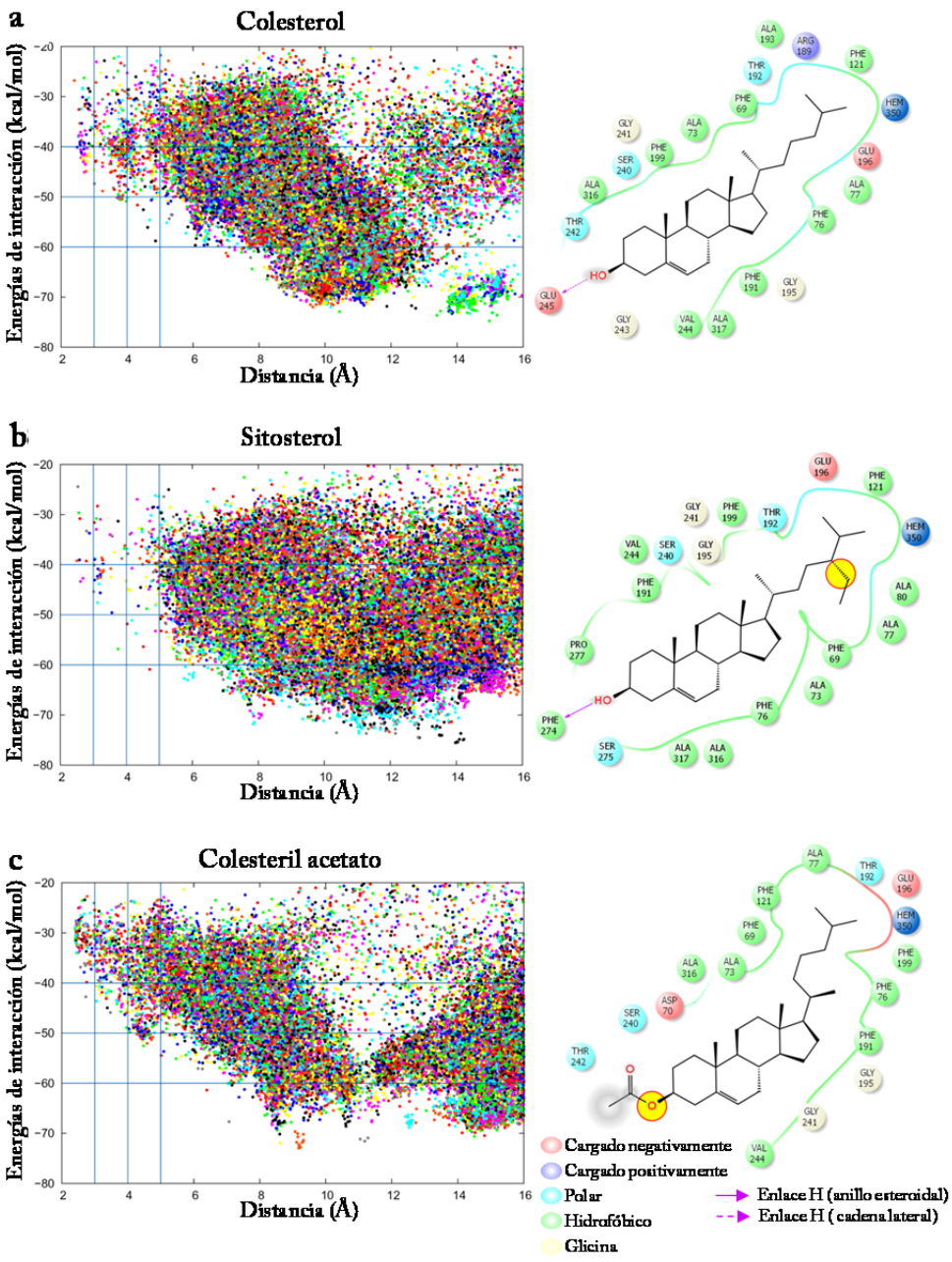

Fig. 23. Resultados de las simulaciones PELE para el colesterol (**a**), sitosterol (**b**) y colesteril acetato (**c**) en su entrada en el sitio activo de *Aae*UPO, incluyendo: (izquierda) gráficas del perfil de energía *vs* la distancia entre el H25 del esteroide y el átomo de oxígeno en el Cpd I de la enzima; y (derecha) las interacciones principales entre el sustrato y la enzima en una estructura representativa para cada uno de los tres esteroides analizados. Los círculos en amarillo señalan las diferencias estructurales con respecto al colesterol.

Los estudios computacionales realizados con los diferentes compuestos esteroidales nos permitieron establecer una correlación directa entre la tasa de conversión obtenida mediante las reacciones enzimáticas y la relación de entrada del sustrato en el sitio activo de la enzima.

4.3.2 Secosteroides

Para la realización de los estudios computacionales del colecalciferol y ergocalciferol, y así poder estudiar el acceso de estos compuestos por el canal de acceso al grupo hemo en *Aae*UPO y r*Cci*UPO, el cofactor hemo se modeló como Cpd I. En los estudios realizados se pudo observar que la entrada de los sustratos, en el caso de *Aae*UPO, es bastante favorable pero, una vez colocados en el canal de acceso al hemo se encuentran con un potencial creciente. En el caso de r*Cci*UPO, la entrada al canal de acceso al hemo es menos abierta por lo cual la entrada del sustrato en la proteína se encuentra más restringida.

Sin embargo, el perfil global de energía para el colecalciferol y ergocalciferol es más favorable en el caso de r*Cci*UPO (65 kcal mol^{-1} y -42 kcal mol^{-1}), que en *Aae*UPO (-40 kcal mol^{-1} y -30 kcal mol^{-1}), respectivamente. Estas diferencias en los perfiles de energía, indican que existe una interacción proteína-ligando más favorable para r*Cci*UPO, lo cual explica la mayor tasa de conversión observada. Por otro lado, para estudiar las diferentes selectividades obtenidas en las reacciones enzimáticas para el colecalciferol y el ergocalciferol con r*Cci*UPO y *Aae*UPO, se analizó la distribución de la distancia relativa entre los átomos de hidrogeno reactivos y los sustratos dentro del sitio activo, por lo cual se tuvieron en cuenta los hidrógenos en las posiciones C-24, C-25, C-26 y C-27 para ambos ligandos. En este sentido, el porcentaje de distancias O-H25 para el colecalciferol y ergocalciferol fue de 54,5% y 36,2% para r*Cci*UPO, y de 27,4% y 25,7% para *Aae*UPO, respectivamente. Así mismo, en las simulaciones realizadas para el colecalciferol con *Aae*UPO, se observó que el porcentaje de distancia O-H24 fue de 19,3%, bastante alta en comparación con los otros casos, lo cual explicaría la formación de productos hidroxilados en esta posición (**Fig. 24**).

Los estudios computacionales realizados con los diferentes secosteroides nos permitieron establecer una correlación directa entre la tasa de conversión obtenida mediante las reacciones enzimáticas y la relación de entrada del sustrato en el sitio activo de la enzima.

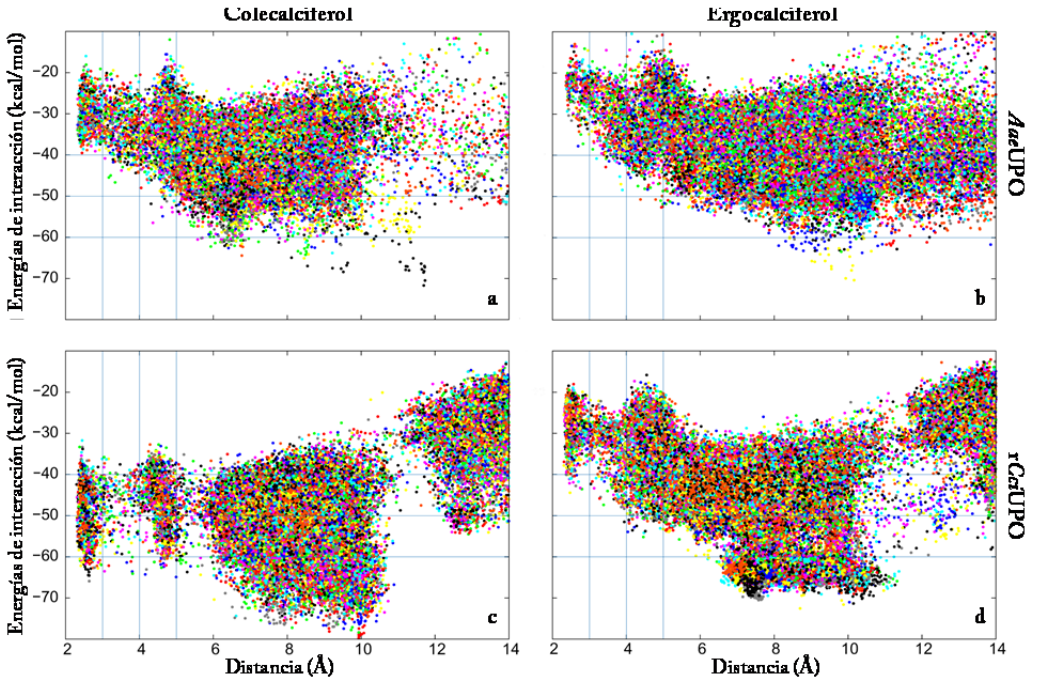

Fig. 24. Resultados de las simulaciones PELE para el colecalciferol (izquierda) y el ergocalciferol (derecha) en su entrada en el sitio activo de *Aae*UPO (**a**, **b**) y r*Cci*UPO (**c**, **d**) incluyendo gráficas del perfil de energía *vs* la distancia de entrada del ligando por el extremo C-25.

En resumen, las peroxigenasas fúngicas estudiadas son capaces de catalizar la oxifuncionalización enzimática de una gran variedad de compuestos alifáticos (ácidos grasos, alcanos, alcoholes, esteroides, secosteroides, etc.) en condiciones suaves y respetuosas con el medio ambiente, al igual que los P450s. En este sentido, ambas comparten un centro activo hemo-tiolato y un compuesto I Fe(IV)=O capaz de transferir un átomo de oxígeno al sustrato. Sin embargo, a diferencia de P450s que son enzimas intracelulares cuya activación requiere NAD(P)H como dador de electrones y una flavín-reductasa auxiliar para la transferencia del electrón al oxígeno (Li , 2001), las peroxigenasas fúngicas son proteínas extracelulares, mucho más estables, y sólo requieren H_2O_2 para su activación y consecuente transferencia de oxígeno al sustrato (Ullrich and Hofrichter, 2007). Debido a las características anteriormente mencionadas, estas

nuevas enzimas pueden ser consideradas como los biocatalizadores de elección para las oxigenaciones enzimáticas.

5. Referencias

Coprinopsis cinerea

5. REFERENCIAS

Andrews DR, Barton DHR, Hesse RH, Pechet MM. 1986. Synthesis of 25-hydroxy- and 1-alpha-25-dihydroxy vitamin D_3 from vitamin D_2 (calciferol). Journal of Organic Chemistry 51: 4819-4828.

Anh DH, Ullrich R, Benndorf D, Svatos A, Muck A, Hofrichter M. 2007. The coprophilous mushroom *Coprinus radians* secretes a haloperoxidase that catalyzes aromatic peroxygenation. Applied and Environmental Microbiology 73: 5477-5485.

Aranda E, Kinne M, Kluge M, Ullrich R, Hofrichter M. 2009. Conversion of dibenzothiophene by the mushrooms *Agrocybe aegerita* and *Coprinellus radians* and their extracellular peroxygenases. Applied Microbiology and Biotechnology 82: 1057-1066.

Batcho AD, Berger DE, Uskokovic MR. 1982. Process and intermediates for the synthesis of vitamin D3 metabolites. Patent (USA) 4310467.

Battistuzzi G, Bellei M, Bortolotti CA, Sola M. 2010. Redox properties of heme peroxidases. Archives of Biochemistry and Biophysics 500: 21-36.

Bauman DR, Bitmansour AD, McDonald JG, Thompson BM, Liang GS, Russell DW. 2009. 25-Hydroxycholesterol secreted by macrophages in response to Toll-like receptor activation suppresses immunoglobulin A production. Proceedings of the National Academy of Science, USA 106: 16764-16769.

Bernhardt R. 2006. Cytochromes P450 as versatile biocatalysts. Journal of Biotechnology 124: 128-145.

Björkhem I. 2013. Five decades with oxysterols. Biochimie, 95. A biologically active metabolite of vitamin D_3. Biochemistry 8: 6: 448-454.

Blunt JW, DeLuca HF. 1969. The synthesis of 25-hydroxycholecalciferol. Biochemistry 8(2): 671-675.

Boddupalli SS, Pramanik BC, Slaughter CA, Estabrook RW, Peterson JA. 1992. Fatty-acid monooxygenation by P450BM-3: Product identification and proposed mechanisms for the sequential hydroxylation reactions. Archives of Biochemistry and Biophysics 292: 20-28.

Bordeaux M, Galarneau A, Drone J. 2012. Catalytic, mild, and selective oxyfunctionalization of linear alkanes: current challenges. Angewandt Chemical International 51: 10712-10723.

Bormann S, Gomez Baraibar A, Ni Y, Holtmann D, Hollmann F. 2015. Specific oxyfunctionalization catalyzed by peroxygenases: opportunities, challenges and solutions. Catalysis Science & Technology 5: 2038-2052.

Brill E, Hannemann F, Zapp J, Brüning G, Jauch J, Bernhardt R. 2014. A new cytochrome P450 system from *Bacillus megaterium* DSM319 for the hydroxylation of 11-keto-β-boswellic acid (KBA). Applied Microbiology Biotechnology 98: 1703-1717.

Capdevila JH, Wei SZ, Helvig C, Falck JR, Belosludtsev Y, Truan G, Graham, Lorence SE, Peterson JA. 1996. The highly stereoselective oxidation of polyunsaturated fatty acids by cytochrome P450BM-3. Journal of Biological Chemistry 271: 22663-22671.

Cherry JR, Lamsa MH, Schneider P, Vind J, Svendsen A, Jones A, Pedersen AH. 1999. Directed evolution of a fungal peroxidase. Nature Biotechnology 17: 379-384.

Diczfalusy U. 2013. On the formation and possible biological role of 25-hydroxycholesterol. Biochimie 95:455-460.

Dolge C, Sass A, Kayser G, Ullrich R, Hofrichter M. 2011. Exploration of r*Cci*APO1 from *Coprinopsis cinerea*: First recombinant aromatic peroxygenase. BIOspektrum, special issue of Proc. VAAM (Association for

General and Applied Microbiology) Annual Conference (Karlsruhe, 3-6 April) 132-132.

Floudas D, Binder M, Riley R, Barry K, Blanchette RA, Henrissat B, Martínez AT, Otillar R, Spatafora JW, Yadav JS, Aerts A, Benoit I, Boyd A, Carlson A, Copeland A, Coutinho PM, de Vries RP, Ferreira P, Findley K, Foster B, Gaskell J, Glotzer D, Górecki P, Heitman J, Hesse C, Hori C, Igarashi K, Jurgens JA, Kallen N, Kersten P, Kohler A, Kües U, Kumar TKA, Kuo A, LaButti K, Larrondo LF, Lindquist E, Ling A, Lombard V, Lucas S, Lundell T, Martin R, McLaughlin DJ, Morgenstern I, Morin E, Murat C, Nolan M, Ohm RA, Patyshakuliyeva A, Rokas A, Ruiz-Dueñas FJ, Sabat G, Salamov A, Samejima M, Schmutz J, Slot JC, St John F, Stenlid J, Sun H, Sun S, Syed K, Tsang A, Wiebenga A, Young D, Pisabarro A, Eastwood DC, Martin F, Cullen D, Grigoriev IV, Hibbett DS. 2012. The Paleozoic origin of enzymatic lignin decomposition reconstructed from 31 fungal genomes. Science 336: 1715-1719.

Fritts CA, Waldroup PW. 2003. Effect of Source and Level of Vitamin D on live performance and bone development in growing broilers. Journal Applied Poultry Research 12: 45-52.

Fuchs C, Schwab W. 2013. Epoxidation, hydroxylation and aromatization is catalyzed by a peroxygenase from *Solanum lycopersicum*. Journal of Molecular Catalysis B: Enzymatic 96: 52- 60.

Glieder A, Farinas ET, Arnold FH. 2002. Laboratory evolution of a soluble, self-sufficient, highly active alkane hydroxylase. Nature Biotechnology 20: 1135-1139.

Gröbe G, Ullrich M, Pecyna M, Kapturska D, Friedrich S, Hofrichter M, Scheibner K. 2011. High-yield production of aromatic peroxygenase by the agaric fungus *Marasmius rotula*. Applied and Industrial Microbiology and Biotechnology Express 1: 31-42.

Hofrichter M, Kellner H, Pecyna MJ, Ullrich R. 2015. Fungal unspecific peroxygenases: hemo-thiolate proteins that combine peroxidase and cytochrome P450 properties. Advances in Experimental Medicine and Biology 851: 341-368.

Hofrichter M, Ullrich R. 2014. Oxidations catalyzed by fungal peroxygenases. Current Opinion in Chemical Biology 19: 116-125.

Hofrichter M, Ullrich R. 2010. New trends in fungal Biooxidation. The Mycota. Industrial applications 10: 425-449.

Hofrichter M, Ullrich R, Pecyna MJ, Liers C, Lundell T. 2010. New and classic families of secreted fungal heme peroxidase. Applied Microbiology and Biotechnology 87: 871-897.

Hofrichter M, Ullric R. 2006. Heme-thiolate haloperoxidases: versatile biocatalysts with biotechnological and environmental significance. Applied Microbiology and Biotechnology 71: 276-288.

Holtmann D, Fraaije MW, Arends IWCE, Opperman DJ, Hollmann F. 2014. The taming of oxygen: biocatalytic oxyfunctionalisations. Chemical Communications 50: 13180-13200.

Hollmann F, Arends I, Buehler K, Schallmey A, Büuhler B. 2011. Enzyme-mediated oxidations for the chemist. Green Chemistry 13: 226-265.

Hrycay EG, Bandiera SM. 2015. The monooxygenase, peroxidase, and peroxygenase properties and reaction mechanisms of cytochrome P450 enzymes. Advances in Experimental Medicine and Biology 851: 1-61.

Hrycay EG, Bandiera SM. 2012. The monooxygenase, peroxidase, and peroxygenase properties of cytochrome P450. Archives of Biochemistry and Biophysics 522: 71-89.

Hudlick T, Reed JW. 2009. Applications of biotransformations and biocatalysis to complexity generation in organic synthesis. Chemical Society Reviews 38: 3117-3132.

Ishimaru A. 1980. On the structure-function relationship of peroxidases and peroxygenase. Bioorganic Chemistry 9: 472-481.

Jean G, Terrat JC, Vanel T, Hurot JM, Lorriaux C, Mayor B, Chazot C. 2008. Daily oral 25-hydroxycholecalciferol supplementation for vitamin D deficiency in haemodialysis patients: effects on mineral metabolism and bone markers. Nephrol Dial Transplant 23: 3670-3676.

Johnston JB, Ouellet H, Podust LM, Ortiz de Montellano PR. 2011. Structural control of cytochrome P450-catalyzed ω-hydroxylation. Archives of Biochemistry and Biophysics 507: 86-94.

Karich A, Kluge M, Ullrich R, Hofrichter M. 2013. Benzene oxygenation and oxidation by the peroxygenase of *Agrocybe aegerita*. Applied and Industrial Microbiology and Biotechnology Express 3: 5.

Kellner H, Luis P, Pecyna MJ, Barbi F, Kapturska D, Krüger D, Zak DR, Marmeisse R, Vandenbol M, Hofrichter M. 2014. Widespread occurrence of expressed fungal secretory peroxidases in forest soils. PLoS ONE 9(4): e95557.

Kinne M, Poraj-Kobielska M, Ullrich R, Nousiainen P, Sipilä J, Scheibner K, Hammel KE, Hofrichter M. 2011. Oxidative cleavage of non-phenolic β-O-4 lignin model dimers by an extracellular aromatic peroxygenase. Holzforschung 65: 673-679.

Kinne M, Zeisig C, Ullrich R, Kayser G, Hammel KE, Hofrichter M. 2010. Stepwise oxygenations of toluene and 4-nitrotoluene by a fungal peroxygenase. Biochemical and Biophysical Research Communications 397: 18-21.

Kinne M, Poraj-Kobielska M, Ralph SA, Ullrich R, Hofrichter M, Hammel KE. 2009. Oxidative cleavage of diverse ethers by an extracellular fungal peroxygenase. The Journal of Biological Chemistry 284(43): 29343-29349.

Kinne M, Poraj-Kobielska M, Aranda E, Ullrich R, Hammel KE, Scheibner K, Hofrichter M. 2009. Regioselective preparation of 5-hydroxypropranolol and 4-hydroxydiclofenac with a fungal peroxygenase. Bioorganic & Medicinal Chemistry Letters 19: 3085-3087.

Kinne M, Ullrich R, Hammel KE, Scheibner K, Hofrichter M. 2008. Regioselective preparation of (R)-2-(4-hydroxyphenoxy) propionic acid with a fungal peroxygenase. Tetrahedron Letters 49: 5950-5953.

Kluge M, Ullrich R, Scheibner K, Hofrichter M. 2014. Formation of naphthalene hydrates in the enzymatic conversion of 1,2-dihydronaphthalene by two fungal peroxydases and subsequent naphthalene formation. Journal of Molecular Catalysis B: Enzymatic 103: 56-60.

Kluge M, Ullrich R, Scheibner K, Hofrichter M. 2012. Stereoselective benzylic hydroxylation of alkylbenzenes and epoxidation of styrene derivatives catalyzed by the peroxygenase of *Agrocybe aegerita*. Green Chemistry 14: 440-446.

Kluge M, Ullrich R, Dolge C, Scheibner K, Hofrichter M. 2009. Hydroxylation of naphthalene by aromatic peroxygenase from *Agrocybe aegerita* proceeds via oxygen transfer from H_2O_2 and intermediary epoxidation. Applied Microbiology and Biotechnology 81: 1071-1076.

Kluge MG, Ullrich R, Scheibner K, Hofrichter M. 2007. Spectrophotometric assay for detection of aromatic hydroxylation catalyzed by fungal haloperoxidase-peroxygenase. Applied Microbiology and Biotechnology 75: 1473-1478.

Krest CM, Onderko EL, Yosca TH, Calixto JC, Karp RF, Livada J, Rittle J, Green MT. 2013. Reactive intermediates in cytochrome P450 catalysis. The Journal of Biological Chemistry 288 (24): 17074-17081.

Kyler KS, Watt DS. 1983. Partial synthesis of (20R)-25-hydroxycholesterol involving a nickel (II)-promoted dienol rearrangement. Journal of the American Chemical Society, 105: 619-621.

Leichtmann GA, Bengoa JM, Bolt MJG, Sitrin MD. 1991. Intestinal absorption of cholecalciferol and 25-hydroxycholecalciferol in pathients with both Crohn's disease and intestinal resection. The American Journal of Clinical Nutrition, 54: 548-552.

Li H. 2001. Cytochrome P450, in: Messerschmidt A, Huber R, Poulos TL, Wieghardt K. (Eds.), Handbook of Metalloproteins. Wiley, Baffins Lane, UK, pp. 267-282

Li HY, Poulos TL. 1997. The structure of the cytochrome P450BM-3 haem domain complexed with the fatty acid substrate, palmitoleic acid. Nature Structural and Molecular Biology 4: 140-146.

Manchand PS, Yiannikouros GP, Belica PS, Madan P. 1995. Nickel-mediated conjugate addition. Elaboration of calcitriol from ergocalciferol. Journal of Organic Chemistry 60: 6574-6581.

Martínez AT, Ruiz-Dueñas FJ, Gutiérrez A, del Río JC, Alcalde M, Liers C, Ullrich R, Hofrichter M, Scheibner K, Kalum L, Vind J, Lund H. 2014. Search, engineering, and applications of new oxidative biocatalysts. Biofuels, Bioproducts and Biorefining 8: 819-835.

May SW. 1999. Applications of oxidoreductases. Current Opinion in Biotechnology 10: 370-375.

Miura Y, Fulco AJ. 1975. ω-1, ω-2 and ω-3 hydroxylation of long-chain fatty-acids, amides and alcohols by a soluble enzyme-system from *Bacillus*

megaterium. Biochimica et Biophysica Acta-Lipids and Lipid Metabolism 388: 305-317.

Morita Y, Yamashita H, Mikami B, Iwamoto H, Aibara S, Terada M, Minami J. 1988. Purification, crystallization, and characterization of peroxidase from *Coprinus cinereus*. Journal of Biochemistry (Tokyo) 103: 693-699.

Munro AW, Leys DG, McLean KJ, Marshall KR, Ost TWB, Daff S, Miles CS, Chapman SK, Lysek DA, Moser CC, Page CC, Dutton PL. 2002. P450BM3: the very model of a modern flavocytochrome. Trends in Biochemical Sciences 27: 250-257.

Narhi LO, Fulco A. 1986. Characterization of a catalytically self-sufficient 119,000-dalton cytochrome-P-450 monooxygenase induced by barbiturates in *Bacillus megaterium*. Journal of Biological Chemistry 261: 7160-7169.

Noble MA, Miles CS, Chapman SK, Lysek DA, Mackay AC, Reid GA, Hanzlik RP, Munro AW. 1999. Roles of key active-site residues in flavocytochrome P450-BM3. Biochemical Journal 339: 371-379.

Orellana M and Guajardo V. 2004. Cytochrome P450 activity and its alteration in different diseases. Revista Médica de Chile 132:85-94.

Ortiz de Montellano PR. Catalytic Mechanisms of Heme Peroxidases. Springer pp 79-107. In: E. Torres, M. Ayala (Eds.). 2010. Biocatalysts Based on Heme Peroxidases, Springer-Verlag Berlin Heidelberg.

Ortiz de Montellano PR. 2010. Hydrocarbon hydroxylation by cytochrome P450 enzymes. Chemical Reviews 110(2): 932-948.

Ortiz de Montellano PR. 2005. Cytochrome P450: Structure, Mechanism, and Biochemistry. Kluwer Academic/Plenum, New York.

Passardi F, Theiler G, Zamocky M, Cosio C, Rouhier N, Teixera F, Margis-Pinheiro M, Ioannidis V, Penel C, Falquet L, Dunand C. 2007. PeroxiBase: The peroxidase database. Phytochemistry 68: 1605-1611.

Pazmiño DET, Winkler M, Glieder A, Fraaije MW. 2010. Monooxygenases as biocatalysts: Classification, mechanistic aspects and biotechnological applications. Journal of Biotechnology 146: 9-24.

Pecyna MJ, Ullrich R, Bittner B, Clemens A, Scheibner K, Schubert R, Hofrichter M. 2009. Molecular characterization of aromatic peroxygenase from *Agrocybe aegerita*. Applied Microbiology and Biotechnology 84: 885-897.

Peng L, Wollenberger U, Kinne M, Hofrichter M, Ullrich R, Scheibner K, Fischer A, Scheller FW. 2010. Peroxygenase based sensor for aromatic compounds. Biosensors and Bioelectronics 26: 1432-1436.

Peng L, Wollenberger U, Hofrichter M, Ullrich R, Scheibner K, Scheller FW. 2010. Bioelectrocatalytic properties of *Agrocybe aegerita* peroxygenase. Electrochimica Acta 55: 7809-7813.

Peter S, Karich S, Ullrich R, Gröbe G, Scheibner K, Hofrichter M. 2014. Enzymatic one-pot conversion of cyclohexane into cyclohexanone: Comparison of four fungal peroxygenases. Journal of Molecular Catalysis B: Enzymatic 103: 47-51.

Peter S, Kinne M, Ullrich R, Kayser G, Hofrichter M. 2013. Epoxidation of linear, branched and cyclic alkenes catalyzed by unspecific peroxygenase. Enzyme and Microbial Technology 52: 370-376.

Peter S, Kinne M, Wang X, Ullrich R, Kayser G, Groves JT, Hofrichter M. 2011. Selective hydroxylation of alkanes by an extracellular fungal peroxygenase, FEBS Journal 278: 3667-3675.

Peters MW, Meinhold P, Glieder A, Arnold FH. 2003. Regio- and enantioselective alkane hydroxylation with engineered P450 BM-3. Journal of the American Chemical Society 125: 13442-13450.

Piontek K, Strittmatter E, Ullrich R, Gröbe G, Pecyna MJ, Kluge M, Scheibner K, Hofrichter M, Plattner DA. 2013. Structural basis of substrate conversion in a new aromatic peroxygenase: P450. Functionality with benefits. The Journal of Biological Chemistry 288: 34767-34776.

Piontek K, Ullrich R, Liers C, Diederichs K, Plattner DA, Hofrichter M. 2010. Crystallization of a 45 kDa peroxygenase/peroxidase from the mushroom *Agrocybe aegerita* and structure determination by SAD utilizing only the haem iron. Acta Crystallographyca 66: 693-698.

Pollard DJ, Woodley JM. 2006. Biocatalysis for pharmaceutical intermediates: the future is now. Trends in Biotechnology 25(2): 66-73.

Poraj-Kobielska M. 2013. Convertion of pharmaceuticals and other drugs by fungal peroxygenases. pp 115. PhD academic dissertation of Zittau-Dresden University (Zittau - Alemania).

Poraj-Kobielska M, Kinne M, Ullrich R, Scheibner K, Hofrichter M. 2012. A spectrophotometric assay for the detection of fungal peroxygenases. Analytical Biochemistry 421: 327-329.

Poraj-Kobielska M, Kinne M, Ullrich R, Scheibner K, Kayser G, Hammel KE, Hofrichter M. 2011. Preparation of human drug metabolites using fungal peroxygenases. Biochemical Pharmacology 82: 789-796.

Poulos TL. 2010. Thirty years of heme peroxidase structural biology. Archives of Biochemistry and Biophysics 500: 3-12.

Ruiz-Dueñas F.J, Martínez A.T. Structural and Functional Features of Peroxidases with a Potential as Industrial Biocatalysts. Springer pp. 37-59. In: E. Torres, M. Ayala (Eds.). 2010. Biocatalysts Based on Heme Peroxidases, Springer-Verlag Berlin Heidelberg.

Scheller U, Zimmer T, Becher D, Schauer F, Schunck WH. 1998. Oxygenation cascade in conversion of *n*-alkanes to α,ω-dioic acids catalyzed by

cytochrome P450 52A3. The Journal of Biological Chemistry 273(49): 32528-32534.

Shoji O, Watanabe Y. 2015. Monooxygenation of small hydrocarbons catalyzed by bacterial cytochrome P450s. Advances in Experimental Medicine and Biology 851: 189-208.

Shoji O, Watanabe Y. 2014. Peroxygenase reactions catalyzed by cytochromes P450. Journal of Biological Inorganic Chemistry 19: 529-539.

Sitrin MD and Bengoa JM. 1987. Intestinal absorption of cholecalciferol and 25-hydroxycholecalciferol in chronic cholestatic liver disease. The American Journal of Clinical Nutrition 46: 1011-1015.

Straathof AJJ, Panke S, Schmid A. 2002. The production of fine chemicals by biotransformations. Current Opinion in Biotechnology 13: 548-556.

Torres Pazmiño DE, Winkler M, Glieder A, Fraaije MW. 2010. Monooxygenases as biocatalysts: Classification, mechanistic aspects and biotechnological applications. Journal of Biotechnology 146: 9-24

Truan G, Komandla MR, Falck JR, Peterson JA. 1999. P450BM-3: Absolute configuration of the primary metabolites of palmitic acid. Archives of Biochemistry and Biophysics 366: 192-198.

Ullrich R, Hofrichter M. 2007. Enzymatic hydroxylation of aromatic compounds. Cellular and Molecular Life Sciences 64: 271-293.

Ullrich R, Hofrichter M. 2005. The haloperoxidase of the agaric fungus *Agrocybe aegerita* hydroxylates toluene and naphthalene. FEBS Letters 579: 6247-6250.

Ullrich R, Nuske J, Scheibner K, Spantzel J, Hofrichter M. 2004. Novel haloperoxidase from the agaric basidiomycete *Agrocybe aegerita* oxidizes aryl alcohols and aldehydes. Applied and Environmental Microbiology 70: 4575-4581.

Urlacher VB, Girhard M. 2012. Cytochrome P450 monooxygenases: an update on perspectives for synthetic application. Trends in Biotechnology 30(1): 26-36.

Vihma V, Tikkanen MJ. 2011. Fatty acid esters of steroids: Synthesis and metabolism in lipoproteins and adipose tissue. Journal of Steroid Biochemistry & Molecular Biology 124: 65-76.

Whitehouse CJC, Bell SG, Wong LL. 2012. P450BM3 (CYP102A1): connecting the dots. Chemical Society Reviews 41: 1218-1260.

Xu F. 2005. Applications of oxidoreductases: Recent progress. Industrial Biotechnology 1: 38-50.

Yarman A, Gröbe G, Neumann B, Kinne M, Gajovic-Eichelmann N, Wollenberger U, Hofrichter M, Ullrich R, Scheibner K, Scheller FW. 2012. The aromatic peroxygenase from *Marasmius rotula* - a new enzyme for biosensor applications. Analytical and Bioanalytical Chemistry 402: 405-412.

Yarman A, Peng L, Wu Y, Bandodkar A, Gajovic-Eichelmann N, Wollenberger U, Hofrichter M, Ullrich R, Scheibner K, Scheller FW. 2011. Can peroxygenase and microperoxidase substitute cytochrome P450 in biosensors. Bioanalytical Reviews 3: 67-94.

Zámocký M, Obinger C. Molecular Phylogeny of Heme Peroxidases. Springer pp. 7-35. In: E. Torres, M. Ayala (Eds.). 2010. Biocatalysts Based on Heme Peroxidases, Springer-Verlag Berlin Heidelberg.

6. Publicaciones

Marasmius rotula

6. PUBLICACIONES

Los principales resultados obtenidos durante la realización de esta Tesis han dado lugar a las siguientes publicaciones y patente:

6.1 Artículos científicos

I. Gutiérrez A., Babot E.D., Ullrich R., Hofrichter M., Martínez A.T., del Río J.C. (2011). Regioselective oxygenation of fatty acids, fatty alcohols and other aliphatic compounds by a basidiomycete hemo-thiolate peroxidase. *Archives of Biochemistry and Biophysics* 514: 33-43.

II. Babot E.D., del Río J.C., Kalum L., Martínez A.T. and Gutiérrez A. (2012). Oxyfunctionalization of aliphatic compounds by a recombinant peroxygenase from *Coprinopsis cinerea*. *Biotechnology and Bioengineering* 110(9): 2323-2332.

III. Babot E.D., del Río J.C., Cañellas M., Sancho F., Lucas F., Guallar V., Kalum L., Lund H., Gröbe G., Scheibner K., Ullrich R., Hofrichter M., Martínez A.T. and Gutiérrez A. (2015) Steroid hydroxylation by basidiomycete peroxygenases: A combined experimental and computational study. *Applied and Environmental Microbiology* 81:4130-4142.

IV. Babot E.D., del Río J.C., Kalum L., Martínez A.T. and Gutiérrez A. (2014). Regioselective hydroxylation in the production of 25-hydroxyvitamin D by *Coprinopsis cinerea* peroxygenase. *ChemCatChem* 7: 283-290.

V. Lucas F., Babot E.D., Cañellas M., del Río J.C., Kalum L., Ullrich R., Hofrichter M., Guallar V., Martínez A.T. and Gutiérrez A. (2016). Molecular determinants for selective C25-hydroxylation of vitamins D_2 and D_3 by fungal peroxygenases. *Catalysis Science & Technology*. 6: 288-295.

6.2 Patente

I. Lund H., Brask J., Kalum L., Gutiérrez Suárez A., Babot E. D., Ullrich R., Hofrichter M., Martínez Ferrer A. T., del Río Andrade J. C. (2013). Enzymatic preparations of diols. WO 2013/004639. PCT/EP2012/062763.

6.1. Publicación I:

Gutiérrez A., Babot E.D., Ullrich R., Hofrichter M., Martínez A.T., del Río J.C. (2011). Regioselective oxygenation of fatty acids, fatty alcohols and other aliphatic compounds by a basidiomycete hemo-thiolate peroxidase. *Archives of Biochemistry and Biophysics* 514: 33-43.

Regioselective oxygenation of fatty acids, fatty alcohols and other aliphatic compounds by a basidiomycete heme-thiolate peroxidase

Ana Gutiérrez[a*], Esteban D. Babot[a], René Ullrich[b], Martin Hofrichter[b], Angel T. Martínez[c], José C. del Río[a]

[a]Instituto de Recursos Naturales y Agrobiología de Sevilla, CSIC, PO Box 1052, E-41080 Seville, Spain

[b]Unit of Environmental Biotechnology, International Graduate School of Zittau, Markt 23, 02763 Zittau, Germany

[c]Centro de Investigaciones Biológicas, CSIC, Ramiro de Maeztu 9, E-28040 Madrid, Spain

* Corresponding author

Abstract:

Reaction of fatty acids, fatty alcohols, alkanes, sterols, sterol esters and triglycerides with the so-called aromatic peroxygenase from *Agrocybe aegerita* was investigated using GC-MS. Regioselective hydroxylation of C12-C20 saturated/unsaturated fatty acids was observed at the ω-1 and ω-2 positions (except myristoleic acid only forming the ω-2 derivative). Minor hydroxylation at ω and ω-3 to ω-5 positions was also observed. Further oxidized products were detected, including keto, dihydroxylated, keto-hydroxy and dicarboxylic fatty acids. Fatty alcohols also yielded hydroxy or keto derivatives of the corresponding fatty acid. Finally, alkanes gave, in addition to alcohols at positions 2 or 3, dihydroxylated derivatives at both sides of the molecule; and sterols showed side-chain hydroxylation. No derivatives were found for fatty acids esterified with sterols or forming triglycerides, but methyl esters were ω-1 or ω-2 hydroxylated. Reactions using $H_2{}^{18}O_2$ established that peroxide is the source of the oxygen introduced in aliphatic hydroxylations. These studies also indicated that oxidation of alcohols to carbonyl and carboxyl groups is produced by successive hydroxylations combined with one dehydration step. We conclude that the *A. aegerita* peroxygenase not only oxidizes aromatic compounds but also catalyzes the stepwise oxidation of aliphatic compounds by hydrogen peroxide, with different hydroxylated intermediates.

Keywords: Peroxidase/peroxygenase, Hydroxylation, Fatty acids, Fatty alcohols, Alkanes, Steroids

Introduction

Recently, a new peroxidase type was discovered in the wood-rotting basidiomycete *Agrocybe aegerita* (in order Agaricales, family Bolbitaceae), which turned out to be a true peroxygenase efficiently transferring oxygen from peroxide to various organic substrates including aromatic compounds, among others [1]. The enzyme was first reported as a haloperoxidase [2], related to the chloroperoxidase of *Leptoxyphium fumago* [3] being able to oxidize non-phenolic aromatic compounds. However, due to its unique ability to epoxidize and hydroxylate aromatic rings by means of hydrogen peroxide, and its low halogenase activity, the enzyme is nowadays mostly referred to as an aromatic peroxygenase [4].

This peroxidase/peroxygenase is able to catalyze reactions formerly assigned to intracellular cytochrome P450 monooxygenases (P450s) [5]. However, unlike P450s, which are intracellular enzymes whose activation requires NAD(P)H as electron donor and auxiliary flavin-reductases, or a second flavin domain, for electron transfer [6], the *A. aegerita* enzyme is a secreted protein, therefore far more stable, and only requires H_2O_2 for function [7]. This peroxidase/peroxygenase combines unique capabilities of P450s such as oxygen transfer, and classic properties of peroxidases such as oxidation of phenolic compounds, but its sequence exhibits no homology to classic peroxidases and P450s, and only little homology (~30%) to ascomycete chloroperoxidase [8]. However, this sequence includes the conserved cysteine residue acting as the fifth heme iron ligand in the two latter enzymes and is, therefore, classified as a heme-thiolate peroxidase [4,9].

The physiological function of *A. aegerita* peroxygenase remains unclear, but its extracellular location and the versatile reactions catalyzed - including peroxygenase, etherase and one-electron abstraction activities, among others - indicate that it could be involved in the unspecific oxidation and detoxification of plant ingredients (e.g., methoxylated phytoalexins) or microbial metabolites and also in the degradation of methoxylated compounds deriving from lignin and other aromatic plant sources [4]. In the latter context, it is interesting that the *A. aegerita* peroxygenase is able to oxidize non-phenolic veratryl alcohol, the

typical substrate of ligninolytic peroxidases, in a broad pH range, while lignin peroxidase and versatile peroxidase are able to oxidize this and related aromatic compounds only under very acidic conditions (around pH 3).

The *A. aegerita* peroxygenase has recently been shown to catalyze a high number of interesting oxidation reactions, including among others, the regioselective epoxidation/hydroxylation of naphthalene, the sulfoxidation of dibenzothiophene and thioanisole, the *N*-oxidation of pyridine, the *O*-dealkylation of alkyl-aryl ethers, the oxidation of aryl alcohols and aldehydes and the bromination of phenol [10-13]. Although its real biological function remains uncertain as mentioned above, the *A. aegerita* peroxygenase has an enormous biotechnological potential, since selective oxo-functionalizations are among the most challenging and desired reactions in organic synthesis and, compared with P450s, has the advantage of being a self-sufficient enzyme (i.e. catalyzing oxygenations without the help of intracellular enzymes providing electrons and reducing power) [7,14]. The authors of the current study demonstrate for the first time the action of the *A. aegerita* peroxygenase on fatty acids, fatty alcohols, alkanes and steroids, and provide information on the regioselectivity and oxidation mechanism (by detailed GC-MS analyses and ^{18}O-labeling) expanding the biotechnological interest of the enzyme by including the area of aliphatic hydroxylations and other oxygenation reactions.

Materials and methods

Enzyme preparation

The extracellular peroxygenase of *A. aegerita* (isoform II, 44 kDa) was produced and purified as described previously [2]. The enzyme preparation was homogeneous by sodium dodecylsulfate-polyacrylamide gel electrophoresis, an exhibited and A_{418}/A_{280} ratio of 1.75. Its specific activity was 117 units·mg^{-1}, where 1 unit represents the oxidation of 1 μmol of veratryl alcohol to veratraldehyde (ε_{310} 9300 M^{-1}·cm^{-1}) in 1 min at 23 ºC and pH 7, in the presence of 2.5 mM H_2O_2. The turnover rate of the purified enzyme on veratryl alcohol was estimated as 85 s^{-1} (with a Michaelis-Menten K_m constant ~2.4 mM).

Model substrates

Twenty-four model aliphatic substrates were used including: **i)** saturated fatty acids such as lauric (dodecanoic), myristic (tetradecanoic), palmitic (hexadecanoic), stearic (octadecanoic) and arachidic (eicosanoic) acids; **ii)** unsaturated fatty acids such as lauroleic (*cis*-9-dodecenoic), myristoleic (*cis*-9-tetradecenoic), palmitoleic (*cis*-9-hexadecenoic), oleic (*cis*-9-octadecenoic), linoleic (*cis*,*cis*-9,12-octadecadienoic) and gondoic (*cis*-11-eicosenoic) acids; **iii)** fatty alcohols such as 1-tetradecanol and 1-hexadecanol; **iv)** alkanes such dodecane, tetradecane, hexadecane and octadecane; **v)** free sterols such as cholesterol and sitosterol; **vi)** sterol esters such as cholesteryl butyrate, cholesteryl caprylate and cholesteryl linoleate; **vii)** the triglyceride trilaurin; and **viii)** the fatty-acid methyl ester methyl laurate. Sitosterol was purchased from Calbiochem, and all the other model substrates were obtained from Sigma-Aldrich.

Enzymatic reactions

Five mL reactions of the above model substrates (1 mM) with the *A. aegerita* peroxygenase (1 U) were performed in 50 mM sodium phosphate buffer (pH 7) at 25 ºC for 2 h, in the presence of 2.5 mM H_2O_2. The substrates were previously dissolved in acetone and added to the buffer (the acetone concentration in the reaction was 15%). In control experiments, substrates were treated under the same conditions (including 2.5 mM H_2O_2) but without enzyme. Enzymatic reactions with ^{18}O-labeled hydrogen peroxide ($H_2{}^{18}O_2$, 90% isotopic content) from Sigma-Aldrich (2% w:v solution) were also performed under the same conditions described above.

After the enzymatic reactions, water was immediately removed in a rotary evaporator, and the products recovered with chloroform, dried under N_2, and redissolved in chloroform for GC-MS analyses. Bis(trimethylsilyl)trifluoro-acetamide (Supelco) in the presence of pyridine was used to prepare trimethylsilyl derivatives.

GC-MS analyses

The GC-MS analyses were performed with a Varian 3800 chromatograph coupled to an ion-trap detector (Varian 4000) using a medium-length fused-

silica DB-5HT capillary column (12 m x 0.25 mm internal diameter, 0.1 μm film thickness) from J&W Scientific, enabling simultaneous elution of the different compound classes [15]. The oven was heated from 120 ºC (1 min) to 380 ºC at 10 ºC·min^{-1}, and held for 5 min. Other temperature program, from 50 ºC to 110 ºC (at 30 ºC·min^{-1}) and then to 320 ºC (at 6 ºC·min^{-1}), was used when necessary. In all GC-MS analyses, the transfer line was kept at 300 ºC, the injector was programmed from 120 ºC (0.1 min) to 380 ºC at 200 ºC·min^{-1} and held until the end of the analysis, and helium was used as carrier gas at a rate of 2 ml·min^{-1}.

Compounds were identified by mass fragmentography, and by comparing their mass spectra with those of the Wiley and NIST libraries and standards, and quantitation was obtained from total-ion peak area, using response factors of the same or similar compounds (those of the saturated substrates and derivatives being in general higher than those of the unsaturated ones). Single-ion chromatographic profiles (of base or other specific ions) were used to estimate compound abundances when two peaks partially overlapped. The relative abundance of products incorporating one to three $^{18}O_2$ atoms in the $H_2{}^{18}O_2$ reactions described above was estimated by peak integration using the corresponding ion with 2, 4 or 6 *m/z* increase (with correction from interfering ions in $H_2{}^{16}O_2$ spectra, when required).

Results

Twenty-four model aliphatic substrates, including a series of saturated and unsaturated fatty acids, one fatty-acid methyl ester, and several fatty alcohols, alkanes, free and esterified sterols and triglycerides were treated with the *A. aegerita* peroxygenase. All the fatty acids and fatty alcohols showed reactivity towards the enzyme. Among the alkanes, only those of shorter chain length were modified. The free sterols were only slightly modified, and the esterified sterols and triglycerides showed no reactivity. The conversion rate, and the reaction products formed were studied by GC-MS as described below.

Fatty-acid oxidation studies

Eleven fatty acids with even carbon number from C_{12} to C_{20} were tested as substrates of the *A. aegerita* peroxygenase (**Table 1**).

Table 1
Conversion of different types of aliphatic compounds by the *A. aegerita* peroxygenase (% of initial content)

Fatty acids	
Lauric acid (C_{12})	36
Lauroleic acid ($C_{12:1}$)	42
Myristic acid (C_{14})	26
Myristoleic acid ($C_{14:1}$)	44
Palmitic acid (C_{16})	24
Palmitoleic acid ($C_{16:1}$)	42
Estearic acid (C_{18})	9
Oleic acid ($C_{18:1}$)	29
Linoleic acid ($C_{18:2}$)	30
Arachidic acid (C_{20})	<5
Gondoic acid ($C_{20:1}$)	23
Fatty acid methyl ester	
Methyl laurate	56
Fatty alcohols	
1-Tetradecanol	41
1-Hexadecanol	15
Alkanes	
Dodecane	<5
Tetradecane	<5
Hexadecane	<5
Octadecane	0
Sterols	
Cholesterol	<5
Sitosterol	<5
Sterol esters	
Cholesteryl butyrate	0
Cholesteryl caprylate	0
Cholesteryl linoleate	0
Triglyceride	
Trilaurin	0

All of them showed reactivity towards the enzyme, although at different extents depending on the chain length, the order of activity as hydroxylation substrates being $C_{12} > C_{14} > C_{16} > C_{18} > C_{20}$.

Six unsaturated fatty acids with the same length as the saturated ones were also tested, all of them being more active than their saturated analogs. It should be mentioned that differences in solubility among the several substrates tested, related to chain length and presence of double bonds, could also influence substrate conversion.

For all the fatty acids, with the exception of myristoleic acid, the alkyl chains were monohydroxylated to give predominantly mixtures of the ω-1 and ω-2 isomers (**Fig. 1**). The position of the hydroxyl group was determined by the mass spectra of their trimethylsilyl derivatives, as illustrated in **Fig. 2** for (ω-1) and (ω-2)-hydroxymyristic acid. These spectra show prominent ions from α-cleavage of the molecular backbone on both sides of the trimethylsilyl group, with characteristic fragments at *m/z* 117 and $[M - CH_3]^+$ for the (ω-1)-hydroxyfatty acids (*m/z* 373 for 13-hydroxymyristic acid, **Fig. 2A**) and at *m/z* 131 and $[M - CH_3CH_2]^+$ for the (ω-2)-hydroxyfatty acids (*m/z* 359 for 12-hydroxymyristic acid, **Fig. 2B**). In all cases, no molecular ions were observed, although they could be readily determined from the fragment corresponding to the loss of a methyl from the trimethylsilyl group $[M - CH_3]^+$ (*m/z* 373 in both hydroxymyristic acid isomers, **Fig. 2**).

The formation of ω-1 and ω-2 derivatives decreased with increasing chain length especially in case of saturated fatty acids (**Fig. 1**). Surprisingly, myristoleic acid formed the ω-2 but not the ω-1 isomer (it was the only fatty acid assayed that did not formed this hydroxylated isomer). On the other hand, the ω-3 to ω-5 and especially the ω positions were also hydroxylated, although with extremely lower efficiency than the ω-1 and ω-2 positions (**Table 2**) being detected in trace amounts in most cases. Hydroxylation beyond the ω-5 position was never observed. Dicarboxylic acids were also detected indicating oxidation of the terminal methyl group, followed by oxidation of the primary alcohol formed to the corresponding acid group.

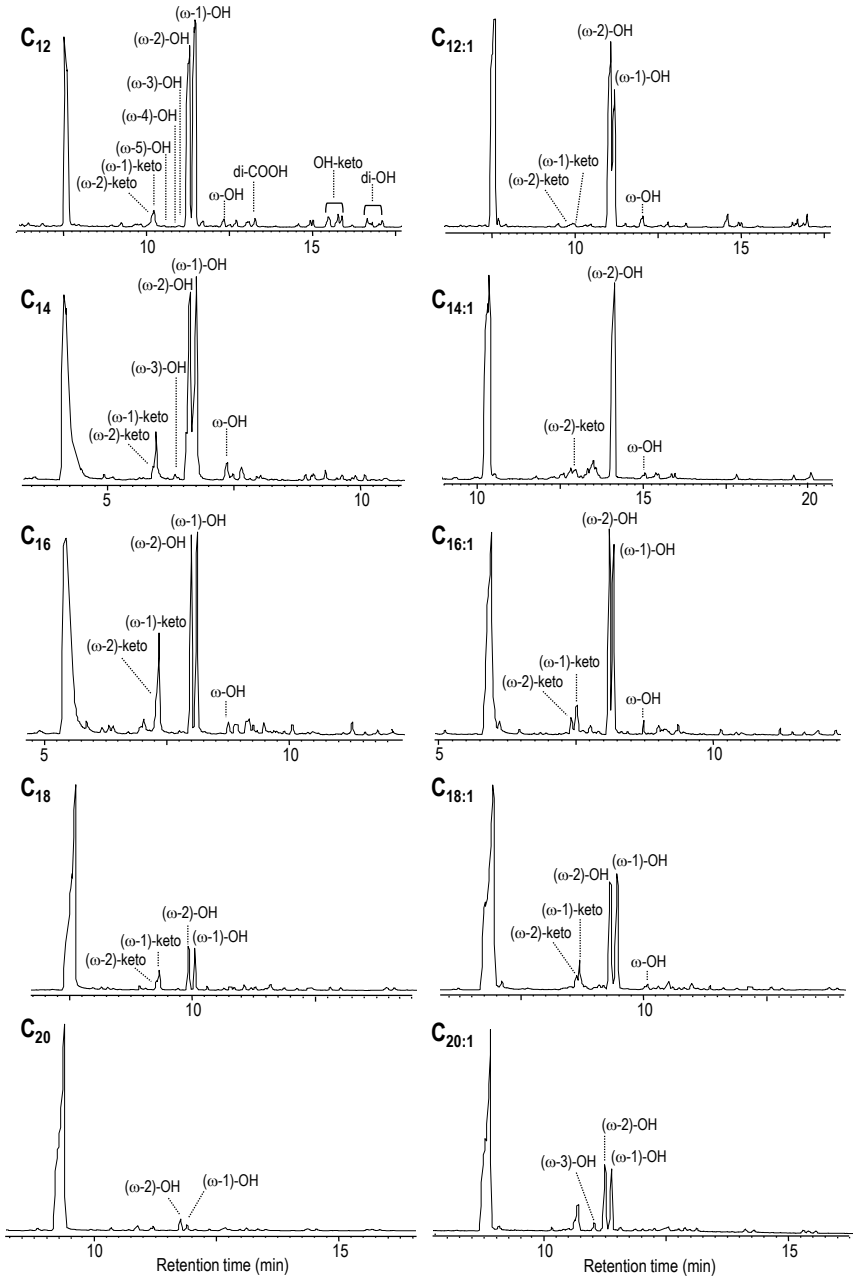

Fig. 1. GC-MS analysis of the peroxygenase reactions with saturated C_{12} to C_{20} (left) and mono-unsaturated $C_{12:1}$ to $C_{20:1}$ (right) fatty acids showing the remaining substrate, and the different ω-1 to ω-2 keto, ω to ω-5 hydroxyl, dicarboxylic, hydroxy-keto and dihydroxy derivatives (see SD, **Fig.S1** for chemical structures, and **Table 1** for quantitative values). The most adequate chromatographic program was used in each case.

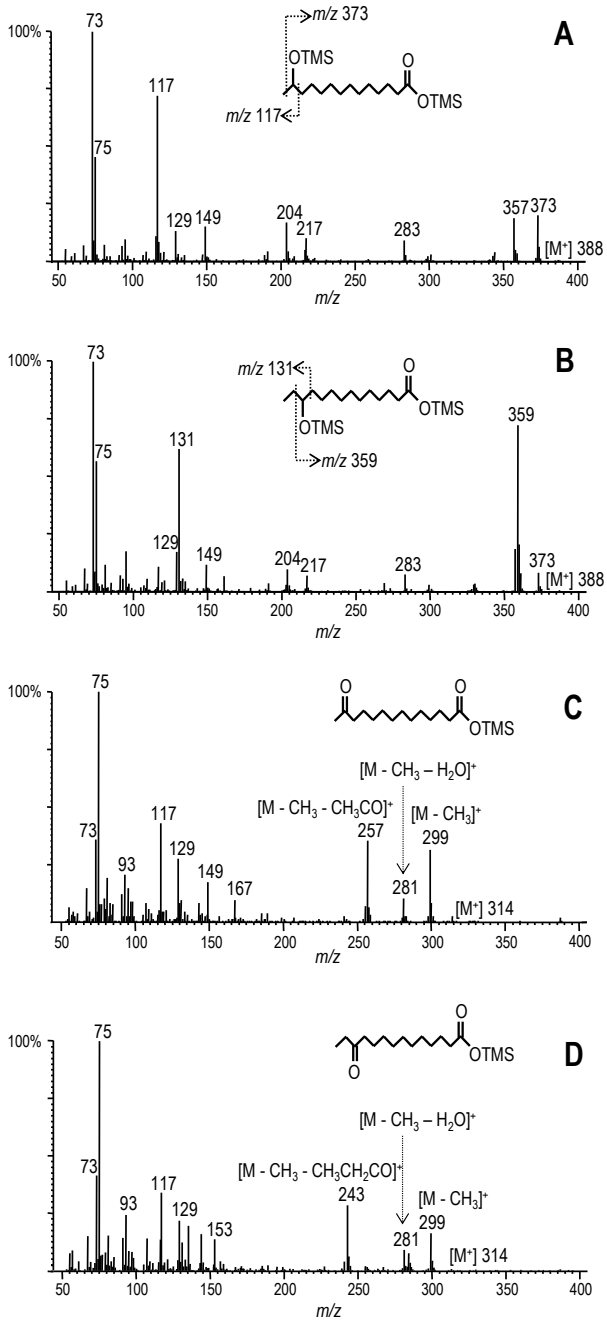

Fig. 2. Mass spectra of ω-1 (**A**) and ω-2 (**B**) monohydroxylated, and ω-1 (**C**) and ω-2 (**D**) keto derivatives of myristic acid (C_{14}) from peroxygenase reactions with myristic acid, as trimethylsilyl (TMS) derivatives.

Table 2

Abundance (relative percentage) of different monohydroxylated, keto, dihydroxylated, keto-hydroxy and dicarboxylic derivatives (at ω to ω-5) identified by GC-MS in the reactions of saturated and unsaturated fatty acids (from 12 to 20 carbons) with the peroxygenase (see **Fig. 1** for chromatographic profiles and SD, **Fig.S1** for chemical structures), and ω-1/ω-2 ratio of the main (monooxygenated) products formed.

	ω-OH	ω-1 OH	ω-2 OH	ω-3 OH	ω-4 OH	ω-5 OH	ω-1 keto	ω-2 keto	di-OH	OH-keto	di-COOH	ω-1/ω-2
C_{12}	1.3	39.7	32.0	0.2	<0.1	<0.1	5.8	1.0	4.4	15.5	0.3	1.4
$C_{12:1}$	3.3	37.4	59.2	0	0	0	<0.1	<0.1	0	0	0	0.6
C_{14}	3.5	34.4	30.5	0.3	0	0	20.8	3.3	0.5	6.2	0.6	1.6
$C_{14:1}$	1.8	0	94.6	0	0	0	0	3.6	0	0	0	0
C_{16}	1.4	23.6	23.6	0.3	0	0	34.5	16.3	0	0	0.3	1.5
$C_{16:1}$	2.5	35.7	47.0	0.1	0	0	10.4	4.4	0	0	0	0.9
C_{18}	<0.1	22.7	27.0	0.1	0	0	32.8	17.0	0	0	0.5	1.3
$C_{18:1}$	1.6	40.8	39.0	0.2	0	0	13.0	5.3	0	0	0	1.2
$C_{18:2}$	1.0	50.2	33.5	2.5	0	0	10.0	2.9	0	0	0	1.7
C_{20}	<0.1	16.0	28.1	0	0	0	38.7	17.3	0	0	0	1.2
$C_{20:1}$	1.2	35.0	38.7	0.4	0	0	18.8	6.0	0	0	0	1.2

An ^{18}O-labeling study, using myristic acid as substrate, and either $H_2{}^{18}O_2$ or $H_2{}^{16}O_2$ as enzyme cosubstrate, was performed to investigate the origin of the oxygen incorporated during the oxygenation of fatty acids. In the reaction using $H_2{}^{18}O_2$, mass spectral analysis of the resulting monohydroxylated fatty acids showed that characteristic fragments for the (ω-1)-hydroxyfatty acid had ~90% shifted from the natural abundance *m/z* 117 and *m/z* 373 found in the unlabeled peroxide reaction (**Fig. 2A**) to *m/z* 119 and *m/z* 375 (**Fig. 3A**), respectively. Likewise, the characteristic fragments for the (ω-2)-hydroxyfatty acid shifted from the natural abundance *m/z* 131 and *m/z* 359 found in the unlabeled peroxide reaction (**Fig. 2B**) to *m/z* 133 and *m/z* 361 (**Fig. 3B**), respectively. In both hydroxyfatty acids, ~10% of the original fragments remained in the $H_2{}^{18}O_2$ reactions due to the 90% ^{18}O isotopic purity of the labeled peroxide used.

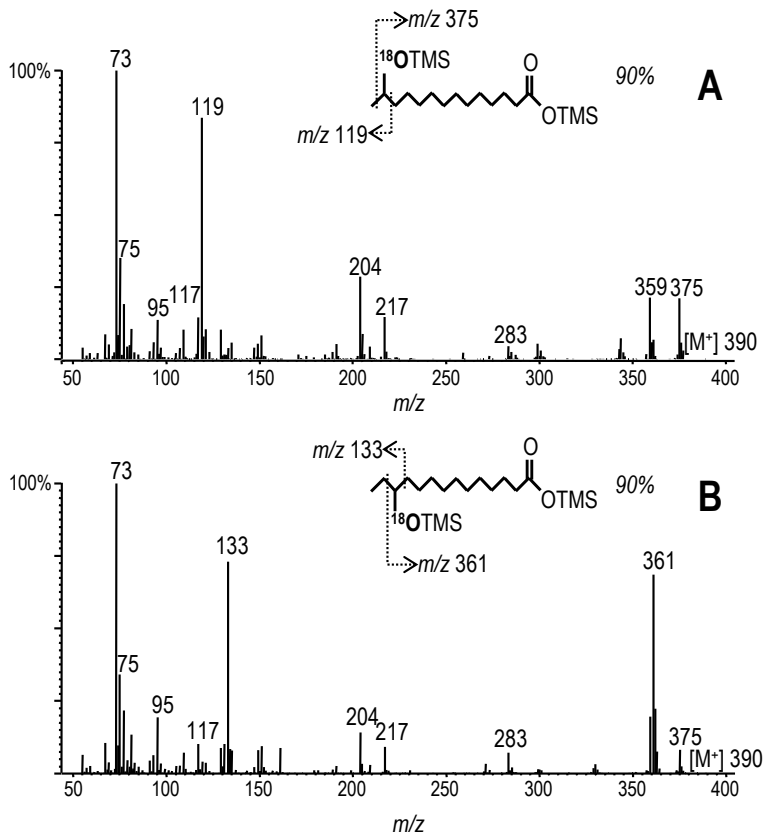

Fig. 3. Mass spectra of ω-1 (**A**) and ω-2 (**B**) ^{18}O-labeled monohydroxylated myristic acid (C_{14}) from peroxygenase reactions with myristic acid in the presence of $H_2{}^{18}O_2$ (90% isotopic purity) as trimethylsilyl (TMS) derivatives.

In addition to hydroxylated derivatives, keto derivatives at positions ω-1 and ω-2 were also identified (**Fig. 1**). The position of the carbonyl group was determined by the mass spectra of the trimethylsilyl derivatives, as shown in **Figs. 2C** and **2D** for (ω-1) and (ω-2)-ketomyristic acid, respectively. No molecular ions were observed in the mass spectra, although they could be determined from the $[M - CH_3]^+$ fragment (*m/z* 299 in both ketomyristic acids). Additional losses of the methylketo $[M - CH_3 - CH_3CO]^+$ or ethylketo $[M - CH_3 - CH_3CH_2CO]^+$ groups from α-cleavage of the carbonyl group in (ω-1) and (ω-2)-ketofatty acids, respectively, produced other diagnostic fragments (at

m/z 257 for 13-ketomyristic acid, and *m/z* 243 for 12-ketomyristic acid). Another characteristic fragments resulted from the loss of a water molecule [M - CH_3 -H_2O]$^+$ (at *m/z* 281 in both ketomyristic acid isomers). The ratio between the two main isomers (ω-1/ω-2) among the total monooxygenated derivatives (hydroxy and ketofatty acids) for the different compounds assayed is shown in **Table 2**. This ratio was very similar for all the saturated fatty acids (from 1.2 to 1.6). Unsaturated fatty acids often showed lower ratios (ranging from 0.6 to 1.2) with the exception of linoleic acid (1.7 ratio), and myristoleic acid that only formed the ω-2 derivative.

In the enzyme-catalyzed reaction of myristic acid with $H_2{}^{18}O_2$, mass spectral analysis of the (ω-1) and (ω-2)-ketofatty acids formed (together with the same hydroxyfatty acids) showed that the above mentioned [M - CH_3]$^+$ fragment (shared by both keto isomers) had ~10% shifted from the natural abundance *m/z* 299 found in the unlabeled peroxide reaction (**Fig. 2**) to *m/z* 301 (spectrum not shown). This ^{18}O-labeling is much lower than the 90% observed during formation of the corresponding hydroxyfatty acids, and revealed ^{18}O loss from the carbonyl formed, due to hydroxyl exchange with water.

Further oxygenation/oxidation of the above mono-substituted hydroxy and keto derivatives were observed in the enzymatic reactions with fatty acids, including dihydroxylated compounds and several combinations of keto and hydroxy derivatives. The chemical structures of all the fatty-acid derivatives identified in the different enzymatic reactions performed are shown in Supplementary data. SD. **Fig. S1**.

With the aim of investigating whether it was necessary that the carboxyl group was in free form for enzyme activity, methyl laurate was assayed as substrate. The results showed that the enzyme is able to transform the methyl esters (**Table 1**). Like in the reaction with free lauric acid, the reaction gave two main monohydroxylated derivatives at ω-1 and ω-2 positions, with a ω-1/ω-2 ratio of 1.3 (similar to that obtained for the free fatty acids).

Fatty-alcohol oxidation studies

Two primary fatty alcohols (1-tetradecanol and 1-hexadecanol) were assayed as substrates for the *A. aegerita* peroxygenase (**Table 1**). Among the reaction products identified (**Fig. 4** and **Fig. S2** of SD), the presence of the

corresponding fatty acids (myristic and palmitic acids, respectively) is noteworthy. The majority of the additional products were hydroxy or keto derivatives at ω-1 and ω-2 positions of the fatty acids (ω-hydroxymyristic and ω-hydroxypalmitic acids were also identified). The ω-1/ω-2 ratio of these monooxygenated derivatives was 1.4 (similar to that obtained directly from myristic and palmitic acids). Some minor peaks were tentatively assigned to monohydroxylated (and keto) derivatives of the fatty alcohols at ω-1 and ω-2 positions, which were more evident in the reaction with tetradecanol. Only traces of the corresponding aldehydes were observed in the reactions.

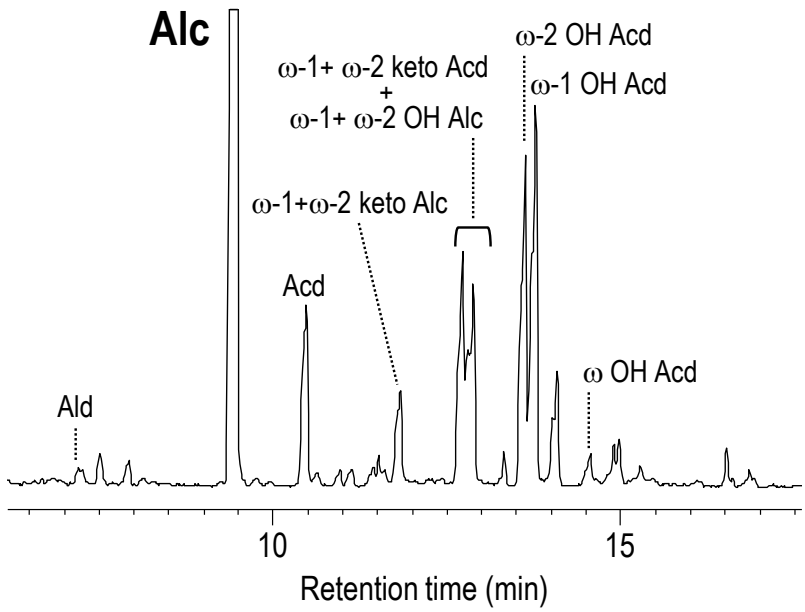

Fig. 4. GC-MS analysis of the peroxygenase reaction with tetradecanol, showing the remaining fatty alcohol substrate (Alc), the corresponding fatty acid (Acd) and its different ω-1 and ω-2 keto, ω to ω-5 hydroxyl, dicarboxylic, hydroxy-keto and dihydroxy derivatives formed (see SD, **Fig. S2** for chemical structures, and **Table 1** for quantitative values). Other minor compounds such as ω-1 and ω-2 keto and hydroxy derivatives of the tetradecanol and traces of the aldehyde (Ald) are also shown.

^{18}O-labeling studies were also performed in the reactions of 1-tetradecanol with the enzyme (and similar results were obtained in the 1-hexadecanol reactions). Incorporation of ^{18}O from $H_2{}^{18}O_2$ to the carboxyl group was observed during the oxidation of 1-tetradecanol to myristic acid (**Fig. 5**). Mass spectral analysis of the myristic acid formed, showed that the characteristic fragment at $[M - CH_3]^+$ had shifted from the natural abundance *m/z* 285 found in the unlabeled peroxide reaction (**Fig. 5A**) to *m/z* 289 (incorporation of two ^{18}O atoms at the carboxyl group) and *m/z* 287 (incorporation of one ^{18}O atom at the carboxyl group) (**Fig. 5B**). The relative abundances of the ^{18}O mono (74%) and bi-labeled (16%) myristic acid, estimated from the corresponding fragment peak areas, are included in **Fig. 5B**, together with their formulae (10% unlabeled acid was also formed due to the partial isotopic purity of the peroxide used).

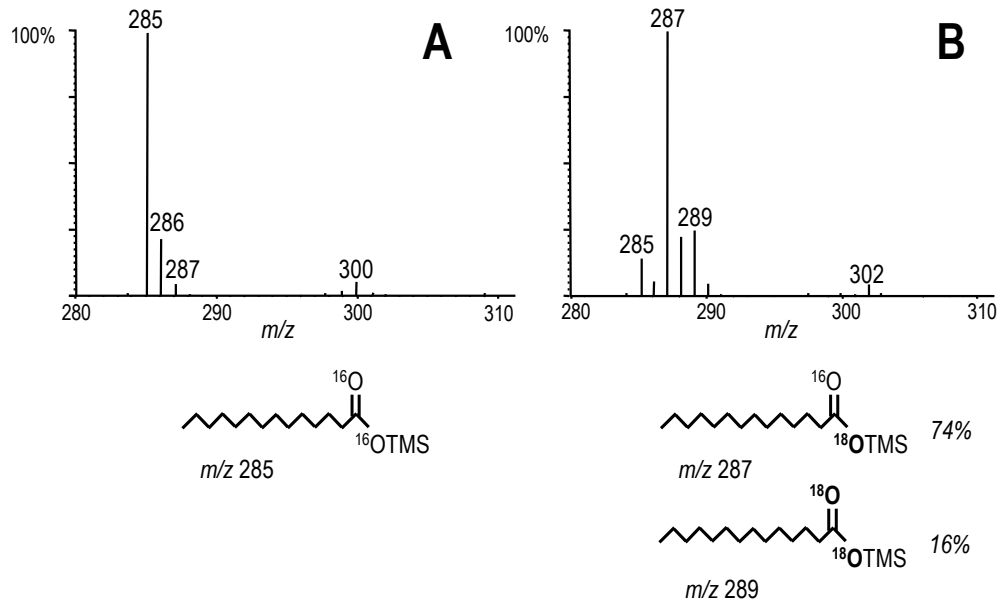

Fig. 5. Mass spectra of myristic acid (C_{14}), from peroxygenase reactions with 1-tetradecanol in the presence of $H_2{}^{16}O_2$ (**A**) and $H_2{}^{18}O_2$ (90% isotopic purity) (**B**), as trimethylsilyl (TMS) derivatives, and formulae for the unlabeled compound found in the **A**, and the mono-, and bi-labeled (top to bottom) compounds found in **B** with indication of their characteristic ions and relative abundances (10% unlabeled acid was also found in the second reaction).

The incorporation of ^{18}O from $H_2{}^{18}O_2$ was also evidenced in the mass spectra of the ω-1 or ω-2 hydroxylated derivatives of myristic acid, formed in the same 1-tetradecanol reaction. The mass spectral analysis showed that the characteristic fragments for the (ω-1) and (ω-2)-hydroxylated derivatives of fatty acids had ~90% shifted from the natural abundance *m/z* 117 and *m/z* 131 to *m/z* 119 and *m/z* 133, respectively (spectra not shown) due to peroxide ^{18}O incorporation. Moreover, the characteristic fragments for the ω-1 at $[M - CH_3]^+$ had shifted from the natural abundance *m/z* 373 found in the unlabeled peroxide reaction (**Fig. 6A**) to *m/z* 379 (incorporation of three ^{18}O atoms), *m/z* 377 (incorporation of two ^{18}O atoms) and *m/z* 375 (incorporation of one ^{18}O atom) (**Fig. 6C**). Likewise, the characteristic fragments for the ω-2 at $[M - CH_3CH_2]^+$ (including both the hydroxyl and carboxyl groups) had shifted from the natural abundance *m/z* 359 found in the unlabeled peroxide reaction (**Fig. 6B**) to *m/z* 365, *m/z* 363 and *m/z* 361 (**Fig. 6D**). The relative abundances of the ^{18}O mono, bi- and tri-labeled hydroxymyristic acid, estimated from the corresponding fragment peak areas, are also included in **Fig. 6C** (ω-1 isomer) and **Fig. 6D** (ω-2 isomer), together with their formulae and fragment generation (0-2% unlabeled hydroxyacid was also formed).

Alkane oxidation studies

Four saturated alkanes (dodecane, tetradecane, hexadecane and octadecane) were tested as *A. aegerita* peroxygenase substrates (**Table 1**). No reactivity with octadecane was observed under the experimental conditions used. It should be noted that hydroxylation of fatty acids with the same chain length (C_{18}) was observed. In contrast, the reactions with dodecane, gave monohydroxylated derivatives at positions 2 and 3. In addition to the monohydroxylated derivatives, products dihydroxylated at the positions 2 and 3 from both ends of the molecule (i.e. α+1 and ω-1/ω-2, or α+2 and ω-1/ω-2) were identified as the predominant compounds. Several combinations of keto and hydroxy derivatives were also formed although in minor amounts (see SD, **Fig. S3**). Unlike that observed in the reactions with fatty acids and fatty alcohols, terminal hydroxylation was not general in the reactions with alkanes. Similar derivatives to those found for dodecane were obtained from tetradecane and hexadecane although in lower amounts.

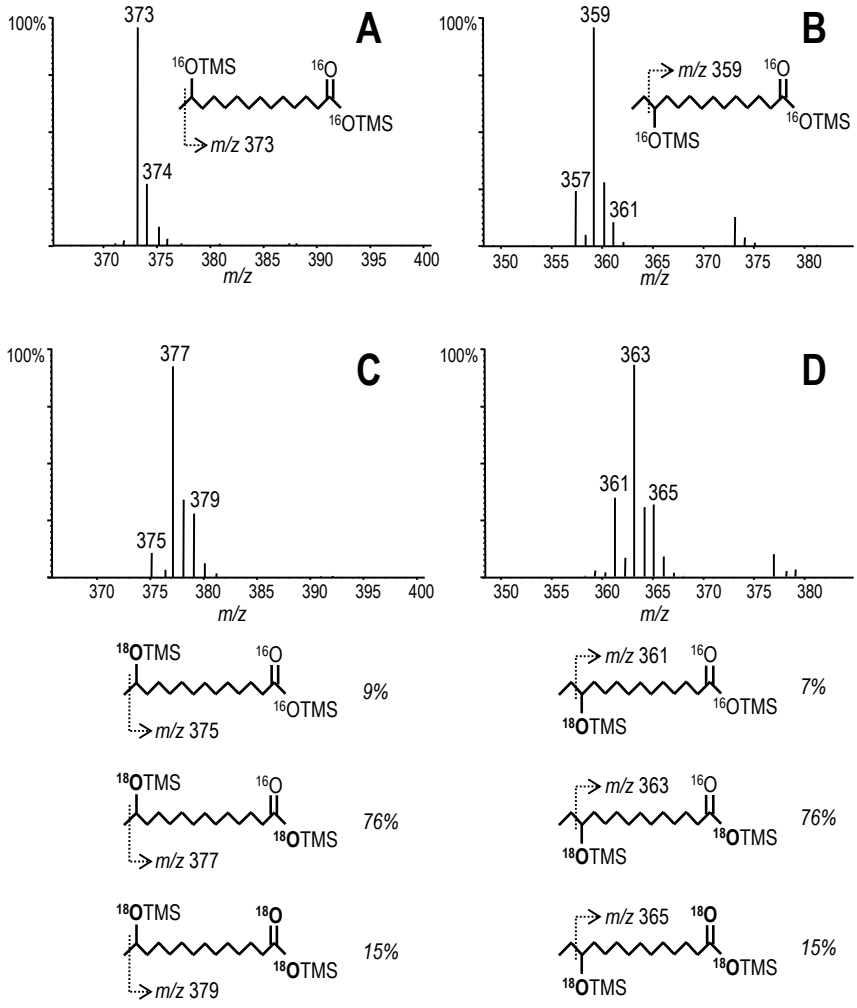

Fig. 6. Mass spectra of ω-1 (**A** and **C**) and ω-2 (**B** and **D**) monohydroxylated myristic acid (C_{14}), from peroxygenase reactions with 1-tetradecanol in the presence of $H_2{}^{16}O_2$ (**A** and **B**) and $H_2{}^{18}O_2$ (90% isotopic purity) (**C** and **D**), as trimethylsilyl (TMS) derivatives, and formulae for the mono-, bi- and tri-labeled (top to bottom) compounds with indication of their characteristic ions and relative abundances in the ω-1 (**C**) and ω-2 (**D**) isomers of hydroxymyristic acid (0-2% unlabeled product was also found).

Steroid oxidation studies

Reactions of both free (cholesterol and sitosterol) and esterified (cholesteryl butyrate, caprylate and linoleate) sterols with the *A. aegerita* peroxygenase were studied (**Table 1**). The enzyme showed low reactivity with free sterols, and only a very low conversion rates were attained under the experimental conditions used. The reaction products of cholesterol were monohydroxylated derivatives at positions C-24, C-25, and C-26 (or C-27) (see SD, **Fig. S4A**) with monohydroxylated C-25 predominating (see SD, **Fig. S4B**). In the reaction with sitosterol, only the monohydroxylated derivatives at positions C-24 and C-25 were observed. On the other hand, in the reactions with cholesterol esters no derivatives were observed.

Triglyceride oxidation studies

In addition of testing the reactivity of free lauric acid and lauric acid methyl ester, the peroxygenase reaction with a glycerol ester of lauric acid (trilaurin) was also studied. Unlike the reaction of free and methylated fatty acid, the triglyceride reaction did not yield any product.

Discussion

A. aegerita peroxygenase and other heme-thiolate enzymes

Heme-containing enzymes using H_2O_2 as electron acceptor (peroxidases) are a fascinating group of biocatalysts with a variety of ecological and biotechnological implications [9]. The current work deals with one of the most novel hemeperoxidase types, the so-called aromatic peroxygenase, that catalyze remarkable reactions such as peroxide-driven oxygen transfer, together with typical peroxidase reactions, being part of a separate peroxidase superfamily for which the name heme-thiolate peroxidases has been suggested [4,9,16]. A similar heme pocket is shared by P450s and results in similar ability to catalyze monooxygenation reactions, although P450s use O_2 as electron acceptor. However, the so-called "peroxide-shunt" exceptionally operates in some of them [17], and an unusual P450 being preferentially activated by H_2O_2 has been described [18]. The main difference between the P450s and peroxygenase reactions concerns formation of the cofactor reactive Compound I (a porphyrin cation-radical Fe^{4+}=O complex) that in peroxidases results from H_2O_2 generated

by oxidases (as shown in **Equation 1** for the peroxygenase reaction with ^{18}O-labeled peroxide); while P450s directly react with O_2 receiving electrons from an associated flavoprotein (or a flavo-domain) [4,19,20]. The subsequent reaction in normal peroxidases involves successive one-electron abstractions from two substrate molecules, while in P450 monooxygenases, and also in peroxygenases, consists of a first hydrogen-atom abstraction (by $Fe^{4+}=O$) coupled to oxygen rebound with hydroxyl transfer to the substrate (regenerating the neutral-porphyrin/ferric resting-state enzyme) (**Equation 2**). The significant deuterium isotopic effect observed in peroxygenase reactions [21] supports the hydrogen abstraction mechanism.

$$P\text{-}Fe^{3+} + H_2{}^{18}O_2 \rightarrow P\text{-}Fe^{3+}[O\text{-}{}^{18}OH]^- + H^+ \rightarrow P^{+\cdot}\text{-}Fe^{4+}={}^{18}O_{(C\text{-}I)} + H_2O \quad \textbf{(1)}$$

$$P^{+\cdot}\text{-}Fe^{4+}={}^{18}O_{(C\text{-}I)} + H\text{-}R \rightarrow [P\text{-}Fe^{4+}\text{-}{}^{18}O...H...R] \rightarrow P\text{-}Fe^{3+} + H{}^{18}O\text{-}R \quad \textbf{(2)}$$

After the first aromatic peroxygenase discovered in *A. aegerita* [2], similar enzymes have been isolated from other basidiomycetes [4,10,22], and genes of heme-thiolate peroxidases have been identified in different basidiomycete genomes [23-25]. Analysis of the sequences available to date suggests several sub-types in this superfamily, the *A. aegerita* heme-thiolate peroxidase being close to five heme-thiolate peroxidase genes identified in the *Coprinopsis cinerea* genome. Interestingly, the best characterized heme-thiolate peroxidase, the ascomycete *L. fumago* chloroperoxidase, does not cluster together with the basidiomycete heme-thiolate peroxidases. The present study shows that the extracellular peroxygenase from *A. aegerita*, previously known as catalyzing H_2O_2-dependent hydroxylations and halogenations of aromatic substrates [1,2], is able to catalyze the regioselective oxygenation/oxidation of different aliphatic compounds, strongly broadening the biotechnological interest of the enzyme, as shown by the new patents deposited.

Oxygenation/oxidation of different types of aliphatic compounds by A. aegerita peroxygenase

The *A. aegerita* peroxygenase shows prominent activity on a wide range of fatty acids yielding a variety of monohydroxylated, keto and dicarboxylic derivatives (and is also active on their methyl esters). P450s also catalyze fatty-acid hydroxylations, as reported for *Bacillus megaterium* P450BM-3 [26]. Under certain conditions, the monohydroxylated isomers from palmitic acid, unlike those from lauric and myristic acids, were further metabolized by P450BM-3 to secondary and tertiary (hydroxy-keto) products. In the peroxygenase reactions, oxidation of hydroxyfatty acids to ketones, diols and hydroxy-ketones was observed with all the fatty acids tested.

The *A. aegerita* peroxygenase also showed oxygenation activity on fatty alcohols, alkanes and free sterols. The activity on alkanes was the lowest among the simple aliphatic compounds assayed. Alkane hydroxylating activity was not observed in wild-type P450BM-3 [27] but a variant after several rounds of directed evolution was able to hydroxylate alkanes [28]. In the peroxygenase reactions with fatty alcohols, most products were hydroxy or keto derivatives of the corresponding fatty acids, and only a minor part of the fatty alcohols, suggesting oxidation of the substrate to the corresponding fatty acid prior to the chain hydroxylation. This differs from the reaction of 1-hexadecanol with P450BM-3, where the only products identified were isomers of hexadecanediol [27]. Moreover, no hydroxylation at the ω position was observed, while ω-hydroxyfatty acids were identified here.

When the reactions with simple aliphatic compounds are taken together, it becomes apparent that the *A. aegerita* peroxygenase would be able to catalyze the stepwise oxygenation of fatty alcohols (or even alkanes) to keto and dicarboxylic acids *via* fatty alcohols and acids, including different hydroxylated intermediates. In P450s, similar cascade oxidations are also produced, although the variety of products formed is lower [29,30].

In the sterol reactions, the conversion rates were very low and limited to the aliphatic side-chain. Maybe the side-chain enters into the same site where alkanes are oxidized in the *A. aegerita* peroxygenase, while P450s have a specific site where steroids are efficiently oxidized [31]. In contrast, the aliphatic chains in sterol esters and triglycerides were not oxidized. Taking into account that the same acids in free form (and also methyl laurate) are substrates of the *A. aegerita*

enzyme, there is seemingly a limitation in molecular size concerning bulky substrate hydroxylation.

Regioselective oxygenation of aliphatic compounds by the A. aegerita peroxygenase

The regioselectivity of *A. aegerita* peroxygenase oxygenation reactions has been investigated here using C_{12} to C_{20} saturated and unsaturated fatty acids, the main products being monohydroxylated derivatives at the ω-1 and ω-2 positions. This regioselectivity is seemingly not chain-length dependent, since when length increased it did not shift between the ω-1 and ω-2 positions, or to contiguous positions. Hydroxylation of fatty acids has been thoroughly studied for P450s, and both similarities and differences with the peroxygenase reaction patterns can be observed [27,32-39]. P450BM-3 has been reported to convert lauric, myristic and palmitic acids to their (ω-1), (ω-2) and (ω-3)-hydroxy derivatives [27,35] but, in contrast with that observed here, the percentage distribution of the regioisomers depends on the chain length (lauric and myristic acids being preferentially hydroxylated at ω-1, while palmitic acid is mainly hydroxylated at the ω-2 position). Regioselectivity changes in P450 hydroxylations suggest a "more selective" active site where the substrate carboxyl group is fixed at the entrance in such a way that the hydroxylation position depends on the length of the fatty-acid chain (Arg47 being involved in fatty-acid fixing at the P450BM-3 active site) [26,40,41]. In contrast, the active site of the *A. aegerita* peroxygenase seems "less selective" in substrate fixation, and hydroxylation is always preferentially produced at the ω-1 and ω-2 positions, which are more favorable than the ω position from the viewpoint of chemical reactivity.

With the *A. aegerita* peroxygenase, a highly regioselective reaction was found for myristoleic acid ($C_{14:1}$) that was hydroxylated at the ω-2 position, and not at the ω-1 position. A similar situation has been described in the oxidation of polyunsaturated arachidonic acid ($C_{20:4}$) by P450BM-3 (yielding 99% ω-2 hydroxylation, 1% ω-3 hydroxylation, and no reaction at ω-1) [36]. However, hydroxylation of saturated fatty acids by P450BM-3, although preferentially produced at the ω-2 carbon, also yields substantial amounts of ω-1 and ω-3 hydroxylated products. Therefore, it seems that the arachidonic molecule imposes additional steric requirements resulting in highly selective hydroxylation

by P450BM-3, and a similar situation would be produced in myristoleic acid oxidation by the peroxygenase.

Interestingly, a relationship between unsaturation and oxygenation regioselectivity was observed in the peroxygenase reactions with C_{12} and C_{16} fatty acids, the ω-1/ω-2 ratio shifting from ~0.8 in the unsaturated to ~1.5 in the saturated fatty acids with the same chain length. A similar result has not been reported in P450 reactions. On the other hand, the *A. aegerita* peroxygenase hydroxylates unsaturated fatty acids in a similar manner as the saturated ones (preferential ω-1 and ω-2 oxygenation in all cases). No epoxidation has been detected in these reactions in contrast with P450BM-3 that caused both hydroxylation and epoxidation of unsaturated fatty acids [33,36]. The regioselectivity of the *A. aegerita* enzyme was also the same for fatty acid methyl esters, but these compounds were not hydroxylated by P450BM-3 [27].

In addition to main hydroxylation at ω-1 and ω-2 positions (and ω-3 to ω-5 low hydroxylation), hydroxylated derivatives at the terminal methyl group of the fatty-acid chain were also identified that were subsequently converted to dicarboxylic acids, both present in low amounts. In contrast, no ω hydroxylation of fatty acids was detected in P450BM-3 reactions [27]. However, some particular P450s preferentially catalyze ω hydroxylations, at the most recalcitrant terminal methyl group [39].

The same regioselectivity observed for fatty-acid oxygenation was observed in the peroxygenase reactions with fatty alcohols and medium-length alkanes, although the latter exhibited symmetric oxygenation at both ends of the molecule. P450BM-3 also shows similar regioselectivity with fatty alcohols and with fatty acids, but does not act on hydrocarbons.

Although the crystal structure of *A. aegerita* peroxygenase has not been reported yet, homology modeling using the *L. fumago* chloroperoxidase crystal structure [42] (PDB entry 1CPO) as template, suggests a more exposed heme than in P450s [40]. A wider active site would be able to accommodate the variety of substrates and perform the variety of oxygenation reactions that peroxygenases are able to catalyze. The crystal structure of the *A. aegerita* peroxygenase will be soon available [43], and this will provide the opportunity to perform a more detailed analysis of the structural bases of its regioselective hydroxylation activity.

Mechanisms of substrate oxygenation/oxidation as revealed using ^{18}O-labeling

The most interesting catalytic property of the secreted *A. aegerita* heme-thiolate peroxidase is the transfer of oxygen to substrate molecules, which has been described as a peroxygenase activity. Reactions with $H_2{}^{18}O_2$ performed in this study revealed that the oxygen introduced in the ω-1 and ω-2 hydroxylation of fatty acids originates from H_2O_2 (90% ^{18}O-labeling in myristic acid hydroxylation) and not from O_2, as in similar reactions catalyzed by P450BM-3 [26]. This difference is consistent with the different mechanisms for Compound I formation in both enzymes, as well as with the common mechanism of substrate hydroxylation by oxygen incorporation from the Compound I iron-oxo complex (see **Equations 1** and **2** for peroxygenase reaction). ^{18}O-labeling was very low (only 10%) after hydroxyl oxidation to keto groups (during peroxygenase reaction with myristic acid) due to hydroxyl exchange with water (in the keto hydration-dehydration equilibrium) after the second hydroxylation yielding the *gem*-diol species.

The ^{18}O-labeling reactions also showed that, in addition to its presence in the hydroxyl (and keto) groups, the $H_2{}^{18}O_2$ oxygen also incorporates into the carboxyl group during the oxidation of 1-tetradecanol to myristic acid (base peak *m/z* 285) and its ω-1 and ω-2 hydroxylated derivatives (**Fig. 7**).

In the first case, ^{18}O-monolabeled (*m/z* 287) and ^{18}O-bilabeled (*m/z* 289) fragments were observed in the mass spectrum of myristic acid, whose integration indicated 74% and 16% abundances, respectively. The ^{18}O-labeling pattern was more complex in the two hydroxylated derivatives of myristic acid. Diagnostic ^{18}O-monolabeled (*m/z* 375 and 361 in the ω-1 and ω-2 derivatives, respectively), ^{18}O-bilabeled (*m/z* 377 and 363), and ^{18}O-trilabeled (m/z 379 and 365) fragments were observed, whose integration indicated 7-9% simple labeling, 76% double-labeling, and 15% triple-labeling. In both cases (myristic and hydroxymyristic acids from 1-tetradecanol), ^{18}O-labeling at the carboxyl group confirms that the oxygen incorporated during aliphatic alcohol oxidation to the corresponding acid is also supplied by H_2O_2 (peroxygenase activity). The relative abundances of the differently labeled products are related to the reaction mechanism commented below.

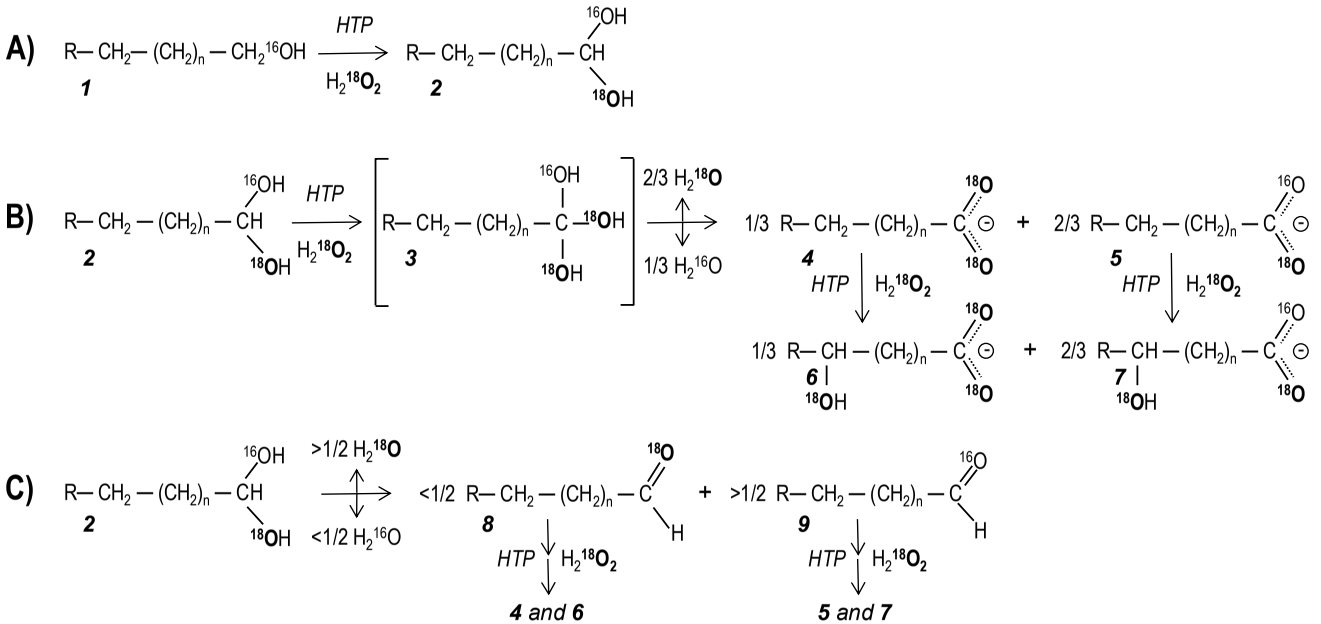

Fig. 7. Possible pathways for *A. aegerita* heme-thiolate peroxidase (HTP) oxidation of fatty alcohols (*1*) to the corresponding hydroxyfatty acids, as revealed using $H_2{}^{18}O_2$, including: **A)** Alcohol hydroxylation to a double ^{18}O-labeled *gem*-diol species (*2*); **B)** Direct oxidation of the *gem*-diol to a *gem*-triol intermediate (*3*) that irreversible dehydrates yielding fatty acids (*4* and *5*) with simple (66%) or double (33%) ^{18}O labeling, which are enzymatically hydroxylated (at the ω-1 position in the scheme) yielding the corresponding hydroxyfatty acids (*6* and *7*); and **C**) *Gem*-diol dehydration yielding ^{18}O labeled (*8*) and unlabeled (*9*) fatty aldehyde that, can exhibit variable hydroxyl exchange with the solvent resulting in reduced ^{18}O-labeling, before being successively hydroxylated by the enzyme yielding the same fatty acids (*4* and *5*) and hydroxyfatty acids (*6* and *7*) as formed in **B**. In the experimental study, lower ^{18}O-labeling percentages were obtained due to the 90% isotopic purity of the $H_2{}^{18}O_2$ used, which also resulted in a low percentage of monolabeled carboxylate.

The first product of fatty alcohol oxidation by the peroxygenase will be a *gem*-diol from C_1 hydroxylation (**Fig. 7A**), which will be either directly hydroxylated (even at the nascent stage) yielding a *gem*-triol intermediate, irreversibly dehydrating to release the acid group (**Fig. 7B**); or first dehydrated pto the corresponding aldehyde and then hydroxylated to the acid group (**Fig. 7C**). The predominant simple-labeling of the carboxyl group in fatty and hydroxyfatty acids (in the latter case accompanied by a second ^{18}O atom at the hydroxyl group) indicates the existence of such dehydration step, resulting in partial loss of the previously introduced ^{18}O-labeling and formation of both ^{16}O and ^{18}O carboxylic group. The same has been shown in stepwise oxidations of ethanol by P450s [29,44]. The ^{18}O-labeling patterns obtained, which are compatible with both oxidation pathways mentioned above, reveal no extensive hydroxyl exchange with the solvent at the aldehyde/*gem*-diol stage, which was hardly detectable in the chromatographic analysis (only aldehyde traces found). In the former aspect, the reaction differs from P450 cascade oxidation of hexadecanol, where complete ^{18}O-hydroxyl exchange with the solvent is produced before the final oxidation to palmitic acid, resulting in ~2 ratio between unlabeled and ^{18}O-monolabeled palmitic acid [30]. Hydroxylation of the aldehyde form was the mechanism suggested in the *A. aegerita* peroxygenase oxidation of benzyl alcohol to benzoic acid, where, in contrast with that observed here, the aldehyde accumulates in substantial amount [45]. However, *gem*-triol intermediates are suggested in several P450-catalyzed reactions, including oxygenation of some of the aliphatic compounds investigated in the present study [30].

Conclusions

The new *A. aegerita* peroxidase combines P450 and typical peroxidase properties, resulting in activation by peroxide and catalysis of monooxygenase-type reactions (peroxygenase activity). Detailed GC-MS analyses revealed that this enzyme is able to oxidize/oxygenate a variety of aliphatic compounds. Therefore, the name "aromatic peroxygenase" should be substituted by “unspecific peroxygenase” and the corresponding entry (EC 1.11.2.1) has been accepted in the IUBMB Enzyme Nomenclature (www.chem.qmul.ac.uk/iubmb/enzyme). In spite of its classical peroxidative (i.e. non-oxygenase) activity, $H_2{}^{18}O_2$ reactions indicated that the enzyme oxidizes

aliphatic alcohols to the corresponding acids by enzymatic hydroxylation and dehydration reactions, taking advantage from its monooxygenase activity (also shown in fatty acid ^{18}O hydroxylation). Interestingly, most of the aliphatic oxygenations catalyzed by the *A. aegerita* peroxygenase (resulting in new hydroxy and keto derivatives) are regioselective taking place at the ω-1 and ω-2 positions, irrespective of the aliphatic chain length (myristoleic acid hydroxylation being only produced at the ω-2 position). This regioselectivity, together with the self-sufficient oxygenase activity, make these new heme-thiolate peroxidases interesting biocatalysts for oxidative modification of different aliphatic compounds.

Acknowledgements

This study was funded by the PEROXICATS (KBBE-2010-4-265397) and BIORENEW (NMP2-CT-2006-026456) EU-projects, and the ELLE (AGL2008-00709) and RAPERO (BIO2008-01533) Spanish MICINN projects co-financed by FEDER funds. J. Rencoret (IRNAS, Seville) is acknowledged for preliminary enzyme assays. E.D. Babot thanks the Spanish CSIC for a JAE fellowship.

References

[1] R. Ullrich, M. Hofrichter, FEBS Lett. 579 (2005) 6247-6250.

[2] R. Ullrich, J. Nuske, K. Scheibner, J. Spantzel, M. Hofrichter, Appl. Environ. Microbiol. 70 (2004) 4575-4581.

[3] M.J. Nuell, G.H. Fang, M.J. Axley, P. Kenigsberg, L.P. Hager, J. Bacteriol. 170 (1988) 1007-1011.

[4] M. Hofrichter, R. Ullrich, M.J. Pecyna, C. Liers, T. Lundell, Appl. Microbiol. Biotechnol. 87 (2010) 871-897.

[5] R. Bernhardt, J. Biotechnol. 124 (2006) 128-145.

[6] H. Li, in: A. Messerschmidt, R. Huber, T.L. Poulos, K. Wieghardt (Eds.), Handbook of metalloproteins, Wiley, Baffins Lane, UK, 2001, pp. 267-282.

[7] R. Ullrich, M. Hofrichter, Cell. Mol. Life Sci. 64 (2007) 271-293.

[8] M.J. Pecyna, R. Ullrich, B. Bittner, A. Clemens, K. Scheibner, R. Schubert, M. Hofrichter, Appl. Microbiol. Biotechnol. 84 (2009) 885-897.

[9] F.J. Ruiz-Dueñas, A.T. Martínez, in: E. Torres, M. Ayala (Eds.), Biocatalysts based on heme peroxidases, Springer-Verlag, Berlin, 2010, pp. 37-59.

[10] E. Aranda, M. Kinne, M. Kluge, R. Ullrich, M. Hofrichter, Appl. Microbiol. Biotechnol. 82 (2009) 1057-1066.

[11] M. Kinne, R. Ullrich, K.E. Hammel, K. Scheibner, M. Hofrichter, Tetrahedron Lett. 49 (2008) 5950-5953.

[12] R. Ullrich, C. Dolge, M. Kluge, M. Hofrichter, FEBS Lett. 582 (2008) 4100-4106.

[13] M.G. Kluge, R. Ullrich, K. Scheibner, M. Hofrichter, Appl. Microbiol. Biotechnol. 75 (2007) 1473-1478.

[14] R. Ullrich, M. Hofrichter, in: The Mycota X: Industrial applications, Springer, Berlin (in press), 2010.

[15] A. Gutiérrez, J.C. del Río, F.J. González-Vila, F. Martín, J. Chromatogr. 823 (1998) 449-455.

[16] M. Hofrichter, R. Ullrich, M. Pecyna, M. Kinne, M.G. Kluge, E. Aranda, C. Liers, M. Poraj-Kobielska, G. Gröbe, B. Bittner, R. Schubert, K.E. Hammel, 16th International Conference on Cytochrome P450. (2009) 83-88.

[17] T.M. Makris, I. Denisov, I. Schlichting, S.G. Sligar, in: P.R. Ortiz de Montellano (Ed.), Cytochrome P450. Structure, mechanisms and biochemistry, Kluwer Academic, New York, 2005.

[18] I. Matsunaga, T. Sumimoto, M. Ayata, H. Ogura, FEBS Lett. 528 (2002) 90-94.

[19] F.J. Ruiz-Dueñas, A.T. Martínez, Microbial Biotechnol. 2 (2009) 164-177.

[20] P.R. Ortiz de Montellano, Cytochrome P450: Structure, mechanism, and biochemistry, Kluwer Academic/Plenum, New York, 2005.

[21] M. Kinne, M. Poraj-Kobielska, S.A. Ralph, R. Ullrich, M. Hofrichter, K.E. Hammel, J. Biol. Chem. 284 (2009) 29343-29349.

[22] D.H. Anh, R. Ullrich, D. Benndorf, A. Svatos, A. Muck, M. Hofrichter, Appl. Environ. Microbiol. 73 (2007) 5477-5485.

[23] F.J. Ruiz-Dueñas, E. Fernández, V. Sáez, M.J. Martínez, A.T. Martínez, in: G. Feijoo, M.T. Moreira (Eds.), Oxidative enzymes as sustainable industrial biocatalysts, USC (ISBN-13: 978-84-614-2824-3), Santiago de Compostela, 2010, pp. 92-97. www.biorenew.org/images/stories/OESIB_2010_Proceedings_Book.pdf.

[24] D. Martínez, J. Challacombe, I. Morgenstern, D.S. Hibbett, M. Schmoll, C.P. Kubicek, P. Ferreira, F.J. Ruiz-Dueñas, A.T. Martínez, P. Kersten, K.E. Hammel, A. Vanden Wymelenberg, J. Gaskell, E. Lindquist, G. Sabat, S.S. Bondurant, L.F. Larrondo, P. Canessa, R. Vicuña, J. Yadav, H. Doddapaneni, V. Subramanian, A.G. Pisabarro, J.L. Lavín, J.A. Oguiza, E. Master, B. Henrissat, P.M. Coutinho, P. Harris, J.K. Magnuson, S.E. Baker, K. Bruno, W. Kenealy, P.J. Hoegger, U. Kues, P. Ramaiya, S. Lucas, A. Salamov, H. Shapiro, H. Tu, C.L. Chee, M. Misra, G. Xie, S. Teter, D. Yaver, T. James, M. Mokrejs, M. Pospisek, I.V. Grigoriev, T. Brettin, D. Rokhsar, R. Berka, D. Cullen, Proc. Natl. Acad. Sci. USA. 106 (2009) 1954-1959.

[25] D. Martínez, L.F. Larrondo, N. Putnam, M.D. Gelpke, K. Huang, J. Chapman, K.G. Helfenbein, P. Ramaiya, J.C. Detter, F. Larimer, P.M. Coutinho, B. Henrissat, R. Berka, D. Cullen, D. Rokhsar, Nat. Biotechnol. 22 (2004) 695-700.

[26] A.W. Munro, D.G. Leys, K.J. McLean, K.R. Marshall, T.W.B. Ost, S. Daff, C.S. Miles, S.K. Chapman, D.A. Lysek, C.C. Moser, C.C. Page, P.L. Dutton, Trends Biochem. Sci. 27 (2002) 250-257.

[27] Y. Miura, A.J. Fulco, Biochim. Biophys. Acta-Lipids Lipid Metab. 388 (1975) 305-317.

[28] A. Glieder, E.T. Farinas, F.H. Arnold, Nat. Biotechnol. 20 (2002) 1135-1139.

[29] L.C. Bell-Parikh, F.P. Guengerich, J. Biol. Chem. 274 (1999) 23833-23840.

[30] U. Scheller, T. Zimmer, D. Becher, F. Schauer, W.H. Schunck, J. Biol. Chem. 273 (1998) 32528-32534.

[31] H. Ouellet, S.H. Guan, J.B. Johnston, E.D. Chow, P.M. Kells, A.L. Burlingame, J.S. Cox, L.M. Podust, P.R.O. de Montellano, n. 77 (2010) 730-742.

[32] L.O. Narhi, A.J. Fulco, J. Biol. Chem. 261 (1986) 7160-7169.

[33] R.T. Ruettinger, A.J. Fulco, J. Biol. Chem. 256 (1981) 5728-5734.

[34] S.S. Boddupalli, R.W. Estabrook, J.A. Peterson, J. Biol. Chem. 265 (1990) 4233-4239.

[35] S.S. Boddupalli, B.C. Pramanik, C.A. Slaughter, R.W. Estabrook, J.A. Peterson, Arch. Biochem. Biophys. 292 (1992) 20-28.

[36] J.H. Capdevila, S.Z. Wei, C. Helvig, J.R. Falck, Y. Belosludtsev, G. Truan, S.E. GrahamLorence, J.A. Peterson, J. Biol. Chem. 271 (1996) 22663-22671.

[37] T. Oster, S.S. Boddupalli, J.A. Peterson, J. Biol. Chem. 266 (1991) 22718-22725.

[38] G. Truan, M.R. Komandla, J.R. Falck, J.A. Peterson, Arch. Biochem. Biophys. 366 (1999) 192-198.

[39] J.B. Johnston, H. Ouellet, L.M. Podust, P.R. Ortiz de Montellano, Arch. Biochem. Biophys. 507 (2011) 86-94.

[40] H.Y. Li, T.L. Poulos, Nature Struct. Biology. 4 (1997) 140-146.

[41] M.A. Noble, C.S. Miles, S.K. Chapman, D.A. Lysek, A.C. Mackay, G.A. Reid, R.P. Hanzlik, A.W. Munro, Biochem. J. 339 (1999) 371-379.

[42] M. Sundaramoorthy, J. Terner, T.L. Poulos, Structure. 3 (1995) 1367-1377.

[43] K. Piontek, R. Ullrich, C. Liers, K. Diederichs, D.A. Plattner, M. Hofrichter, Acta Crystallogr. F. 66 (2010) 693-698.

[44] F.P. Guengerich, C.D. Sohl, G. Chowdhury, Arch. Biochem. Biophys. 507 (2011) 126-134.

[45] M. Kinne, C. Zeisig, R. Ullrich, G. Kayser, K.E. Hammel, M. Hofrichter, Biochem. Biophys. Res. Commun. 397 (2010) 18-21.

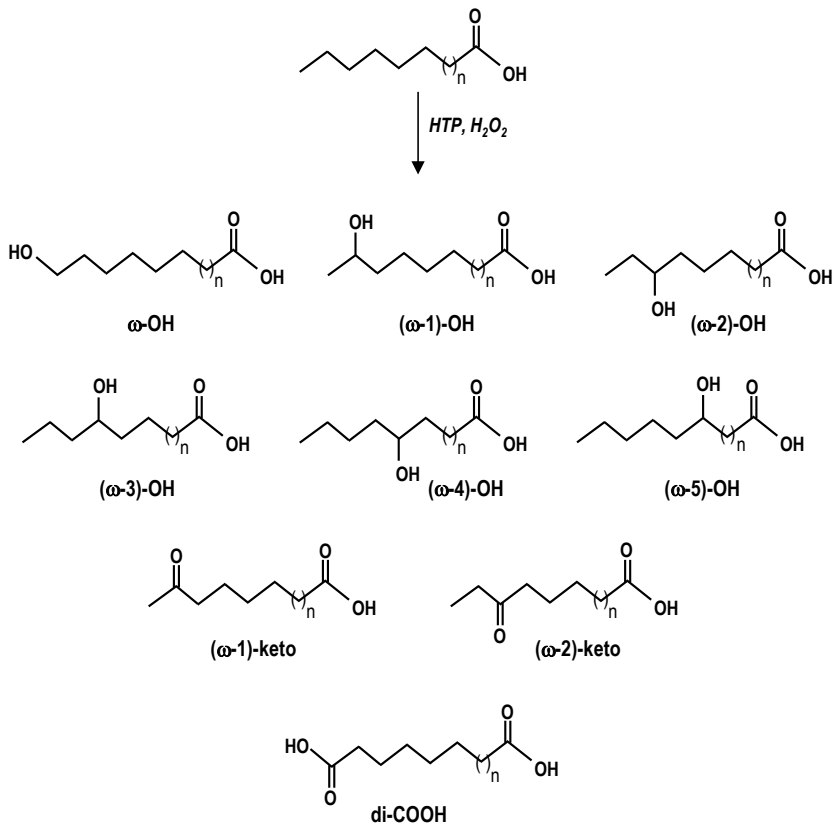

Fig. S1. Chemical structures of the main oxidation products identified in the peroxygenase reactions with fatty acids, including ω to ω-5 hydroxylated derivatives, ω-1 and ω-2 keto derivatives, and dicarboxylic fatty acids.

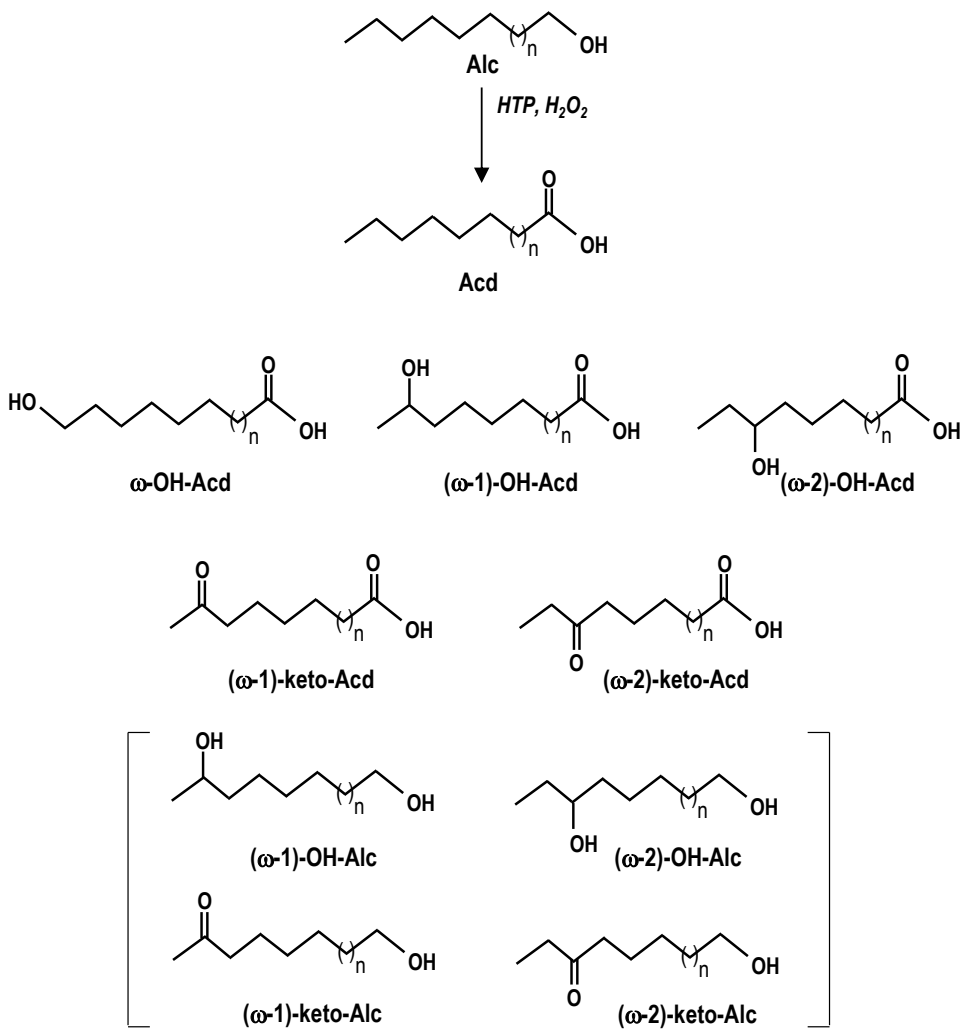

Fig. S2. Chemical structures of the main oxidation products identified in the peroxygenase reactions with fatty alcohols, including fatty acids (Acd) and their ω to ω-2 hydroxylated, and ω-1 and ω-2 keto derivatives. Minor compounds such as ω-1 and ω-2 hydroxy and keto derivatives of the fatty alcohols (Alc) are also shown in brackets.

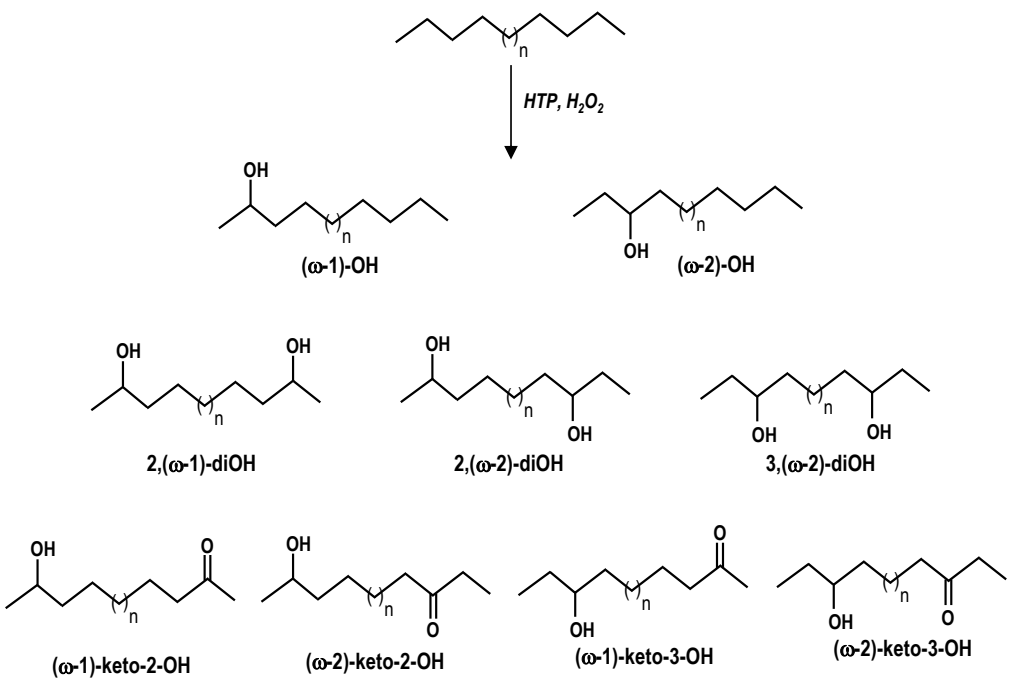

Fig. S3. Chemical structures of the main oxidation products identified in the peroxygenase reactions with alkanes, including monohydroxylated (positions 2 and 3), and dihydroxylated (positions 2 and ω-1, 2 and ω-2, and 3 and ω-2) fatty alcohols, and ketofatty alcohols ((ω-1) and (ω-2)-keto-2-hydroxyfatty alcohol; and (ω-1) and (ω-2)-keto-3-hydroxyfatty alcohol).

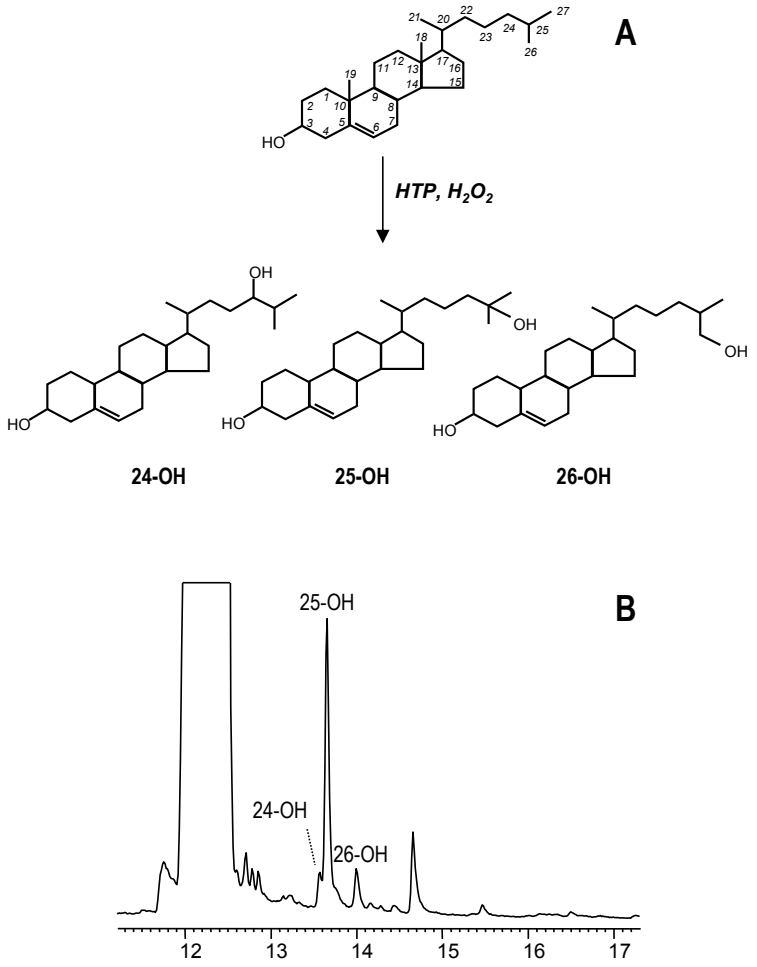

Fig. S4. Chemical structures of the main oxidation products identified in the peroxygenase reactions with cholesterol including 24-hydroxy, 25-hydroxy and 26-hydroxycholesterol (**A**), and GC-MS analysis of these products (**B**).

6.1. Publicación II:

Babot E.D., del Río J.C., Kalum L., Martínez A.T. and Gutiérrez A. (2012). Oxyfunctionalization of aliphatic compounds by a recombinant peroxygenase from *Coprinopsis cinerea*. *Biotechnology and Bioengineering* 110(9): 2323-2332.

Oxyfunctionalization of aliphatic compounds by a recombinant peroxygenase from *Coprinopsis cinerea*

Esteban D. Babot[a], José C. del Río[a], Lisbeth Kalum[b], Angel T. Martínez[c] and Ana Gutiérrez[a*]

[a]Instituto de Recursos Naturales y Agrobiología de Sevilla, CSIC, Reina Mercedes 10, E-41012 Seville, Spain

[b]Novozymes A/S, Krogshoejvej 36, 2880 Bagsvaerd, Denmark

[c]Centro de Investigaciones Biológicas, CSIC, Ramiro de Maeztu 9, E-28040 Madrid, Spain

* Corresponding author

Abstract:

The goal of this study is the selective oxyfunctionalization of aliphatic compounds under mild and environmentally-friendly conditions using a low-cost enzymatic biocatalyst. This could be possible taking advantage from a new peroxidase type that catalyzes monooxygenase reactions with H_2O_2 as the only cosubstrate (peroxygenase). With this purpose, recombinant peroxygenase, from gene mining in the sequenced genome of *Coprinopsis cinerea* and heterologous expression using an industrial fungal host, is tested for the first time on aliphatic substrates. The reaction on free and esterified fatty acids and alcohols, and long-chain alkanes was followed by gas chromatography, and the different reaction products were identified by mass spectrometry. Regioselective hydroxylation of saturated/ unsaturated fatty acids was observed at the ω-1 and ω-2 positions (only at the ω-2 position in myristoleic acid). Alkyl esters of fatty acids and monoglycerides were also ω-1 or ω-2 hydroxylated, but di- and triglycerides were not modified. Fatty alcohols yielded hydroxy derivatives at the ω-1 or ω-2 positions (diols) but also fatty acids and their hydroxy derivatives. Interestingly, the peroxygenase was able to oxyfunctionalize alkanes giving, in addition to alcohols at positions 2 or 3, dihydroxylated derivatives at both sides of the molecule. The predominance of mono- or dihydroxylated derivatives seems related to the higher or lower proportion of acetone, respectively, in the reaction medium. The recombinant *C. cinerea* peroxygenase appears as a promising

biocatalyst for alkane activation and production of aliphatic oxygenated derivatives, with better properties than the previously reported peroxygenase from *Agrocybe aegerita*, and advantages related to its recombinant nature for enzyme engineering and industrial production.

Keywords: Peroxygenase; hydroxylation; alkanes; fatty alcohols; fatty acids

Introduction

Selective hydroxylation of C-H bonds provides a mean to obtain drug intermediates, natural product derivatives, and different fine chemicals. However, selective oxyfunctionalization of organic substrates can be a significant problem in organic synthesis since these reactions are often carried out with strong oxidizing agents and occur with little regioselectivity. Enzymes are capable of avoiding these limitations catalyzing the selective oxyfunctionalization of organic substrates under mild and environmentally-friendly conditions (Pazmino et al., 2010). Members of the cytochrome P450 monooxygenase (P450) superfamily are notable examples of such catalysts (Ortiz de Montellano, 2005).

A few years ago, a new peroxidase type was discovered in the wood/litter rotting basidiomycete *Agrocybe aegerita* (Ullrich et al., 2004) which turned out to be a true peroxygenase efficiently transferring oxygen from peroxide to various organic substrates (Hofrichter et al., 2010). This peroxygenase is able to catalyze reactions formerly assigned to intracellular P450s (Bernhardt, 2006). However, unlike P450s that are intracellular enzymes whose activation requires NAD(P)H as electron donor and auxiliary flavin-reductases (or a second flavin domain) for electron transfer to O_2 (Li, 2001), the *A. aegerita* enzyme is a secreted protein that only requires H_2O_2 for activation (Ullrich and Hofrichter, 2007). This peroxygenase combines the above unique capabilities of P450s for oxygen transfer (in two-electron oxidations) and classic properties of peroxidases such as (one electron) oxidation of phenolic and other substrates. The *A. aegerita* peroxygenase has been shown to catalyze a high number of interesting oxygenation reactions on aromatic compounds (Hofrichter et al., 2010) and recently, the action of this enzyme on some aliphatic compounds was demonstrated for the first time expanding the biotechnological interest of the

enzyme (Peter et al., 2011; Gutiérrez et al., 2011). Therefore, the enzyme, first described as a haloperoxidase and later mostly referred to as aromatic peroxygenase (APO) can be now named "unspecific peroxygenase" (UPO) since the corresponding entry (EC 1.11.2.1) has been accepted in the IUBMB Enzyme Nomenclature (www.chem.qmul.ac.uk/iubmb/enzyme).

After the first basidiomycete peroxygenase discovered in *A. aegerita* (Ullrich et al., 2004), similar enzymes have also been found in a few related fungi such as *Coprinellus radians* and *Marasmius rotula*, and there are indications for their widespread occurrence in the fungal kingdom (Anh et al., 2007; Hofrichter et al., 2010; Gröbe et al., 2011). Database research with the gene of *A. aegerita* peroxygenase as a probe revealed peroxygenase genes in diverse organisms (Pecyna et al., 2009). These include *Coprinopsis cinerea* (synonym: *Coprinus cinereus*), a dung dwelling mushroom whose genome, sequenced by the Broad Institute, is available for annotated gene search at the Joint Genome Institute (JGI; www.jgi.doe.gov). Very recently, over one-hundred peroxygenase-type genes (encoding enzymes of the heme-thiolate peroxidase superfamily) have been identified during the analysis of 24 basidiomycete genomes (Floudas et al., 2012). The wild-type *C. cinerea* peroxygenase has not been isolated and characterized to date, but one of the peroxygenase genes from its genome (JGI model CC1G_08427T0) was heterologously expressed by Novozymes A/S (Bagsvaerd, Denmark) being covered by an international patent (WO/2008/119780). This first recombinant peroxygenase can be a powerful biocatalytic tool for synthetic applications because of potential high expression yield, and possibility to tailor-make its catalytic and operational properties using protein engineering tools. Here, the reaction of recombinant *C. cinerea* peroxygenase with aliphatic compounds including challenging alkane activation is evaluated for the first time. The final aim will be to incorporate the new peroxygenase to the group of recombinant hemeperoxidases, including the *C. cinerea* peroxidase (Morita et al., 1988; Cherry et al., 1999), that are commercially available (from Novozymes and other companies) for large scale applications (such as bleaching and dye-transfer prevention in detergent formulations) (Xu, 2005).

Materials and Methods

Enzyme preparations

The recombinant peroxygenase used in this study corresponds to gene model CC1G_08427T0 from the sequenced *C. cinerea* genome available at JGI (www.jgi.doe.gov). The corresponding protein (*C. cinerea* genome ID 7429) was produced by heterologous expression using a Novozymes *Aspergillus oryzae* industrial host system (patent WO/2008/119780) and purified using a combination of S-Sepharose and SP-Sepharose ion-exchange chromatography. The recombinant peroxygenase preparation is an electrophoretically homogeneous glycoprotein with a molecular mass around 44 kDa (a non-uniform glycosylation pattern was observed), a typical UV-vis spectrum with a Soret band at 418 nm, and the ability to oxygenate different aromatic compounds (Dolge et al. 2011) with a specific activity of approximately 100 $U \cdot mg^{-1}$ (measured as described below). The wild-type peroxygenase included in the present study for comparative purposes (*A. aegerita* isoform II, 46 kDa) was provided by R. Ullrich and M. Hofrichter (University of Zittau, Germany) after its isolation from cultures of *A. aegerita* grown in soybean-peptone medium, and subsequent purification using a combination of Q-Sepharose and SP-Sepharose and Mono-S ion-exchange chromatographic steps (Ullrich et al. 2004). One enzyme activity unit was defined as the amount of enzyme oxidizing 1 μmol of veratryl alcohol to veratraldehyde (ε_{310} 9300 $M^{-1} \cdot cm^{-1}$) in 1 min at 24 °C, pH 7, in the presence of 0.5 mM H_2O_2 (2.5 mM H_2O_2 in the case of the *A. aegerita* peroxygenase).

Model substrates

A series of model aliphatic substrates (from Sigma-Aldrich) was used including: i) saturated fatty acids such as lauric (dodecanoic), myristic (tetradecanoic), palmitic (hexadecanoic) and stearic (octadecanoic) acids; ii) unsaturated fatty acids such as myristoleic (*cis*-9-tetradecenoic) and oleic (*cis*-9-octadecenoic) acids; iii) fatty alcohols such as 1-tetradecanol; iv) alkanes such as tetradecane, *cis*-1-tetradecene, and *trans*-7-tetradecene; and v) fatty acid esters such as methyl myristate, myristyl myristate, octyl octanoate, monomyristin (1-myristoylglycerol), dimyristin (1,2-dimyristoylglycerol) and trimyristin.

Enzymatic reactions

Five mL reactions of the model substrates (0.1 mM, except alkanes at 0.3 mM concentration) with the *C. cinerea* peroxygenase (1 U) were performed in 50 mM sodium phosphate buffer (pH 7) at 25 ºC at different reaction times (30, 60 and 120 min), in the presence of 0.5 mM H_2O_2. The substrates were previously dissolved in acetone and added to the buffer (acetone concentration in most reactions was 15%). In the alkane reactions three concentrations of acetone were used (20%, 40% and 60%). In control experiments, substrates were treated under the same conditions (including 0.5 mM H_2O_2) but without enzyme. Reactions with the *A. aegerita* peroxygenase were also performed under the same conditions as *C. cinerea* peroxygenase (except the 2.5 mM H_2O_2 concentration). Products were recovered from the reactions by liquid-liquid extraction with methyl *tert*-butyl ether and dried under N_2. Bis(trimethylsilyl)trifluoroacetamide (Supelco) was used to prepare trimethylsilyl (TMS) derivatives that were analyzed by gas chromatography-mass spectrometry (GC-MS).

GC-MS analyses

The analyses were performed with a Varian 3800 chromatograph coupled to an ion-trap detector (Varian 4000) using a medium-length fused-silica DB-5HT capillary column (12 m x 0.25 mm internal diameter, 0.1 μm film thickness) from J&W Scientific (Gutiérrez et al., 1998). The oven was heated from 120 ºC (1 min) to 300 ºC (15 min) at 10 ºC·min^{-1}. The injector was programmed from 60 ºC (0.1 min) to 300 ºC (28 min) at 200 ºC·min^{-1}. A second temperature program, from 50 ºC to 90 ºC (2 min) at 30 ºC·min^{-1}, and then to 250 ºC (2 min) at 8 ºC·min^{-1} (with the injector kept at 250 ºC) was also used. In all analyses, the transfer line was kept at 300 ºC and helium was used as carrier gas (2 ml·min^{-1}). Compounds were identified by mass fragmentography and comparing their mass spectra with those of the Wiley and NIST libraries and standards, and quantification was obtained from total-ion peak area, using response factors of the same or similar compounds. Single-ion chromatographic profiles were used to estimate compound abundances when two peaks partially overlapped.

Results and discussion

This work deals with evaluation of the first recombinant peroxygenase, representative for a new superfamily of heme-thiolate peroxidases with a cysteine residue as the fifth ligand of the heme iron (Hofrichter et al., 2010) as a biocatalyst for the oxyfunctionalization of different aliphatic compounds. Here it is shown for the first time how this recombinant peroxygenase, which was obtained by mining the sequenced *C. cinerea* genome followed by heterologous expression in *A. oryzae*, is similar or even superior to the best described peroxygenase of *A. aegerita* (Ullrich et al., 2004) catalyzing the regioselective oxygenation of different aliphatic compounds. With this purpose, free and esterified fatty acids (as alkyl and glycerol esters), fatty alcohols and long-chain alkanes were tested as substrates of the recombinant *C. cinerea* peroxygenase. The reactivity of the *A. aegerita* peroxygenase on some aliphatic compounds was recently reported (Gutiérrez et al., 2011) and in the present study parallel reactions with this wild-type (non-recombinant) peroxygenase were carried out for comparison. All the compounds assayed showed reactivity towards the new enzyme except the di- and triglycerides, and the esters of long-chain fatty acids with long-chain alcohols. The conversion rate and the reaction products formed were studied by GC-MS.

Fatty-acid reactions

Saturated fatty acids with even carbon number from C_{12} to C_{18} were tested as substrates of the *C. cinerea* peroxygenase (**Table 1**). All of them showed reactivity towards the enzyme although at different extents, myristic and palmitic acids attaining almost complete transformation after 30 min. The reactions of these compounds with the *A. aegerita* peroxygenase showed the same tendency related to chain length (**Table 1**) but with lower efficiency under the same reaction conditions (≤ 50% that of the *A. aegerita* peroxygenase). For the fatty acids tested, the alkyl chains were monohydroxylated by the enzyme to give predominantly mixtures of the ω-1 and ω-2 isomers (**Fig. 1A**, **Table 2)**. The position of the hydroxyl group was identified from the mass spectra of TMS derivatives (Gutiérrez et al., 2011). In addition to hydroxylated derivatives, keto derivatives at positions ω-1 and ω-2 were also identified (**Fig. 1**).

Table 1
Conversion of different types of aliphatic compounds by the *C. cinerea* and *A. aegerita* peroxygenases within 30 min reaction (% of substrate transformed).

Substrate	*C. cinerea* peroxygenase	*A. aegerita* peroxygenase
Fatty acids		
Lauric acid (C_{12})	45	25
Myristic acid (C_{14})	98	41
Palmitic acid (C_{16})	93	40
Stearic acid (C_{18})	72	31
Myristoleic acid ($C_{14:1}$)	53	43
Oleic acid ($C_{18:1}$)	68	60
Fatty acid esters		
Methyl myristate	94	50
Myristyl myristate	0	0
Octyl octanoate	40	36
Monomyristin	47	18
Dimyristin	0	0
Trimyristin	0	0
Fatty alcohols		
1-Tetradecanol	72	72
Alkanes/alkenes		
Tetradecane	52	24
1-Tetradecene	1	0
7-Tetradecene	81	13

Most probably, these compounds were formed because the reactions were performed with non-limiting hydrogen peroxide concentration, and peroxygenase leads to further oxidation of the monohydroxylated compounds. This results in carbonyl compounds which originate from dehydration of

geminal diol intermediates, as previously demonstrated by the authors in ^{18}O labeling studies with the *A. aegerita* peroxygenase (Gutiérrez et al., 2011).

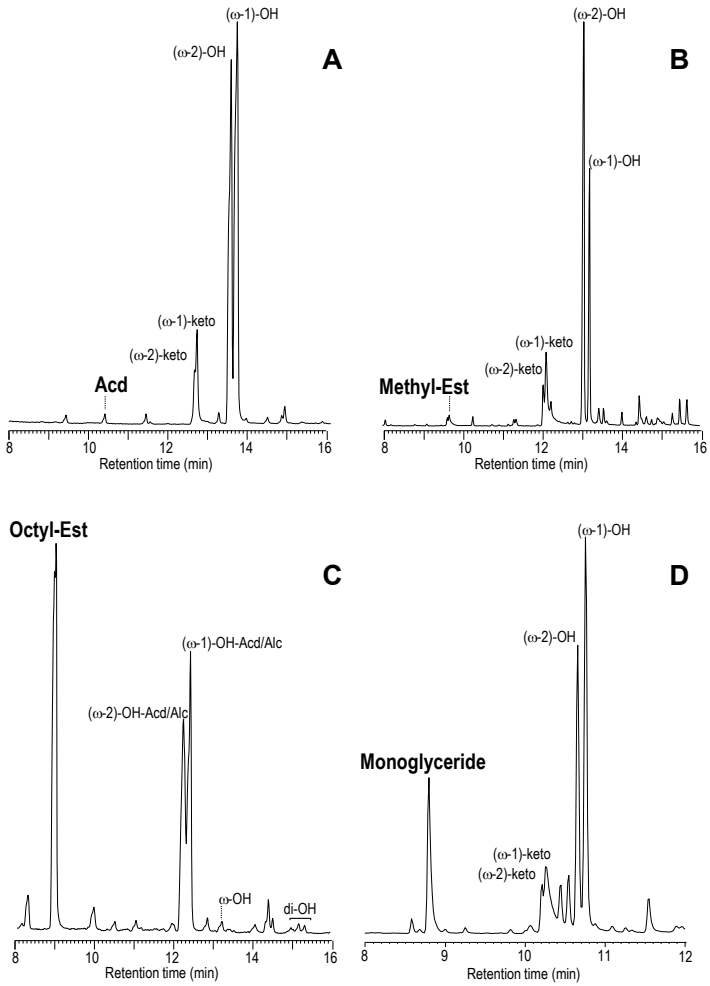

Fig. 1. GC-MS analysis of the recombinant *C. cinerea* peroxygenase reactions (at 30 min) with myristic acid (**A**), methyl myristate (**B**), octyl octanoate (**C**) and glyceryl myristate (**D**) showing the remaining substrates (Acd: acid, Methyl-Est: acid methyl ester, Octyl-Est: acid octyl ester, Monoglyceride: acid monoglyceryl ester) and the ω-1 and ω-2 monohydroxy and keto derivatives.

Table 2

Abundance (relative percentage) of the different hydroxylated and keto derivatives (at ω-1 and ω-2 positions) identified by GC-MS in the reactions of free (R=H) saturated, unsaturated ($C_{14:1}$ and $C_{18:1}$) and esterified (R=methyl, glyceryl, octyl) fatty acids (from 12 to 18 carbons) with the recombinant *C. cinerea* peroxygenase.

Substrate	**(ω-1)-OH**	**(ω-2)-OH**	**(ω-1)-keto**	**(ω-2)-keto**
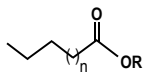	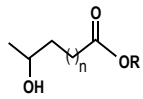	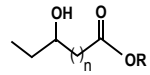	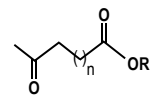	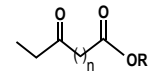
Saturated fatty acids				
Lauric acid (R=H, n=8)	57.0	43.0	-	-
Myristic acid (R=H, n=10)	49.5	43.0	6.9	0.7
Palmitic acid (R=H, n=12)	38.4	52.9	6.7	2.1
Stearic acid (R=H, n=14)	31.5	50.2	12.5	5.6
Unsaturated fatty acids				
Myristoleic acid (R=H, n=10; $C_{14:1}$)	-	100	-	-
Oleic acid (R=H, n=14; $C_{18:1}$)	33.3	66.8	-	-
Fatty acid esters				
Methyl myristate (R=CH_3, n=10)	21.1	43.4	24.3	11.3
Octyl octanoate (R=C_8H_{13}, n=4)	49.7	50.3	-	-
Monomyristin (R=$C_3H_7O_3$, n=10)	33.8	22.8	16.7	4.7

The abundance of the different monohydroxylated and keto derivatives (at ω-1 and ω-2) for the fatty acids assayed is shown in **Table 2**. The results show that the regioselectivity of *C. cinerea* peroxygenase in these oxygenation reactions is seemingly chain-length dependent, since when length increased it shifted from the ω-1 to the ω-2 position. The ratio between the two main isomers (ω-1/ω-2) among the total monooxygenated derivatives (hydroxy- and ketofatty acids) is >1 for lauric (dodecanoic, C_{12}) and myristic (tetradecanoic, C_{14}) acids and <1 for palmitic (hexadecanoic, C_{16}) and stearic (octadecanoic, C_{18}) acids. In contrast, with the *A. aegerita* peroxygenase the ω-1/ω-2 ratio is >1 for the four fatty acids (Gutiérrez et al., 2011). Hydroxylation of fatty acids has been thoroughly studied for P450s (Miura and Fulco, 1975; Narhi and Fulco, 1986; Boddupalli et al., 1992; Truan et al., 1999; Johnston et al., 2011) and both similarities and differences with the peroxygenase reaction patterns are observed. The *Bacillus megaterium* P450BM-3 has been reported to convert lauric, myristic and palmitic acids to their (ω-1), (ω-2) and (ω-3)-hydroxy derivatives and as found in the reactions with *C. cinerea* peroxygenase the percentage distribution of the regioisomers depends on the chain length. In this aspect, the *C. cinerea* peroxygenase is more similar to P450s than to *A. aegerita* peroxygenase, which maintain the same regioselectivity regardless the fatty acid chain length.

Two unsaturated fatty acids, namely myristoleic and oleic acids, were also tested as substrates of the *C. cinerea* peroxygenase. The reaction with oleic acid followed a similar pattern as that of the saturated fatty acid (stearic acid) giving monohydroxylated derivatives at the ω-1 and ω-2 positions, with predominance of the latter. The conversion of this compound with the *A. aegerita* peroxygenase was produced with similar efficiency and gave monohydroxylated derivatives at the ω-1 and ω-2 positions, with predominance of the former. On the other hand, a highly strict regioselectivity was observed in the hydroxylation of myristoleic acid that was exclusively hydroxylated at the ω-2 position, and not at the ω-1 position, with both peroxygenases. The latter situation is similar to that described in the oxidation of polyunsaturated arachidonic acid ($C_{20:4}$) by P450BM-3. As mentioned above, hydroxylation of saturated fatty acids by P450BM-3, although preferentially produced at the ω-2 carbon, also yields substantial amounts of ω-1 and ω-3 hydroxylated products. However, in the case of arachidonic acid, 99% ω-2 hydroxylation is produced by this P450 (Capdevila et al., 1996). It seems that the arachidonic molecule imposes additional steric requirements resulting in highly selective hydroxylation by

P450BM-3, and a similar situation would be produced in myristoleic acid oxidation by the peroxygenases.

Fatty-acid ester reactions

With the aim of investigating whether it was necessary that the carboxyl group was in free form for peroxygenase activity, several esters of fatty acids - namely methyl myristate, myristyl myristate, octyl octanoate and mono-, di- and trimyristin - were assayed as substrates of *C. cinerea* peroxygenase (**Table 1**). The results show that the enzyme is able to transform some of these esters at different extents, giving monohydroxylated derivatives (**Table 2**). Like with free myristic acid, the reaction with methyl myristate (**Fig. 1B**) was very efficient and the substrate was almost completely transformed within 30 min. Two main monohydroxylated derivatives at ω-1 and ω-2 positions were obtained, although the hydroxylation in the latter position was predominant in this case. In addition to methyl myristate, the ester of myristic acid with the long chain myristyl alcohol was also tested. However, this reaction did not yield any product, most probably due to steric hindrance, since both free compounds, myristic acid and tetradecanol (see below) were transformed by the peroxygenase. Using octyl octanoate as substrate (**Fig. 1C**) a conversion of 40% was produced at 30 min, giving mainly monohydroxylated derivatives at ω-1 and ω-2 positions in similar proportion (**Table 2**). When the mass spectra of these compounds were studied in more detail it was observed that there were derivatives at ω-1 and ω-2 positions from both ends of the molecule, corresponding to the alcohol and acid moieties. For a better identification of the isomers, the reaction products were analyzed using a longer chromatographic column and isothermal oven heating. The four monohydroxylated derivatives were easily discerned by monitoring the characteristic mass fragments at *m/z* 127 and *m/z* 199 in single-ion chromatograms (**Fig. 2**), and diagnostic mass spectra were obtained from selected scans with minimal peak overlapping (**Fig. 3**). The mass spectra of the TMS ether derivative of octyl octanoate hydroxylated at ω-1 position, either on the acyl or the alcohol moiety, show the characteristic base peak at *m/z* 117 from the α-cleavage of the TMS group, while the two isomers at ω-2 position show the characteristic base peak at *m/z* 131 from the α-cleavage of the TMS group.

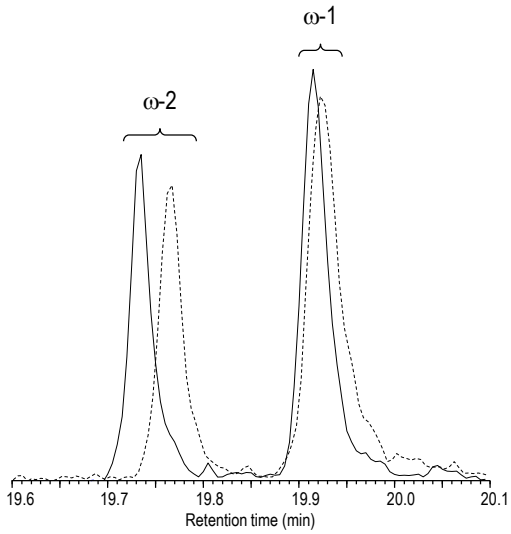

Fig. 2. Single-ion chromatograms of the recombinant *C. cinerea* peroxygenase reaction (30 min) with octyl octanoate (**Fig. 1C**) showing the four hydroxy derivatives at the ω-1 and ω-2 positions of the acid moiety in the *m/z* 199 profile (continuous line), and the alcohol moiety in the *m/z* 127 profile (dashed line).

The key to distinguish if the hydroxyl group is located on the acyl or in the alcohol moiety of the ester molecule relies on the mass fragment arisen from the cleavage of the ester bond (Marques et al., 2007). The presence of a hydroxyl group (as TMS ether derivative) in the acyl moiety (at either ω-1 or ω-2 positions) produces a fragment at *m/z* 199 from the loss of the alcohol group of the ester, together with an additional loss of a methyl from the TMS group. If the hydroxyl group occurs in the alcohol moiety (at either ω-1 or ω-2 positions), then the acyl moiety is not hydroxylated and the fragment from the cleavage of the ester bond is at *m/z* 127. Besides the monohydroxylated derivatives, several dihydroxylated derivatives at ω-1 and ω-2 positions from both ends of the molecule and terminal monohydroxylation (ω derivatives) were also present although in trace amounts. The peroxygenase reaction with a glycerol ester of myristic acid (monomyristin) (**Fig. 1D**) gave also the corresponding two ω-1 and ω-2 monohydroxylated derivatives, with the former predominating. The conversion was 47% at 30 min reaction. In contrast, the reaction of dimyristin and trimyristin did not yield any product.

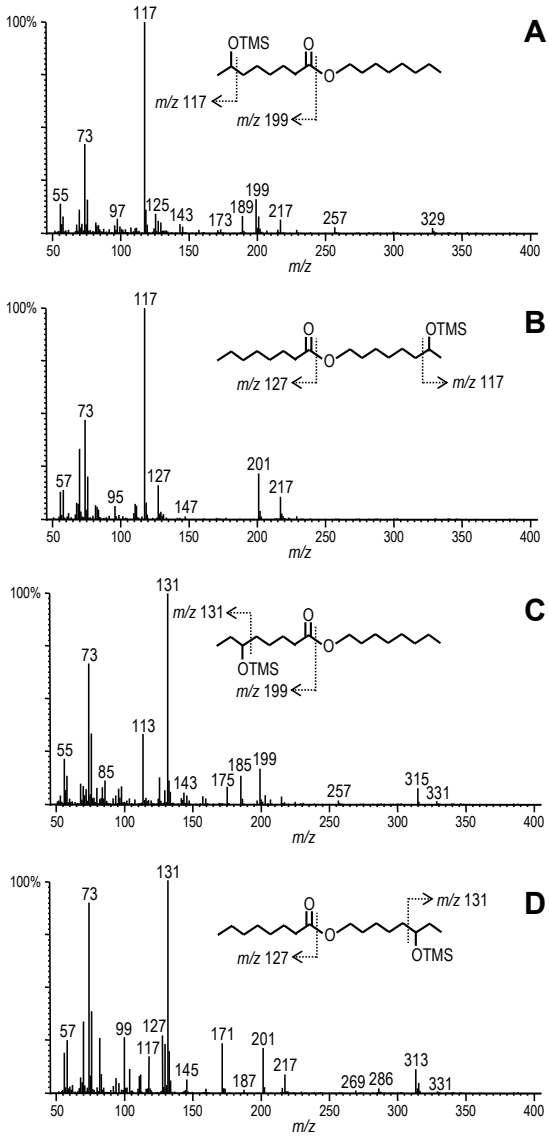

Fig. 3. Mass spectra of ω-1 (**A** and **B**) and ω-2 (**C** and **D**) monohydroxylated derivatives at the acid (**A** and **C**) and alcohol (**B** and **D**) moieties from peroxygenase reactions with octyl octanoate, as TMS derivatives, from selected scans in **Fig. 2**.

Taking into account that the same acids in free form (and also as methyl and monoglyceryl esters) are substrates of the *C. cinerea* enzyme, there is seemingly a limitation in molecular size concerning bulky substrate hydroxylation. Reactions

of methyl myristate, octyl octanoate and monomyristin with *A. aegerita* peroxygenase gave good conversion yields although lower than those obtained with the *C. cinerea* peroxygenase (**Table 1**). Monohydroxylated derivatives at ω-1 and ω-2 positions were also identified with the ω-1 derivatives predominating. In contrast, P450BM-3 was reported as unable to hydroxylate fatty acid methyl esters (Miura and Fulco, 1975). This seems related to the above discussed P450 regioselectivity hydroxylating fatty acids, which is due to a "more selective" active site where the free carboxyl group of the substrate is fixed at the entrance (by P450BM-3 Arg47) in such a way that the hydroxylation position depends on the length of the fatty-acid chain (Li and Poulos, 1997; Noble et al., 1999; Munro et al., 2002). Although a similar regioselectivity is exhibited by the *C. cinerea* peroxygenase, as discussed above, the mechanism is probably more related to the shape (and length) of the active-site channel than to the presence of a residue anchoring the carboxyl group, since free fatty acids and their methyl esters exhibit similar peroxygenase reactivities. The first fungal peroxygenase has been crystallized (Piontek et al., 2010) and structural-functional studies on this and other members of this superfamily will provide the clues required to explain this and other aspects of their catalysis.

Fatty-alcohol reactions

A primary fatty alcohol (1-tetradecanol) was assayed as substrate for the *C. cinerea* peroxygenase. High conversion (72%) was attained at 30 min (**Table 1**) and several reaction products were identified (**Fig. 4**) including the corresponding fatty acid (myristic acid) and the hydroxy derivatives at the ω-1 and ω-2 positions of the fatty alcohol (1,13- and 1,12-tetradecanediol, respectively) and fatty acid (13- and 12-hydroxymyristic acids, respectively) (**Table 3**). Only traces of the corresponding aldehyde were observed in the reactions. The mass spectra of the TMS derivatives of 1,13- and 1,12-tetradecanediol, shown in **Fig. 5**, are characterized by the fragments at *m/z* 117 and *m/z* 131, typical for the ω-1 and ω-2 hydroxy derivatives, respectively.

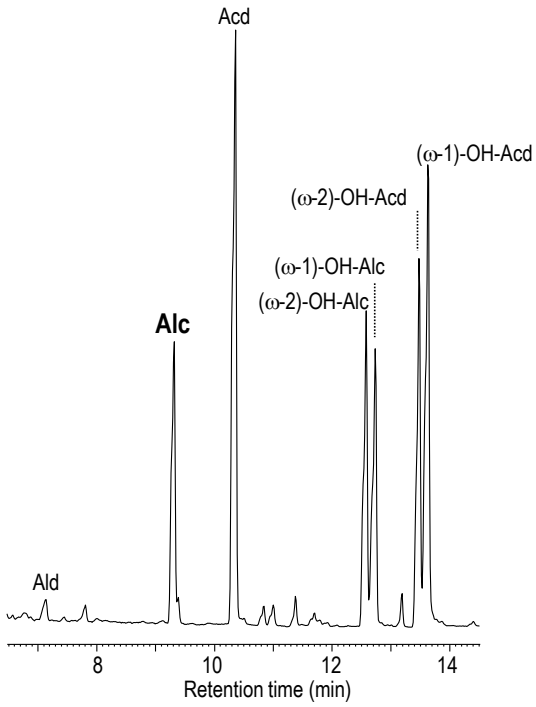

Fig. 4. GC-MS analysis of the recombinant *C. cinerea* peroxygenase reactions with tetradecanol at 30 min showing the remaining fatty alcohol substrate (Alc), its ω-1 and ω-2 monohydroxy derivatives, the corresponding fatty acid (Acd) formed, and the fatty acid ω-1 and ω-2 monohydroxy derivatives. Traces of aldehyde (Ald) formed are also shown.

The relative abundances of the different derivatives after 30 min reaction (**Table 3**) show that myristic acid is the main product of the *C. cinerea* peroxygenase reaction with tetradecanol. Therefore, it was deduced that hydroxylation at position 1 resulting in fatty acid formation (via the aldehyde and the intermediates mentioned below) takes place more rapidly than hydroxylation at the ω-1 and ω-2 positions to form the diols. In longer reaction times (**Table 3**) it can be observed how the amount of diols does not change noticeably whereas the hydroxyl fatty acids increase paralleling the decrease of fatty acids. The oxidation of fatty alcohols to the corresponding acids takes places by enzymatic hydroxylation and dehydration reactions taking advantage from the enzyme monooxygenase activity, as previously demonstrated for the *A. aegerita* peroxygenase using ^{18}O labeling (Gutiérrez et al., 2011).

Table 3

Abundance (relative percentage) of the different hydroxylated derivatives identified by GC-MS in the reactions of a fatty alcohol (tetradecanol) with recombinant *C. cinerea* peroxygenase at 30 min (t-30), 60 min (t-60) and 120 min (t-120) reaction times (Alc: alcohol, Acd: acid).

Substrate	(ω-1)-OH-Alc	(ω-2)-OH-Alc	Acd	(ω-1)-OH-Acd	(ω-2)-OH-Acd
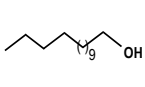	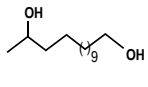	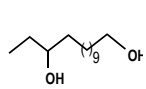	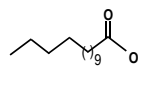	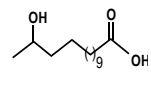	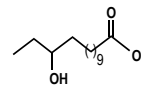
t-30	6.4	7.2	75.8	5.9	4.7
t-60	7.8	9.0	60.7	12.4	10.1
t-120	4.1	5.9	47.2	23.4	19.4

It is noteworthy that this hydroxylation is produced at the terminal position (-CH_2OH) (and not at the subterminal ones as the main reactions described above) which would be favored by the presence of a functional group. This can also explain the predominance of fatty acids and their hydroxylated derivatives over the derivatives of the fatty alcohols (diols) in the *C. cinerea* peroxygenase reactions with fatty alcohols. Similar conversion yield (**Table 1**) and predominance of fatty acid derivatives was observed in the reaction of tetradecanol with the *A. aegerita* peroxygenase. This differs from the reaction of 1-hexadecanol with P450BM-3, where the only products identified were isomers of hexadecanediol and the formation of the fatty acid was not produced (Miura and Fulco, 1975).

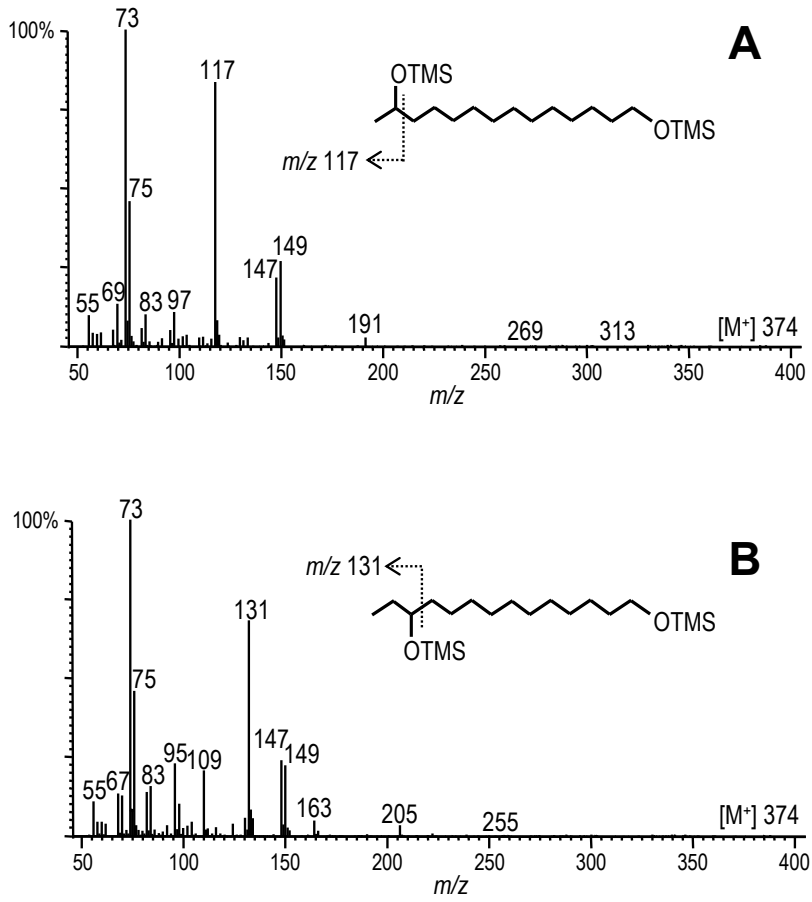

Fig. 5. Mass spectra of ω-1 (**A**) and ω-2 (**B**) monohydroxylated derivatives from peroxygenase reactions with tetradecanol (see **Fig. 4**), as TMS derivatives.

Alkane reactions

Linear alkanes are difficult to hydroxylate. The alkane C-H bond is extremely inert because of its high bond strength. Additionally, the similarity of methylene C-H bond strengths in a linear alkane and the lack of functional groups that can serve to direct catalysis make selective hydroxylation of these compounds especially interesting. In this work, a linear saturated long-chain alkane, *n*-tetradecane, was tested as *C. cinerea* peroxygenase substrate (**Table 1**). A 52% conversion rate was attained at 30 min reaction (in 20% acetone), which increased with reaction time (up to 55% and 62% after 60 and 120 min,

respectively). Several products including monohydroxylated derivatives at positions 2 or 3, dihydroxylated derivatives at positions 2 or 3 from both ends of the molecule (i.e. 2 and ω-1/ω-2, or 3 and ω-1/ω-2) and several combinations of keto and hydroxy derivatives were identified (**Fig. 6A**). The mass spectra of the TMS ethers of the mono- and dihydroxylated derivatives of tetradecane are shown in **Fig. 7**. Those of the monohydroxylated derivatives at positions 2 and 3 exhibited the typical fragments from the α-cleavage of the TMS group at *m/z* 117 and *m/z* 131, respectively. The other fragments of the α-cleavage of the TMS group are *m/z* 271 and *m/z* 257 for the 2 and 3 isomers, respectively. The molecular ions were not observed although, as in the case of fatty acids, they could be determined from the fragment corresponding to the loss of a methyl from the TMS group (*m/z* 271 for both isomers). The mass spectra of the TMS ethers of the dihydroxylated derivatives also exhibited the typical fragments at *m/z* 117 and *m/z* 131 arisen from the α-cleavage of the TMS group. Hence, the mass spectrum of 2,13-tetradecanediol (2, ω-1 dihydroxy alkanes) produces the fragment at *m/z* 117 from both sides of this symmetrical molecule, the mass spectrum of 2,12-tetradecanediol (2, ω-2 dihydroxy alkanes) produces the fragments at *m/z* 117 and *m/z* 131 from the 2 and the ω-2 sides of the molecule, and the mass spectrum of 3,12-tetradecanediol (3, ω-2 dihydroxy alkanes) produces the fragment at *m/z* 131 from both sides of this symmetrical molecule. The abundance of the different derivatives formed at several reaction times is shown in **Table 4**. Interestingly, dihydroxy and hydroxy-keto derivatives are predominant and monohydroxy derivatives are present in very low amounts in the reactions with 20% acetone. The predominance of dihydroxylated over monohydroxylated derivatives was also observed in the reactions with the *A. aegerita* peroxygenase (data not shown) with a substrate conversion of 24% (**Table 1**). It is worth mentioning that the enzymatic production of dihydroxylated derivatives (diols) is of great industrial interest and a patent has been recently filed on the use of fungal peroxygenase with this purpose (patent WO 2013/004639 A2).

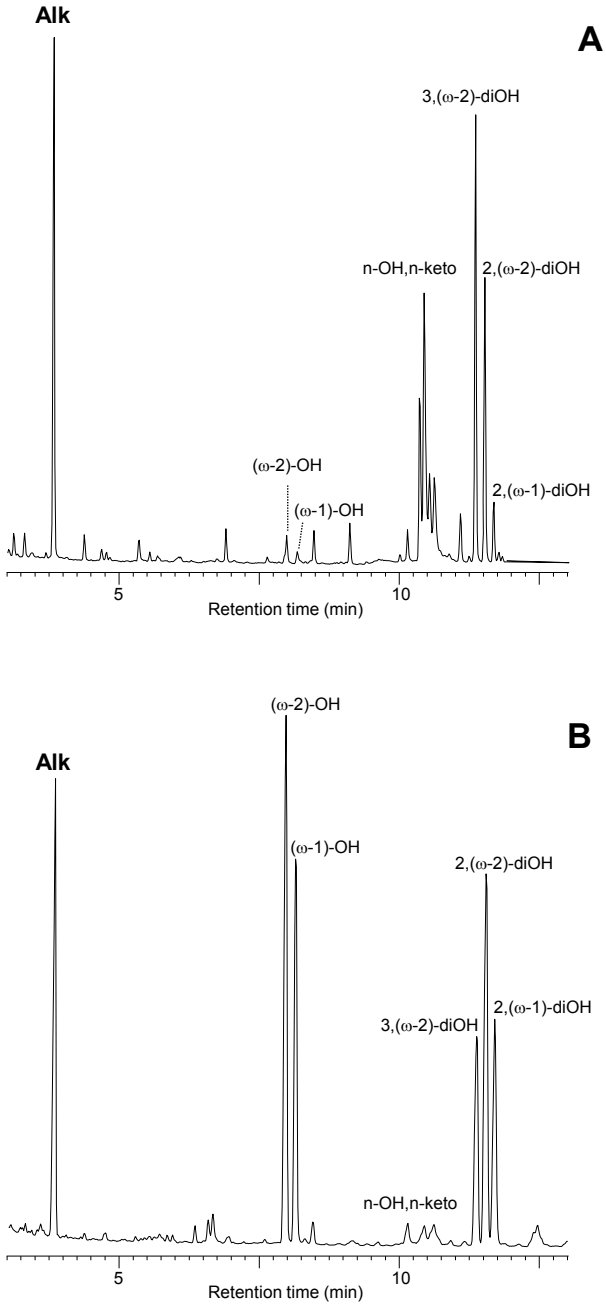

Fig. 6. GC-MS analysis of the recombinant *C. cinerea* peroxygenase reactions with tetradecane at 120 min in the presence of 20% (**A**) and 40% (**B**) acetone, showing the remaining alkane (Alk), and the ω-1 to ω-2 monohydroxy, hydroxy-keto and dihydroxy derivatives formed.

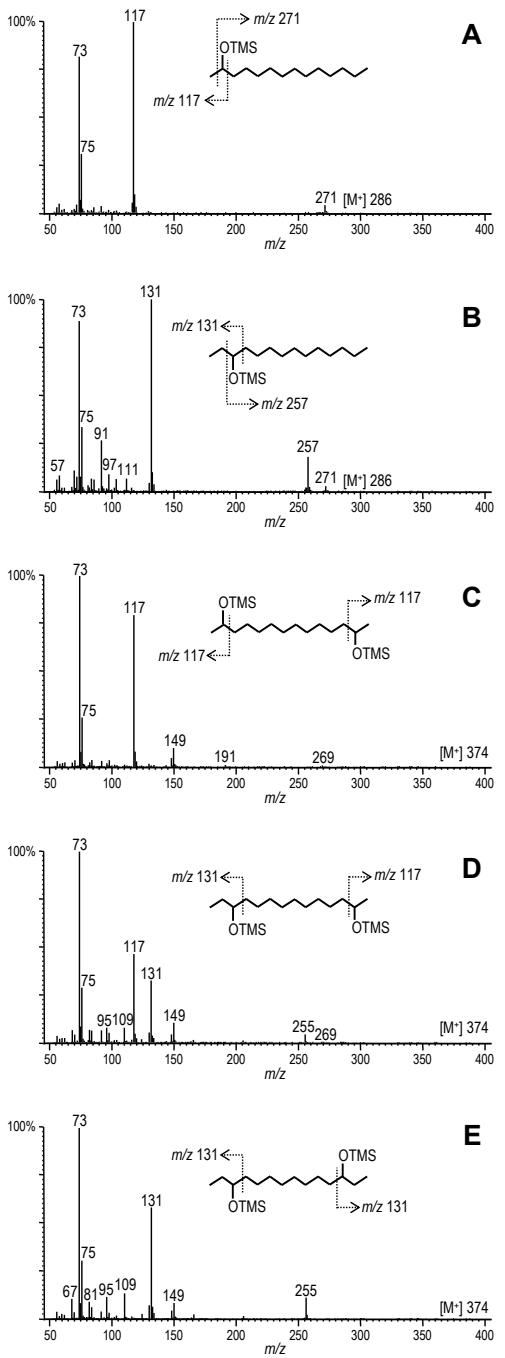

Fig. 7. Mass spectra of ω-1 (**A**) and ω-2 (**B**) monohydroxylated derivatives, and 2, (ω-1)-diOH (**C**); 2, (ω-2)-diOH (**D**) and 3, (ω-1)-diOH dihydroxylated (**E**) derivatives from peroxygenase reactions with tetradecane (**Fig. 6**), as TMS derivatives.

Table 4

Abundance (relative percentage) of the different hydroxylated derivatives identified by GC-MS in the reactions of an alkane (tetradecane) with the *C. cinerea* peroxygenase at 30 min (t-30), 60 min (t-60) and 120 min (t-120) reaction times, with different acetone concentrations (20% and 40%).

Substrate	(ω-1)-OH	(ω-2)-OH	2,(ω-1)-diOH	2,(ω-2)-diOH	3,(ω-2)-diOH	n-keto, n-OH
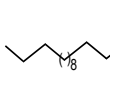	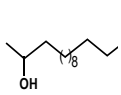	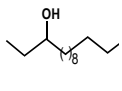	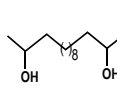	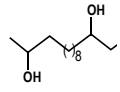	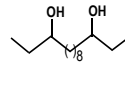	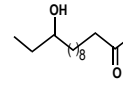
20% acetone						
t-30	2.0	4.0	3.8	10.0	10.6	69.6
t-60	1.0	2.2	2.8	13.0	16.0	65.0
t-120	1.0	1.9	1.7	9.5	15.0	70.1
40% acetone						
t-30	35.8	44.7	4.6	8.0	4.4	2.5
t-60	29.9	38.6	7.0	12.2	6.9	5.5
t-120	27.0	36.2	8.2	14.2	8.2	6.3

Since the enzymatic oxidation of alkanes in aqueous solutions is limited by their low solubility in water, the acetone concentration in the reactions of *C. cinerea* peroxygenase with tetradecane was increased to 40%. A higher conversion of substrate was attained in the latter case, after 30 min (64%), 60 min (71%) and 120 min (74%). Moreover, although the same reaction products were identified in the reactions with the two acetone concentrations (20% and 40%) the relative proportion of these products was definitely different (**Fig. 6B, Table 4**). With 40% acetone, the monohydroxylated derivatives were predominant, although a relatively high amount of dihydroxylated derivatives were still formed. Therefore, the predominance of mono-or dihydroxylated

derivatives seems related to the higher or lower proportion of acetone in the reaction. Similar results were obtained with the *A. aegerita* peroxygenase with an increase in substrate conversion from 24% to 45% (at 30 min) and predominance of monohydroxylated derivatives when the acetone concentration passed from 20% to 40% (data not shown). Then, the proportion of acetone was increased up to 60% and only monohydroxylated derivatives were identified in the reaction with *C. cinerea* peroxygenase (and also with *A. aegerita* peroxygenase). The predominance of dihydroxylated derivatives over the monohydroxylated ones observed in the reactions with 20% acetone, would be due to the higher solubility of the products (monohydroxylated derivatives) in the reaction medium compared with the substrate (alkane) that favors the preferential hydroxylation of the alcohols over the alkanes. At higher concentration of acetone in the reaction medium the alkanes become more soluble and both reactions are competing.

In addition to tetradecane, two unsaturated alkanes (*cis*-1-tetradecene and *trans*-7-tetradecene) were also tested as substrates of the *C. cinerea* peroxygenase (**Table 1**). Surprisingly, the former alkene did not show reactivity towards the enzyme (only traces of monohydroxylated derivatives were identified). The existence of a terminal double bond may have influenced the enzyme reactivity. In contrast, a high conversion (81%) was attained with *trans*-7-tetradecene and monohydroxylated derivatives at 2 (28%) and 3 (63%) positions were predominant over the dihydroxylated ones (9%), since 40% acetone was used in these reactions. On the other hand, a very much lower reactivity of *trans*-7-tetradecene was attained in the reaction with the *A. aegerita* peroxygenase, where a predominance of monohydroxylated derivatives at the 2 (57%) over the 3 (43%) positions was observed.

The oxyfunctionalization of hydrocarbons under mild conditions constitute a challenge of modern chemistry. Here it has been shown that *C. cinerea* peroxygenase introduce oxygen into a wide variety of molecules, including both saturated and unsaturated hydrocarbons in a selective manner, which is of interest for the synthesis of fine and bulk chemicals. Alkane hydroxylating activity was not observed in wild-type P450BM-3 (Miura and Fulco, 1975) although protein engineering by directed evolution and site-directed mutagenesis has generated variants able to hydroxylate alkanes of short to medium chain lengths (Glieder et al., 2002; Peters et al., 2012). The fact that only free fatty acids and alcohols, and not fatty acid methyl esters or alkanes, are

hydroxylated by wild-type P450BM-3 suggests the electrostatic binding of the substrate polar functional group to the enzyme. This would not be the case for the fungal peroxygenases, which are able to hydroxylate free and esterified fatty acids, alcohols and also alkanes. However, some regioselectivity change of *C. cinerea* peroxygenase is observed for higher chain-length substrates. Most probably this is related to the active-site access channel shape in this peroxygenase, as discussed for the fatty-acid esters.

Conclusions

Fungal peroxygenase, a novel biocatalyst for oxyfunctionalization of a variety of aliphatic compounds, will be commercially available to generate industrially useful products after the heterologous expression of a basidiomycete peroxygenase gene (from the *C. cinerea* genome) in an industrial host organism. The recombinant enzyme obtained is evaluated for the first time in the hydroxylation of long chain alkanes, fatty alcohols and free and esterified fatty acids. Interestingly, most of the aliphatic hydroxylations catalyzed are regioselective giving rise to both the ω-1 and ω-2 derivatives. An interesting exception is myristoleic acid hydroxylation giving rise exclusively to the ω-2 derivative. It is worth mentioning that the recombinant *C. cinerea* peroxygenase is also able to hydroxylate different long chain alkanes, giving rise to the corresponding diols in addition to the monohydroxylated derivatives. This is a challenging reaction, due to the extremely low reactivity of these compounds, that is not efficiently produced when a peroxygenase from a different basidiomycete (*A. aegerita*) is used. The above regioselectivity, together with its self-sufficient oxygenase activity (i.e. the ability to catalyze oxygenations without the help of intracellular flavo-enzymes and the requirement of a source of reducing power) and its expression in a suitable host organism make this first recombinant peroxygenase an interesting industrial biocatalyst for oxidative modification of different aliphatic compounds.

Acknowledgements

This study was funded by the PEROXICATS (KBBE-2010-4-265397) EU project. E.D. Babot thanks the Spanish CSIC for a JAE fellowship co-financed by FSE. R. Ullrich and M. Hofrichter are acknowledged for providing wild-type

A. aegerita peroxygenase preparation. The authors have no conflict of interest to declare.

References

Anh DH, Ullrich R, Benndorf D, Svatos A, Muck A, Hofrichter M. 2007. The coprophilous mushroom *Coprinus radians* secretes a haloperoxidase that catalyzes aromatic peroxygenation. Appl. Environ. Microbiol. 73: 5477-5485.

Bernhardt R. 2006. Cytochromes P450 as versatile biocatalysts. J. Biotechnol. 124: 128-145.

Boddupalli SS, Pramanik BC, Slaughter CA, Estabrook RW, Peterson JA. 1992. Fatty-acid monooxygenation by P450Bm-3: Product identification and proposed mechanisms for the sequential hydroxylation reactions. Arch. Biochem. Biophys. 292: 20-28.

Capdevila JH, Wei SZ, Helvig C, Falck JR, Belosludtsev Y, Truan G, GrahamLorence SE, Peterson JA. 1996. The highly stereoselective oxidation of polyunsaturated fatty acids by cytochrome P450BM-3. J. Biol. Chem. 271: 22663-22671.

Cherry JR, Lamsa MH, Schneider P, Vind J, Svendsen A, Jones A, Pedersen AH. 1999. Directed evolution of a fungal peroxidase. Nat. Biotechnol. 17: 379-384.

Dolge C, Sass A, Kayser G, Ullrich R, Hofrichter M. 2011. Exploration of r*Cci*APO1 from *Coprinopsis cinerea*: First recombinant aromatic peroxygenase. BIOspektrum, special issue of Proc. VAAM (Association for General and Applied Microbiology) Annu. Confer. (Karlsruhe, 3-6 April), 132-132.

Floudas D, Binder M, Riley R, Barry K, Blanchette RA, Henrissat B, Martínez AT, Otillar R, Spatafora JW, Yadav JS, Aerts A, Benoit I, Boyd A, Carlson A, Copeland A, Coutinho PM, de Vries RP, Ferreira P, Findley K, Foster B, Gaskell J, Glotzer D, Górecki P, Heitman J, Hesse C, Hori C, Igarashi K, Jurgens JA, Kallen N, Kersten P, Kohler A, Kües U, Kumar TKA, Kuo A, LaButti K, Larrondo LF, Lindquist E, Ling A, Lombard V, Lucas S, Lundell T, Martin R, McLaughlin DJ, Morgenstern I, Morin E, Murat C, Nolan M, Ohm RA, Patyshakuliyeva A, Rokas A, Ruiz-Dueñas FJ, Sabat G, Salamov A, Samejima M, Schmutz J, Slot JC, St John F, Stenlid J, Sun H, Sun S, Syed K, Tsang A, Wiebenga A, Young D, Pisabarro A, Eastwood DC, Martin F, Cullen D, Grigoriev IV, Hibbett DS. 2012. The Paleozoic origin of enzymatic lignin decomposition reconstructed from 31 fungal genomes. Science 336: 1715-1719.

Glieder A, Farinas ET, Arnold FH. 2002. Laboratory evolution of a soluble, self-sufficient, highly active alkane hydroxylase. Nat. Biotechnol. 20: 1135-1139.

Gröbe G, Ullrich M, Pecyna M, Kapturska D, Friedrich S, Hofrichter M, Scheibner K. 2011. High-yield production of aromatic peroxygenase by the agaric fungus *Marasmius rotula* . AMB Express 1: 31-42.

Gutiérrez A, Babot ED, Ullrich R, Hofrichter M, Martínez AT, del Río JC. 2011. Regioselective oxygenation of fatty acids, fatty alcohols and other aliphatic compounds by a basidiomycete heme-thiolate peroxidase. Arch. Biochem. Biophys. 514: 33-43.

Gutiérrez A, del Río JC, González-Vila FJ, Martín F. 1998. Analysis of lipophilic extractives from wood and pitch deposits by solid-phase extraction and gas chromatography. J. Chromatogr. 823: 449-455.

Hofrichter M, Ullrich R, Pecyna MJ, Liers C, Lundell T. 2010. New and classic families of secreted fungal heme peroxidases. Appl. Microbiol. Biotechnol. 87: 871-897.

Johnston JB, Ouellet H, Podust LM, Ortiz de Montellano PR. 2011. Structural control of cytochrome P450-catalyzed w-hydroxylation. Arch. Biochem. Biophys. 507: 86-94.

Li H. 2001. Cytochrome P450, in: Messerschmidt A, Huber R, Poulos TL, Wieghardt K. (Eds.), Handbook of metalloproteins. Wiley, Baffins Lane, UK, pp. 267-282

Li HY, Poulos TL. 1997. The structure of the cytochrome p450BM-3 haem domain complexed with the fatty acid substrate, palmitoleic acid. Nature Struct. Biology 4: 140-146.

Marques G, Gutiérrez A, del Río JC. 2007. Chemical characterization of lignin and lipophilic fractions from leaf fibers of curaua (*Ananas erectifolius*). J. Agric. Food Chem. 55: 1327-1336.

Miura Y, Fulco AJ. 1975. w-1, w-2 and w-3 hydroxylation of long-chain fatty-acids, amides and alcohols by a soluble enzyme-system from *Bacillus megaterium*. Biochim. Biophys. Acta-Lipids Lipid Metab. 388: 305-317.

Morita Y, Yamashita H, Mikami B, Iwamoto H, Aibara S, Terada M, Minami J. 1988. Purification, crystallization, and characterization of peroxidase from *Coprinus cinereus*. J. Biochem. (Tokyo) 103: 693-699.

Munro AW, Leys DG, McLean KJ, Marshall KR, Ost TWB, Daff S, Miles CS, Chapman SK, Lysek DA, Moser CC, Page CC, Dutton PL. 2002. P450BM3: the very model of a modern flavocytochrome. Trends Biochem. Sci. 27: 250-257.

Narhi LO, Fulco A. 1986. Characterization of a catalytically self-sufficient 119,000-dalton cytochrome-P-450 monooxygenase induced by barbiturates in *Bacillus megaterium*. J. Biol. Chem. 261: 7160-7169.

Noble MA, Miles CS, Chapman SK, Lysek DA, Mackay AC, Reid GA, Hanzlik RP, Munro AW. 1999. Roles of key active-site residues in flavocytochrome P450 BM3. Biochem. J. 339: 371-379.

Ortiz de Montellano PR. 2005. Cytochrome P450: Structure, mechanism, and biochemistry. Kluwer Academic/Plenum, New York.

Pazmino DET, Winkler M, Glieder A, Fraaije MW. 2010. Monooxygenases as biocatalysts: Classification, mechanistic aspects and biotechnological applications. J. Biotechnol. 146: 9-24.

Pecyna MJ, Ullrich R, Bittner B, Clemens A, Scheibner K, Schubert R, Hofrichter M. 2009. Molecular characterization of aromatic peroxygenase from *Agrocybe aegerita*. Appl. Microbiol. Biotechnol. 84: 885-897.

Peter S, Kinne M, Wang X, Ullrich R, Kayser G, Groves JT, Hofrichter M. 2011. Selective hydroxylation of alkanes by an extracellular fungal peroxygenase. FEBS J. 278: 3667-3675.

Peters MW, Meinhold P, Glieder A, Arnold FH. 2012. Regio- and enantioselective alkane hydroxylation with engineered P450 BM-3. J. Am. Chem. Soc. 125: 13442-13450.

Piontek K, Ullrich R, Liers C, Diederichs K, Plattner DA, Hofrichter M. 2010. Crystallization of a 45 kDa peroxygenase/peroxidase from the mushroom *Agrocybe aegerita* and structure determination by SAD utilizing only the haem iron. Acta Crystallogr. F 66: 693-698.

Truan G, Komandla MR, Falck JR, Peterson JA. 1999. P450BM-3: Absolute configuration of the primary metabolites of palmitic acid. Arch. Biochem. Biophys. 366: 192-198.

Ullrich R, Hofrichter M. 2007. Enzymatic hydroxylation of aromatic compounds. Cell. Mol. Life Sci. 64: 271-293.

Ullrich R, Nuske J, Scheibner K, Spantzel J, Hofrichter M. 2004. Novel haloperoxidase from the agaric basidiomycete *Agrocybe aegerita* oxidizes aryl alcohols and aldehydes. Appl. Environ. Microbiol. 70: 4575-4581.

Xu F. 2005. Applications of oxidoreductases: Recent progress. Industr. Biotechnol. 1: 38-50.

6.1. Publicación III:

Babot E.D., del Río J.C., Cañellas M., Sancho F., Lucas F., Guallar V., Kalum L., Lund H., Gröbe G., Scheibner K., Ullrich R., Hofrichter M., Martínez A.T. and Gutiérrez A. (2015) Steroid hydroxylation by basidiomycete peroxygenases: A combined experimental and computational study. *Applied and Environmental Microbiology* 81:4130-4142.

Este artículo fue seleccionado como uno de los cinco mejores de entre los publicados en el volumen 81 de la revista *Applied and Environmental Microbiology* y se escogió como portada para dicho volumen.

Steroid hydroxylation by basidiomycete peroxygenases: A combined experimental and computational study

Esteban D. Babot,[a] José C. del Río,[a] Marina Cañellas,[b,c] Ferran Sancho,[b,c] Fátima Lucas,[b] Víctor Guallar,[b,d] Lisbeth Kalum,[e] Henrik Lund,[e] Glenn Gröbe,[f] Katrin Scheibner,[f] René Ullrich,[g] Martin Hofrichter,[g] Angel T. Martínez[h] and Ana Gutiérrez[a*]

[a]Instituto de Recursos Naturales y Agrobiología de Sevilla, CSIC, Reina Mercedes 10, E-41012 Seville, Spain

[b]Joint BSC-CRG-IRB Research Program in Computational Biology, Barcelona Supercomputing Center, Jordi Girona 29, E-08034 Barcelona, Spain

[c]Anaxomics Biotech, Balmes 89, E-08008 Barcelona, Spain

[d]ICREA, Passeig Lluís Companys 23, E-08010 Barcelona, Spain

[e]Novozymes A/S, Krogshoejvej 36, 2880 Bagsvaerd, Denmark

[f]JenaBios GmbH, Orlaweg 2, 00743 Jena, Germany

[g]TU Dresden, Department of Bio- and Environmental Sciences, Markt 23, 02763 Zittau, Germany

[h]Centro de Investigaciones Biológicas, CSIC, Ramiro de Maeztu 9, E-28040 Madrid, Spain

* Corresponding author

Abstract:

The goal of this study is the selective oxyfunctionalization of steroids under mild and environmentally friendly conditions using fungal enzymes. With this purpose, peroxygenases from three basidiomycete species were tested for the hydroxylation of a variety of steroidal compounds, using H_2O_2 as the only cosubstrate. Two of them are wild-type enzymes from *Agrocybe aegerita* and *Marasmius rotula*, and the third one is a recombinant enzyme from *Coprinopsis cinerea*. The enzymatic reactions on free and esterified sterols, steroid hydrocarbons, and ketones were monitored by gas chromatography, and the products were identified by mass spectrometry. Hydroxylation at the side chain over the steroidal rings was preferred, with the 25-hydroxyderivatives predominating. Interestingly, antiviral and other biological activities of 25-

hydroxycholesterol have been reported recently (M. Blanc et al., Immunity 38:106-118, 2013, http://dx.doi.org/10.1016/j.immuni.2012.11.004). However, hydroxylation in the ring moiety and terminal hydroxylation at the side chain also was observed in some steroids, the former favored by the absence of oxygenated groups at C-3 and by the presence of conjugated double bonds in the rings. To understand the yield and selectivity differences between the different steroids, a computational study was performed using Protein Energy Landscape Exploration (PELE) software for dynamic ligand diffusion. These simulations showed that the active-site geometry and hydrophobicity favors the entrance of the steroid side chain, while the entrance of the ring is energetically penalized. Also, a direct correlation between the conversion rate and the side chain entrance ratio could be established that explains the various reaction yields observed.

Keywords: basidiomycete peroxygenases, steroids, selective hydroxylation, GC–MS, PELE simulation.

Introduction

Steroids represent an important class of natural compounds that are widespread in nature and have a multitude of pharmacological properties. Indeed, steroids are ranked among the most marketed medical products and represent the second largest category next to antibiotics. The physiological activity of steroids depends on their structures, including the oxidation state of the rings, and the type, number, and regio- and stereoposition of the functional groups attached (1). It is known that even minor changes in the structure of steroids can highly affect their biological activity, which has promoted countless studies on the modification of naturally occurring steroids in search of new and more active compounds (2). Among these modifications, hydroxylation is one of the most important reactions in steroid oxyfunctionalization.

Hydroxylation serves to increase the polarity of the rather hydrophobic steroids, and hydroxylated steroids often express a higher level of biological activity than their less polar nonhydroxylated analogs. Moreover, hydroxylation can be used to develop intermediates for further synthesis by offering access to otherwise inaccessible sites of the steroid molecule. These modifications have

been obtained mostly by applying microorganisms (1), with only a few examples where isolated enzymes were used. Members of the cytochrome P450 monooxygenase (P450s) superfamily are notable examples of such enzymatic catalysts, since, because of their catalytic versatility, they would perfectly meet the requirements of chemical synthesis (3, 4). However, large-scale applications are not yet feasible due to the intrinsic properties of these oxygenases (5), whose activation requires NAD(P)H as an electron donor and auxiliary flavin-reductases (or a second flavin domain) for electron transfer to O_2 (6).

A few years ago, a new peroxidase type was discovered in the wood-dwelling basidiomycete *Agrocybe aegerita* (7), which turned out to be a true peroxygenase efficiently transferring oxygen from peroxide to various organic substrates (8). This peroxygenase is able to catalyze reactions formerly assigned only to P450s (9). However, unlike P450s, which are intracellular enzymes whose activation often requires an auxiliary enzyme and a source of reducing power, the *A. aegerita* enzyme is a secreted protein; therefore, it is far more stable and requires only H_2O_2 for activation (8). The *A. aegerita* peroxygenase has been shown to catalyze numerous interesting oxygenation reactions on aromatic compounds (10), and recently, the action of this enzyme on aliphatic compounds was demonstrated, expanding its biotechnological interest (11, 12). The enzyme, first described as a haloperoxidase and later mostly referred to as aromatic peroxygenase (APO), now is named "unspecific peroxygenase" (UPO; EC 1.11.2.1).

After the first peroxygenase of *A. aegerita* (7), similar enzymes also have been found in other basidiomycetes, such as *Coprinellus radians* (13) and *Marasmius rotula* (14), and there are indications for their widespread occurrence in the fungal kingdom (15). Recently, over 100 peroxygenase-type genes (encoding enzymes of the heme-thiolate peroxidase superfamily) have been identified during the analysis of 24 basidiomycete genomes (16), including *Coprinopsis cinerea* (17). The wild-type *C. cinerea* peroxygenase has not been isolated to date from this fungus, but one of the peroxygenase genes from its genome (protein model 7249, available from the Joint Genome Institute [JGI; http://genome.jgi.doe.gov/Copci1]) was heterologously expressed by Novozymes A/S (Bagsvaerd, Denmark). This first recombinant peroxygenase can be a powerful biocatalyst for synthetic applications because of the potentially high expression yield and the possibility of tuning its catalytic and operational properties using protein engineering tools. Recently, the ability of this

recombinant peroxygenase in the oxyfunctionalization of several aliphatic compounds was demonstrated (18).

Here, the efficiency of three different peroxygenases, namely, the wild enzymes from *A. aegerita* (*Aae*UPO) and *M. rotula* (*Mro*UPO) and the recombinant enzyme from *C. cinerea* (r*Cci*UPO), in oxyfunctionalization of a variety of steroidal compounds (including free and esterified sterols, steroid hydrocarbons, and ketones) is evaluated for the first time. All three fungi are agaric basidiomycetes, but they belong to different families of the order *Agaricales*, and they also differ to some extent from an ecophysiological point of view. *M. rotula* (family *Marasmiaceae*) is a fungus that stands between white rotters and litter decomposers, because it preferably colonizes small twigs of broad-leaved trees (*Fagus*, *Quercus*, and *Acer*). *C. cinerea* (family *Psathyrellaceae*) naturally dwells on older dung and in soils rich in organic nitrogen (i.e., it is a specialized litter decomposer). *A. aegerita* (family *Bolbitaceae*) is a wood-dwelling fungus that causes an unspecific white rot on trunks and stumps of broad-leaved trees (e.g., *Populus* and *Acer* species). However, it would be daring to conclude from these evolutionary and ecological differences that the UPOs of these fungi must be different.

In addition to the experimental assays, where the products from the reaction of a variety of steroids with the three abovementioned peroxygenases were analyzed by gas chromatographymass spectrometry (GC-MS), a set of representative molecules was selected for computational simulations with *Aae*UPO (for which a crystal structure is available) to get further insights into the molecular determinants that affect the reactivity of the different steroid types. All simulations followed an identical protocol where, after appropriate preparation of the protein with heme as compound I [the two-electron oxidized cofactor containing an Fe(IV)=O porphyrin cation radical complex], each substrate was placed at the entrance of the heme access channel, still in the solvent. From there the substrate explored both the entrance pathway and the active site using Protein Energy Landscape Exploration (PELE) software (19, 20). From the information provided by the energy profiles and trajectories, analyses of the effect of the structural differences between the substrates and their peroxygenase reactivity could be rationalized.

Materials and methods

Enzymes

r*Cci*UPO was provided by Novozymes A/S (Bagsvaerd, Denmark). This recombinant enzyme corresponds to the protein model 7249 from the sequenced *C. cinerea* genome, available at the JGI (http://genome.jgi.doe.gov/Copci1), expressed in *Aspergillus oryzae* (40). The protein was purified using a combination of S-sepharose and SP-sepharose ion-exchange chromatography. The recombinant peroxygenase preparation is an electrophoretically homogeneous glycoprotein with a molecular mass of around 44 kDa (a nonuniform glycosylation pattern was observed), a typical UV-visible (UV-Vis) spectrum with a Soret band at 418 nm, and the ability to oxygenate different aromatic compounds with a specific activity of approximately 100 U · mg^{-1} (measured as described below).

The *Aae*UPO and *Mro*UPO enzymes are two wild-type peroxygenases isolated from cultures of *A. aegerita* DSM 22459 and *M. rotula* DSM 25031, deposited at the German Collection of Microorganisms and Cell Cultures (Braunschweig, Germany). *Aae*UPO was produced in suspensions of soybean meal and purified by several steps of fast protein liquid chromatography (FPLC) using different ion exchangers (SP-sepharose, MonoQ, and MonoS) with size exclusion chromatography (Superdex 75) as the final isolation step. The final protein fraction had a molecular mass of 46 kDa with one enriched isoform (*Aae*UPO II). This isoform was used in the present study (7, 21). *Mro*UPO was purified by FPLC to apparent homogeneity, confirmed by sodium dodecyl sulfate-polyacrylamide gel electrophoresis (SDS-PAGE) under denaturing conditions, and showed a molecular mass of 32 kDa and an isoelectric point of pH 5.0 to 5.3. The UV-visible spectra of the enzymes showed a characteristic maximum around 420 nm (Soret band of heme-thiolate proteins) (14).

All media and columns used for enzyme isolation were purchased from GE Healthcare Life Sciences. One UPO activity unit is defined as the amount of enzyme oxidizing 1 μmol of veratryl alcohol to veratraldehyde (ε310, 9,300 M^{-1} · cm^{-1}) in 1 min at 24 °C, pH 7 (the optimum for peroxygenase activity), after addition of H_2O_2 (0.5 mM H_2O_2 in r*Cci*UPO reaction mixtures and 2.5 mM H_2O_2 in *Aae*UPO and *Mro*UPO reaction mixtures).

Steroids

The model steroid compounds (from Sigma-Aldrich) used in the enzymatic reactions include (i) free sterols, such as cholesterol, campesterol, ergosterol, sitosterol, and stigmasterol; (ii) steroid ketones, such as cholestan-3-one, 4-cholesten-3-one, cholesta-3,5-dien-7-one, and testosterone; (iii) steroid hydrocarbons, such as cholestane, cholesta-3,5-diene, and pregnane; and (iv) sterol esters, such as cholesteryl acetate, cholesteryl butyrate, and cholesteryl caprylate (see **Fig. 1**).

Enzymatic reactions

Reactions of the model steroids (0.05 mM concentration) with the three peroxygenases (1 U) were performed in 5 ml vials containing 50 mM sodium phosphate (pH 7 in *Aae*UPO and r*Cci*UPO reactions and pH 5.5 in *Mro*UPO reactions) at 40 °C and a 60 min reaction time in the presence of H_2O_2 (0.5 mM in r*Cci*UPO reactions and 2.5 mM in *Aae*UPO and *Mro*UPO reactions). Prior to use, the substrates were dissolved in acetone and added to the buffer to give a final acetone concentration of 40% (vol/vol) in most cases. In control experiments, substrates were treated under the same conditions (including 0.5 mM and 2.5 mM H_2O_2) but without enzyme. Products were recovered by liquid-liquid extraction with methyl *tert*butyl ether and dried under N_2. *N*,*O*-Bis(trimethylsilyl)trifluoroacetamide (Supelco) was used to prepare trimethylsilyl (TMS) derivatives that were analyzed by GC-MS.

GC-MS analyses

The GC-MS analyses were performed with a Varian 3800 chromatograph coupled to an ion-trap detector (Varian 4000) using a medium-length fused-silica DB-5HT capillary column (12 m by 0.25 mm internal diameter, 0.1 μm film thickness) from J&W Scientific (22). The oven was heated from 120 °C (1 min) to 300 °C (15 min) at 10 °C · min^{-1}. The injector was programmed from 60 °C (0.1 min) to 300 °C (28 min) at 200 °C · min^{-1}. The transfer line was kept at 300 °C, and helium was used as the carrier gas (2 ml · min^{-1}). For some analyses, a Shimadzu GC-MS QP2010 Ultra with a fused-silica DB-5HT capillary column (30m by 0.25 mm internal diameter, 0.1 μm film thickness) also was used. The oven was heated from 120°C (1 min) to 300°C (15 min) at 5°C·min^{-1}.

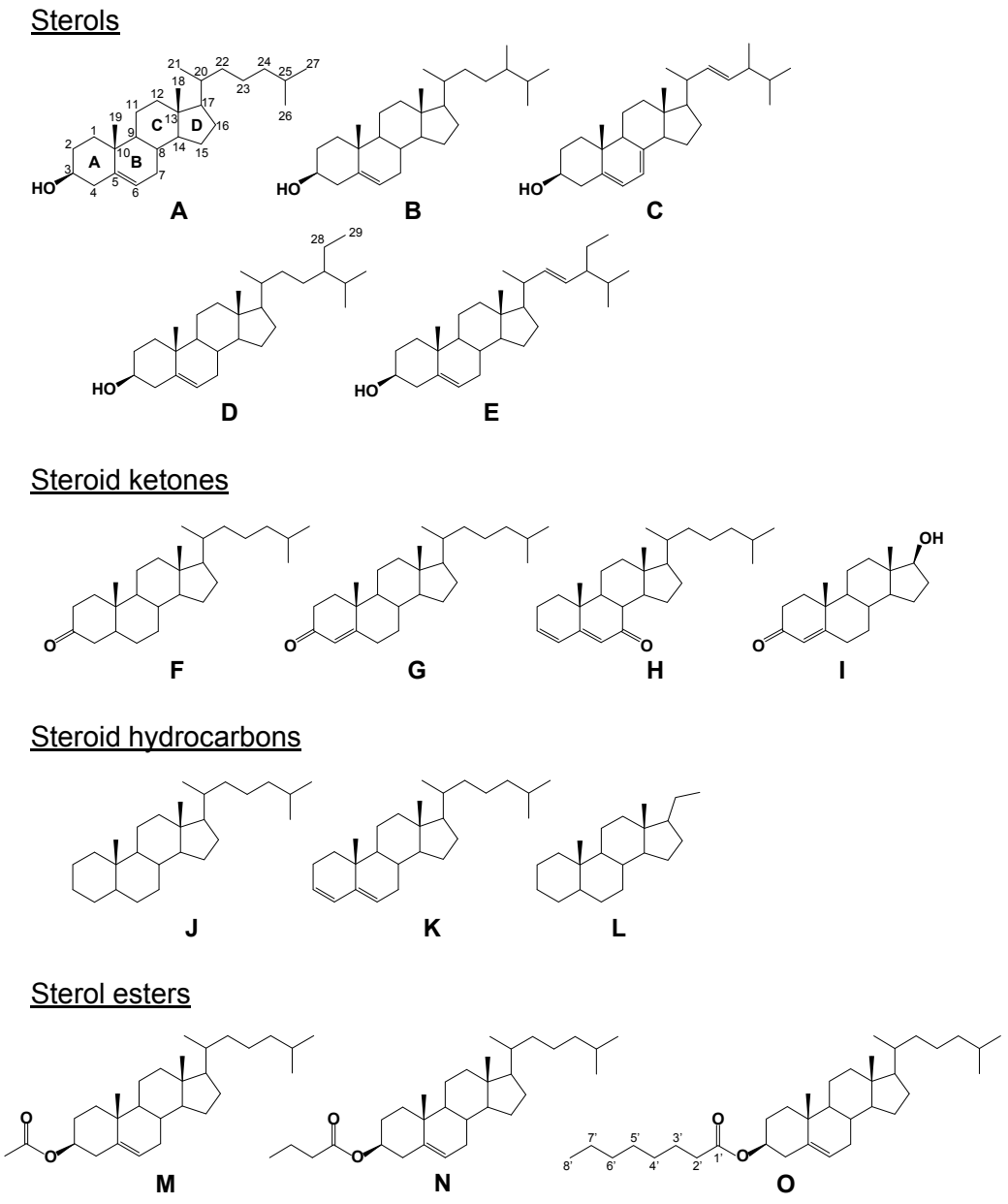

Fig 1. Chemical structures of the different steroid compounds tested as substrates of the peroxygenases including: i) free sterols such as cholesterol (**A**), campesterol (**B**), ergosterol (**C**), sitosterol (**D**) and stigmasterol (**E**); ii) steroid ketones such as cholestan-3-one (**F**), 4-cholesten-3-one (**G**), cholesta-3,5-dien-7-one (**H**) and testosterone (**I**); iii) steroid hydrocarbons such as cholestane (**J**), cholesta-3,5-diene (**K**) and pregnane (**L**); and iv) sterol esters such as cholesteryl acetate (**M**), cholesteryl butyrate (**N**) and cholesteryl caprylate (**O**).

The injection was performed at 300°C, and the transfer line was kept at 300°C. Compounds were identified by mass fragmentography and comparing their mass spectra with those of the Wiley and NIST libraries and standards. Quantification was obtained from total-ion peak area, using response factors of the same or similar compounds. Data from replicates were averaged, and in all cases (substrate conversion and relative abundance of reaction products) the standard deviations were below 3.5% of the mean values.

PELE computational analyses

For the computational study, eight representative compounds (cholesterol, sitosterol, cholestan-3-one, cholesta-3,5-dien-7-one, cholestane, cholesta-3,5-diene, cholesteryl acetate, and cholesteryl caprylate) were prepared and PELE simulations performed.

The starting structure for all PELE simulations was the *Aae*UPO 2.19 Å resolution crystal (PDB entry 2YOR) (23). As the optimum pH for peroxygenase activity is 7, the structure was prepared accordingly using Schrodinger's Protein Preparation Wizard (24) and H++ web server (25). Histidines were δ-protonated, with the exception of His-82 (ε-protonated) and His-118 and His-251 (double protonated). All acidic residues were deprotonated, except Asp-85, which was kept in its protonated state. The eight ligands studied in this section were optimized with Jaguar 7.8 (Schrödinger, LLC, New York, NY) at the DFT/M06 level with the 6-31G** basis and a PBF implicit solvent in order to obtain their electrostatic potential atomic charges. Finally, the heme site was modeled as compound I after being fully optimized in the protein environment with quantum mechanics/molecular mechanics (QM/MM) using QSite 5.7 (Schrödinger).

Once the initial protein structure was prepared, the optimized ligands were placed manually in identical positions at the entrance of the protein's binding pocket and PELE (20) simulations were performed. PELE is a Monte Carlo-based algorithm that produces new configurations through a sequential ligand and protein perturbation, side-chain prediction, and minimization steps. New configurations then are filtered with a Metropolis acceptance test, where the energy is described with an all-atom OPLS force field (26) and a surface-generalized Born solvent (27). In this way it is possible to locate and characterize local and global minima structures for the most favorable protein-ligand

interactions. PELE has been used successfully in a number of ligand migration studies with both small and large substrates (28–30). In this work, PELE was set up first to drive the ligands inside the protein until the center of mass was less than 10 Å from the compound I oxygen. After that, simulation proceeded by allowing a free exploration of the enzyme active site by the ligand. The results presented are based on ~350 48-h trajectories for each ligand.

Results

The efficiency of three peroxygenases (*Aae*UPO, *Mro*UPO, and r*Cci*UPO) hydroxylating 15 steroidal compounds (including free and esterified sterols, steroid hydrocarbons, and ketones) was experimentally evaluated, and the reaction products were analyzed by GC-MS. To rationalize the results obtained with the different steroid types, substrate diffusion simulations were performed with PELE (20), providing energy profiles and ligand trajectories, as described in the final section.

Free sterol reactions. Free C_{27} (cholesterol), C_{28} (campesterol and ergosterol), and C_{29} (sitosterol and stigmasterol) sterols (**Fig. 1A** to **E**, respectively) were tested as UPO substrates (**Table 1**). Cholesterol was converted to a larger extent than the other sterols, although the individual enzymes showed differences in their performance (after 60 min): r*Cci*UPO completely (100%) transformed the substrate, followed by *Aae*UPO (64%) and *Mro*UPO (23%). The reaction products of cholesterol were oxygenated derivatives at the C-24, C-25, and C-26/C-27 positions of the side chain (**Fig. 1** depicts atom numbering), with the monohydroxylated C-25 derivative predominating (**Table 2**). Interestingly, a strict regioselectivity was observed in the reaction of cholesterol with r*Cci*UPO, yielding 25-hydroxycholesterol as the sole reaction product.

The position of the hydroxyl group was determined by the mass spectra of the TMS derivatives, as found for 25-hydroxycholesterol (see **Fig. S1** in the supplemental material). The spectrum includes the molecular ion (*m/z* 546) and a characteristic ion at *m/z* 131, resulting from C-24–C-25 bond cleavage, together with additional fragments. Likewise, the spectra of monohydroxylated derivatives at C-24 and C-26 (not shown) showed, in addition to the molecular ion at *m/z* 546, the characteristic fragment at *m/z* 131, described above, and that

at *m/z* 145 from the C-23–C-24 bond cleavage. In the *Aae*UPO and *Mro*UPO reactions, further oxidized compounds (carboxycholesterol) at C-26/C-27 were identified (with a molecular ion at *m/z* 560 and the above-described characteristic fragment at *m/z* 145), although they were in small amounts.

Table 1

Conversion of different types of steroid compounds by the r*Cci*UPO, *Aae*UPO, and *Mro*UPO peroxygenases within a 60-min reaction.

	% substrate transformed by:		
Substrate	r*Cci*UPO	*Aae*UPO	*Mro*UPO
Free sterols			
Cholesterol	100	64	23
Campesterol	30	47	10
Ergosterol	6	10	7
Sitosterol	6	13	4
Stigmasterol	2	2	5
Steroid ketones			
Cholestan-3-one	54	42	12
4-Cholesten-3-one	100	67	14
Cholesta-3,5-dien-7-one	97	57	39
Testosterone	0	0	0
Steroid hydrocarbons			
Cholestane	14	3	1
Cholesta-3,5-diene	34	18	23
Pregnane	0	0	37
Sterol esters			
Cholesteryl acetate	34	16	5
Cholesteryl butyrate	7	1	1
Cholesteryl caprylate	0	0	0

Table 2

Abundance of the different oxygenated derivatives identified by GC-MS in the reactions of free sterols with r*Cci*UPO, *Aae*UPO, and *Mro*UPO peroxygenases.

	Abundance (relative %) of derivative with:				
Derivative	24-OH	25-OH	26/27-OH	28-OH	26/27-COOH
Cholesterol					
r*Cci*UPO	-	100	-	-	-
*Aae*UPO	6	80	9	-	5
*Mro*UPO	-	89	6	-	5
Campesterol					
r*Cci*UPO	-	85	15	-	-
*Aae*UPO	-	99	1	-	-
*Mro*UPO	-	98	2	-	-
Ergosterol					
r*Cci*UPO	-	100	-	-	-
*Aae*UPO	-	100	-	-	-
*Mro*UPO	-	100	-	-	-
Sitosterol					
r*Cci*UPO	-	52	-	48	-
*Aae*UPO	-	94	-	6	-
*Mro*UPO	-	100	-	-	-
Stigmasterol					
r*Cci*UPO	-	100	-	-	-
*Aae*UPO	-	100	-	-	-
*Mro*UPO	-	100	-	-	-

The C_{28} sterols, especially ergosterol, were transformed to a lesser extent than cholesterol (**Table 1**). *Aae*UPO showed more reactivity toward campesterol and ergosterol than the other peroxygenases. The reaction of ergosterol was strictly regioselective, with 25-hydroxyergosterol being the only reaction product identified in all cases (**Table 2**). The reaction with campesterol also was highly regioselective, giving the 25-hydroxyderivative as the main product, although hydroxylation at C-26 also was observed (especially in the r*Cci*UPO reaction). Likewise, the three peroxygenases showed low reactivity with the C_{29} sterols, and only very low conversion rates (<13%) were attained (**Table 1**). In the reaction with stigmasterol, only the monohydroxylated derivative at C-25 was observed, whereas with sitosterol, nearly the same amount of 28-hydroxysitosterol was formed by r*Cci*UPO (and a small amount by *Aae*UPO) (**Table 2**).

Steroid ketone reactions. Cholestan-3-one, 4-cholesten-3-one, cholesta-3,5-dien-7-one, and testosterone (**Fig. 1F** to **I**, respectively) were tested as UPO substrates (**Table 1**). r*Cci*UPO was the most efficient enzyme in transforming steroid ketones except testosterone, which was not modified by any of the three peroxygenases, followed by *Aae*UPO and *Mro*UPO. The unsaturated 4-cholesten-3-one and cholesta-3,5-dien-7-one were completely transformed by r*Cci*UPO, and the saturated cholestan-3-one also was significantly transformed (54%).

The three ketones were predominantly monohydroxylated at C-25 (**Table 3**). In the case of cholestan-3-one, the regioselectivity was strict, since only the 25-monohydroxylated derivative was formed by the three enzymes, and the same was observed in the reactions of 4-cholesten-3-one with r*Cci*UPO and *Mro*UPO. However, in the reaction with *Aae*UPO, monohydroxylation at the 4-cholesten-3-one terminal positions (C-26/C-27) also was observed, although as a minor proportion. Interestingly, in the reaction of the diunsaturated cholesta-3,5-dien-7-one, hydroxylation in the steroidal ring also was produced, being especially pronounced in the *Mro*UPO reaction.

Table 3

Abundance of the different oxygenated derivatives identified by GC-MS in the reactions of steroid ketones with r*Cci*UPO, *Aae*UPO, and *Mro*UPO peroxygenases.

	Abundance (relative %) of derivative with:			
Derivative	25-OH	26/27-OH	x-OH	x,25-diOH
Cholestan-3-one				
r*Cci*UPO	100	-	-	-
*Aae*UPO	100	-	-	-
*Mro*UPO	100	-	-	-
4-Cholesten-3-one				
r*Cci*UPO	100	-	-	-
*Aae*UPO	93	7	-	-
*Mro*UPO	100	-	-	-
Cholesta-3,5-dien-7-one				
r*Cci*UPO	93	-	-	7
*Aae*UPO	87	5	4	4
*Mro*UPO	56	-	39	5

The mass spectra of the TMS derivatives of the three 25-monohydroxylated ketones (not shown) showed the above-described characteristic fragment at *m/z* 131 (from C-24–C-25 bond cleavage). No molecular ions for the saturated and monounsaturated ketones were observed, although the molecular masses could be determined from the $[M-15]^+$ fragments (at *m/z* 459 and *m/z* 457, respectively). However, the mass spectrum of the 25-hydroxyderivative of the diunsaturated ketone showed a molecular ion (*m/z* 470) in addition to the *m/z* 131 and $[M-15]^+$ fragments. Likewise, the 26-hydroxyderivative of 4-cholesten-3-one showed a molecular ion (*m/z* 472) in addition to the *m/z* 131 and $[M-15]^+$ fragments. The diunsaturated cholesta-3,5-dien-7-one yielded the mono- and dihydroxyderivatives, with one hydroxylation at the steroidal ring. The most prominent fragment in the mass spectrum of the monohydroxylated derivative

(see **Fig. S2A** in the supplemental material) corresponded to the molecular ion at *m/z* 470. Other characteristic fragments were observed, but the position of the hydroxyl group in the ring could not be determined. The mass spectrum of the dihydroxylated derivative (see **Fig. S2B**) showed the characteristic fragment at *m/z* 131. Additionally, a molecular ion (*m/z* 558) and other characteristic fragments were found, but, like in the monohydroxylated derivative, the position of the hydroxyl group in the ring could not be determined.

Steroid hydrocarbon reactions. Cholestane, cholesta-3,5-diene, and pregnane (**Fig. 1J** to **L**, respectively) were tested as UPO substrates (**Table 1**). Cholestane, and especially cholesta-3,5-diene, were transformed by the three peroxygenases, with r*Cci*UPObeing the most efficient one. In contrast, pregnane was modified only by *Mro*UPO.

The reaction products of these hydrocarbons are shown in **Table 4**. Whereas the reaction of cholestane was 100% regioselective at C-25, cholesta-3,5-diene gave several di- and trihydroxylated derivatives at the steroidal ring, in addition to the 25-hydroxyderivatives (mainly formed by r*Cci*UPO). Among the dihydroxylated derivatives at the ring core, the ones with hydroxylation at C-3 and C-6 are noteworthy (**Fig. 2A** and **B**). In these reactions, the saturation of one double bond and displacement of the other one (to C-4) took place. Therefore, the 3,5-diene structure in the substrate was transformed into a 3,6-dihydroxy-4-ene structure. Likewise, the C-3 and C-4 dihydroxylated derivatives lost the double bond at C-3, yielding a 3,4-dihydroxy-5-ene structure. The reaction of pregnane with *Mro*UPO gave several monohydroxylated derivatives at the steroid ring (97% of reaction products), together with a further oxidized derivative (3% 3-ketopregnane) (see **Fig. S3** in the supplemental material), although the position of the hydroxyl group could not be determined.

The mass spectra of the 25-hydroxycholestane and 25-hydroxycholesta-3,5-diene TMS derivatives (not shown) showed the characteristic fragment at *m/z* 131, as well as other characteristic ($[M-15]^+$, $[M-90]^+$, and $[M-90-15]^+$) fragments. The mass spectrum of 3,6-dihydroxycholest-4-ene (**Fig. 2A**), whose formation is described above, showed a molecular ion (*m/z* 546) and a base peak at *m/z* 403 considered characteristic of the 4-ene-6-hydroxy structure (31) together with other fragments (including $[M-15]^+$, $[M-90]^+$, and $[M-15-90]^+$).

Table 4

Abundance of the different oxygenated derivatives identified by GC-MS in the reactions of steroid hydrocarbons with r*Cci*UPO, *Aae*UPO, and *Mro*UPO peroxygenases.

	Abundance (relative %) of derivative with:					
Derivative	25-OH	x-OH	x,25-diOH	3,4-diOH-5-en	3,6-diOH-4-en	3,6,25-triOH-4-en
Cholestane						
r*Cci*UPO	100	_	_	_	_	_
*Aae*UPO	100	_	_	_	_	_
*Mro*UPO	100	_	_	_	_	_
Cholesta-3,5-diene						
r*Cci*UPO	36	_	14	3	18[a]	29
AaeUPO	3	_	20	35	31[b]	11
*Mro*UPO	_	_	1	36	61[c]	2
Pregnane						
r*Cci*UPO	_	_	_	_	_	_
*Aae*UPO	_	_	_	_	_	_
*Mro*UPO	_	100[d]	_	_	_	_

[a] Including 3,6-diOH-4-en (14%) and 3,6-diOH-4-en (4%).

[b] Including 3,6-diOH-4-en (28%) and 3,6-diOH-4-en (3%).

[c] Including 3,6-diOH-4-en (50%) and 3,6-diOH-4-en (11%).

[d] Including 97% hydroxy and 3% keto derivatives (see **Fig. S3** in the supplemental material).

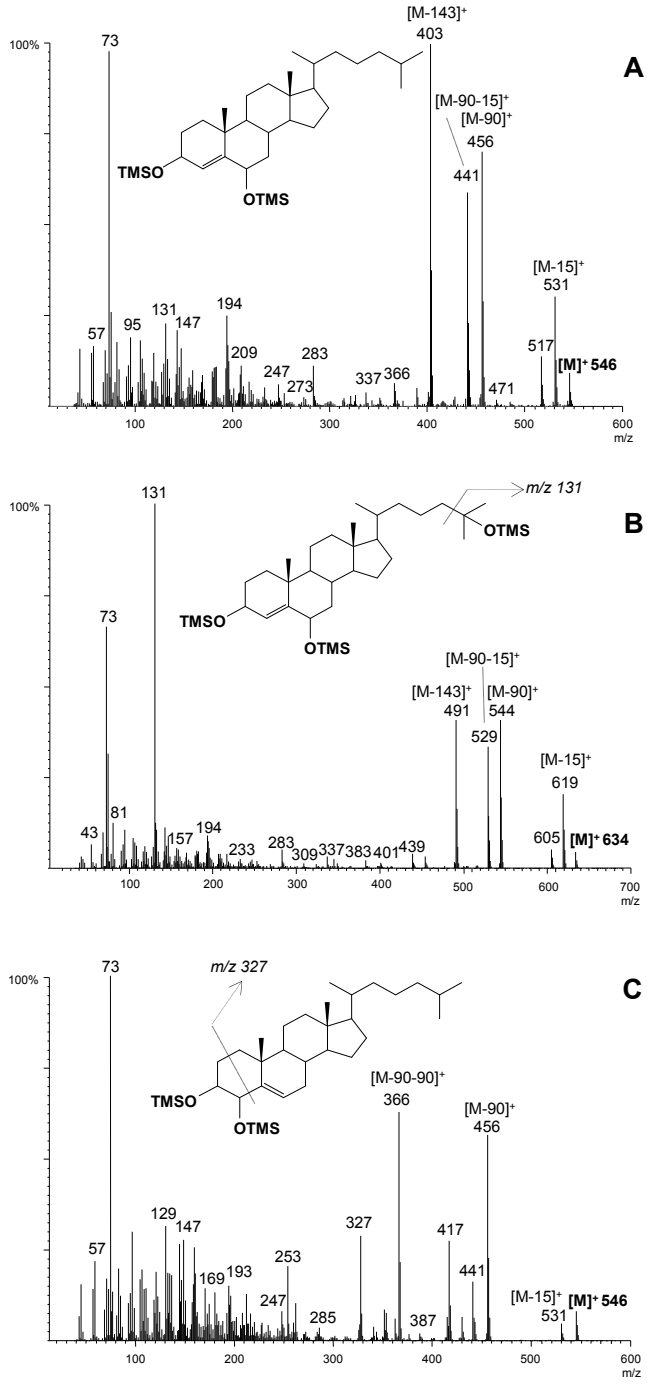

Fig 2. Mass spectra of 3,6-dihydroxycholest-4-ene (**A**), 3,6,25-trihydroxycholest-4-ene (**B**) and 3,4-dihydroxycholest-5-ene (**C**) from peroxygenase reactions with cholesta-3,5-diene (structure **K** in **Fig. 1**), as TMS derivatives.

The mass spectrum of 3,6,25-trihydroxycholest-4-ene (**Fig. 2B**) showed a molecular ion (*m/z* 634) and the characteristic fragment at *m/z* 131, together with the three additional fragments mentioned above. The mass spectrum of 3,4-dihydroxycholest-4-ene (**Fig. 2C**) showed a molecular ion (*m/z* 546) and the characteristic fragment at *m/z* 327, together with other fragments (three additional fragments mentioned above plus $[M-90-90]^+$). Finally, the mass spectrum of x,25-dihydroxycholesta-3,5-diene (not shown; where "x" denotes the unknown position of hydroxylation in the ring) showed a molecular ion (*m/z* 544) and the characteristic fragment at *m/z* 131, together with other fragments ($[M-15]^+$ and $[M-90]^+$), but the position of the hydroxyl in the steroid ring could not been determined.

Sterol ester reactions. Cholesteryl acetate, butyrate, and caprylate (**Fig. 1M** to **O**, respectively) were tested as UPO substrates (**Table 1**). The best results were obtained with r*Cci*UPO and cholesteryl acetate, reaching a conversion yield of 34%. Cholesteryl caprylate was not modified by any of the three peroxygenases. In the reactions of sterol esters, the 25-hydroxyderivative was the only product identified. The mass spectra (not shown) showed the characteristic fragment at *m/z* 131 and molecular ions at *m/z* 544 and *m/z* 428 for cholesteryl butyrate and acetate, respectively.

Computational analyses

The molecular structures of eight representative steroids, and that of the *Aae*UPO (PDB entry 2YOR) enzyme, were prepared at the optimal pH for peroxygenase reactions. PELE simulations were performed, providing energy profiles and ligand trajectories. The driving criterion for the simulations was to reduce the distance between the oxygen atom of the peroxygenase compound I and the center of mass of the ligand. From the results of the simulations, we computed the fractions of ligand that entered by the C-25 end and the fractions that entered by the C-3 end. The structures closest to the reactive oxygen then were analyzed as described below. Further detail on energy profiles and interaction maps for each studied steroid in the heme active site are available in the supplemental material (including supplemental computational results and **Fig. S4** to **S9**). A direct correlation between the percentage of substrate conversion (**Table 1**) and the percentage of entrance by C-25 was observed (**Fig.**

3). In the case of cholestane, the fact that it remains 3.6 Å away from the reactive oxygen (see **Fig. S7**) justifies its reduced reactivity.

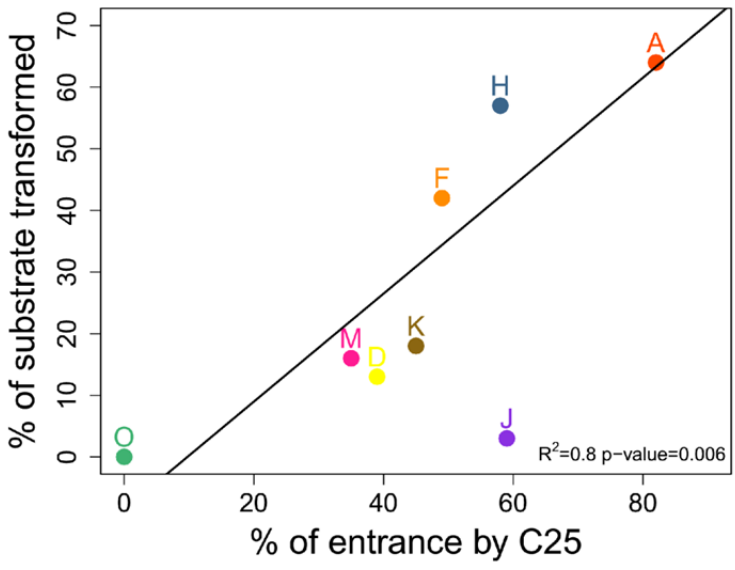

Fig 3. Correlation plot for steroid conversion rate (**Table 1**) and steroid (side chain) entrance by C-25 to the enzyme active site. Computational results were computed from PELE diffusion simulations (20) of eight selected steroids on the molecular structure of *Aae*UPO (PDB entry 2YOR). For steroid (**A** to **K**) identification, see the legend to **Fig. 1**. Cholestane (compound **J**) has been removed from the correlation plot (discussed in the text).

A comparison of PELE simulations (binding energy versus distance between substrate C-25 and compound I oxygen) for sidechain hydroxylation of two free sterols and one esterified sterol (cholesterol, sitosterol, and cholesteryl acetate) is shown in **Fig. 4**, which also includes the main interactions in a representative structure with the ligand at reaction distance from compound I. Cholesterol has the best fraction (82%) of entrance trajectories (**Fig. 3**). The reason for this is a very hydrophobic heme access channel of peroxygenase, which favors the entrance of the apolar C-25 side.

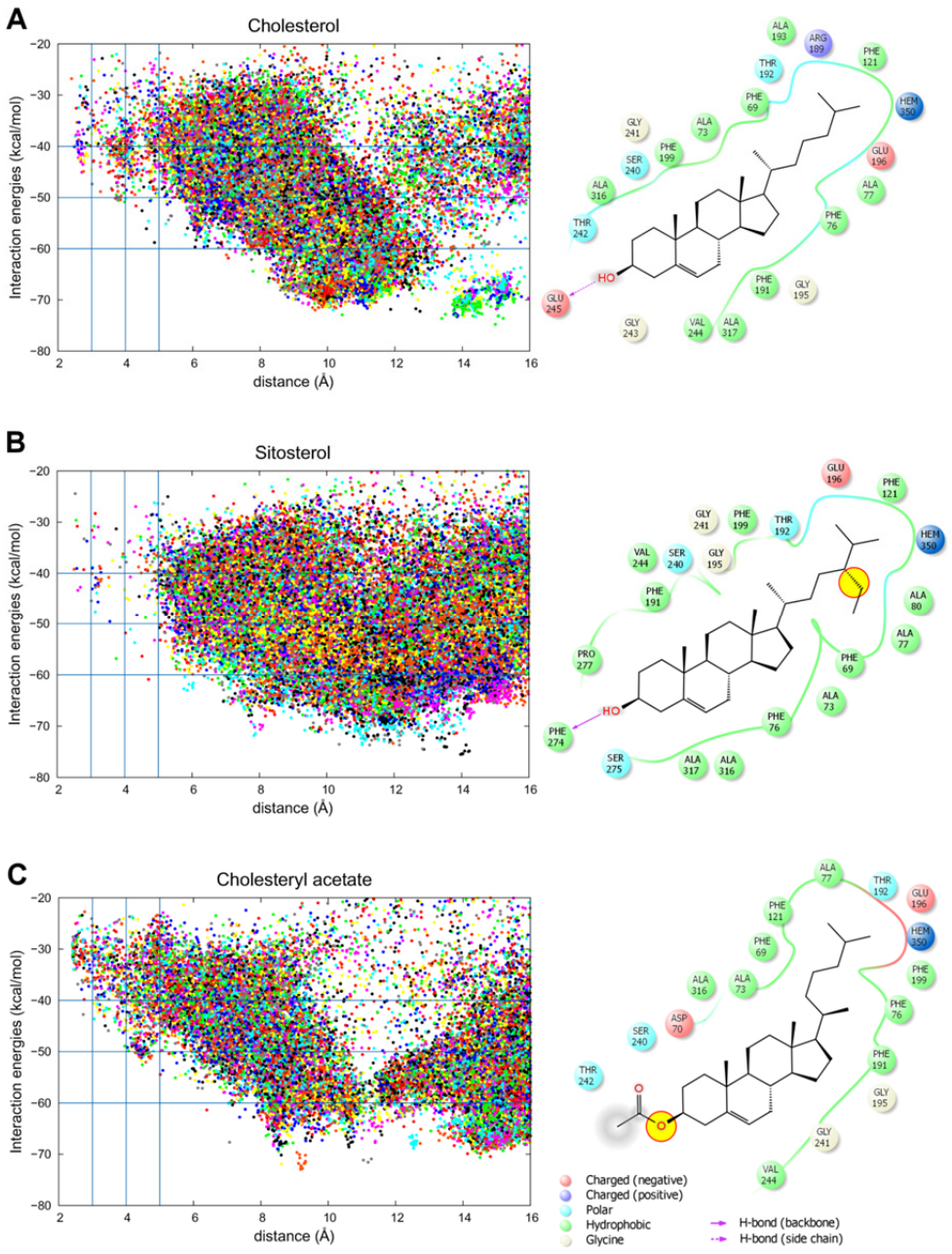

Fig 4. Results from PELE (20) simulations for cholesterol (**A**), sitosterol (**B**), and cholesteryl acetate (**C**) diffusion at the active site of the *Aae*UPO, including (left) plots of the energy profile versus the distance between the steroid H25 and the oxygen atom in enzyme compound I and (right) main interactions between the substrate and the enzyme in a representative structure for each of the three steroids analyzed. The yellow circles identify structural differences relative to the structure of cholesterol.

With the side chain in the active site, the molecule then is further stabilized by a hydrogen bond with Glu245 on the surface of the protein (**Fig. 4A**). Reaction at C-24 and C-26/C-27 also is possible, despite the lower reactivity of secondary and primary carbons compared to that of tertiary C-25, due to the favorable minima with these carbons well positioned for reaction (see **Fig. S4** in the supplemental material).

Compared with cholesterol, sitosterol contains an extra ethyl group. This large substituent impedes the access of the substrate to the active site, which is reflected by the lower fraction of structures entering the protein through the C-25 side (39%) compared with cholesterol (**Fig. 3**). In particular, at the active site the C-28 and C-29 groups clash with Ala77 and Thr192 and reduce considerably the number of structures approaching the heme (**Fig. 4B**). In addition to C-25, some reaction can be expected at C-28, since the ligand also approaches a favorable distance for the reaction of this additional secondary carbon (data not shown). In spite of its similar structure, the fraction of cholestan-3-one entrance trajectories (49%) also is lower than that found for cholesterol (**Fig. 3**), and the distance between C-25 and the compound I oxygen is longer (see **Fig. S5** in the supplemental material). This is most probably because cholestan-3-one is incapable of hydrogen bonding to Glu245. In the case of cholesta-3,5-dien-7-one, a better approachfrom the ring side, due to the two double bonds present (see **Fig. S6**), results in the observed ring hydroxylation.

Cholesteryl acetate has an ester bond at the C-3 hydroxyl, and as in the case of the ketones described above, binding for C-25 oxidation no longer is favored by the hydrogen bond with Glu245 (**Fig. 4C**), resulting in lower entrance trajectories (35%) than those for cholesterol (**Fig. 3**); however, an approach from the opposite side did not result in ring hydroxylation. Cholesteryl caprylate has a longer acyl chain than the cholesteryl acetate described above, and (as seen in **Fig. S9** in the supplemental material) it does not approach the heme group from either side (the large hydrophobic chains would favor interactions with the protein to avoid solvent exposure).

Finally, cholesta-3,5-diene has a very interesting reactivity, due to the presence of two double bonds at C-3 and C-5 and the lack of the C-3 hydroxyl mentioned above, that resulted in similar entrance by both C-25 and C-3 positions (**Fig. 5A** and **B**, respectively). This explains the fraction of

hydroxylated products at the steroid rings, with many of them being additions to its double bonds. In contrast, the bulkier saturated C-5 and C-6 in cholestane (and consequent loss of planarity) impedes a suitable binding of the ligand when it enters by C-25, and a very small number of structures come close enough to the compound I oxygen (see **Fig. S7** in the supplemental material), explaining the low reactivity of this compound (cholesterol is converted by 64%, while cholestane is converted by only 3%) (**Fig. 3**).

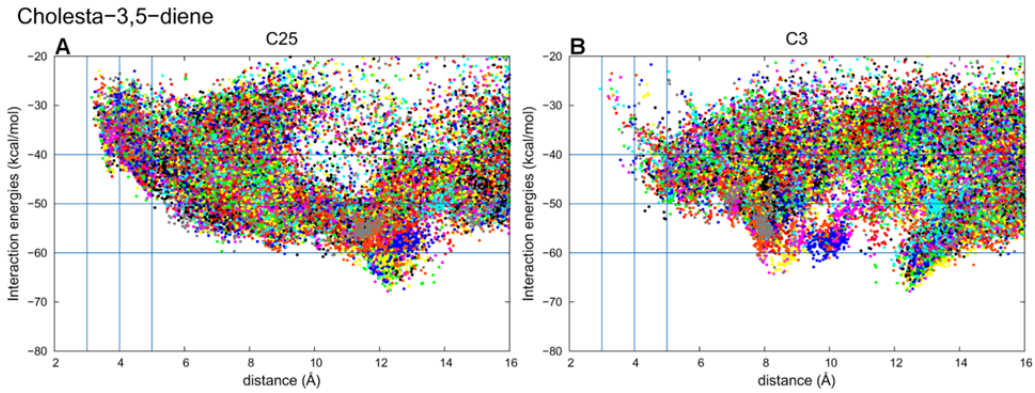

Fig 5. Results from PELE (20) simulations for cholesta-3,5-diene diffusion at the active site with C-25 (**A**) or C-3 (**B**) approaching the heme cofactor of the *Aae*UPO.

Discussion

Despite significant progress in the development of efficient biocatalysts, there is still a great demand for cost-efficient and economical biotechnologies to produce valuable steroids. Most work has been dedicated to steroid modifications catalyzed by whole microbial cells (1). The present work deals with the oxyfunctionalization of steroids using fungal peroxygenases, relatively young representatives of the superfamily of heme-thiolate peroxidases that are characterized by the presence of a cysteine residue as the fifth ligand of the heme iron and their peroxygenase activity (8). Several steroids differing in their structures, including free and esterified sterols and steroid ketones and

hydrocarbons, were tested as substrates of peroxygenases from three basidiomycete species. The relationships between the structure of the different substrates, the enzyme reactivity, and the reaction products obtained are discussed below. A combined experimental and computational approach shows that there is not a unique factor that determines the hydroxylation profile; instead, it is a result of the sum of many structural factors, concerning both the steroid mol- ecule and the enzyme active site. These include the polar/apolar character of C-3/C-7 ring groups, the presence of double bonds in the steroidal rings, and the length and character of the alkyl C-17 chain, which affect the ligand entrance ratio on the C-25 side.

Relationships between steroid structure and conversion yield

The influence of the C-17 alkyl chain, oxidation/unsaturation of the rings, and esterification of the C-3 hydroxyl group on the steroid conversions is discussed below.

(i) ***Alkyl chain at C17.*** The influence of the steroid alkyl side chain substitution and unsaturation was shown by the different extents of transformation obtained for C_{27}, C_{28}, and C_{29} sterols. The C_{27} cholesterol was completely transformed by r*Cci*UPO, while the other sterols were transformed to a lesser extent by this and the two other peroxygenases. The presence of a methyl or ethyl group at C-24 makes it progressively more difficult to hydroxylate campesterol and sitosterol, as illustrated in **Fig. 6**. Moreover, the double bond at C-22, in addition to the methyl or ethyl group at C-24, made ergosterol and stigmasterol more difficult to be hydroxylated (by the three peroxygenases) than the above-described campesterol and sitosterol. The influence of a shorter side chain was shown by comparing the hydroxylation of pregnane (with an ethyl group at C-17) and other steroid hydrocarbons (e.g., cholestane). The presence of a two-carbon (instead of eightcarbon) alkyl chain prevents hydroxylation by r*Cci*UPO and *Aae*UPO and, in contrast, promotes hydroxylation by *Mro*UPO, which takes place in the steroidal ring (not in the side chain). Finally, the absence of an alkyl chain at C-17, like in testosterone (having instead a hydroxyl group), completely prevents its hydroxylation by the three fungal peroxygenases (compared with up to 100% conversion of 4-cholesten-3-one).

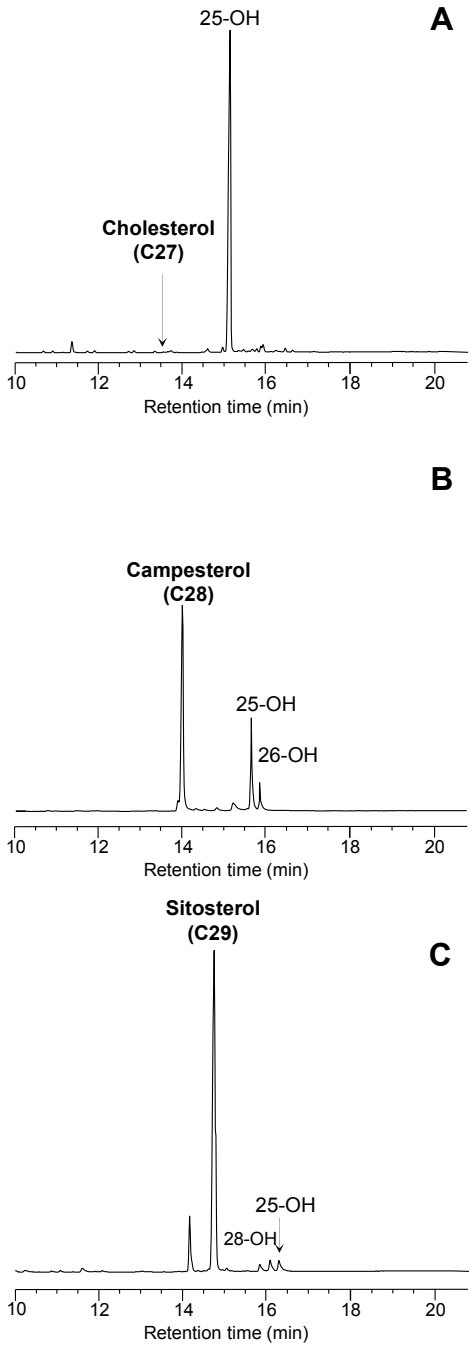

Fig 6. GC-MS analysis of the r*Cci*UPO reaction (at 60 min) with cholesterol (**A**), campesterol (**B**), and sitosterol (**C**) (depicted in **Fig. 1**) showing the remaining substrates and the monohydroxylated derivatives at C-25, C-26, and C-28 of the side chain.

The good conversion produced in the reactions of peroxygenases with cholesterol and the differences observed in the conversion of sterols with different alkyl chain sizes, like sitosterol, are explained by computational results. In general terms, the polarity of the substituent group at C-3 has a positive correlation with the ligand rate entrance by the C-25 side. This is due to the hydrophobic character of the protein access channel to the heme that contains numerous phenylalanine residues. Moreover, the presence of a hydroxyl group in C-3 (of cholesterol and other sterols) increases the ligand rate entrance by the C-25 side and stabilizes the ligand in a suitable catalytic position (a good catalytic position is assumed when the distance between the hydrogen in C-25 and the compound I oxygen is around 2.4 Å) due to a hydrogen bond with Glu245. These two factors correlate perfectly with the high activity shown for cholesterol. However, although sitosterol also has a hydroxyl group in C-3, it is not able to access the heme site by the C-25 end in the same way as cholesterol due to the bulkier alkyl chain in C-17 that clashes with residues in the heme access channel (namely, Thr192, Ala77, Phe69, Phe121, and Phe199).

(ii) ***Oxidation/unsaturation degree of the rings.*** Steroids differing in the oxidation state of the ring were tested, including steroid hydrocarbons, sterols, and steroid ketones. Whereas r*Cci*UPO completely converted both cholesterol and 4-cholesten-3-one, *Aae*UPO and *Mro*UPO oxidized the ketone with lower efficiency. The contrary was reported for P450s (e.g., CYP27A1), which hydroxylated steroids with a 3-oxo-Δ^4 structure at a much higher rate than those with a 3-hydroxy-Δ^5 structure (32). Therefore, the structural differences between 4-cholesten-3-one and cholesterol, which are the planarity of the sterol A-ring and the electronic properties resulting from a keto versus hydroxyl substituent at C-3, seemingly affect the peroxygenase activity. The computational results revealed that the polar character of the hydroxyl and oxo groups in the sterols and steroid ketones affects in a positive way the ligand entrance rate by C-25, which correlates with the high activity that these compounds show compared with the corresponding steroid hydrocarbons.

On the other hand, although differences were observed between the three peroxygenases, the presence and number of double bonds in the rings of steroid hydrocarbons and ketones significantly increases their hydroxylation degree. This is illustrated in **Fig. 7**, where better *Aae*UPO conversion of cholesta-3,5-

diene and cholesta-3,5-dien-7-one, compared with that of the corresponding saturated molecules (cholestane and cholestan-3-one), is shown. The C-25 side entrance and the placement of the steroid hydrocarbons in a proper catalytic position are determined by the presence or absence of double bonds.

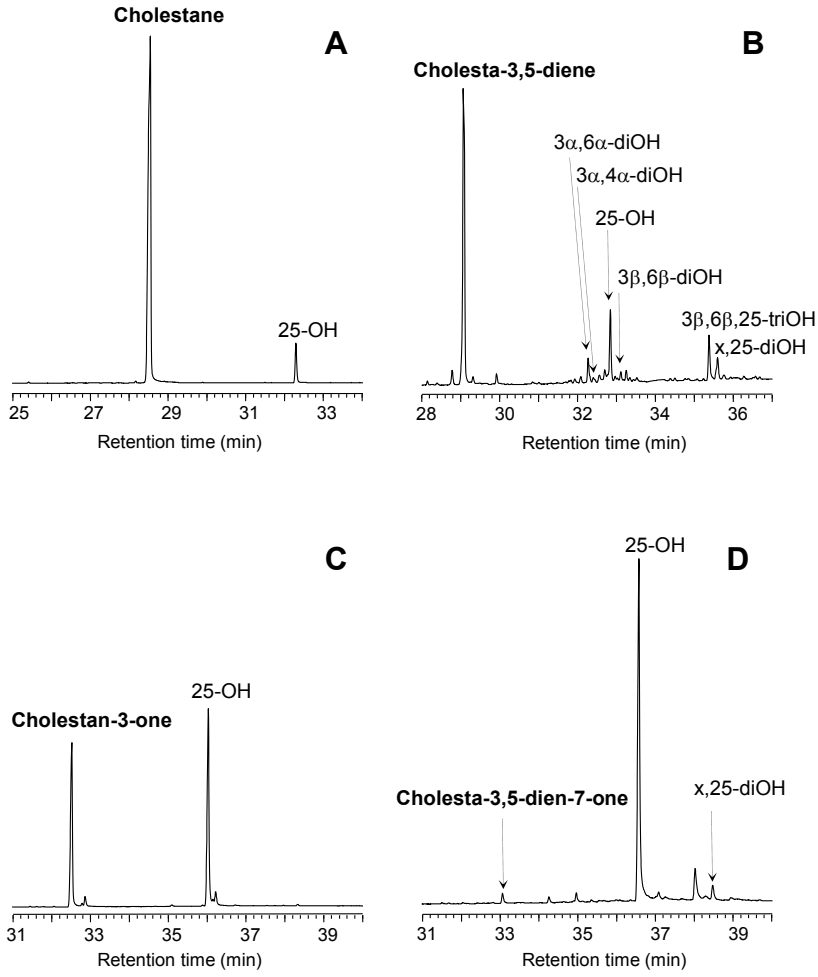

Fig 7. GC-MS analysis of the r*Cci*UPO reaction (at 60 min) with cholestane (A), cholesta-3,5-diene (B), cholestan-3-one (C), and cholesta-3,5-diene-7-one (D) (depicted in **Fig. 1**) showing the remaining substrates and the mono-, di-, and trihydroxylated derivatives included in **Table 4** (x denotes the unknown position of hydroxylation in the ring).

These reduce the volume of the steroid ring, facilitating its entrance in the active site, and provide proper curvature to the substrate for an optimal approach to the heme. Therefore, both the apolar nature of the two extremes of the molecule and the presence of double bonds in cholesta-3,5-diene facilitate access to the heme from both sides, C-3 and C-25, and its correct placement for reaction. However, neither the substrate entrance nor its placement in the active site are as suitable as they are in sterols and steroid ketones. In the case of cholestane, the entrance to the heme site is hampered by the larger sp^3 groups at C-3, C-4, C-6, and C-7. This can be better observed by comparing the energy profiles of this compound (see **Fig. S7** in the supplemental material) to those of cholesta-3,5-diene (see **Fig. S8**) and observing the very different occupation of the binding site. In addition, the higher reactivity of alkenes than alkanes leads to addition of hydroxyl groups to the double bonds in the steroidal rings in cholesta-3,5-diene, which is not observed in cholestane. Concerning the two ketones compared in **Fig. 7C** and **D**, although both have a similar ratio for C-25 entrance, cholestan-3-one can be hydroxylated at only C-25, while cholesta-3,5-dien-7-one shows some additional hydroxylation due to the higher reactivity of the alkenes mentioned above. Moreover, as in the case of the steroid hydrocarbons, the two double bonds in the steroid ketone ring will facilitate the entrance and proper positioning of the substrate at the peroxygenase active site.

Due to the above-described effects, although the conversion rates of cholestan-3-one are lower than those of cholesterol (the best steroid substrate of the basidiomycete peroxygenases), they are increased by the presence of double bonds in the steroid ring, and cholestan-3,5-dien-7-one hydroxylation rates are in the same order of those obtained for cholesterol.

(iii) ***Esterified hydroxyl group at C3.*** With the aim of investigating whether the hydroxyl group at C-3, in free form, is necessary for maximal peroxygenase activity, three esters of cholesterol with organic acids of different chain lengths were assayed as substrates. The experimental results revealed that the presence of an esterifying group hampers substrate conversion, and that this effect is directly correlated with increasing chain length of the fatty acid. In sterol esters, hydroxylation (at C-25) only of the side chain of the sterol was observed and not at the acyl moiety, despite *Aae*UPO and r*Cci*UPO being found to efficiently hydroxylate fatty acids (11, 18).

The computational analyses revealed that in the sterol esters, the C-25 entrance rate is decreased with respect to cholesterol due to the presence of hydrophobic alkyl chains at the ester site. In the case of cholesteryl caprylate, which is not transformed by any of the peroxygenases, the long unsubstituted hydrocarbon chain tends to "anchor" the substrate away from the heme site by interacting with different groups on the protein surface. Since both ends are hydrophobic, interactions with the protein minimize the solvent exposure but restrain the ligand from reaching the heme, which explains the lack of activity for this compound.

Relationships between steroid structure and regioselectivity. In general, the reactions of the three fungal peroxygenases with the different steroids proceed with remarkable regioselectivity and result in the formation of the 25-hydroxyderivatives as the main products. The complete conversion of cholesterol by r*Cci*UPO to produce 25-hydroxycholesterol is noteworthy, since this compound is widely used, displaying an array of pharmacological actions *in vitro* and in cell-based systems (33), as discussed below. Different alkyl chains at C-17 seemingly do not influence the regioselectivity in *Aae*UPO and *Mro*UPO reactions (see below) but affect that of r*Cci*UPO, since cholesterol is C-25 hydroxylated with a strict (100%) regioselectivity, whereas for campesterol and sitosterol, hydroxylation at terminal C-26/C-27 (15%) and subterminal C-28 (48%), respectively, also was observed. On the other hand, the double bond at C-22 in ergosterol and stigmasterol seemingly influences the strict regioselectivity of the hydroxylation at C-25. Minor hydroxylation at the terminal positions of the steroid branched side chain by *Aae*UPO and *Mro*UPO also leads in some cases (e.g., cholesterol) to formation of the C-26/C-27-carboxylated derivatives, in addition to the C-26/C-27-hydroxylated ones. This is because of the further oxidation (successive hydroxylation and dehydration reactions) of the monohydroxylated products, as previously demonstrated in ^{18}O-labeling oxygenation studies with *Aae*UPO and $H_2{}^{18}O_2$ (11).

Hydroxylation at positions other than C-25 occurs in cases that show a high (energetically favorable) occupation of binding positions near any of these centers, as demonstrated for *Aae*UPO by computational studies. In particular, the case of cholesterol hydroxylation at C-24 is due to interactions between the substrate and the protein that include a local minima for C-24, which is slightly

more favorable than that for C-25. Hydroxylation at C-25 (tertiary C-H bond) is electronically preferred by its lower C-H bond strength compared with that of the secondary and primary C-H bonds (34). In contrast, steric constraints rather than the differential electronic properties of the C-H bonds have been reported to govern the regioselectivity of the reaction of steroids (cholesterol and 4-cholesten-3-one) with P450s (CYP125A1) where terminal oxidation was preferred (35).

Interestingly, in addition to hydroxylation at the side chain, some hydroxylated derivatives at the steroid core are formed when oxygen groups are lacking at C-3, such as in cholesta-3,5-dione, cholesta-3,5-diene, or pregnane. Indeed, the presence of a hydroxyl or oxo group at this position seems to prevent the hydroxylation of the steroidal core. On the other hand, the presence of two conjugated double bonds in the ring seems to favor the hydroxylation at the steroidal core, especially by *Aae*UPO and *Mro*UPO, as evidenced in the reaction of cholesta-3,5-diene yielding 3,6-dihydroxycholest-4-ene and 3,4-dihydroxycholest-5-ene, as mentioned above. The mechanism of this double (at C-3 and C-6 or at C-3 and C-4) hydroxylation implies the displacement of one of the cholesta-3,5-diene double bonds to the intermediate (C-4 or C-5) position and the saturation of the other.

Significance of side-chain versus ring hydroxylation. It has been shown that the reactions of the peroxygenases from the three different basidiomycetes occurred generally with noteworthy regioselectivity, and hydroxylation at the side chain over the steroidal ring was preferred, with the 25-hydroxyderivatives predominating. From a biochemical point of view, side-chain and steroid nucleus oxidation have been confirmed to be independent processes, at least in some microorganisms (1). Side-chain hydroxylation is usually a prestep in side-chain degradation in most microbial systems that oxidize steroids. The initial step of the side-chain oxidation of sterols (and other C_{27} steroids) is hydroxylation at C-26 or C-27, followed by a complex sequence of reactions involving different enzymes (some of them still unidentified) that produce the elimination of side chain at C-17 and then steroidal nucleus oxidation. However, further oxidative degradation on the C-17 side chain may not occur when hydroxylation is produced at C-25 (instead of C-26 or C-27). This has been observed using 25-hydroxylated cholesterol as the substrate (36),

concluding that C-25 hydroxylation must be a distinct reaction from that of the usual cholesterol side chain degradation pathway. Indeed, the authors do not consider that steroid metabolism is a specific function of UPOs, not as much as it is the oxidation of alkanes, alkenes, ethers, or aromatics. Rather, UPOs represent a catalytic system ("extracellular liver") that, irrespective of a particular structure, can nonspecifically oxidize diverse compounds emerging in the fungus microenvironment. In this context, unspecific detoxification surely is more important than specific degradation.

Interestingly, a previously unrecognized biological (antiviral) role for 25-hydroxycholesterol, which is selectively formed by the r*Cci*UPO as discussed above, has been highlighted recently (37). Indeed, that study revealed 25-hydroxycholesterol as the only oxysterol notably upregulated following macrophage infection or activation by interferons. This antiviral effect is specific to 25-hydroxycholesterol, because other related (enzymatically generated) oxysterols, such as 19-hydroxychoesterol and 7-hydroxycholesterol, fail to repress viral infection. 25-Hydroxycholesterol has been reported to have a high potency to inhibit a broad spectrum of viruses from high to low physiological concentrations depending on lipid conditions and virus-host cell system. Likewise, other recent studies also revealed 25-hydroxycholesterol as a potential antiviral therapeutic (38). Independent of its known regulatory effect on metabolism, 25-hydroxycholesterol impairs viral entry at the virus-cell fusion step by inducing cellular membrane changes. Because 25-hydroxycholesterol can permeate through membranes, it likely modifies cellular membranes to exert its antiviral effect. Moreover, in addition to interfering with viral entry and replication, 25-hydroxycholesterol also amplifies the activation of immune cells and increases the production of immune mediators (39).

Final remarks. The first crystal structure of a fungal peroxygenase (23), from the basidiomycete *A. aegerita* (*Aae*UPO), was used in the computational simulations included in the present study. The availability of more peroxygenase crystal structures, including those from *C. cinerea* and *M. rotula*, will provide the opportunity to correlate the different regioselectivities in steroid oxygenation described here with the architecture of the active site and other structural features. Such information will permit us to engineer these self-sufficient

monooxygenases (whose activation depends on a peroxide source) as new and robust industrial biocatalysts for the pharmaceutical and fine-chemical sectors.

In conclusion, in the present work, the ability of three different fungal peroxygenases to catalyze the regioselective hydroxylation of a variety of steroids is shown for the first time. Generally, hydroxylation at the side chain over the steroid ring was preferred, with 25-hydroxyderivatives being the main products formed. It has been observed that some structural features of the steroid substrates, such as the presence and length of the alkyl chain at C-17 and the presence of oxygen groups and/or conjugated double bonds in the steroid ring system, influence substrate conversion and guide the regioselectivity of the reactions. A better understanding of the mechanistic aspects of hydroxylation in combination with the development of suitable biocatalysts would be the basis for efficient steroid hydroxylation bioprocesses using new enzymes with self-sufficient mono(per)oxygenase activities.

Acknowledgements

This study was supported by the INDOX (KBBE-2013-7-613549), PEROXICATS (KBBE-2010-4-265397), and PELE (ERC-2009-Adg 25027) EU projects.

We have no conflicts of interest to declare.

References

1. Donova MV, Egorova OV. 2012. Microbial steroid transformations: current state and prospects. Appl Microbiol Biotechnol 94:1423–1447. http://dx.doi.org/10.1007/s00253-012-4078-0.
2. Beneventi E, Ottolina G, Carrea G, Panzeri W, Fronza G, Lau PCK. 2009. Enzymatic Baeyer-Villiger oxidation of steroids with cyclopentadecanone monooxygenase. J Mol Catal B Enzym 58:164–168. http://dx.doi.org/10.1016/j.molcatb.2008.12.009.
3. Ortiz de Montellano PR. 2005. Cytochrome P450: structure, mechanism, and biochemistry. Kluwer Academic/Plenum, New York, NY.
4. Urlacher VB, Girhard M. 2012. Cytochrome P450 monooxygenases: an update on perspectives for synthetic application. Trends Biotechnol 30:26-36. http://dx.doi.org/10.1016/j.tibtech.2011.06.012.

5. van Beilen JB, Funhoff EG. 2005. Expanding the alkane oxygenase toolbox: new enzymes and applications. Curr Opin Biotechnol 16:308–314. http://dx.doi.org/10.1016/j.copbio.2005.04.005.
6. Li H. 2001. Cytochrome P450, p 267–282. *In* Messerschmidt A, Huber R, Poulos TL, Wieghardt K (ed), Handbook of metalloproteins, vol 1. Wiley, Chichester, United Kingdom.
7. Ullrich R, Nuske J, Scheibner K, Spantzel J, Hofrichter M. 2004. Novel haloperoxidase from the agaric basidiomycete *Agrocybe aegerita* oxidizes aryl alcohols and aldehydes. Appl Environ Microbiol 70:4575–4581. http://dx.doi.org/10.1128/AEM.70.8.4575-4581.2004.
8. Hofrichter M, Ullrich R. 2014. Oxidations catalyzed by fungal peroxygenases. Curr Opin Chem Biol 19:116–125. http://dx.doi.org/10.1016/j.cbpa.2014.01.015.
9. Bernhardt R. 2006. Cytochromes P450 as versatile biocatalysts. J Biotechnol 124:128–145. http://dx.doi.org/10.1016/j.jbiotec.2006.01.026.
10. Hofrichter M, Ullrich R, Pecyna MJ, Liers C, Lundell T. 2010. New and classic families of secreted fungal heme peroxidases. Appl Microbiol Biotechnol 87:871–897. http://dx.doi.org/10.1007/s00253-010-2633-0.
11. Gutiérrez A, Babot ED, Ullrich R, Hofrichter M, Martínez AT, del Río JC. 2011. Regioselective oxygenation of fatty acids, fatty alcohols and other aliphatic compounds by a basidiomycete heme-thiolate peroxidase. Arch Biochem Biophys 514:33–43. http://dx.doi.org/10.1016/j.abb.2011.08.001.
12. Peter S, Kinne M, Wang X, Ullrich R, Kayser G, Groves JT, Hofrichter M. 2011. Selective hydroxylation of alkanes by an extracellular fungal peroxygenase. FEBS J 278:3667-3675. http://dx.doi.org/10.1111/j.1742-4658.2011.08285.x.
13. Anh DH, Ullrich R, Benndorf D, Svatos A, Muck A, Hofrichter M. 2007. The coprophilous mushroom *Coprinus radians* secretes a haloperoxidase that catalyzes aromatic peroxygenation. Appl Environ Microbiol 73:5477-5485. http://dx.doi.org/10.1128/AEM.00026-07.
14. Gröbe G, Ullrich M, Pecyna M, Kapturska D, Friedrich S, Hofrichter M, Scheibner K. 2011. High-yield production of aromatic peroxygenase by the agaric fungus *Marasmius rotula*. AMB Express 1:31–42. http://dx.doi.org/10.1186/2191-0855-1-31.
15. Pecyna MJ, Ullrich R, Bittner B, Clemens A, Scheibner K, Schubert R, Hofrichter M. 2009. Molecular characterization of aromatic peroxygenase from *Agrocybe aegerita*. Appl Microbiol Biotechnol 84:885–897. http://dx.doi.org/10.1007/s00253-009-2000-1.
16. Floudas D, Binder M, Riley R, Barry K, Blanchette RA, Henrissat B, Martínez AT, Otillar R, Spatafora JW, Yadav JS, Aerts A, Benoit I, Boyd A, Carlson A, Copeland A, Coutinho PM, de Vries RP, Ferreira P, Findley K, Foster B, Gaskell J, Glotzer D, Górecki P, Heitman J, Hesse C, Hori C, Igarashi K, Jurgens JA, Kallen N, Kersten P, Kohler A, Kües U, Kumar TKA, Kuo A, LaButti K, Larrondo LF, Lindquist E, Ling A, Lombard V, Lucas S, Lundell T, Martin R, McLaughlin DJ, Morgenstern I, Morin E, Murat C, Nolan M, Ohm RA, Patyshakuliyeva A, Rokas A, Ruiz-Dueñas FJ, Sabat G, Salamov A, Samejima M, Schmutz J, Slot JC, St John F, Stenlid J, Sun H, Sun S, Syed

K, Tsang A, Wiebenga A, Young D, Pisabarro A, Eastwood DC, Martin F, Cullen D, Grigoriev IV, Hibbett DS. 2012. The Paleozoic origin of enzymatic lignin decomposition reconstructed from 31 fungal genomes. Science 336:1715-1719. http://dx.doi.org/10.1126/science.1221748.

17. Stajich JE, Wilke SK, Ahren D, Au CH, Birren BW, Borodovsky M, Burns C, Canback B, Casselton LA, Cheng CK, Deng JX, Dietrich FS, Fargo DC, Farman ML, Gathman AC, Goldberg J, Guigo R, Hoegger PJ, Hooker JB, Huggins A, James TY, Kamada T, Kilaru S, Kodira C, Kues U, Kupfert D, Kwan HS, Lomsadze A, Li WX, Lilly WW, Ma LJ, Mackey AJ, Manning G, Martin F, Muraguchi H, Natvig DO, Palmerini H, Ramesh MA, Rehmeyer CJ, Roe BA, Shenoy N, Stanke M, Ter Hovhannisyan V, Tunlid A, Velagapudi R, Vision TJ, Zeng QD, Zolan ME, Pukkila PJ. 2010. Insights into evolution of multicellular fungi from the assembled chromosomes of the mushroom *Coprinopsis cinerea* (*Coprinus cinereus*). Proc Natl Acad Sci U S A 107:11889–11894. http://dx.doi.org/10.1073/pnas.1003391107.
18. Babot ED, del Río JC, Kalum L, Martínez AT, Gutiérrez A. 2013. Oxyfunctionalization of aliphatic compounds by a recombinant peroxygenase from *Coprinopsis cinerea*. Biotechnol Bioeng 110:2332. http://dx.doi.org/10.1002/bit.24904.
19. Cossins BP, Hosseini A, Guallar V. 2012. Exploration of protein conformational change with PELE and meta-dynamics. J Chem Theory Comput 8:959–965. http://dx.doi.org/10.1021/ct200675g.
20. Borrelli KW, Vitalis A, Alcantara R, Guallar V. 2005. PELE: protein energy landscape exploration. A novel Monte Carlo based technique. J Chem Theory Comput 1:1304 – 1311.
21. Ullrich R, Liers C, Schimpke S, Hofrichter M. 2009. Purification of homogeneous forms of fungal peroxygenase. Biotechnol J 4:1619–1626. http://dx.doi.org/10.1002/biot.200900076.
22. Gutiérrez A, del Río JC, González-Vila FJ, Martín F. 1998. Analysis of lipophilic extractives from wood and pitch deposits by solid-phase extraction and gas chromatography. J Chromatogr 823:449–455. http://dx.doi.org/10.1016/S0021-9673(98)00356-2.
23. Piontek K, Strittmatter E, Ullrich R, Grobe G, Pecyna MJ, Kluge M, Scheibner K, Hofrichter M, Plattner DA. 2013. Structural basis of substrate conversion in a new aromatic peroxygenase: cytochrome P450 functionality with benefits. J Biol Chem 288:34767–34776. http://dx.doi.org/10.1074/jbc.M113.514521.
24. Sastry GM, Adzhigirey M, Day T, Annabhimoju R, Sherman W. 2013. Protein and ligand preparation: parameters, protocols, and influence on virtual screening enrichments. J Comput Aided Mol Des 27:221–234. http://dx.doi.org/10.1007/s10822-013-9644-8.
25. Anandakrishnan R, Aguilar B, Onufriev AV. 2012. H__3.0: automating pK prediction and the preparation of biomolecular structures for atomistic molecular modeling and simulations. Nucleic Acids Res 40:W537-W541. http://dx.doi.org/10.1093/nar/gks375.
26. Kaminski GA, Friesner RA, Tirado-Rives J, Jorgensen WL. 2001. Evaluation and reparametrization of the OPLS-AA force field for proteins via comparison with accurate

quantum chemical calculations on peptides. J Phys Chem B 105:6474–6487. http://dx.doi.org/10.1021/jp003919d.
27. Bashford D, Case DA. 2000. Generalized born models of macromolecular solvation effects. Annu Rev Phys Chem 51:129–152. http://dx.doi.org/10.1146/annurev.physchem.51.1.129.
28. Linde D, Pogni R, Cañellas M, Lucas F, Guallar V, Baratto MC, Sinicropi A, Sáez-Jiménez V, Coscolín C, Romero A, Medrano FJ, Ruiz-Dueñas FJ, Martínez AT. 2014. Catalytic surface radical in dyedecolorizing peroxidase: a computational, spectroscopic and directed mutagenesis study. Biochem J 50:5096–5107. http://dx.doi.org/10.1042/BJ20141211.
29. Hernández-Ortega A, Lucas F, Ferreira P, Medina M, Guallar V, Martínez AT. 2011. Modulating O2 reactivity in a fungal flavoenzyme: involvement of aryl-alcohol oxidase Phe-501 contiguous to catalytic histidine. J Biol Chem 286:41105–41114. http://dx.doi.org/10.1074/jbc.M111.282467.
30. Lucas MF, Guallar V. 2012. An atomistic view on human hemoglobin carbon monoxide migration processes. Biophys J 102:887–896. http://dx.doi.org/10.1016/j.bpj.2012.01.011.
31. Brooks CJW, Henderson W, Steel G. 1973. Use of trimethylsilyl ethers in characterization of natural sterols and steroid diols by gas chromatography mass spectrometry. Biochim Biophys Acta 296:431–445. http://dx.doi.org/10.1016/0005-2760(73)90101-X.
32. Norlin M, von Bahr S, Bjorkhem I, Wikvall K. 2003. On the substrate specificity of human CYP27A1: implications for bile acid and cholestanol formation. J Lipid Res 44:1515-1522. http://dx.doi.org/10.1194/jlr.M300047-JLR200.
33. Diczfalusy U. 2013. On the formation and possible biological role of 25-hydroxycholesterol. Biochimie 95:455–460. http://dx.doi.org/10.1016/j.biochi.2012.06.016.
34. Johnston JB, Ouellet H, Podust LM, Ortiz de Montellano PR. 2011. Structural control of cytochrome P450-catalyzed _-hydroxylation. Arch Biochem Biophys 507:86–94. http://dx.doi.org/10.1016/j.abb.2010.08.011.
35. Ouellet H, Guan SH, Johnston JB, Chow ED, Kells PM, Burlingame AL, Cox JS, Podust LM, de Montellano PR. 2010. *Mycobacterium tuberculosis* CYP125A1, a steroid C27 monooxygenase that detoxifies intracellularly generated cholest-4-en-3-one. Mol Microbiol 77:730–742. http://dx.doi.org/10.1111/j.1365-2958.2010.07243.x.
36. Wang KC, Wang PH, Lee SS. 1997. Microbial transformation of protopanaxadiol and protopanaxatriol derivatives with *Mycobacterium* sp. (NRRL B-3805). J Nat Prod 60:1236-1241. http://dx.doi.org/10.1021/np970331y.
37. Blanc M, Hsieh WY, Robertson KA, Kropp KA, Forster T, Shui GH, Lacaze P, Watterson S, Griffiths SJ, Spann NJ, Meljon A, Talbot S, Krishnan K, Covey DF, Wenk MR, Craigon M, Ruzsics Z, Haas J, Angulo A, Griffiths WJ, Glass CK, Wang YQ, Ghazal P. 2013. The transcription factor STAT-1 couples macrophage synthesis of

25-hydroxycholesterol to the interferon antiviral response. Immunity 38:106–118. http://dx.doi.org/10.1016/j.immuni.2012.11.004.
38. Liu SY, Aliyari R, Chikere K, Li GM, Marsden MD, Smith JK, Pernet O, Guo HT, Nusbaum R, Zack JA, Freiberg AN, Su LS, Lee B, Cheng GH. 2013. Interferon-inducible cholesterol-25-hydroxylase broadly inhibits viral entry by production of 25-hydroxycholesterol. Immunity 38:92–105. http://dx.doi.org/10.1016/j.immuni.2012.11.005.
39. Gold ES, Diercks AH, Podolsky I, Podyminogin RL, Askovich PS, Treuting PM, Aderem A. 2014. 25-Hydroxycholesterol acts as an amplifier of inflammatory signaling. Proc Natl Acad Sci U S A 111:10666-10671. http://dx.doi.org/10.1073/pnas.1404271111.
40. Schnorr KM, Ullrich R, Scheibner K, Kluge MG, Hofrichter M. October 2008. Fungal peroxygenases and methods of application. World Intellectual Property Organization patent WO/2008/119780.

Supplemental Computational Results

Free and esterified sterols

Cholesterol (compound A in **Fig. 1**) has the best fraction of trajectories entering by the C25 side (82%) (**Fig. 3**). The reason for this is a hydrophobic entrance to the heme side which favors the entrance by the apolar side of the ligand. Then in the active site the molecule is further stabilized by a hydrogen bond with Glu245 on the surface of the protein (**Fig. 4A**). Reactions at C24 (**Fig. S4A**) and C26/C27 (**Fig. S4C** and **D**) are possible despite the less favorable breaking of secondary and primary C-H bonds due to the presence of minima with these hydrogens well positioned for reaction with compound I. In particular C24 approaches the heme with a more favorable interaction energy than C25.

Sitosterol (compound D in **Fig. 1**) contains an extra ethyl group at C24. This large substituent impedes the entrance of the substrate in the active site, which is reflected by the lower fraction of structures entering the protein through C25 side (39% opposed to 82% for compound A) (**Fig. 3**). In particular, at the active site the C28 and C29 groups clash with Ala77 and Thr192 which reduces considerably the number of structures capable of approaching the heme at a reactive distance (**Fig. 4B**). Some reaction can nevertheless be expected at C28 due to the fact that simulations show that the ligand approaches the heme to a favorable distance for reaction at this secondary carbon.

Steroid ketones

Cholestan-3-one (compound F in **Fig. 1**) has a ketone in C3 instead of an alcohol and a single bond between C5 and C6. This ligand is not able to enter the binding pocket as well as compound A (**Fig. S5**). First the fraction of entrances by the C25 side is reduced (from 82% to 49%) and second the distance between the reactive hydrogen and the oxygen atom in cholestan-3-one is slightly longer (2.5 Å in A to 2.8 Å in F). This will have an effect in the reactivity of the compound and in particular will favor reaction at the most labile hydrogen (H25 being tertiary) since the number of reactive positions is considerably reduced (when compared to cholesterol). Interaction of the ligand in the active site is less favorable than cholesterol due to the fact that cholestan-3-one is incapable of hydrogen bonding to Glu245.

Cholesta-3,5-dien-7-one (compound H in **Fig. 1**) does not have the alcohol in C3, instead it has a ketone in C7 and an extra double bond at C3-C4. This molecule has an identical activity as cholesterol (57% substrate conversion vs. 64). Here the entrance by the C25 side is reduced (from 82% in cholesterol to 58% in cholesta-3,5-dien-7-one) probably due to the apolar nature of the steroid ring on the external side (C3) (**Fig. S6**). This also justifies reaction observed in the ring due to the presence of the double bond and C3 which can place itself correctly in the active site. However the hydrogen present on a carbon atom with an sp2 hybridization has lower reactivity (similar to a primary carbon) which can explain the low percentage of product at the steroid ring.

Steroid hydrocarbons

Cholestane (compound J in **Fig. 1**) lacks the polar alcohol group in C3, which increases the fraction of entrance by this side of the ligand, but most importantly the bulkier saturated C5 and C6 (and consequent loss of planarity) impedes a suitable placement of the ligand in the binding site when it enters by C25. For this reason a low number of structures come close enough to the oxygen atom in cholestane (**Fig. S7**) which explains the low reactivity of this compound (cholesterol is converted by 64% while only 3% for cholestane).

Cholesta-3,5-diene (compound K in **Fig. 1**) has a very interesting reactivity due to the presence of two double bonds at C3 and C5. Also the lack of any polar group leads to a less favorable entrance by C25 (82% for A and 45% for K)

(**Fig. 3**). This compound should also be compared to cholesta-3,5-dien-7-one as they only differ by the presence of a ketone group at C7 (**Figs. S6** and **S8**). This group has a considerable effect in reactivity. First it decreases the fraction of entrances by C3 (55% for K vs. 42% for H), thus increasing the conversion of the reactants to products (18% for K 57% and for H). Second, the more favorable entrance by C3 for cholesta-3,5-diene increases the fraction of hydroxylated products at the steroid rings. It is also interesting to note that many of these products are additions to the double bond.

Sterol esters

Cholesteryl acetate (compound M in **Fig. 1**) has almost the same structure as cholesterol but with an ester instead of a hydroxyl group in the C3. For this reason, the entrance to the protein by this side (**Fig. 3**) is favoured compared to cholesterol, while the opposite occurs at the C25 side (82% for cholesterol and 35% for cholesteryl acetate) (**Fig. 3**). Moreover, the binding position of the ligand in the C25 oxidation is no longer favoured by the hydrogen bond with Glu245 (**Fig. 4**).

Cholesteryl caprylate (compound O in **Fig. 1**) is similar to cholesteryl acetate but with a larger alkyl chain in the ester group. PELE simulations show that the ligand does not approach the heme group from the C25 side (**Fig. S9**) nor by the C3 (data not shown). The reason for this is the large hydrophobic chains that favor interactions with the protein to avoid solvent exposure. An unusual binding mode occurs for this molecule where a strong minimum energy structure is observed that hinders the correct placement of the molecule in the active site by either end.

Supplemental Figures

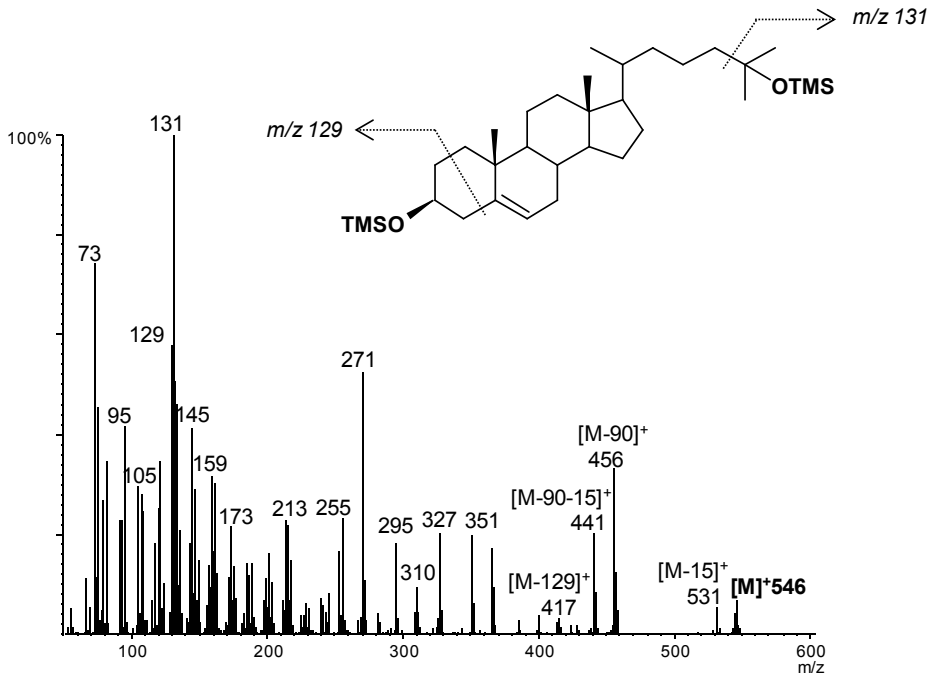

Fig S1. Mass spectrum of 25-hydroxycholesterol from peroxygenase reactions with cholesterol (see **Fig. 1**), as TMS derivative.

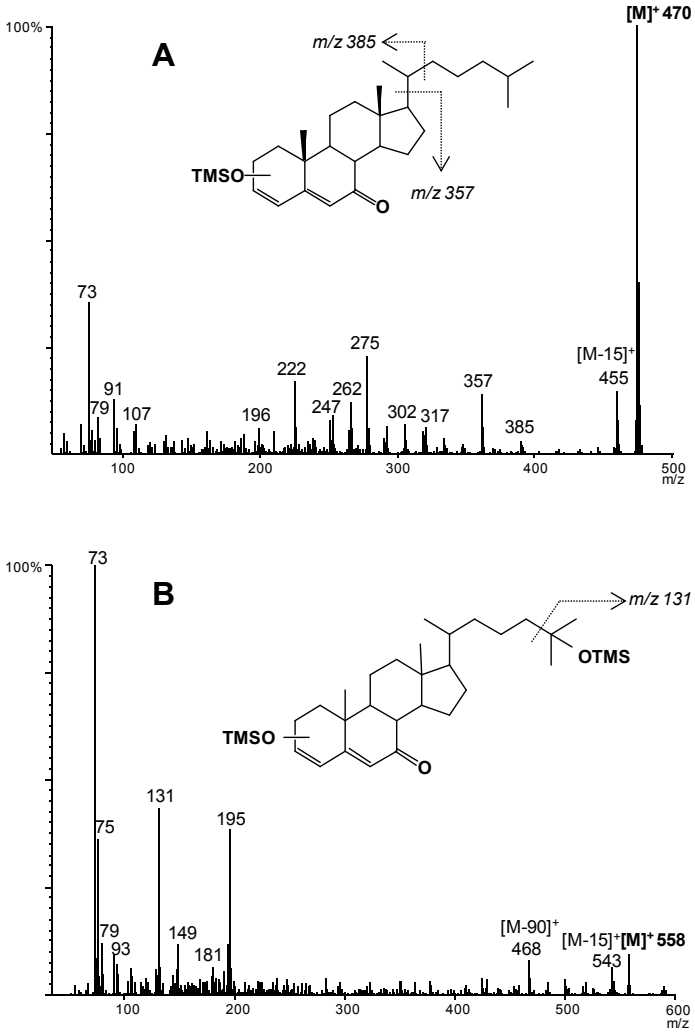

Fig S2. Mass spectra of x-hydroxycholesta-3,5-diene-7-one (**A**) and x,25-dihydroxycholesta-3,5-diene-7-one (**B**) from peroxygenase reactions with cholesta-3,5-diene-7-one (see **Fig. 1**), as TMS derivatives.

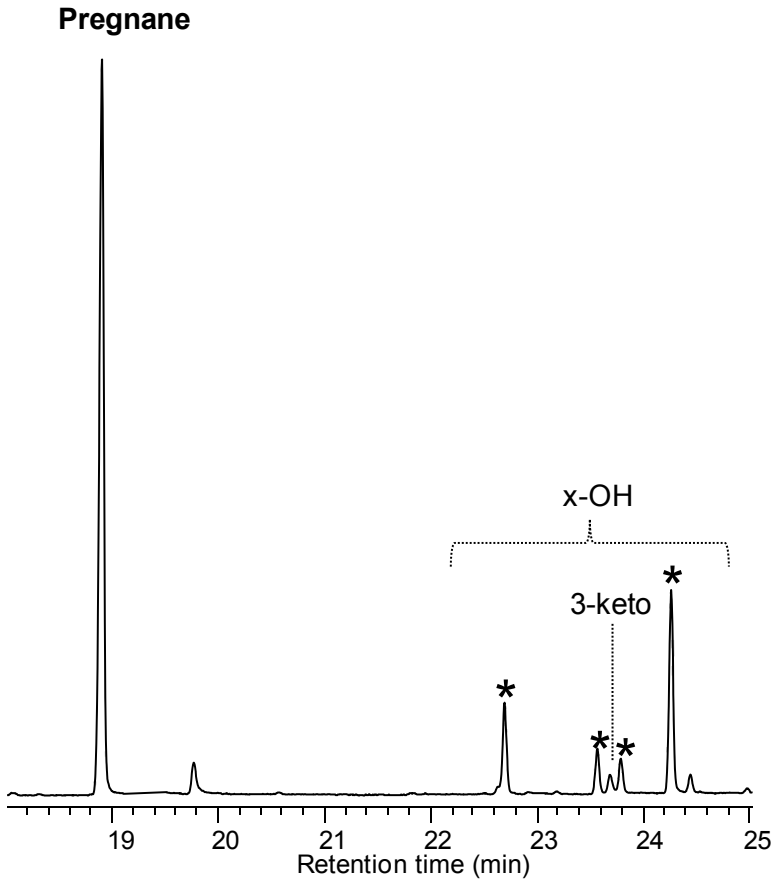

Fig S3. GC-MS analysis of the *Mroi*UPO reaction (at 60 min) with pregnane (see **Fig. 1**) showing the remaining substrate and the monohydroxylated derivatives (x denotes the unknown position of hydroxylation in the ring).

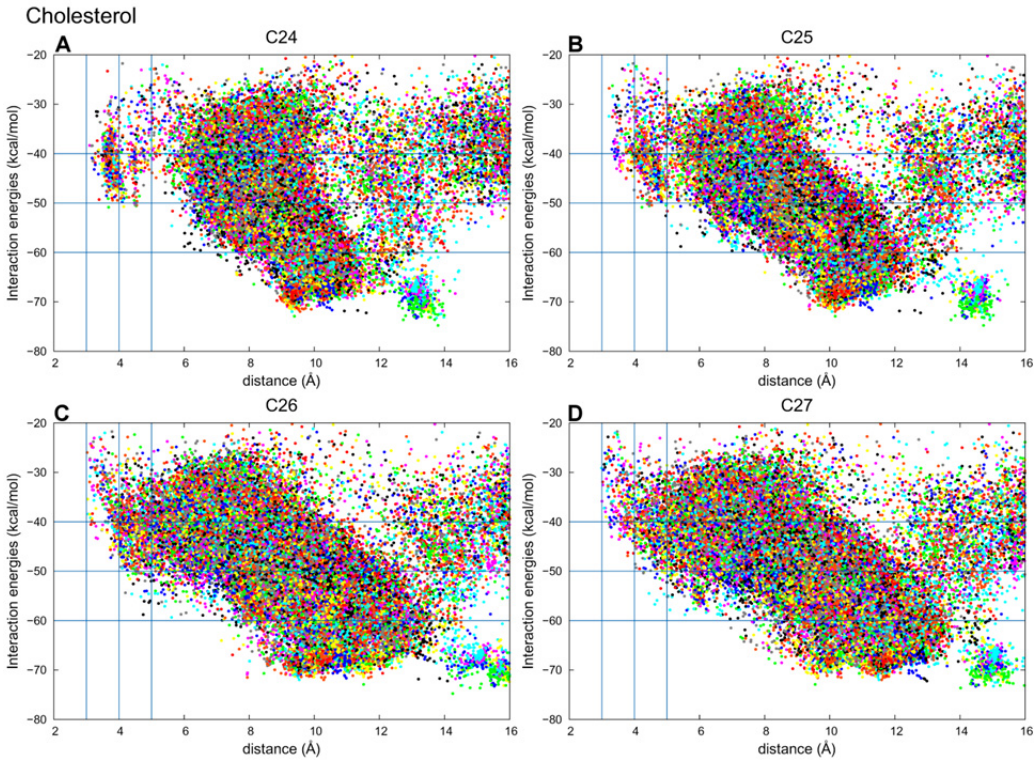

Fig S4. Results from PELE simulations for cholesterol (compound A in **Fig. 1**). The distances plotted correspond to the C24 (**A**), C25 (**B**), C26 (**C**) or C27 (**D**) atoms to the oxygen atom in *Aae*UPO compound I.

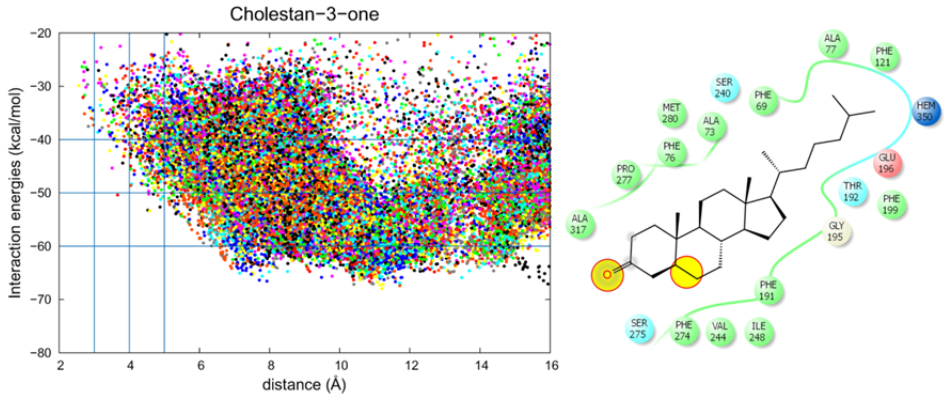

Fig S5. Results from PELE simulations for cholestan-3-one (compound **F** in **Fig. 1**) diffusion at the active site of the *Aae*UPO including: *(left)* Plots of the energy profile *vs.* the distance between the steroid H25 and the oxygen atom in enzyme compound I; and (*right*) Main interactions between cholestan-3-one and the enzyme in a representative structure in the binding site. The yellow circles identify structural differences relative to cholesterol.

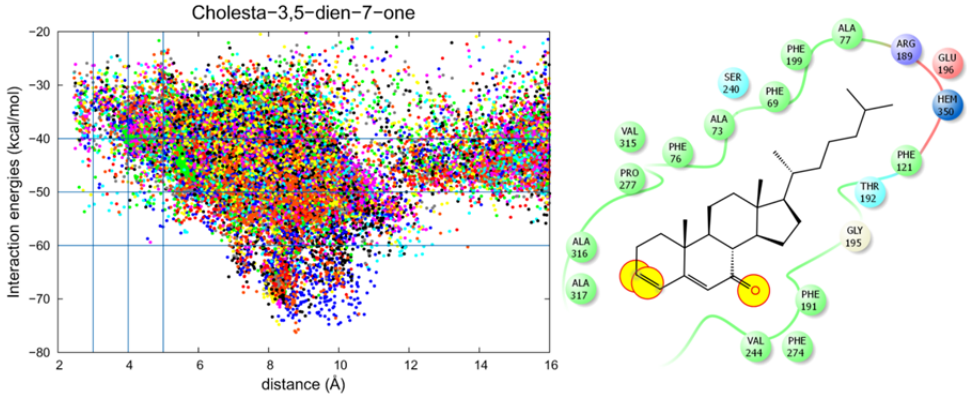

Fig S6. Results from PELE simulations for cholesta-3,5-dien-7-one (compound **H** in **Fig. 1**) diffusion at the active site with C25 approaching the heme cofactor of the *Aae*UPO, including: (*left*) Plots of the energy profile *vs.* the distance between the steroid H25 atom and the oxygen atom in enzyme compound I; and (*right*) Main interactions between cholesta-3,5-dien-7-one and the enzyme in a representative structure in the binding site. The yellow circles identify structural differences relative to cholesterol.

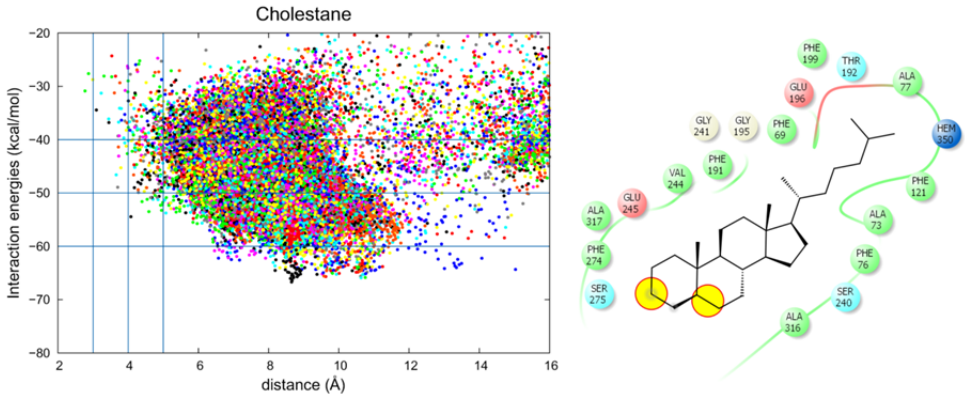

Fig S7. Results from PELE simulations for cholestane (compound **J** in **Fig. 1**) diffusion at the active site with C25 approaching the heme cofactor of the *Aae*UPO, including: (*left*) Plots of the energy profile *vs* the distance between the steroid C25 atom and the oxygen atom in enzyme cholestane; and (*right*) Main interactions between cholestane and the enzyme in a representative structure in the binding site. The yellow circles identify structural differences relative to cholesterol.

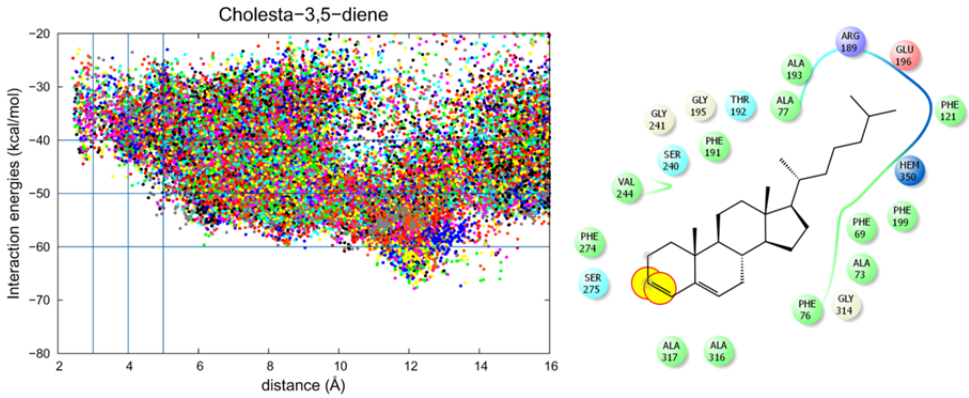

Fig S8. Results from PELE simulations for cholesta-3,4-diene (compound **K** in **Fig. 1**) diffusion at the active site with C25 approaching the heme cofactor of the *Aae*UPO, including: (*left*) Plots of the energy profile *vs.* the distance between the steroid H25 atom and the oxygen atom in enzyme compound I; and (*right*) Main interactions between cholesta-3,4-diene and the enzyme in a representative structure in the binding. The yellow circles identify structural differences relative to cholesterol.

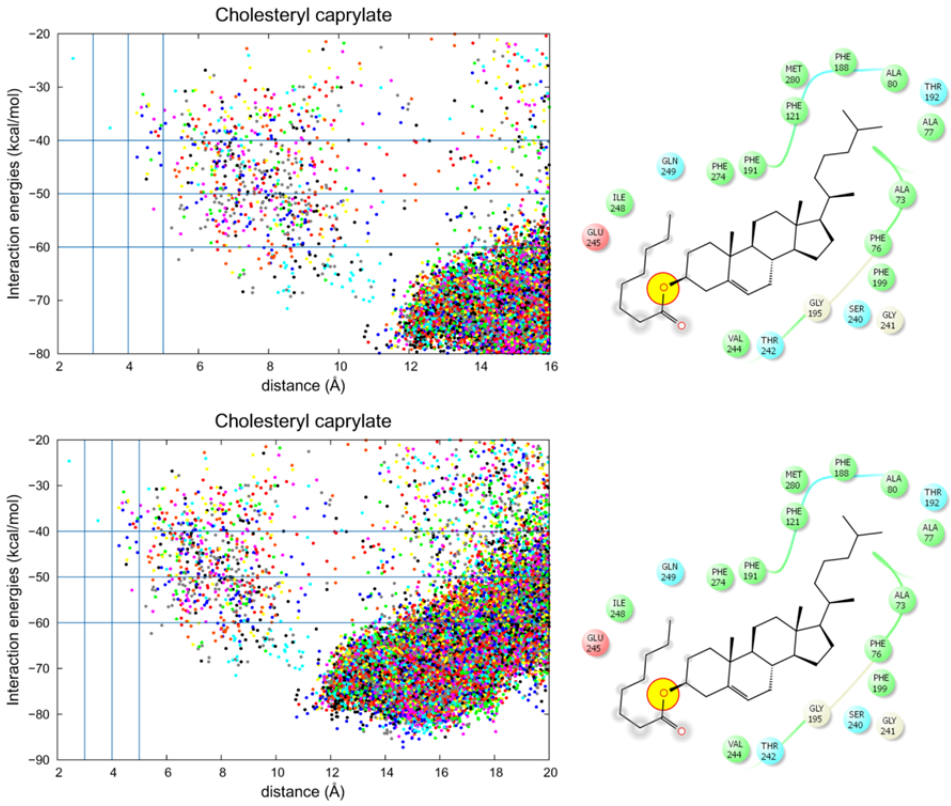

Fig S9. Results from PELE simulations for cholesteryl caprylate (compound **O** in **Fig. 1**) diffusion at the active site with C25 approaching the heme cofactor of the *Aae*UPO, including: (*left*) Plots of the energy profile *vs.* the distance between the steroid H25 atom and the oxygen atom in enzyme compound I; and (*right*) Main interactions between cholesteryl caprylate and the enzyme in a representative structure in the binding site. The yellow circles identify structural differences relative to cholesterol.

6.1. Publicación IV:

Babot E.D., del Río J.C., Kalum L., Martínez A.T. and Gutiérrez A. (2014). Regioselective hydroxylation in the production of 25-hydroxyvitamin D by *Coprinopsis cinerea* peroxygenase. *ChemCatChem* 7: 283-290.

Regioselective hydroxylation in the production of 25-hydroxyvitamin D by *Coprinopsis cinerea* peroxygenase

Esteban D. Babot[a], José C. del Río[a], Lisbeth Kalum[b], Angel T. Martínez[c] and Ana Gutiérrez[a*]

[a]Instituto de Recursos Naturales y Agrobiología de Sevilla, CSIC, Reina Mercedes 10, E-41012 Seville, Spain

[b]Novozymes A/S, Krogshoejvej 36, 2880 Bagsvaerd, Denmark

[c]Centro de Investigaciones Biológicas, CSIC, Ramiro de Maeztu 9, E-28040 Madrid, Spain

* Corresponding author

Abstract:

Monohydroxylated metabolites of vitamin D_3 (cholecalciferol) and vitamin D_2 (ergocalciferol), generically known as 25-hydroxycalciferol, are better for several diseases and other applications than vitamin D (calciferol). This work relates to a novel biotechnological approach for the preparation of 25-hydroxycalciferols, starting from the readily available cholecalciferol and ergocalciferol. It includes the regioselective (100%) hydroxylation of these compounds (at the C-25 position) under mild and environmentally-friendly conditions using a peroxidase from the fungus *Coprinopsis cinerea* (gene model CC1G_08427T0 from the sequenced genome) that catalyzes monooxygenation with H_2O_2 as the only cosubstrate (peroxygenase). Hydroxylation of cholecalciferol and ergocalciferol is a true peroxygenation, as demonstrated by incorporation of ^{18}O from $H_2{}^{18}O_2$ into the products. The peroxygenase has additional advantages related to its recombinant nature, enabling enzyme engineering and low-cost overexpression in an industrial host. Therefore, the peroxygenase is a promising biocatalyst for the production of vitamin D active metabolites.

Keywords: cholecalciferol, ergocalciferol, peroxygenase, 25-hydroxyvitamin D, vitamin D.

Introduction

Vitamin D (calciferol) includes a group of liposoluble secosteroids that are essential in the homeostasis of calcium and phosphate through the regulation of hundreds of genes in animal metabolism.[1] Vitamin D deficiency is a great concern for human health because it causes rickets in children and osteomalacia in adults. An inadequate amount of vitamin D can increase the risk of bone fractures in elderly people and, more recently, it has been associated to an increased risk of cancers, cardiovascular diseases, immunodeficiency, and diabetes.[1, 2] Cholecalciferol (vitamin D_3, **Figure 1A**) and ergocalciferol (vitamin D_2 ; **Figure 1B**) can be obtained through dietary intake.

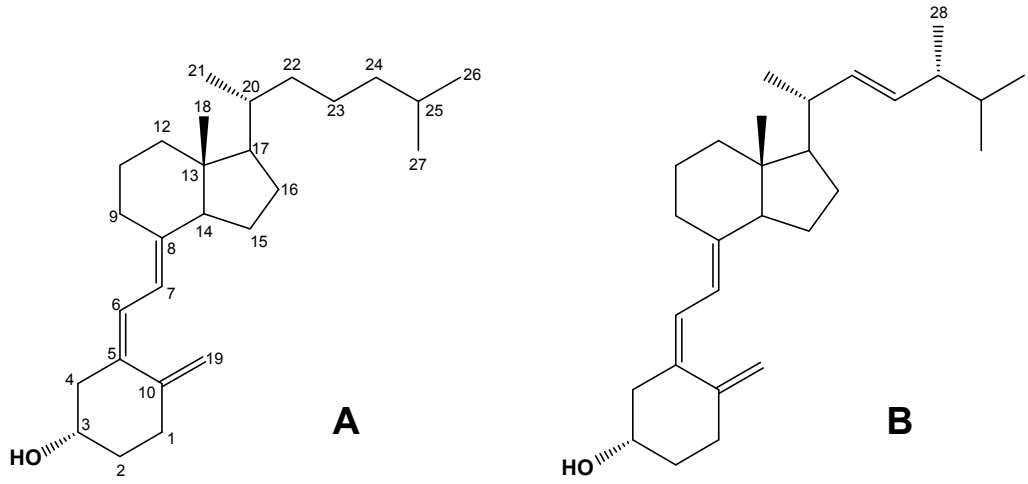

Figure 1. Chemical structures of the two vitamin D forms, cholecalciferol (vitamin D_3, **A**) and ergocalciferol (vitamin D_2, **B**), tested as substrates of the recombinant peroxygenase.

Vitamin D_3, derived from cholesterol metabolism in animals, is naturally present in foods, such as fish, meat, eggs, and milk, whereas vitamin D_2 is present in commercially irradiated mushrooms and yeast,[3] where it is formed from fungal ergosterol.[4] Additionally, vitamin D_3 is produced in human skin and converted to active hydroxylated metabolites in the liver and kidneys, as

described in **Figure 2**. 25-Hydroxyvitamin D_3 (25-hydroxycholecalciferol) is the first metabolically active, and the major form, of circulating vitamin D (used to detect vitamin deficiency), whereas 1α,25-dihydroxyvitamin D3 (calcitriol) is the major active form. Vitamin D_2 obtained from our diet undergoes an analogous set of activation steps to give 25-hydroxyergocalciferol and 1α,25-dihydroxyergocalciferol.

It has been shown that for diseases, such as hyperglycemia, chronic kidney disease, and for anephric patients, supplementation with 25-hydroxycholecalciferol has a positive effect[5–7] owing to, in some cases, the extrarenal hydroxylation of this metabolite.[6] Similar findings have also been reported for Crohn's disease and intestinal resection, as well as for chronic cholestatic liver disease.[8, 9] In addition to the physiological interest in 25-hydroxycholecalciferol for human health, this compound has also raised interest for the feeding of poultry[10–13] and other farm animals.[14] The poor-quality skeletons of broiler chickens is currently a serious problem that has a negative influence on the economic benefits of rearing these birds. The addition of 25-hydroxycholecalciferol into feed mixtures has been shown to have a favorable effect.[10] Therefore, both vitamin D_3, D_2, and their hydroxylated derivatives are approved food additives.[15]

In addition to the biosynthesis of naturally hydroxylated vitamin D_3 by animals, and production of hydroxylated vitamin D_2 from fungal ergosterol by UV irradiation, chemical synthesis (total or partial) for the production of these active compounds has attracted much interest, and several approaches have been reported.[11, 16–22] As a sustainable alternative, biotechnological approaches have been investigated, including microbial oxygenations in the production of vitamin D derivatives.[23, 24] Moreover, enzymes (monooxygenases containing both heme and flavin cofactors) are capable of catalyzing the selective oxyfunctionalization of organic substrates under mild and environmentally friendly conditions.[25] Members of the cytochrome P450 monooxygenase (P450) superfamily are remarkable examples of such catalysts.[26–29] However, large-scale applications are limited because of the intrinsic properties of P450s.[30]

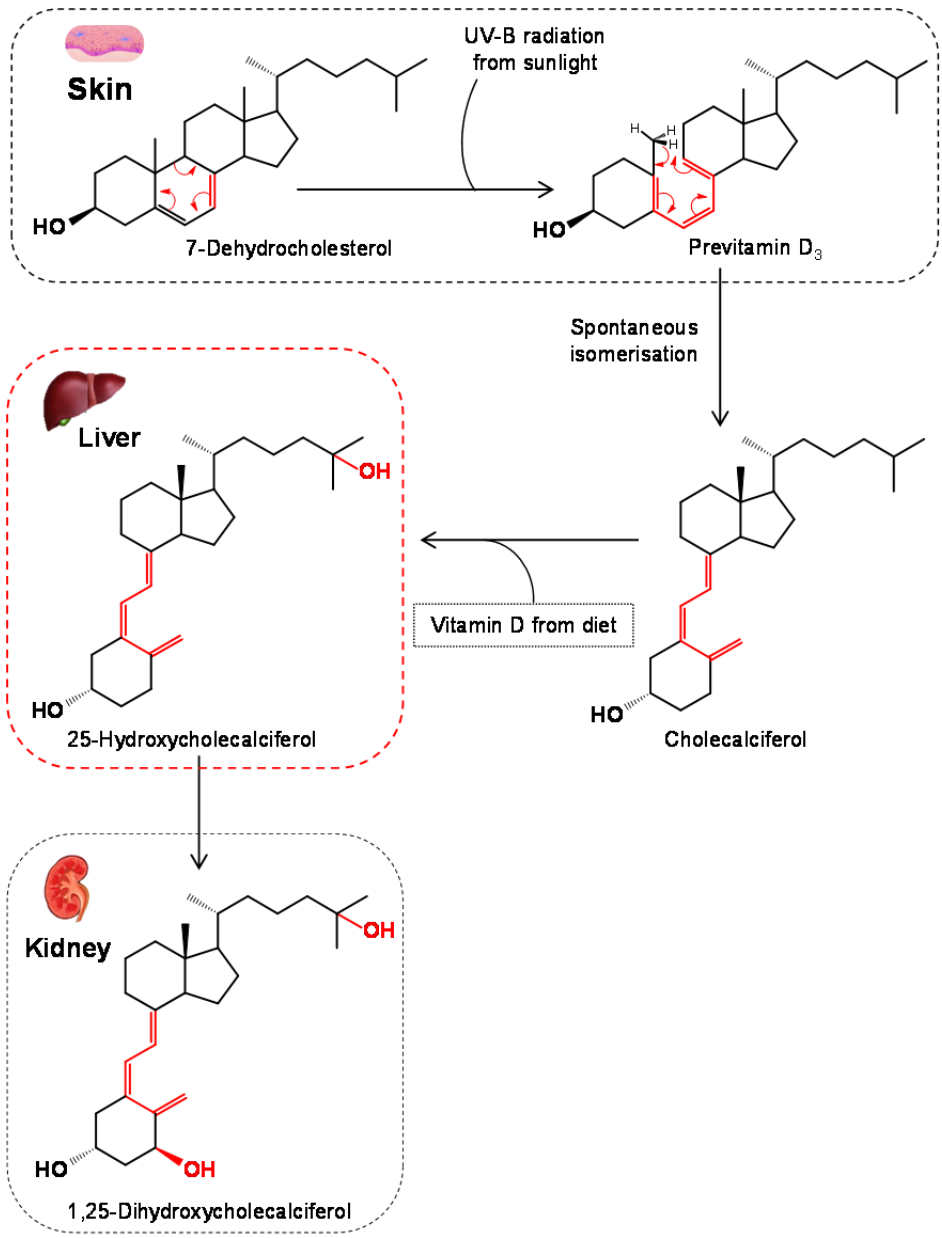

Figure 2. Human metabolism of vitamin D_3 showing the key metabolites. On exposure to UV light in the skin, provitamin D_3 (7-dehydrocholesterol) is converted to previtamin D_3, which is isomerized to more stable vitamin D_3 (cholecalciferol) via a thermally induced transformation. Vitamin D_3, either cutaneously formed or taken in the diet, is then hydroxylated in the liver to 25-hydroxyvitamin D_3 (25-hydroxycholecalciferol). Finally, 25-hydroxyvitamin D_3 is hydroxylated again, primarily in the kidney, to give 1α,25-dihydroxyvitamin D_3 (calcitriol), the major biologically active form of vitamin D.

Recently, a new type of peroxidase was discovered in the basidiomycete *Agrocybe aegerita*[31] that turned out to be a true peroxygenase efficiently transferring oxygen from peroxide to various organic substrates.[32–34] Only a few similar enzymes have been characterized from related fungi, but there are indications of their widespread occurrence.[35–37] For example, over 100 related genes, classified in the new superfamily of heme–thiolate peroxidases,[33, 38] have recently been identified in the screening of 24 sequenced genomes of basidiomycetes,[39] including *Coprinopsis cinerea*. To date, wild peroxygenase has not been isolated from *C. cinerea* cultures, but the corresponding genes from the genome were heterologously expressed by Novozymes A/S (Bagsvaerd, Denmark).[40] The monooxygenation ability of one of these recombinant enzymes (protein ID 7249 from the *C. cinerea* genome available at the JGI; http://genome.jgi.doe.gov/Copci1) has recently been exploited for the hydroxylation of fatty acids, fatty alcohols, and long-chain alkanes.[41] Herein, the ability and efficiency of the recombinant *C. cinerea* peroxygenase in the hydroxylation of vitamin D_3 and D_2, is evaluated for the first time.

Results

The current work proposes a biotechnological approach to obtain both 25-hydroxycholecalciferol and 25-hydroxyergocalciferol starting from readily available and low-cost cholecalciferol and ergocalciferol, respectively, by using an enzyme from *C. cinerea*, which is representative of the new fungal peroxidases with monooxygenase activity (peroxygenases) first described in *A. aegerita*. With this purpose, the reaction of the latter secosterols with the recombinant peroxygenase was studied, and the substrate conversion rate and product identification were carried out by GC-MS.

Enzymatic hydroxylation of cholecalciferol at C-25 position

Firstly, cholecalciferol (**Figure 1A**) was tested as a peroxygenase substrate. The GC-MS analysis of the reaction revealed that this compound was completely transformed by the *C. cinerea* enzyme within 60 min (**Figure 3A**). The control reaction without peroxygenase is shown in **Figure 3B**.

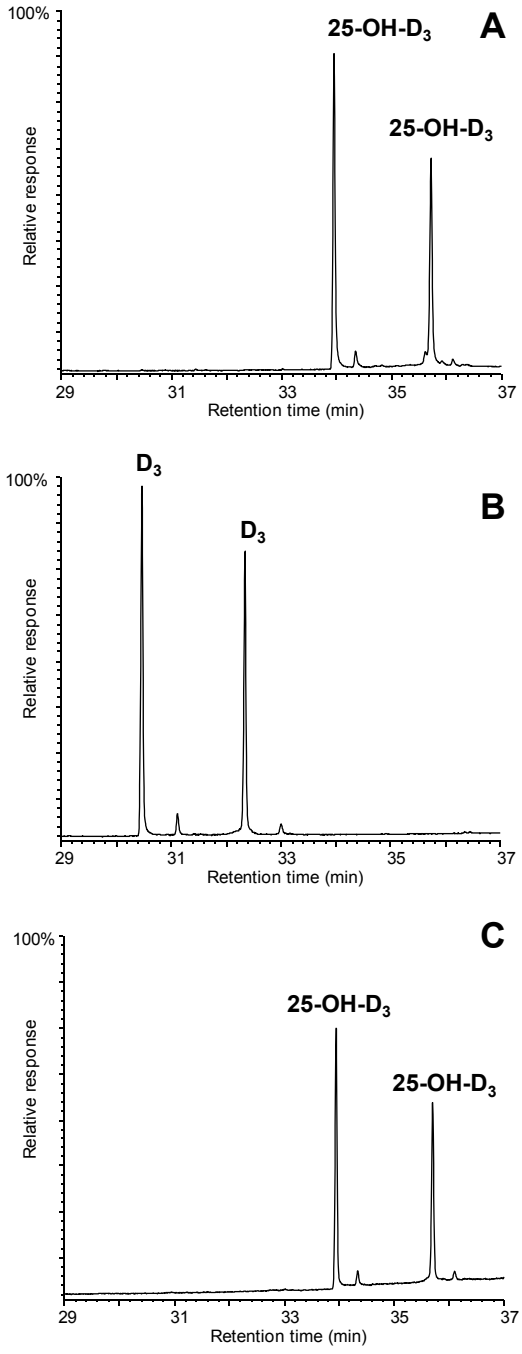

Figure 3. GC-MS analysis of the *C. cinerea* peroxygenase reaction (at 60 min) with cholecalciferol (see **Figure 1A**) showing product formation (**A**), control without enzyme (**B**), and 25-hydroxycholecalciferol standard (**C**), as TMS derivatives. In all cases the isopyro (left) and pyro (right) isomers from secosteroid thermal rearrangement are obtained.

The conversion showed strict regioselectivity and provided 25-hydroxycholecalciferol exclusively (100% yield), as confirmed by comparison to a true standard of this compound (**Figure 3C**), which showed an identical retention time.

The double peaks observed in the chromatograms for each substrate and product (**Figure 3**) correspond to the isopyro (19β, 9β) and pyro (19α, 9α) isomers formed by thermal rearrangement involving ring-B closure, which vitamin D and its hydroxylated derivatives undergo because of the temperature at which GC-MS EI(+) analysis is carried out. Indeed, the presence of the two isomers during GC separation is a useful indication that a secosteroid of the vitamin D-type was injected into the system.[42] Therefore, both the chromatographic profiles (**Figure 3**) and the mass spectra discussed below (**Figure 4**) correspond to the isomerized secosteroids.

The position of the hydroxyl group at C-25 was established by mass spectrometry of the trimethylsilyl (TMS) derivative. The spectrum in **Figure 4A** shows a prominent ion from C-24/C-25 bond cleavage, with a characteristic fragment at *m/z* 131 and a molecular ion at *m/z* 544. Additionally, characteristic fragments at *m/z* 529 ($[M-15]^+$), *m/z* 454 ($[M-90]^+$), *m/z* 439 ($[M-90-15]^+$), *m/z* 349 ($[M-90-90-15]^+$), and *m/z* 413, were also present. The spectrum of standard 25-hydroxycholecalciferol is shown in the inset of **Figure 4A**, and is identical to that obtained from the peroxygenase reaction. It should be noted that the mass spectra in **Figure 4** are from vitamin D pyroderivatives in which ring-B is cyclized, even if the secosteroid is illustrated, because GC-MS spectra of non-isomerized vitamin D have not yet been described.[42] The NMR spectra of the reaction product confirmed the formation of 25-hydroxylated vitamin D_3 (unprotonated C-25 with δ_C=71.3 ppm, and other signals listed in the Experimental Section).

An ^{18}O-labeling study, using cholecalciferol as substrate and $H_2{}^{18}O_2$ as enzyme co-substrate, was performed to investigate the origin of the oxygen atom incorporated during oxygenation. The results showed that oxygen originating from ^{18}O-labeled peroxide ($H_2{}^{18}O_2$) was completely incorporated into 25-hydroxycholecalciferol.

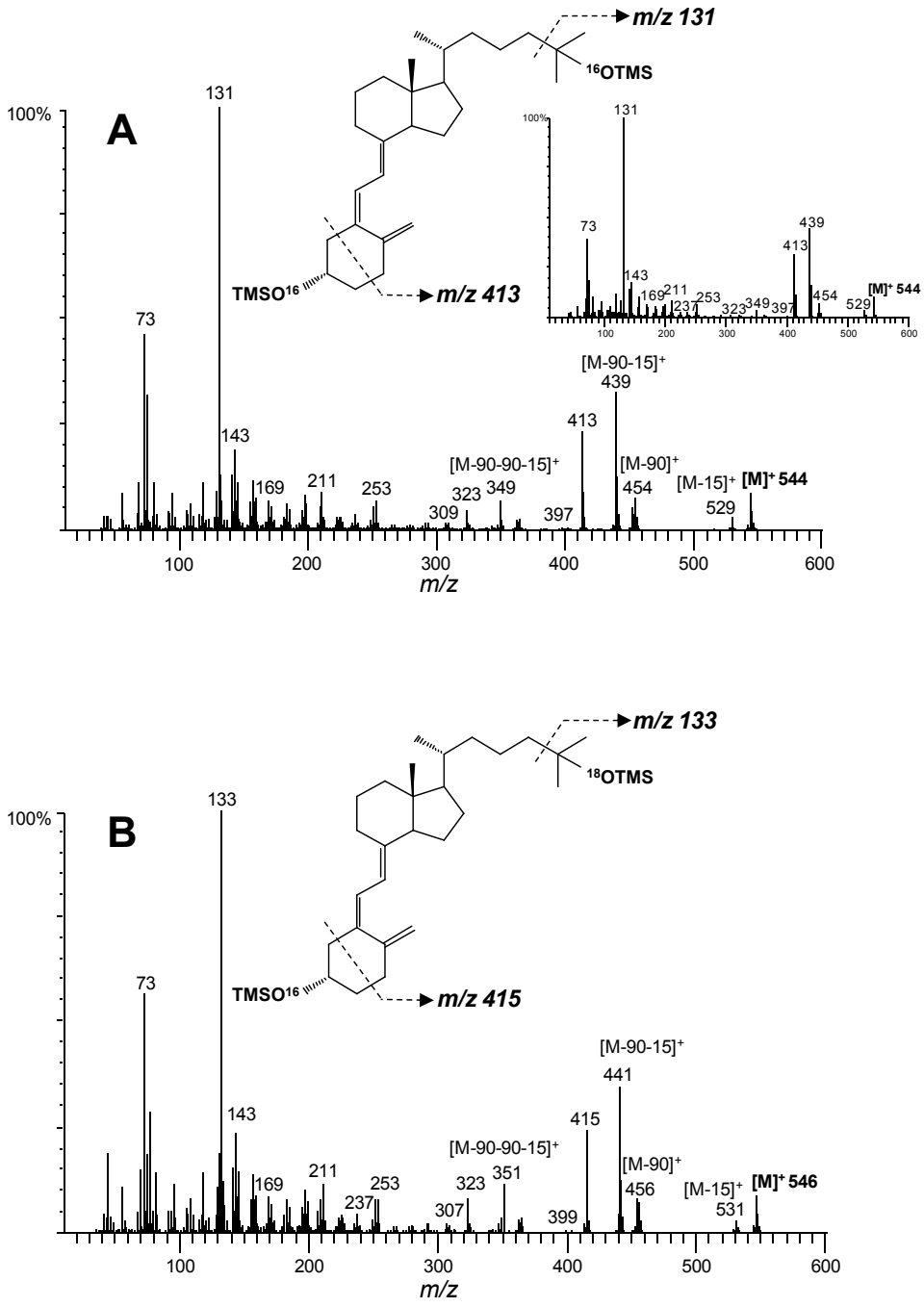

Figure 4. Mass spectra of 25-hydroxycholecalciferol from *C. cinerea* peroxygenase reaction with cholecalciferol in the presence of $H_2{}^{16}O_2$ (**A**) (inset is the mass spectrum of standard compound 25-hydroxycholecalciferol) and $H_2{}^{18}O_2$ (90% isotopic purity) (**B**), as TMS derivatives.

Mass spectral analysis of the resulting monohydroxylated cholecalciferol (**Figure 4B**) showed that the characteristic fragments had approximately 90% shifted from the natural abundance at *m/z* 544, *m/z* 529, *m/z* 454, *m/z* 439, *m/z* 349, *m/z* 131, and *m/z* 413 found in the unlabeled peroxide reaction to *m/z* 546, *m/z* 531, *m/z* 456, *m/z* 441, *m/z* 351, *m/z* 133, and *m/z* 415, respectively (~10% of the original frag fragments remained in the $H_2{}^{18}O_2$ reactions owing to the 90% ^{18}O isotopic purity of the labeled peroxide).

Enzymatic hydroxylation of ergocalciferol at C-25 position

Hydroxylation of ergocalciferol (**Figure 1B**), the artificial form of vitamin D derived from UV irradiation of ergosterol, was also studied. The peroxygenase from *C. cinerea* showed similar efficiency, in the transformation of ergocalciferol, to that of cholecalciferol after 60 min incubation, resulting in 90% substrate conversion (**Figure 5A** and **B**) although the conversion was slower as found at shorter incubation times (data not shown). This reaction also showed strict regioselectivity, 25-hydroxyergocalciferol being the only product formed (90% yield), confirmed by comparison with a standard (**Figure 5C**). The position of the hydroxyl group at C-25 was established from the mass spectrum (**Figure 6**), which was identical to that of a standard (**Figure 6**, inset). The spectrum shows a prominent ion from C-24/C-25 bond cleavage, with a characteristic fragment at *m/z* 131 and a molecular ion at *m/z* 556. Additionally, characteristic fragments at *m/z* 541 ($[M-15]^+$), *m/z* 466 ($[M-90]^+$), *m/z* 451 ($[M-90-15]^+$), and *m/z* 361 ($[M-90-90-15]^+$), were also present in the spectrum. In a similar manner to the reaction with cholecalciferol, the peaks of the two pyroisomers are found in the chromatogram (**Figure 5**), and the mass spectra in **Figure 6** are from isomerized vitamin D derivatives. The NMR spectra of the reaction product confirmed the formation of 25-hydroxylated vitamin D_2 (unprotonated C-25 with δ_C=72.5 ppm, and other signals listed in the Experimental Section).

Similar to the cholecalciferol reaction, ^{18}O-labeling showed that oxygen originating from ^{18}O-labeled peroxide ($H_2{}^{18}O_2$) was completely incorporated into 25-hydroxyergocalciferol. Mass spectral analysis (**Figure 6B**) showed that the characteristic fragments for the 25-hydroxyergocalciferol had approximately 90% shifted from the natural abundance at *m/z* 556, *m/z* 541, *m/z* 466, *m/z* 451, *m/z* 361, and *m/z* 131 found in the unlabeled peroxide reaction to *m/z* 558, *m/z* 543, *m/z* 468, *m/z* 441, *m/z* 363, and *m/z* 133, respectively.

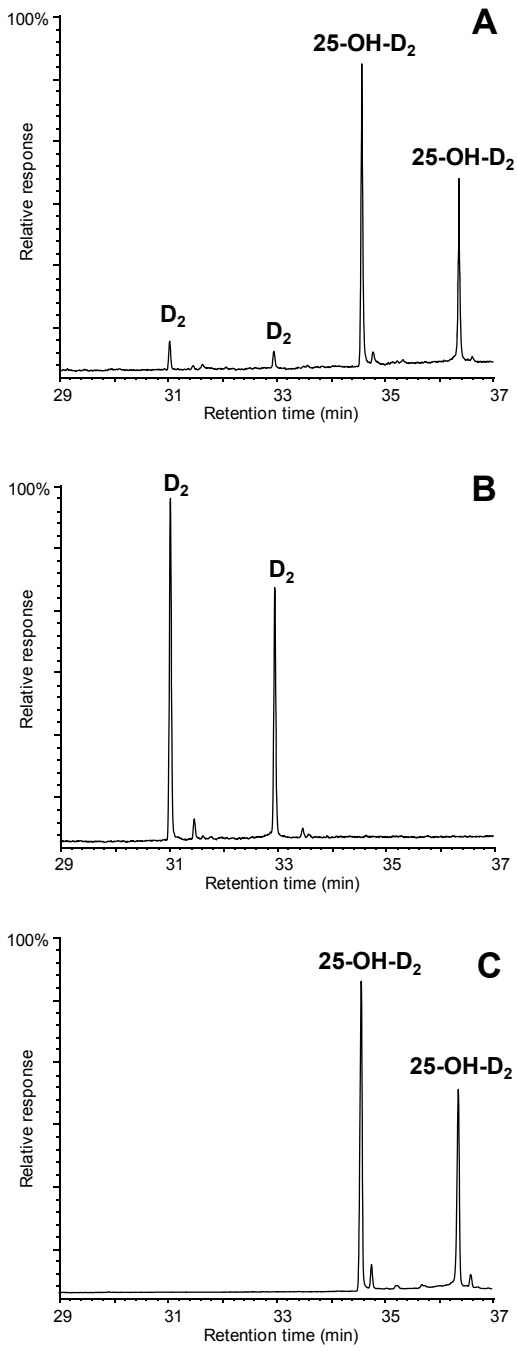

Figure 5. GC-MS analysis of the *C. cinerea* peroxygenase reaction (at 60 min) with ergocalciferol (see **Figure 1B**) showing product formation (**A**), control without enzyme (**B**), and 25-hydroxyergocalciferol standard (**C**), as TMS derivatives. In all cases the isopyro (left) and pyro (right) isomers from secosteroid thermal rearrangement are obtained.

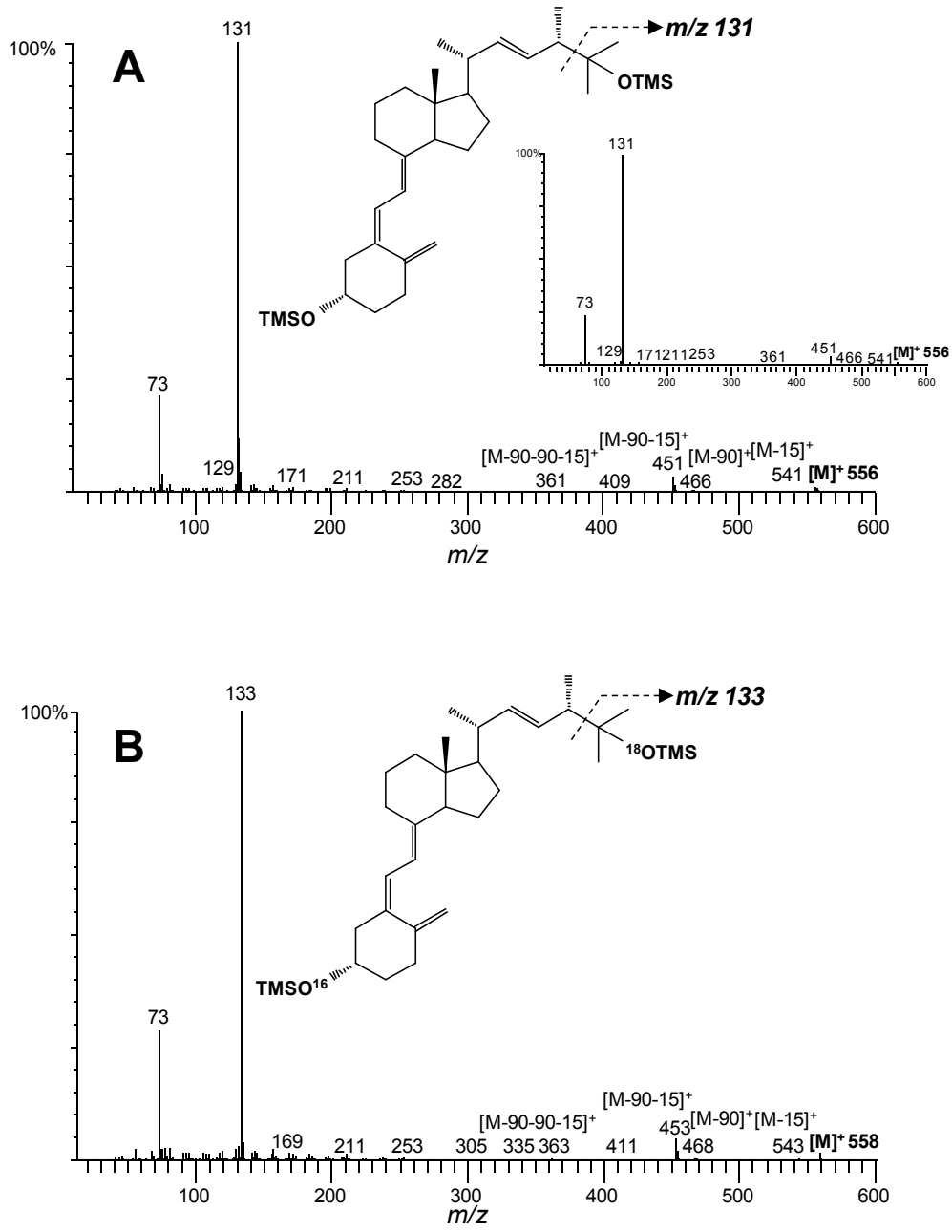

Figure 6. Mass spectra of 25-hydroxyergocalciferol from *C. cinerea* peroxygenase reaction with ergocalciferol in the presence of $H_2{}^{16}O_2$ (**A**) (inset is the mass spectrum of standard compound 25-hydroxyergocalciferol) and $H_2{}^{18}O_2$ (90% isotopic purity) (**B**), as TMS derivatives.

Discussion

It has been demonstrated that the 25-hydroxylated metabolites of vitamin D, including 25-hydroxycholecalciferol and 25-hydroxyergocalciferol, are considerably better therapeutic agents for several diseases than vitamin D itself, owing to their direct biological activity and better intestinal absorption in some cases.[5, 8, 9] Likewise, these hydroxylated compounds also find applications as animal-feed supplements (and are superior to vitamin D itself), especially when their subsequent metabolic conversion is diminished.[10, 43, 44] On the other hand, despite some controversy on which oral formulation of vitamin D (vitamin D_3 or D_2) is preferred, and although there are reports that certain animal species discriminate against vitamin D_2, in humans vitamin D_2 and D_3 seem to be essentially equipotent in the prevention and cure of rickets and possibly other vitamin D actions in the body.[6] The recognition that both forms of 25-hydroxyvitamin D exhibit several advantages relative to vitamin D has generated great interest in the chemical synthesis of these compounds.[11, 16–20] However, these reactions often require strong oxidizing agents, include several steps, are expensive, and occur with little regioselectivity in the hydroxylation steps.

In contrast to chemical synthesis, the peroxygenase from the *C. cinerea* genome is highly selective, and can hydroxylate the C-25 position of both vitamin D_3 and D_2 to provide the biologically active hydroxylated forms by means of environmentally friendly and potentially unexpensive reactions. This enzyme, the sequence of which is also available from GenBank (XM_001831858), shares 63% of mature protein sequence with the first described and cloned basidiomycete peroxygenase from *A. aegerita*. Similarities include the catalytically relevant Cys36 (87% identity in the Lys15–Gly66 region around this heme-iron ligand), Arg189 and Glu196 (involved in reactions with peroxide), as well as four (Phe76, Phe121, Phe191, and Phe199) of the five phenylalanine residues at the heme access cavity of the *A. aegerita* peroxygenase, and two cysteine residues (Cys284 and Cys327).[45] These structural similarities justify the similar oxygenation activities reported in a recent comparison of two basidiomycete peroxygenases.[41] However, the *C. cinerea* enzyme is superior for vitamin D_2/D_3 hydroxylation, resulting in the 90-100% conversion rates reported herein, whereas 45-77% conversion was obtained with the *A. aegerita* and *Marasmius rotula* peroxygenases under the same reaction conditions (unpublished).

Selective hydroxylation of vitamin D by the recombinant *C. cinerea* peroxygenase, as shown here by MS and NMR analysis, is in agreement with the described subterminal oxygenation of fatty acids, fatty alcohols, and alkanes by this enzyme,[41] as well as by the *A. aegerita* peroxygenase.[46, 47] It is worth noting that the structural features of the vitamin D_2 side chain, such as the methyl group at C-24 and the double bond at C-22, did not preclude the hydroxylation at C-25. In the above reactions, the basidiomycete enzymes act as true peroxygenases, as confirmed by the labeled oxygen of $H_2{}^{18}O_2$ being incorporated into the formed products. The same was shown previously, for the peroxygenase-catalyzed oxygenation of several aliphatic[46] and aromatic compounds,[34] in a series of reactions that could also be useful for preparing specifically labeled molecules for diagnostic purposes. The enzymatic reactions described herein could be used for the selective hydroxylation of totally or partially chemically synthesized cholecalciferol (or ergocalciferol) or, more interestingly, could be applied to natural ergocalciferol obtained by UV irradiation of ergosterol, a sterol characteristic of fungi.[48] The latter UV reaction is possible because the ergosterol ring-B is doubly unsaturated, compared with the monounsaturated ring in the main sterols of plant (sitosterol) and animal (cholesterol) origin (7-dehydrocholesterol is a precursor of both cholesterol and vitamin D_3). The chemistry of aliphatic- (and aromatic-) substrate oxygenation by the basidiomycete peroxygenases[49, 50] is the same as that operating in P450s,[27] both enzymes share a heme–thiolate active center and a Fe^{IV}=O compound that transfers the oxygen atom to the substrate in a two-electron oxidation. However, unlike P450s, which are intracellular enzymes whose activation requires NAD(P)H as an electron donor and auxiliary flavin reductases (or a second flavin domain) for electron transfer to O_2 (as shown using $^{18}O_2$),[51] the basidiomycete peroxygenases are secreted proteins, therefore, are far more stable, and only require H_2O_2 for (direct) activation and subsequent oxygen transfer to the substrate.[34, 52] Owing to the above characteristics, these new basidiomycete enzymes can be considered as the biocatalysts of choice for enzymatic oxygenations.

The above reasoning is especially true for the vitamin D hydroxylation reactions described above because, in addition to their chemical selectivity, high conversion rates were obtained resulting in almost complete transformation in a short reaction time. The efficiency of these peroxygenase reactions is similar to that recently found for the oxygenation of some alkylbenzenes and styrene

derivatives,[53] but is much higher than that reported for most peroxygenase reactions, such as fatty acid or alkane oxygenations, which often result in several products (at ω-1 and ω-2 positions) with different oxidation degrees (from hydroxyl to carbonyl groups).[41, 46, 47] Therefore, the production of biologically active vitamin D forms from both cholecalciferol and ergocalciferol adds to the list of interesting oxygenation reactions that basidiomycete peroxygenase can catalyze,[46, 47, 54-58] occupying a preeminent position owing to the high degree of regioselectivity of the enzymatic bioconversion. Moreover, the recombinant nature of the *C. cinerea* peroxygenase used, after successful expression in the industrial host *Aspergillus oryzae*,[40] permits over expression of the enzyme (as a low-cost product) and tailoring of its properties by protein engineering tools, if necessary, to improve industrial applicability.

Conclusions

Fungal peroxygenase, a novel biocatalyst for environmentally friendly oxyfunctionalization of a variety of aromatic and aliphatic compounds, first described in *A. aegerita*, is now available for application in enzymatic reactions after the heterologous expression of a *C. cinerea* peroxygenase gene in an industrial host organism. The recombinant enzyme obtained is evaluated for the first time in the hydroxylation of vitamin D, including both the cholecalciferol and ergocalciferol forms. The 100% regioselectivity in the hydroxylation at the C-25 position, together with its self-sufficient oxygenase activity (i.e. the ability to catalyze oxygenations without the help of intracellular enzymes providing electrons and reducing power, as in the case of P450s), and its overexpression in a suitable host organism, make this recombinant heme–thiolate peroxidase an interesting industrial biocatalyst for the synthesis of 25-hydroxycalciferol.

Experimental Section

Enzyme

The recombinant peroxygenase used in this study corresponds to gene model CC1G_08427T0 from the sequenced *C. cinerea* genome available at the JGI (http://genome.jgi.doe.gov/copci1) and GenBank (XM_001831858). The corresponding protein (*C. cinerea* genome ID 7249) was produced by heterologous expression using a Novozymes *Aspergillus oryzae* industrial host

system,[40] and purified using a combination of S-Sepharose and SP-Sepharose ion-exchange chromatography. The recombinant peroxygenase preparation is an electrophoretically homogeneous glycoprotein with a molecular mass around 44 kDa (a non-uniform glycosylation pattern was observed), a typical UV–VIS spectrum with a Soret band at 418 nm, and the ability to oxygenate different aromatic compounds (Dolge et al., 2011) with a specific activity of approximately 100 U mg^{-1} measured with veratryl alcohol. One enzyme activity unit was defined as the amount of enzyme oxidizing 1 μmol of veratryl alcohol to veratraldehyde (ε_{310} 9300 $M^{-1}\cdot cm^{-1}$) in 1 min at 24 ºC, pH 7, in the presence of 0.5 mM H_2O_2.

Secosteroid substrates and standards

Vitamin D_3, also known as calciol or cholecalciferol ((5Z,7E)-(3S)-9,10-seco-5,7,10(19)-cholestatrien-3-ol), and vitamin D_2, also known as ercalciol or ergocalciferol ((5Z,7E,22E)-(3S)-9,10-seco-5,7,10(19),22-ergostatetraen-3-ol), were tested as substrates of the *C. cinerea* peroxygenase. 25-Hydroxyvitamin D_3, also known as calcidiol or 25-hydroxycholecalciferol ((5Z,7E)-(3S)-9,10-seco-5,7,10(19)-cholestatriene-3,25-diol), and 25-hydroxyvitamin D_2, also known as ercalcidiol or 25-hydroxyergocalciferol ((5Z,7E,22E)-(3S)-9,10-seco-5,7,10(19),22-ergostatetraene-3,25-diol), were used as standards for GC-MS analyses. All the compounds were from Sigma-Aldrich.

Enzymatic reactions

Reactions of cholecalciferol and ergocalciferol (0.05 mM) with the *C. cinerea* peroxygenase (1 U) were performed in 5 mL of 50 mM sodium phosphate (pH 7) at 40 ºC at 60 min reaction time, in the presence of 0.5 mM H_2O_2. The substrates were previously dissolved in acetone, and added to the buffer (the acetone concentration in the reaction was 40%). In control experiments, the substrates were treated under the same conditions (including 0.5 mM H_2O_2) but without enzyme. Enzymatic reactions with ^{18}O-labeled hydrogen peroxide ($H_2{}^{18}O_2$, 90% isotopic content) from Sigma-Aldrich (2% w:v solution) were also performed under the same conditions described above.

After the enzymatic reactions, products were recovered by liquid-liquid extraction with methyl tert-butyl ether, dried under N_2, and redissolved in

chloroform for GC-MS analyses. Bis(trimethylsilyl)trifluoroacetamide (Supelco) in the presence of pyridine was used to prepare TMS derivatives. An internal standard was added after the enzymatic reactions to determine product yields.

GC-MS analyses

The GC-MS analyses were performed with a Shimadzu GC-MS QP2010 Ultra, using a fused-silica DB-5HT capillary column (30 m x 0.25 mm internal diameter, 0.1 μm film thickness) from J&W Scientific.[59] The oven was heated from 120 °C (1 min) to 300 °C (15 min) at 5 °C·min^{-1}. The injection was performed at 300 °C, the transfer line was kept at 300 °C, and helium was used as carrier gas.

Compounds were identified by mass fragmentography, and by comparing their mass spectra with those of the Wiley and NIST libraries and standards, and quantitation was obtained from total-ion peak area, using response factors of the same reaction products (25-hydroxycholecalciferol and 25-hydroxyergocalciferol). These two standards were also used (as external standards for calculation of product yields). The relative abundance of the hydroxylated product incorporating one $^{18}O_2$ atom in the $H_2{}^{18}O_2$ reactions described above was estimated by peak integration using the corresponding ion with 2 *m/z* increase (with correction from interfering ions in $H_2{}^{16}O_2$ spectra, when required).

NMR analyses

The structure of 25-hydroxy products was confirmed by ^{1}H, ^{13}C and HSQC NMR spectroscopy (the latter spectrum enabling assignment in the 1D spectra). Spectra of both the products and the standards were acquired. The NMR spectra were acquired on a Bruker Biospin (Billerica, MA) AVANCE 500 MHz spectrometer fitted with a cryogenically cooled 5-mm TCI gradient probe with inverse geometry (proton coils closest to the simple).

25-hydroxycholecalciferol: ^{1}H-NMR (500 MHz, $CDCl_3$) δ 2.17 (1H, m, 1-H), 2.40 (1H, m, 1-H), 1.67 (1H, m, 2-H), 1.92 (1H, m, 2-H), 3.95 (1H, bm, 3-H), 2.57 (1H, dd, *J*= 3.7, 13.1 Hz, 4-H), 6.23 (1H, d, *J*= 11.2 Hz, 6-H), 6.03 (1H, d, *J*= 11.2 Hz, 7-H), 1.67 (1H, m, 9-H), 2.82 (1H, m, 9-H), 1.47 (2H, m, 11-H), 1.29 (1H, m, 12-H), 2.06 (1H, m, 12-H), 1.28 (1H, m, 14-H),

1.53 (1H, m, 15-H), 1.66 (1H, m, 15-H), 1.27 (1H, m, 16-H), 1.87 (1H, m, 16-H), 1.98 (1H, m, 17-H), 0.55 (3H, s, 18-H), 4.82 (1H, m, 19-H), 5.05 (1H, m, 19-H), 1.38 (1H, m, 20-H), 0.94 (1H, d, *J*= 6.5 Hz, 21-H), 1.06 (1H, m, 22-H), 1.37 (1H, m, 22-H), 1.23 (1H, m, 23-H), 1.42 (1H, m, 23-H), 1.39 (1H, m, 24-H), 1.44 (1H, m, 24-H), 1.22 (3H, s, 26-H), 1.22 (3H, s, 27-H). ^{13}C-NMR (500 MHz, $CDCl_3$) δ 32.1 (C-1), 35.3 (C-2), 69.4 (C-3), 46.1 (C-4), 135.2 (C-5), 122.2 (C-6), 117.7 (C-7), 142.4 (C-8), 29.2 (C-9), 145.3 (C-10), 22.4 (C-11), 40.7 (C-12), 46.0 (C-13), 56.7 (C-14), 23.7 (C-15), 27.8 (C-16), 56.5 (C-17), 12.2 (C-18), 112.6 (C-19), 36.3 (C-20), 19.0 (C-21), 36.6 (C-22), 21.0 (C-23), 44.6 (C-24), 71.3 (C-25), 29.5 (C-26), 29.4 (C-27).

25-hydroxyergocalciferol: ^{1}H-NMR (500 MHz, $CDCl_3$) δ 2.18 (1H, m, 1-H), 2.40 (1H, m, 1-H), 1.68 (1H, m, 2-H), 1.92 (1H, m, 2-H), 3.95 (1H, m, 3-H), 2.29 (1H, dd, *J*= 13.0, 7.3 Hz, 4-H), 2.57 (1H, dd, *J*= 13.0, 3.7 Hz, 4-H), 6.23 (1H, d, *J*= 11.3 Hz, 6-H), 6.03 (1H, d, *J*= 11.3 Hz, 7-H), 1.68 (1H, m, 9-H), 2.83 (1H, m, 9-H), 1.46 (2H, m, 11-H), 1.31 (1H, m, 12-H), 1.96 (1H, m, 12-H), 1.34 (1H, m, 14-H), 1.54 (1H, m, 15-H), 1.68 (1H, m, 15-H), 1.26 (1H, m, 16-H), 1.71 (1H, m, 16-H), 1.99 (1H, m, 17-H), 0.56 (3H, s, 18-H), 4.81 (1H, m, 19-H), 5.04 (1H, m, 19-H), 2.07 (1H, m, 20-H), 1.04 (3H, d, *J*= 6.7 Hz, 21-H), 5.37 (1H, dd, *J*= 15.3, 8.3 Hz, 22-H), 5.30 (1H, dd, *J*= 15.3, 8.2 Hz, 23-H), 2.11 (1H, m, 24-H), 1.13 (3H, s, 26-H), 1.17 (3H, s, 27-H), 1.00 (3H, d, *J*= 6.9 Hz, 28-H). ^{13}C-NMR (500 MHz, $CDCl_3$) δ 32.1 (C-1), 35.3 (C-2), 69.3 (C-3), 46.1 (C-4), 135.3 (C-5), 122.6 (C-6), 117.7 (C-7), 142.2 (C-8), 29.1 (C-9), 145.2 (C-10), 22.4 (C-11), 40.6 (C-12), 46.0 (C-13), 56.4 (C-14), 23.7 (C-15), 27.9 (C-16), 56.5 (C-17), 12.4 (C-18), 112.6 (C-19), 40.6 (C-20), 21.1 (C-21), 139.2 (C-22), 129.3 (C-23), 48.3 (C-24), 72.5 (C-25), 26.5 (C-26), 27.2 (C-27), 15.8 (C-28).

Acknowledgements

This study was funded by the INDOX (KBBE-2013-7-613549) EU-project, and by the HIPOP (BIO2011-26694) project of the Spanish Ministry of Economy and Competitiveness. J. Jimenez-Barbero is acknowledged for helpful discussion on NMR results, and Manuel Angulo (CITIUS, University of Seville) for providing technical assistance in the NMR analyses as well as help in NMR data interpretation.

[1] D. D. Bikle. *Chemistry & Biology*. 2014, 21, 319-329.

[2] M. F. Holick. *N. Engl. J. Med*. 2007, 357, 266-281.

[3] E. E. Hohman, B. R. Martin, P. J. Lachcik, D. T. Gordon, J. C. Fleet, C. M. Weaver. *J. Agric. Food Chem*. 2011, 59, 2341-2346.

[4] P. Urbain, F. Singler, G. Ihorst, K. Biesalski, H. Bertz. *Eur. J. Clin. Nutr*. 2011, 65, 965-971.

[5] G. Jean, J. C. Terrat, T. Vanel, J. M. Hurot, C. Lorriaux, B. Mayor, C. Chazot. *Nephrol. Dial. Transplant*. 2008, 23, 3670-3676.

[6] G. Jones. *Annu. Rev. Nutr*. 2013, 33, 23-44.

[7] N. R. Buck, W. Claerhout, B. H. Leuenberger, E. Stoecklin, K. Urban, S. Wolfram *Patent (USA).* 2013, US 20130210782 A1.

[8] M. D. Sitrin, J. M. Bengoa. *Amer. J. Clin. Nutr*. 1987, 46, 1011-1015.

[9] G. A. Leichtmann, J. M. Bengoa, M. J. G. Bolt, M. D. Sitrin. *Amer. J. Clin. Nutr*. 1991, 54, 548-552.

[10] M. Michalczuk, D. Pietrzak, J. Niemiec, J. Mroczk. *Pol. J. Food Nutr. Sci*. 2010, 60, 121-126.

[11] C. A. Fritts, P. W. Waldroup. *Journal of Applied Poultry Research*. 2003, 12, 45-52.

[12] S. Käppeli, E. Frohlich, S. G. Gebhardt-Henrich, A. Pfulg, H. Schäublin, R. Zweifel, H. Wiedmer, H. H. Stoffel. *Arch. Geflügelk*. 2011, 75, 179-184.

[13] J. M. Hernández. *Patent (USA)*. 2013, US 20130137662 A1.

[14] C. Simoes-Nunes, G. M. Weber. *Patent (European)*. 2004, EP 1516540 B1.

[15] Scientifc Panel Members. *EFSA J*. 2005, 224, 1-35.

[16] J. W. Blunt, H. F. Deluca. *Biochemistry*. 1969, 8, 671-675.

[17] P. S. Manchand, G. P. Yiannikouros, P. S. Belica, P. Madan. *J. Org. Chem*. 1995, 60, 6574-6581.

[18] D. R. Andrews, D. H. R. Barton, R. H. Hesse, M. M. Pechet. *J. Org. Chem*. 1986, 51, 4819-4828.

[19] K. S. Kyler, D. S. Watt. *J. Am. Chem. Soc*. 1983, 105, 619-621.

[20] A. D. Batcho, D. E. Berger, M. R. Uskokovic. *Patent (USA)*. 1982, 4310467.

[21] G. D. Zhu, W. H. Okamura. *Chemical Reviews*. 1995, 95, 1877-1952.

[22] S. Fuse, Y. Mifune, N. Tanabe, T. Takahashi. *Org. Biomol. Chem*. 2012, 10, 5205-5211.

[23] J. Sasaki, A. Miyazaki, M. Saito, T. Adachi, K. Mizoue, K. Hanada, S. Omura. *Appl. Microbiol. Biotechnol*. 1992, 38, 152-157.

[24] K. Takeda, T. Asou, A. Matsuda, K. Kimura, K. Okamura, R. Okamoto, J. Sasaki, T. Adachi, S. Omura. *Journal of Fermentation and Bioengineering*. 1994, 78, 380-382.

[25] D. E. T. Pazmino, M. Winkler, A. Glieder, M. W. Fraaije. *J. Biotechnol*. 2010, 146, 9-24.

[26] P. R. Ortiz de Montellano. 2005. *Cytochrome P450: Structure, mechanism, and biochemistry*, 3rd Ed., Kluwer Academic/Plenum, New York.

[27] R. Bernhardt. *J. Biotechnol*. 2006, 124, 128-145.

[28] Y. Yasutake, T. Nishioka, N. Imoto, T. Tamura. *ChemBioChem*. 2013, 14, 2284-2291.

[29] K. Yasuda, M. Endo, S. Ikushiro, M. Kamakura, M. Ohta, T. Sakaki. *Biochem. Biophys. Res. Commun*. 2013, 434, 311-315.

[30] J. B. van Beilen, E. G. Funhoff. *Curr. Opin. Biotechnol*. 2005, 16, 308-314.

[31] R. Ullrich, J. Nuske, K. Scheibner, J. Spantzel, M. Hofrichter. *Appl. Environ. Microbiol*. 2004, 70, 4575-4581.

[32] R. Ullrich, M. Hofrichter. *FEBS Lett*. 2005, 579, 6247-6250.

[33] M. Hofrichter, R. Ullrich, M. J. Pecyna, C. Liers, T. Lundell. *Appl. Microbiol. Biotechnol*. 2010, 87, 871-897.

[34] M. Hofrichter, R. Ullrich. *Curr. Opin. Chem. Biol*. 2014, 19, 116-125.

[35] D. H. Anh, R. Ullrich, D. Benndorf, A. Svatos, A. Muck, M. Hofrichter. *Appl. Environ. Microbiol*. 2007, 73, 5477-5485.

[36] G. Gröbe, M. Ullrich, M. Pecyna, D. Kapturska, S. Friedrich, M. Hofrichter, K. Scheibner. *AMB Express*. 2011, 1, 31-42.

[37] M. J. Pecyna, R. Ullrich, B. Bittner, A. Clemens, K. Scheibner, R. Schubert, M. Hofrichter. *Appl. Microbiol. Biotechnol*. 2009, 84, 885-897.

[38] F. J. Ruiz-Dueñas, A. T. Martínez, In *Biocatalysts based on heme peroxidases* (Torres, E. and Ayala, M., eds), 2010, pp. 37-59, Springer-Verlag, Berlin.

[39] D. Floudas, M. Binder, R. Riley, K. Barry, R. A. Blanchette, B. Henrissat, A. T. Martínez, R. Otillar, J. W. Spatafora, J. S. Yadav, A. Aerts, I. Benoit, A. Boyd, A. Carlson, A. Copeland, P. M. Coutinho, R. P. de Vries, P. Ferreira, K. Findley, B. Foster, J. Gaskell, D. Glotzer, P. Górecki, J. Heitman, C. Hesse, C. Hori, K. Igarashi, J. A. Jurgens, N. Kallen, P. Kersten, A. Kohler, U. Kües, T. K. A. Kumar, A. Kuo, K. LaButti, L. F. Larrondo, E. Lindquist, A. Ling, V. Lombard, S. Lucas, T. Lundell, R. Martin, D. J. McLaughlin, I. Morgenstern, E. Morin, C. Murat, M. Nolan, R. A. Ohm, A. Patyshakuliyeva, A. Rokas, F. J. Ruiz-Dueñas, G. Sabat, A. Salamov, M. Samejima, J. Schmutz, J. C. Slot, F. St.John, J. Stenlid, H. Sun, S. Sun, K. Syed, A. Tsang, A. Wiebenga, D. Young, A. Pisabarro, D. C. Eastwood, F. Martin, D. Cullen, I. V. Grigoriev, D. S. Hibbett. *Science*. 2012, 336, 1715-1719.

[40] M. J. Pecyna, K. M. Schnorr, R. Ullrich, K. Scheibner, M. G. Kluge, M. Hofrichter. *Patent (International)*. 2008, WO 2008/119780 A2.

[41] E. D. Babot, J. C. del Río, L. Kalum, A. T. Martínez, A. Gutiérrez. *Biotechnol. Bioeng.* 2013, 110, 2332.

[42] H. L. J. Makin, D. B. Gower. 2010. *Steroid analysis*, Springer, NY.

[43] H. F. de Luca, J. W. Blunt. *Patent (USA)*. 1971, 3565924.

[44] L. Stark, J. G. Yarger, S. Perry. *Patent (USA)*. 1997, 5695794.

[45] K. Piontek, E. Strittmatter, R. Ullrich, G. Grobe, M. J. Pecyna, M. Kluge, K. Scheibner, M. Hofrichter, D. A. Plattner. *J. Biol. Chem*. 2013, 288, 34767-34776.

[46] A. Gutiérrez, E. D. Babot, R. Ullrich, M. Hofrichter, A. T. Martínez, J. C. del Río. *Arch. Biochem. Biophys*. 2011, 514, 33-43.

[47] S. Peter, M. Kinne, X. Wang, R. Ulrich, G. Kayser, J. T. Groves, M. Hofrichter. *FEBS J*. 2011, 278, 3667-3675.

[48] J. D. Weete, S. R. Gandhi, In *The Mycota* (Brambl, R. and Marzluf, G. A., eds), 1996, pp. 421-428, Springer Verlag, Berlin.

[49] X. S. Wang, S. Peter, M. Kinne, M. Hofrichter, J. T. Groves. *J. Am. Chem. Soc*. 2012, 134, 12897-12900.

[50] X. S. Wang, S. Peter, R. Ullrich, M. Hofrichter, J. T. Groves. *Angew. Chem*. 2013, 52, 9238-9241.

[51] H. Li, In *Handbook of metalloproteins* (Messerschmidt, A., Huber, R., Poulos, T. L., and Wieghardt, K., eds), 2001, pp. 267-282, Wiley, Baffins Lane, UK.

[52] R. Ullrich, M. Hofrichter. *Cell. Mol. Life Sci*. 2007, 64, 271-293.

[53] M. Kluge, R. Ullrich, K. Scheibner, M. Hofrichter. *Green Chem*. 2012, 14, 440-446.

[54] E. Aranda, M. Kinne, M. Kluge, R. Ullrich, M. Hofrichter. *Appl. Microbiol. Biotechnol*. 2009, 82, 1057-1066.

[55] M. Kinne, R. Ullrich, K. E. Hammel, K. Scheibner, M. Hofrichter. *Tetrahedron Lett*. 2008, 49, 5950-5953.

[56] R. Ullrich, C. Dolge, M. Kluge, M. Hofrichter. *FEBS Lett*. 2008, 582, 4100-4106.

[57] M. G. Kluge, R. Ullrich, K. Scheibner, M. Hofrichter. *Appl. Microbiol. Biotechnol*. 2007, 75, 1473-1478.

[58] A. Gutiérrez, E. D. Babot, R. Ullrich, M. Hofrichter, A. T. Martínez, J. C. del Río, J. Brask, H. Lund, L. Kalum. *Patent (International)*. 2011, 12249-EP-EPA, WO2013-004639A2.

[59] A. Gutiérrez, J. C. del Río, F. J. González-Vila, F. Martín. *J. Chromatogr*. 1998, 823, 449-455.

6.1. Publicación V:

Lucas F., Babot E.D., Cañellas M., del Río J.C., Kalum L., Ullrich R., Hofrichter M., Guallar V., Martínez A.T. and Gutiérrez A. 2016. Molecular determinants for selective C25-hydroxylation of vitamins D_2 and D_3 by fungal peroxygenases. *Catalysis Science & Technology*. 6: 288-295.

Molecular determinants for selective C_{25}-hydroxylation of vitamins D_2 and D_3 by fungal peroxygenases

Fátima Lucas,‡*[a] Esteban D. Babot,‡[b] Marina Cañellas,‡[a,c] José C. del Río,[b] Lisbeth Kalum,[d] René Ullrich,[e] Martin Hofrichter,[e] Victor Guallar,[a,f] Angel T. Martínez[g] and Ana Gutiérrez*[b].

[a] Joint BSC-CRG-IRB Research Program in Computational Biology, Barcelona Supercomputing Center, Jordi Girona 29, E-08034 Barcelona, Spain. E-mail: fatima.lucas@bsc.es

[b] Instituto de Recursos Naturales y Agrobiología de Sevilla, CSIC, Reina Mercedes 10, E-41012 Seville, Spain. E-mail: anagu@irnase.csic.es; Fax: +32 954624002; Tel: +32 954624711

[c] Anaxomics Biotech, Balmes 89, E-08008 Barcelona, Spain

[d] Novozymes A/S, Krogshoejvej 36, 2880 Bagsvaerd, Denmark

[e] TU Dresden, Department of Bio- and Environmental Sciences, Markt 23, 02763 Zittau, Germany

[f] ICREA, Passeig Lluís Companys 23, E-08010 Barcelona, Spain

[g] Centro de Investigaciones Biológicas, CSIC, Ramiro de Maeztu 9, E- 28040 Madrid, Spain

‡ These three authors equally contributed to this work

* Corresponding author

Abstract:

Hydroxylation of vitamin D by *Agrocybe aegerita* and *Coprinopsis cinerea* peroxygenases was investigated in a combined experimental and computational study. 25-Monohydroxylated vitamin D_3 (cholecalciferol) and D_2 (ergocalciferol), compounds of high interest in human health and animal feeding, can be obtained through reaction with both fungal enzymes. Differences in conversion rates and, especially, in site selectivity were nevertheless observed. To rationalize the results, diffusion of D_2 and D_3 on the molecular structure of the two enzymes was performed with PELE software. In good agreement with experimental conversion yields, simulations indicate more favorable energy profiles for the substrates' entrance in than for *A. aegerita* enzyme. On the other hand, GC-MS

analyses show that while a full regioselective conversion into the active C_{25} form is catalyzed by C. cinerea peroxygenase for D_2 and D_3, *A. aegerita* yielded a mixture of the hydroxylated D_3 products. From the molecular simulations, relative distance distributions between the haem compound I oxygen and H_{24}/H_{25} atoms (hydrogens on C_{24} and C_{25} respectively) were plotted. Results show large populations for O-H_{25} distances below 3 Å for D_2 and D_3 in *C. cinerea* in accordance with the high reactivity observed for this enzyme. In *A. aegerita*, however, cholecalciferol has similar populations (below 3 Å) for O-H_{25} and O-H_{24} which can justify the hydroxylation observed in C_{24}. In the case of ergocalciferol, due to the bulky methyl group in position C_{24}, very few structures are found with O-H_{24} distances below 3 Å and thus, as expected, reaction was only observed at C_{25} position.

Introduction

Selective oxygenations of aliphatic compounds are among the most challenging reactions in organic chemistry for the regio and/or stereo specific synthesis of pharmaceuticals and fine chemicals. Monooxygenases catalyzing such hydroxylation reactions include cytochromes P450, a family of haem proteins playing a variety of physiological roles but often requiring an auxiliary flavoenzyme (or flavin-containing module) and a source of reducing power to be activated by O_2, two facts that limit their biotechnological applicability.

Recently, a new peroxidase type, which shares the active-site architecture and reaction mechanism of cytochromes P450, but has the advantage of being activated directly by H_2O_2, was isolated from *Agrocybe aegerita*,[46] and later identified in a variety of sequenced basidiomycete genomes including that of *Coprinopsis cinerea*.[14] Due to the above characteristics, these unspecific peroxygenases (EC 1.11.2.1) have a huge biotechnological potential as self-sufficient monooxygenases,[10,20] for hydroxylation of both aromatic[2,3,25-28,43-45] and aliphatic compounds.[4,16,34]

The *A. aegerita* enzyme has been the most widely investigated basidiomycete peroxygenase, but recent studies have shown that the *C. cinerea* enzyme has comparative advantages related to its high conversion yield/selectivity for some

hydroxylation reactions, and its production as a recombinant protein in an industrial expression host (by Novozymes, Bagsvaerd, Denmark).[5,7]

Hydroxylation of vitamin D for the selective production of its active C_{25}-hydroxylated derivatives is one of the reactions where the *C. cinerea* peroxygenase can be of biotechnological interest (**Fig. 1**).[6] Supplementation with 25-hydroxyvitamin D has a positive effect in different human diseases,[12,21,22,29,42] and also raises considerable interest for feeding broiler chickens[15,18,24,33] and other farm animals,[41] to reduce skeleton problems caused by rapid growth and reduced mobility. Therefore, the use of a peroxygenase in vitamin D hydroxylation represents an attractive alternative to the chemical synthesis.

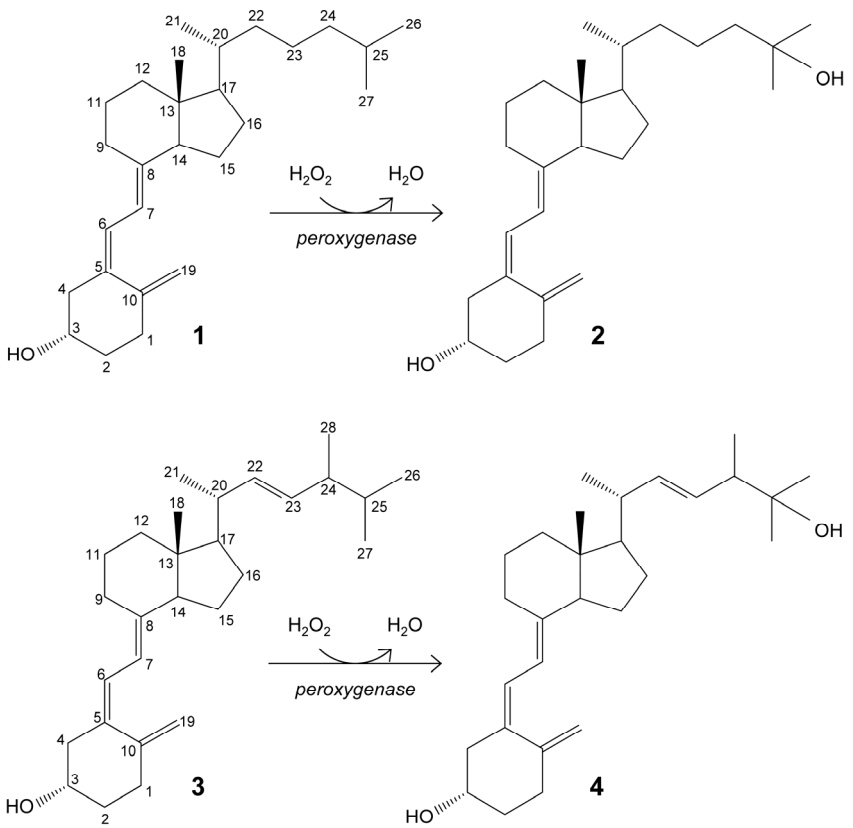

Fig. 1. Enzymatic conversion of cholecalciferol (vitamin D_3; **1**) and ergocalciferol (vitamin D_2; **3**) into their bioactive 25-hydroxylated derivatives (**2** and **4**) by basidiomycete peroxygenases.

The goal of the present work was to rationalize the differences observed in cholecalciferol and ergocalciferol (vitamins D_3 and D_2, respectively) conversion rates and site selectivity by the *A. aegerita* and *C. cinerea* peroxygenases. The work presented here consists first of the enzymatic conversion of these compounds by the two peroxygenases, under the same reaction conditions, and gas chromatography-mass spectrometry (GC-MS) analyses to identify all reaction products. Then, energy profiles and binding modes of vitamins D_2 and D_3 were determined by structure-based computational simulations, using the PELE software.[11,13] Finally, differences in site selectivity were investigated through the analysis of the most favorable binding orientations in the active site. Results show that molecular simulations can effectively discriminate experimentally observed differences in conversion rates and site selectivity.

Results and discussion

Experimental hydroxylation reactions

Conversion of cholecalciferol and ergocalciferol was experimentally determined for both the *A. aegerita* and *C. cinerea* peroxygenases. In the case of cholecalciferol (0.1 mM), GC-MS analyses of the reaction mixture revealed that this compound was completely (100%) converted by the *C. cinerea* enzyme within 60 min reaction (**Fig. 2C**) as compared with the control reaction without peroxygenase (**Fig. 2A**). In the *A. aegerita* peroxygenase reaction up to 90% conversion was observed (**Fig. 2B**). In the case of ergocalciferol (**Figs. 2D-F**), a conversion of 85% was produced by *C. cinerea* while in *A. aegerita* reaction 81% product was observed. When higher substrate concentrations were tested (e.g. 0.5 mM) higher differences in the conversion rates by the two enzymes were observed (40-50% and 20% conversions by the *C. cinerea* and *A. aegerita* peroxygenases, respectively).

Moreover, cholecalciferol and ergocalciferol conversion by the *C. cinerea* peroxygenase showed a strict site selectivity since it gave exclusively 25-hydroxycalciferol. Likewise, conversion by the *A. aegerita* enzyme of ergocalciferol yielded exclusively 25-hydroxyergocalciferol but for cholecalciferol a mixture of products was observed.

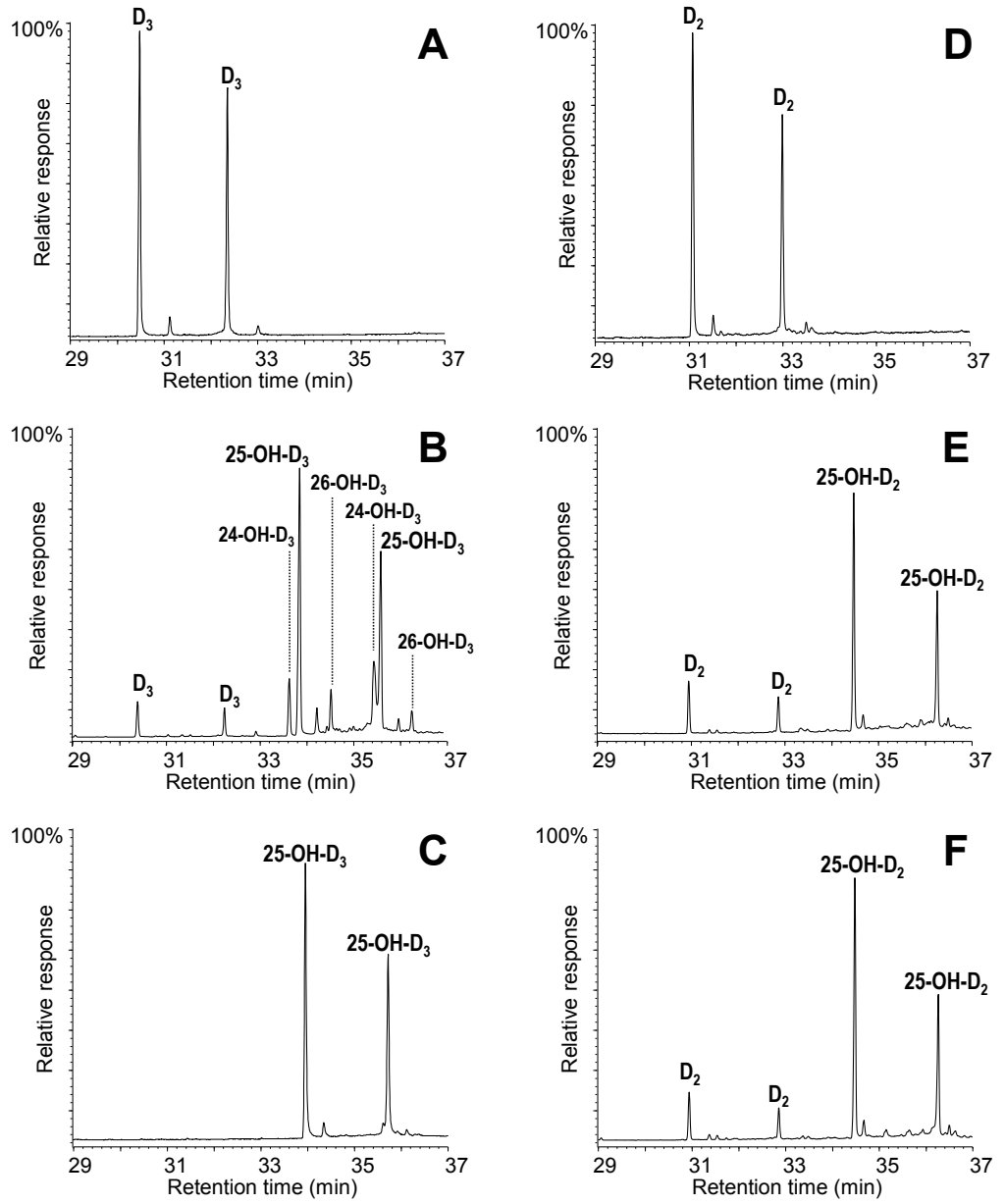

Fig. 2. GC-MS analyses of cholecalciferol (left) and ergocalciferol (right) hydroxylation by the *A. aegerita* (**B**, **E**) and *C. cinerea* peroxygenases (**C**, **F**), compared with a control without enzyme showing the substrate peaks (**A**, **D**), as TMS derivatives from 60-min reactions. In all cases the isopyro (left) and pyro (right) isomers from secosteroid thermal rearrangement are obtained (two small peaks in **A** and **D** correspond to minor additional isomers).

The products include 25-hydroxycholecalciferol (64% of the initial substrate) together with 24-hydroxycholecalciferol (21%) and 26/27-hydroxycholecalciferol (7%), as confirmed by comparison with true standards showing identical retention times and mass spectra. The double peaks observed in the chromatograms for both substrate and product (**Fig. 2**) correspond to the isopyro (19β, 9β) and pyro (19α, 9α) isomers formed by thermal rearrangement involving ring-B closure, that vitamin D and its hydroxylated derivatives undergo due to the temperature at which GC-MS EI(+) is carried out. Indeed, the presence of the two isomers during GC separation is a useful indication that a secosteroid of the vitamin D type was injected into the system.[32] The position of the hydroxyl group at the target C_{25} position was established by MS of the TMS derivative. The spectrum shows a prominent ion from C_{24}-C_{25} bond cleavage, with characteristic fragment at m/z 131 and molecular ion at m/z 544. Additionally, characteristic fragments at m/z 529 ([M-15]+), m/z 454 ([M-90]+), m/z 439 ([M-90-15]+), m/z 349 ([M-90-90-15]+) and m/z 413, were also present. Therefore, both the chromatographic profiles and the mass spectra correspond to the isomerized secosteroids.

Peroxygenase structure

A superimposition of the general structure and the haem pocket residues in the *A. aegerita* and *C. cinerea* peroxygenases is shown in **Fig. 3**. The main differences are two longer loops (**Fig. 3A**, arrows) and the substitution of Phe69 by Met69 (**Fig. 3B**, red label) in the *C. cinerea* enzyme. All other haem pocket residues, including the proximal cysteine acting as the fifth ligand of the haem iron (Cys36) and the distal glutamic acid and arginine involved in haem activation by H_2O_2 (Glu169 and Arg189),[35] are conserved in the two enzymes. Moreover, differences in the channel providing access to the haem cofactor and the neighbor residues at the channel entrance are shown in **Fig. 4**.

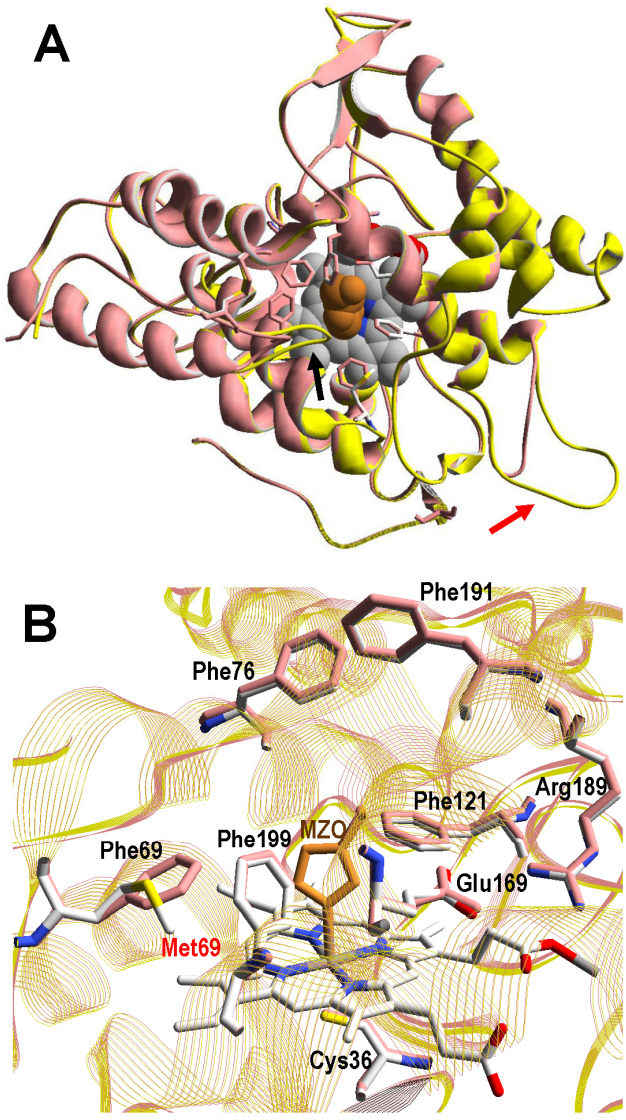

Fig. 3. Comparison of peroxygenase molecular structures. **A**) General superimposition with the *A. aegerita* and *C. cinerea* proteins as pink and yellow ribbons, respectively. The haem group (CPK-colored spheres) and several haem pocket residues (pink- and CPK-colored sticks, respectively) are shown, and two larger loops in the second enzyme are indicated by arrows. **B**) Haem pocket residues in the *A. aegerita* (pink sticks) and *C. cinerea* (CPK-colored sticks) peroxygenases (red label indicates non-conserved methionine in position 69 of the latter enzyme). A hypothetical product molecule identified as 4-hydroxymethylimidazole is shown in A (brown-colored vdW spheres) and B (MZ0, brown-colored sticks).[35] From *A. aegerita* PDB 2YOR, and *C. cinerea* homology model (provided as **Supplemental file 1**).

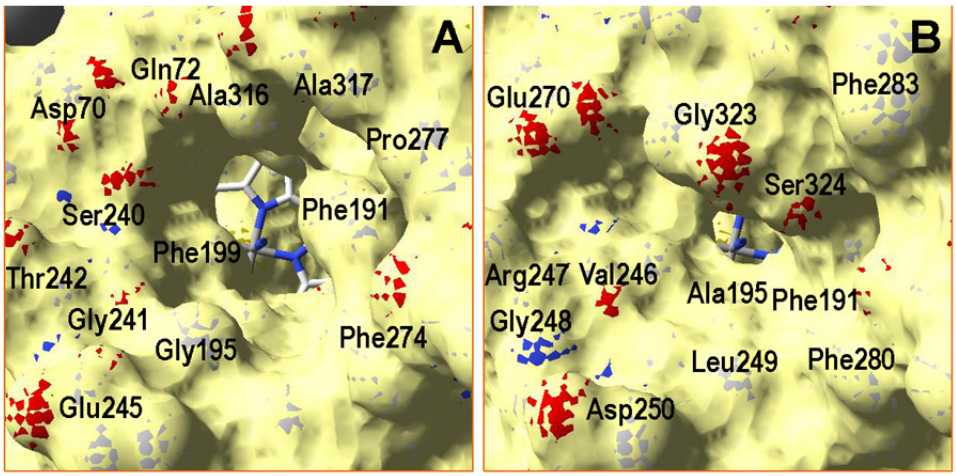

Fig. 4. Solvent access surfaces showing differences in the size of the haem (CPK-colored sticks) access channel in the peroxygenases of *A. aegerita* (**A**) and *C. cinerea* (**B**). Several neighbor residues are shown as CPK-colored vdW spheres, including Gly323 and Ser324 contributing to occlude the haem channel in the *C. cinerea* enzyme.

Computational modeling

Ligand diffusion energy profiles

For the simulations of cholecalciferol and ergocalciferol access to the H_2O_2-activated haem in the *A. aegerita* and *C. cinerea* peroxygenases, the haem cofactor was modeled as compound I (a FeIV=O, porphyrin cation radical). The substrate was placed close to the entrance of the haem-access channel of the proteins prepared at the optimal pH for peroxygenase activity (pH 7). This initial location was identified using SiteMap,[40] and from there, the ligand was spawned inside the protein by PELE,[11] following the distance between the reactive O atom in the haem compound I and the cholecalciferol/ergocalciferol C_{25} atom (**Fig. 1**).

PELE simulations were done in two stages: first the substrate is perturbed to reduce the C_{25}-O distance and, when this distance is below 5 Å, the substrate is free to explore the active site cavity (at the haem distal side) with a 15 Å restrain. In the first step, the ligand is perturbed with a combination of large and small translations and rotations, ranging from 0.5 to 1.5 Å for translations, and

0.05 to 0.25 radians for rotations. However, during the second stage, translation range is reduced (0.75-0.25 Å) to perform a finer active site exploration. The plots shown in Fig. 5 correspond to three 48 h simulations each with 80 processors, and show the substrate-C_{25} to haem-O distance vs. the interaction energy between the protein and the substrate at each of the different poses explored.

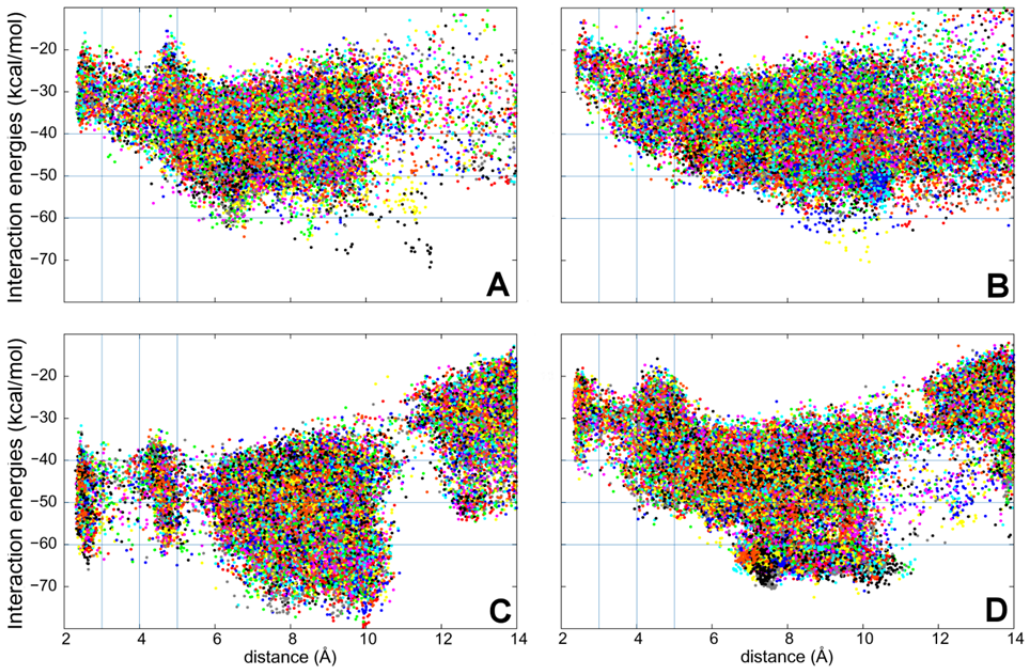

Fig. 5. Interaction energies vs. ligand distances from PELE simulations for cholecalciferol (left) and ergocalciferol (right) entrance by the C_{25} end in the peroxygenases from *A. aegerita* (**A, B**) and *C. cinerea* (**C**, **D**). The distances shown (Å) are between the reactive O atom in the haem compound I and the calciferol C_{25} (for substrate numbering see **Fig. 1**).

Simulations show that for the *A. aegerita* peroxygenase the entrance of the substrates from the surface of the protein is quite favorable but then, the access to the activated haem is obtained against an uphill potential (**Figs. 5A,B**). For the *C. cinerea* enzyme the entrance is less open than in the *A. aegerita*

peroxygenase and, for this reason, we observed a constrained access to the protein (at around 12 Å). However, the overall energy profile is more favorable, in particular for cholecalciferol (**Fig. 5C**). Once inside the protein, the ligand must surpass smaller barriers to reach the haem. From **Fig. 5** it is clear that *C. cinerea* peroxygenase has the most favorable energy profiles and well defined minima in the active site (with C_{25}-O distance around 3 Å). **Fig. 5A/5C** show that binding of cholecalciferol at the haem site, is more favorable in the *C. cinerea* peroxygenase (-65 kcal/mol) than in the *A. aegerita* enzyme (-40 kcal/mol). This difference comes from the fact that the first protein has a tighter binding pocket (see below). In the case of ergocalciferol **Fig. 5B/5D**, also binding is more favorable in the *C. cinerea* (-42 kcal/mol) than in the *A. aegerita* enzyme (-30 kcal/mol). These differences in the energy profiles, which indicate a more favorable protein-ligand interaction in *C. cinerea*, can explain the higher conversion rate observed for the two compounds in this peroxygenase.

Ligand binding

If we overlap cholecalciferol's positions for the entire PELE simulations for both proteins, we find two main orientations in the active site, as shown in **Fig. 6**. The two orientations in **Fig. 6B** correspond to the two minima observed in cholecalciferol's diffusion in the *C. cinerea* peroxygenase (**Fig. 5C**). One of the minima (in green) is found at binding distance to the haem O, and a second (in blue), about 5 Å away from the haem oxygen (**Fig. 5C**). The ligand's positions observed in the *C. cinerea* peroxygenase are also found in the *A. aegerita* enzyme (**Fig. 6A**), although they do not correspond to energy minima (**Fig. 5A**). Likewise, ergocalciferol can adopt two main positions in the binding pocket, although the minima (**Fig. 5D**) are less marked than found for cholecalciferol (**Fig. 5C**).

When cholecalciferol is in an optimal reacting position, it is held in place by *C. cinerea*/*A. aegerita* peroxygenase Val77/Ala77, Phe121/Phe121, Thr192/Thre192, Ala195/Gly195, Phe199/Phe199 and Glu196/Glu196 (**Fig. S1**). Noteworthy is that Phe69 also contributes to substrate positioning in *A. aegerita* peroxygenase, but the homologous Met69 of the *C. cinerea* enzyme (**Fig. 3B**) is placed away from cholecalciferol and does not appear to have any effect on its position in the active site. Ergocalciferol, however, with an extra methyl group in position C_{24} and with a C_{22}-C_{23} double bond (**Fig. 1**), is positioned in a

slightly different manner in the active site, and residues in position 69 (phenylalanine and methionine) now interacts with the ligand (red arrows in **Fig. S2**). This extra constraint could be responsible for the lower reactivity observed for D_2 in both peroxygenases. The influence of side-chain structure (alkyl substituent and unsaturation presence) on the activity of the *A. aegerita* and *C. cinerea* peroxygenases was evidenced in the reaction of these enzymes with different sterols (**Table S1**).

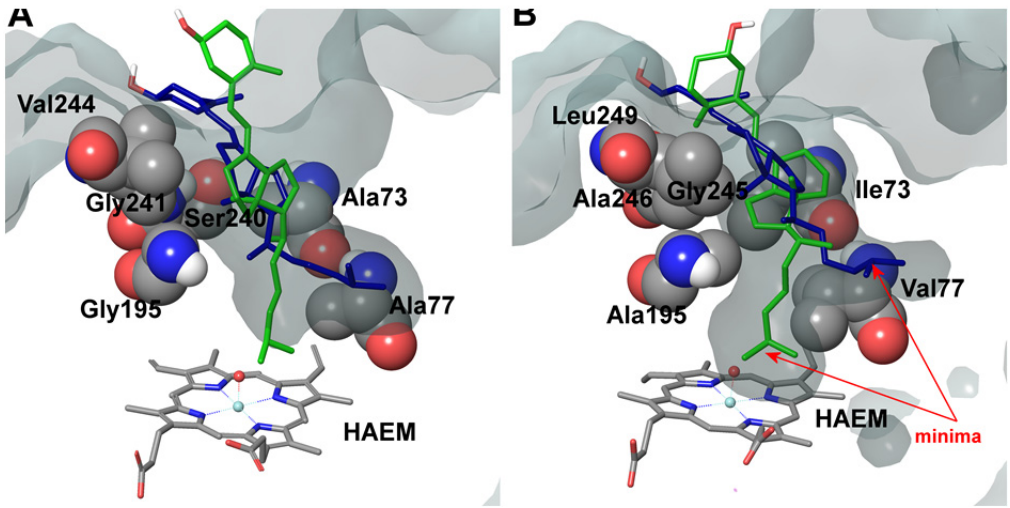

Fig. 6. Superposition of cholecalciferol main active site positions (as liquorice) obtained in PELE simulations on the *A. aegerita* (**A**) and *C. cinerea* (**B**) peroxygenases. Haem cofactor also in liquorice and selected residues as vdW spheres. The protein's active site access is shown as a surface.

Inspection of the haem entrance when both ligands are in the active site, reveals a better wrapping of the protein around the ligands in *C. cinerea* peroxygenase, compared with the *A. aegerita* enzyme. This in mainly due to the larger loop, where Gly323 is located, which is smaller in the *A. aegerita* peroxygenase (**Fig. 3A**, black arrow). These are better illustrated in the haem-access channel of both peroxygenases in **Fig. 4**, where the position of the above Gly323 is shown. The narrower access to the haem in *C. cinerea* is also the result

of several hydrophobic amino acid substitutions. Replacements to larger side chains in C. cinerea are dominant with: Ala73/Ile73, Ala77/Val77, Gly195/Ala195, Gly241/Ala246 and Val244/Leu249; and only one to a smaller amino acid, Ser240/Gly245. Due to the larger entrance cavity of the *A. aegerita* peroxygenase, both substrates remained solvent exposed at the C_2 end. In contrast, more favorable interactions are established at the final substrate position inside the tighter channel of the *C. cinerea* peroxygenase, which presents extra interactions on the protein surface. The combination of the surface interactions, along with a tighter haem cavity, result in the improved interaction energies seen for D_2 and D_3 in this protein.

Site selectivity

To investigate the different site selectivities observed for D_2 and D_3 hydroxylation by *A. aegerita* and *C. cinerea* peroxygenases, we haveanalysed the relative distance distribution of the substrates' reactive hydrogen atoms in the active site. We have considered as reactive those that can approach the haem compound I oxygen atom close enough to react. Thus, we have taken into account hydrogen atoms in positions C_{24}, C_{25}, C_{26} and C_{27} for both ligands, in addition to C_{28} hydrogen atoms for ergocalciferol. We have selected all structures (from the PELE simulations) where the distance between H-O is below 5 Å and interaction energies below -20 kcal/mol for D_2 and -30 kcal/mol for D_3. When the relative frequency of these distances was computed (**Fig. 7**) it can be seen that for *C. cinerea* the O-H_{25} frequency is dominant for both compounds. Similar conclusions were obtained for both enzymes and substrates when the distribution of angles Fe=O-H37 was computed for the different reactive positions in the cholecalciferol and ergocalciferol side-chains (**Fig. S3**).

The percentage of O-H_{25} distances below 3 Å in *C. cinerea* is 54.5% for D_3 and 36.2% for D_2, whereas in *A. aegerita* it is 27.4% and 25.7%, respectively. Moreover, in the D_3 simulations in *A. aegerita*, the fraction of structures with O-H_{24} below 3 Å is 19.3% which is quite high when compared to the other cases. In fact, the fraction of O-H_{25} distances is only 1.4 times superior to O-H_{24} while for the other systems it ranges between 10 to 20 times. This higher fraction of reactive O-H_{24} distances can explain the observed formation of C_{24} hydroxylated products in cholecalciferol. To sum up, and in agreement with experimental results, from the relative frequencies in *C. cinerea* peroxygenase, and also for

ergocalciferol in *A. aegerita*, we would expect a completely regioselective reaction in C_{25}. In contrast, for cholecalciferol in *A. aegerita* enzyme, it seems that hydroxyl addition is possible not only in C_{25} position, but also in other carbons (C_{24} and C_{26}/C_{27}).

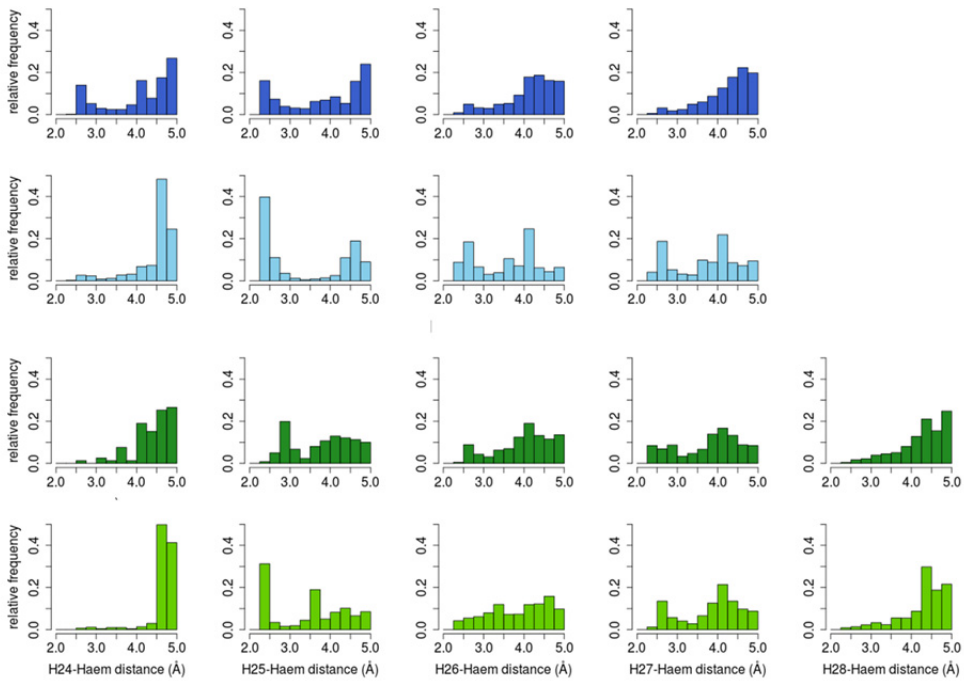

Fig. 7. Relative distance distributions of cholecalciferol (blue) and ergocalciferol (green) reactive hydrogen atoms to haem compound-I oxygen. Histograms for *A. aegerita* are in dark colours, and in light colours for *C. cinerea*.

Conclusions

Atomic level simulations have been used here to rationalize the differences observed for ergocalciferol and cholecalciferol's conversion rates and site selectivity in two peroxygenases. The overall improved energy profiles in *C. cinerea*, the presence of favorable minima, and a high fraction of favorable O-H_{25} distances agrees well with experimentally higher conversion rates.

The main structural differences between the *A. aegerita* and *C. cinerea* peroxygenases that modify the access of cholecalciferol to the activated haem are Ala73/Ile73, Ala77/Val77, Gly195/Ala195, Gly241/Ala246 and Val244/Leu249 changes, all larger amino acids with only Ser240/Gly245 to a smaller one. These larger hydrophobic side chains augment the interaction of D_2 and D_3 substrate with *C. cinerea*. The better conversion rates observed for *C. cinerea* peroxygenase do not originate in the active site itself (where Phe69 is replaced by Met69), but instead in the ligand access to the active site, and especially in the entrance to the protein. In particular, the larger loop hosting Gly323 creates a barrier that reduces the size of the entrance channel in the *C. cinerea* peroxygenase. This, along with a tighter cavity, is reflected in the more favorable interaction energies.

Although the improved reactivity of *C. cinerea* does not appear to be affected by the larger Phe69 side chain, it does hinder the entrance of ergocalciferol relative to cholecalciferol. The presence of an extra methyl group that interacts directly with position 69 in both proteins lowers the reactivity of this compound. Finally, computed relative frequency of distances between the activated haem oxygen and the hydrogen atoms in C_{24} and C_{25} show that, despite the more favourable hydroxylation on tertiary carbons, reaction at cholecalciferol C_{24} occurs when the ratio of favourable $O\text{-}H_{25}/O\text{-}H_{24}$ distances decreases.

Materials and methods

Enzymes and chemicals

Peroxygenase (isoform II) was isolated from *A. aegerita* DSM 22459 grown in soybean medium using a combination of SP-Sepharose chromatography and Mono-P chromatofocusing.[46] A. aegerita DSM 22459 is deposited at the Deutsche Stammsammlung für Mikroorganismen und Zellkulturen Braunschweig (Germany). *C. cinerea* peroxygenase was provided by Novozymes A/S (Bagsvaerd, Denmark). The enzyme corresponds to the protein model 7249 from the sequenced *C. cinerea* genome available at the JGI (http://genome.jgi.doe.gov/Copci1), which was expressed in *Aspergillus oryzae* and purified using a combination of S-Sepharose and SP-Sepharose ion-exchange chromatography (patent WO/2008/119780). One peroxygenase unit is defined as the amount of enzyme oxidizing 1 μmol of veratryl alcohol to veratraldehyde (ε_{310} 9300 $M^{-1}\cdot cm^{-1}$) in 1 min at 24 °C, pH 7, after addition of

0.5 mM H_2O_2 in the *C. cinerea* peroxygenase reactions and 2.5 mM H_2O_2 in those with the *A. aegerita* peroxygenase.

Vitamin D_3, also known as calciol or cholecalciferol ((5*Z*,7*E*)-(3*S*)-9,10-seco-5,7,10(19)-cholestatrien-3-ol; **Fig. 1**, structure **1**), was tested as substrate of the *A. aegerita* and *C. cinerea* peroxygenases. 25-Hydroxyvitamin D_3, also known as calcidiol or 25-hydroxycholecalciferol ((5*Z*,7*E*)-(3*S*)-9,10-seco-5,7,10(19)-cholestatriene-3,25-diol; **Fig. 1** structure **2**), was used as standard for gas chromatography-mass spectrometry (GC-MS) analyses. Vitamin D_2, also known as ercalciol or ergocalciferol ((5*Z*,7*E*,22*E*)-(3*S*)-9,10-seco-5,7,10(19),22-ergostatetraen-3-ol; **Fig. 1**, structure **3**), was also tested as substrate of the two peroxygenases. 25-Hydroxyvitamin D_2, also known as ercalcidiol or 25-hydroxyergocalciferol ((5*Z*,7*E*,22*E*)-(3*S*)-9,10-seco-5,7,10(19),22-ergostatetraene-3,25-diol; **Fig. 1**, structure **4**), was also used as standard for GC-MS analyses. All compounds were from Sigma-Aldrich.

Enzymatic reactions

Reactions of cholecalciferol and ergocalciferol (0.1 and 0.5 mM) with the *A. aegerita* and *C. cinerea* peroxygenases (1 U) were performed in 5 mL of 50 mM sodium phosphate, pH 7, at 40 ºC for 60 min, in the presence of 0.5 mM H_2O_2. The substrates were previously dissolved in acetone, and added to the buffer (the acetone concentration in the reaction was 40%). In control experiments, the substrates were treated under the same conditions (including H_2O_2) but without enzyme. After the enzymatic reactions, products were recovered by liquid-liquid extraction with methyl tert-butyl ether, dried under N_2, and redissolved in chloroform for GC-MS analyses. Bis(trimethylsilyl)trifluoroacetamide (Supelco) in the presence of pyridine was used to prepare trimethylsilyl (TMS) derivatives. An internal standard was added after the enzymatic reactions to determine product yields.

GC-MS analyses

GC-MS analyses were performed with a Shimadzu QP2010 Ultra equipment, using a fused-silica DB-5HT capillary column (30 m x 0.25 mm internal diameter, 0.1 μm film thickness) from J&W Scientific.[17] The oven was heated from 120 ºC (1 min) to 300 ºC (15 min) at 5 ºC·min^{-1}. The injection

was performed at 300 ºC, the transfer line was kept at 300 ºC, and helium was used as carrier gas. Compounds were identified by mass fragmentography, and by comparing their mass spectra with standards, and quantitation was obtained from total-ion peak area, using molar response factors obtained from cholecalciferol, ergocalciferol, 25-hydroxycholecalciferol and 25-hydroxyergocalciferol standards. The two latter compounds were also used as external standards for calculation of product yields.

PELE and other computational analyses

The starting structures for PELE simulations were the *A. aegerita* peroxygenase crystal (2YOR)[35] and a homology model for the *C. cinerea* peroxygenase structure obtained using 2YOR as template.[9] As the optimum pH for peroxygenase activity is 7, the structures were prepared accordingly using Schrodinger's Protein Preparation Wizard[36] and H++ web server.[1] Histidines were δ-protonated, with the exception of His82 (ε-protonated) and His118 and His251 (double protonated). All acidic residues were deprotonated, except Asp85 that was kept in its protonated state. The ergocalciferol and cholecalciferol molecules were optimized with Jaguar[38] at the DFT/M06 level with the 6-31G** basis and a PBF implicit solvent in order to obtain their electrostatic potential atomic charges. Finally, the haem site was modeled as thiolate-ligated compound I after being fully optimized in the protein environment with quantum mechanics/molecular mechanics (QM/MM) using QSite.[39] The electronic calculations show three unpaired electrons: two located on the oxoiron group and a third on the heme and less than 1% spin contamination.

Once the initial protein structure was prepared and ligands optimized, these were placed manually in identical positions at the entrance of the haem-access channel and PELE simulations were performed.[11] PELE is a Monte Carlo based algorithm that produces new configurations through a sequential ligand and protein perturbation, side chain prediction and minimization steps, freely available at https://pele.bsc.es. New configurations are then filtered with a Metropolis acceptance test, where the energy is described with an all-atom OPLS force field[23] and a surface generalized Born solvent 8. In this way it is possible to locate and characterize local and global minima structures for the

most favorable protein-ligand interactions. PELE has been successfully used in a number of ligand migration studies with both small and large substrates [19,30,31].

Distance and angle distributions were computed after screening all structures from PELE simulations by interaction energy and distance to the compound I oxygen. Structures that showed interaction energies below -20 kcal/mol for ergocalciferol and -30 kcal/mol for cholecalciferol were selected. Reactive hydrogen atoms where considered below 5 Å to the compound I oxygen atom for the distance analysis and 3Å for the angle study (angles are much more sensitive and thus only near attack conformations were selected). All the selected structures where then used to compute the relative frequencies of the ligand's hydrogen atoms at reactive distances to the haem oxygen and Fe=O-H and O-H-C angles.

Acknowledgements

This work was supported by the INDOX (KBBE-2013-7-613549) and PELE (ERC-2009-Adg 25027) EU projects, and by the BIO2011-26694 and CTQ2013-48287 projects of the Spanish Ministry of Economy and Competitiveness.

Electronic Supplementary Information (ESI) available: Molecular model for *C. cinerea* peroxygenase obtained using the *A. aegerita* crystal structure as template. See DOI: 10.1039/b000000x/.

1. R. Anandakrishnan, B. Aguilar and A. V. Onufriev, *Nucleic Acids Res.*, 2012, **40,** W537-W541.
2. E. Aranda, M. Kinne, M. Kluge, R. Ullrich and M. Hofrichter, *Appl. Microbiol. Biotechnol.*, 2009, **82,** 1057-1066.
3. E. Aranda, R. Ullrich and M. Hofrichter, *Biodegradation*, 2010, **21,** 267-281.
4. E. D. Babot, J. C. del Río, M. Cañellas, F. Sancho, F. Lucas, V. Guallar, L. Kalum, H. Lund, G. Gröbe, K. Scheibner, R. Ullrich, M. Hofrichter, A. T. Martínez and A. Gutiérrez, *Appl. Environ. Microbiol.*, 2015, **81,** 4130-4142.
5. E. D. Babot, J. C. del Río, L. Kalum, A. T. Martínez and A. Gutiérrez, *Biotechnol. Bioeng.*, 2013, **110,** 2332.

6. E. D. Babot, J. C. del Río, L. Kalum, A. T. Martínez and A. Gutiérrez, *Chemcatchem*, 2014,(on line).

7. E. D. Babot, J. C. del Río, L. Kalum, A. T. Martínez and A. Gutiérrez, *Chemcatchem*, 2014,(on line).

8. D. Bashford and D. A. Case, *Annual Review of Physical Chemistry*, 2000, **51,** 129-152.

9. L. Bordoli, F. Kiefer, K. Arnold, P. Benkert, J. Battey and T. Schwede, *Nat. Protoc.*, 2009, **4,** 1-13.

10. S. Bormann, A. G. Baraibar, Y. Ni, D. Holtmann and F. Hollmann, *Catal. Sci. Technol.*, 2015, **5,** 2038-2052.

11. K. W. Borrelli, A. Vitalis, R. Alcantara and V. Guallar, *J. Chem. Theory Comput.*, 2005, **1,** 1304-1311.

12. N. R. Buck, W. Claerhout, B. H. Leuenberger, E. Stoecklin, K. Urban and S. Wolfram, *Patent (USA)*, 2013,US 20130210782 A1.

13. B. P. Cossins, A. Hosseini and V. Guallar, *J. Chem. Theory Comput.*, 2012, **8,** 959-965.

14. D. Floudas, M. Binder, R. Riley, K. Barry, R. A. Blanchette, B. Henrissat, A. T. Martínez, R. Otillar, J. W. Spatafora, J. S. Yadav, A. Aerts, I. Benoit, A. Boyd, A. Carlson, A. Copeland, P. M. Coutinho, R. P. de Vries, P. Ferreira, K. Findley, B. Foster, J. Gaskell, D. Glotzer, P. Górecki, J. Heitman, C. Hesse, C. Hori, K. Igarashi, J. A. Jurgens, N. Kallen, P. Kersten, A. Kohler, U. Kües, T. K. A. Kumar, A. Kuo, K. LaButti, L. F. Larrondo, E. Lindquist, A. Ling, V. Lombard, S. Lucas, T. Lundell, R. Martin, D. J. McLaughlin, I. Morgenstern, E. Morin, C. Murat, M. Nolan, R. A. Ohm, A. Patyshakuliyeva, A. Rokas, F. J. Ruiz-Dueñas, G. Sabat, A. Salamov, M. Samejima, J. Schmutz, J. C. Slot, F. St.John, J. Stenlid, H. Sun, S. Sun, K. Syed, A. Tsang, A. Wiebenga, D. Young, A. Pisabarro, D. C. Eastwood, F. Martin, D. Cullen, I. V. Grigoriev and D. S. Hibbett, *Science*, 2012, **336,** 1715-1719.

15. C. A. Fritts and P. W. Waldroup, *Journal of Applied Poultry Research*, 2003, **12,** 45-52.

16. A. Gutiérrez, E. D. Babot, R. Ullrich, M. Hofrichter, A. T. Martínez and J. C. del Río, *Arch. Biochem. Biophys.*, 2011, **514,** 33-43.

17. A. Gutiérrez, J. C. del Río, F. J. González-Vila and F. Martín, *J. Chromatogr.*, 1998, **823,** 449-455.

18. J. M. Hernández, *Patent (USA)*, 2013,US 20130137662 A1.

19. A. Hernández-Ortega, F. Lucas, P. Ferreira, M. Medina, V. Guallar and A. T. Martínez, *J. Biol. Chem.*, 2011, **286,** 41105-41114.

20. M. Hofrichter and R. Ullrich, *Curr. Opin. Chem. Biol.*, 2014, **19,** 116-125.

21. G. Jean, J. C. Terrat, T. Vanel, J. M. Hurot, C. Lorriaux, B. Mayor and C. Chazot, *Nephrol. Dial. Transplant.*, 2008, **23,** 3670-3676.

22. G. Jones, *Annu. Rev. Nutr.*, 2013, **33,** 23-44.

23. G. A. Kaminski, R. A. Friesner, J. Tirado-Rives and W. L. Jorgensen, *J. Phys. Chem. B*, 2001, **105,** 6474-6487.

24. S. Käppeli, E. Frohlich, S. G. Gebhardt-Henrich, A. Pfulg, H. Schäublin, R. Zweifel, H. Wiedmer and H. H. Stoffel, *Arch. Geflügelk.*, 2011, **75,** 179-184.

25. A. Karich, M. Kluge, R. Ullrich and M. Hofrichter, *AMB Express*, 2013, **3:5,**

26. M. Kinne, C. Zeisig, R. Ullrich, G. Kayser, K. E. Hammel and M. Hofrichter, *Biochem. Biophys. Res. Commun.*, 2010, **397,** 18-21.

27. M. Kluge, R. Ullrich, C. Dolge, K. Scheibner and M. Hofrichter, *Appl. Microbiol. Biotechnol.*, 2009, **81,** 1071-1076.

28. M. Kluge, R. Ullrich, K. Scheibner and M. Hofrichter, *Green Chem.*, 2012, **14,** 440-446.

29. G. A. Leichtmann, J. M. Bengoa, M. J. G. Bolt and M. D. Sitrin, *Amer. J. Clin. Nutr.*, 1991, **54,** 548-552.

30. D. Linde, R. Pogni, M. Cañellas, F. Lucas, V. Guallar, M. C. Baratto, A. Sinicropi, V. Sáez-Jiménez, C. Coscolín, A. Romero, F. J. Medrano, F. J. Ruiz-Dueñas and A. T. Martínez, *Biochem. J.*, 2014, on-line doi:10.1042/BJ20141211,

31. M. F. Lucas and V. Guallar, *Biophys. J.*, 2012, **102,** 887-896.

32. Makin, H. L. J. and D. B. Gower. Steroid analysis. Springer, NY, 2010.

33. M. Michalczuk, D. Pietrzak, J. Niemiec and J. Mroczk, *Pol. J. Food Nutr. Sci.*, 2010, **60,** 121-126.

34. S. Peter, M. Kinne, X. Wang, R. Ulrich, G. Kayser, J. T. Groves and M. Hofrichter, *FEBS J.*, 2011, **278,** 3667-3675.

35. K. Piontek, E. Strittmatter, R. Ullrich, G. Grobe, M. J. Pecyna, M. Kluge, K. Scheibner, M. Hofrichter and D. A. Plattner, *J. Biol. Chem.*, 2013, **288,** 34767-34776.

36. G. M. Sastry, M. Adzhigirey, T. Day, R. Annabhimoju and W. Sherman, *Journal of Computer-Aided Molecular Design*, 2013, **27,** 221-234.

37. J. C. Schöneboom, S. Cohen, H. Lin, S. Shaik and W. Thiel, *J. Am. Chem. Soc.*, 2004, **126,** 4017-4034.

38. Schrödinger. Jaguar 7.8. LCC, New York, 2011.

39. Schrödinger. QSite 5.7. LCC, New York, 2011.

40. Schrödinger. SiteMap 2.5. LCC, New York, 2011.

41. C. Simoes-Nunes and G. M. Weber, *Patent (European)*, 2004,EP 1516540 B1.

42. M. D. Sitrin and J. M. Bengoa, *Amer. J. Clin. Nutr.*, 1987, **46,** 1011-1015.

43. R. Ullrich, C. Dolge, M. Kluge and M. Hofrichter, *FEBS Lett.*, 2008, **582,** 4100-4106.

44. R. Ullrich and M. Hofrichter, *FEBS Lett.*, 2005, **579,** 6247-6250.

45. R. Ullrich and M. Hofrichter, *Cell. Mol. Life Sci.*, 2007, **64,** 271-293.

46. R. Ullrich, J. Nuske, K. Scheibner, J. Spantzel and M. Hofrichter, *Appl. Environ. Microbiol.*, 2004, **70,** 4575-4581.

Supporting Information

The Supporting Information shows the main interactions of cholecalciferol and ergocalciferol at the peroxygenase heme access channel (**Fig. S1** and **S2**, respectively), the effect of side-chain structure on the conversion rates of five sterols by the *A. aegerita* and *C. cinerea* peroxygenases (**Table S1**), and distributions of estimated Fe=O-H and O-H-C angles in the peroxygenase reactions with cholecalciferol and ergocalciferol (**Fig. S3**).

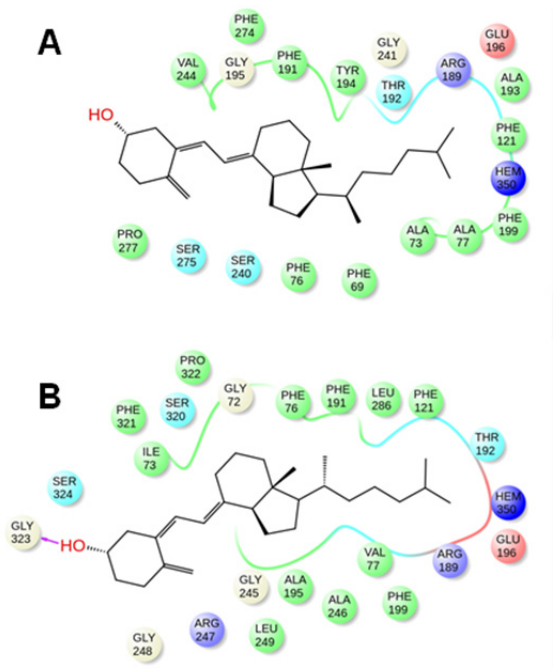

Fig. S1. Main interactions (below 3 Å) for cholecalciferol with the peroxygenases of *A. aegerita* (**A**) and *C. cinerea* (**B**).

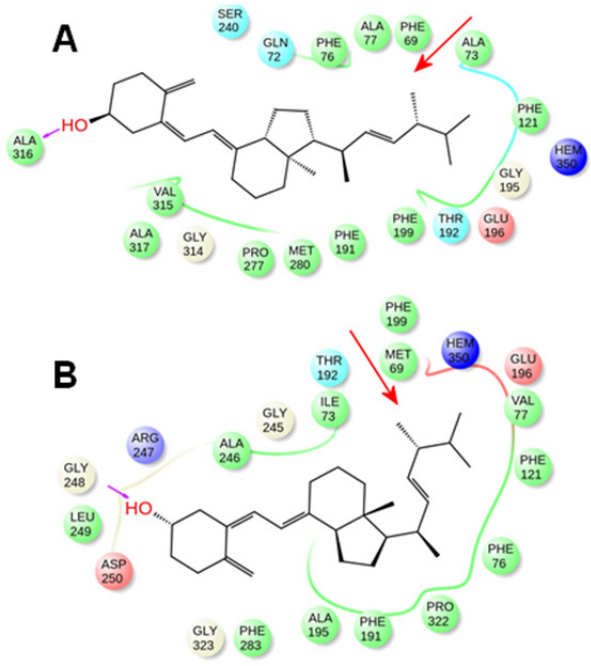

Fig. S2. Main interactions (below 3 Å) for ergocalciferol with the peroxygenases of *A. aegerita* (**A**) and *C. cinerea* (**B**).

Table S1. Conversion degree of steroids with different side-chains (**A-E**: cholesterol, campesterol, ergosterol, sitosterol and stigmasterol, respectively) by *A. aegerita* and *C. cinerea* peroxygenases[a].

		Conversion (%)	
		A. aegerita peroxygenase	*C. cinerea* peroxygenase
A	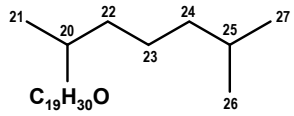	64	100
B	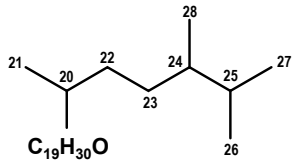	47	30
C	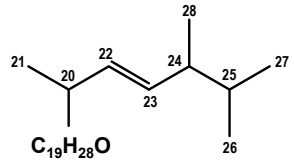	10	6
D	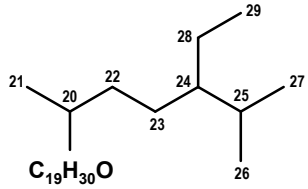	13	6
E	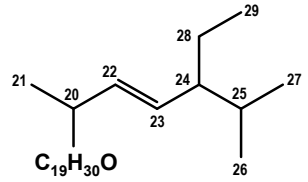	2	2

[a]From E. D. Babot, J. C. del Río, M. Cañellas, F. Sancho, F. Lucas, V. Guallar, L. Kalum, H. Lund, G. Gröbe, K. Scheibner, R. Ullrich, M. Hofrichter, A. T. Martínez, and A. Gutiérrez. 2015. Steroid hydroxylation by basidiomycete peroxygenases: A combined experimental and computational study. *Appl. Environ. Microbiol.* 81:4130-4142

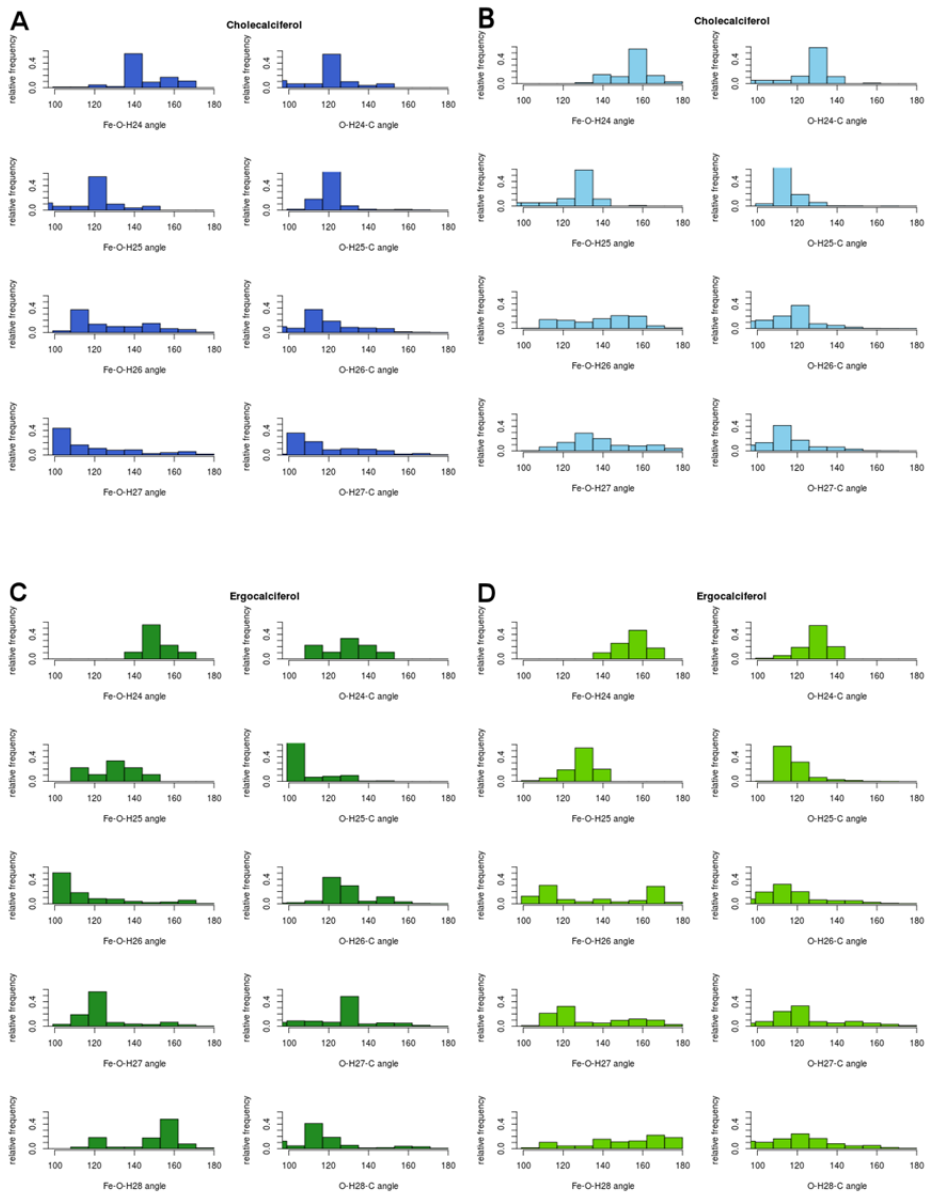

Fig. S3. Relative distributions of computed Fe=O-H and O-H-C angles for the reactions of *A. aegerita* (**A**, **C**) and *C. cinerea* (**B**, **D**) peroxygenases at the C_{24}, C_{25}, C_{26} and C_{27}, positions of cholecalciferol (blue) and ergocalciferol (green) and the C_{28} position of ergocalciferol. Structures were filtered by energy and distance between the pertinent hydrogen atom and the haem compound I oxygen (below 3 Å). QM/MM studies for $P450_{cam}$[b] show that in a pre-arranged reactive position camphor adopts angles of 130º for Fe=O-H and 170º for O-H-C. While for that latter no correlation is found to the theoretical predictions, in the case of Fe=O-H_{24} angles between 120 and 140º are favoured in C_{24} for cholecalciferol reacting with

A. aegerita (**A**) in agreement with the experimentally observed formation of 21% product in this position. In the case of the remaining 3 reactions, few structures are found with angles below 145º. In the case of Fe=O-H_{25} (as expected) all compounds present favourable angles. Analogous to the case of the distance distribution analysis, no conclusions can be made for the reactivity of C_{26}, C_{27} and C_{28}. [b]J. C. Schöneboom, S. Cohen, H. Lin, S. Shaik and W. Thiel, J. Am. Chem. Soc., 2004, 126, 4017-4034.

6.2. Patente I:

Lund H., Brask J., Kalum L., Gutiérrez Suárez A., Babot E. D., Ullrich R., Hofrichter M., Martínez Ferrer A. T., del Río Andrade J. C. (2013). Enzymatic preparations of diols. WO 2013/004639. PCT/EP2012/062763.

ENZYMATIC PREPARATION OF DIOLS

Reference to a Sequence Listing

This application contains a Sequence Listing in computer readable form. The computer readable form is incorporated herein by reference.

BACKGROUND OF THE INVENTION

Field of the Invention

The present invention relates to the use of polypeptides having peroxygenase activity for site specific oxidation of aliphatic hydrocarbons.

Background

A peroxygenase denoted AaP from the agaric basidiomycete strain *Agrocybe aegerita* (strain TM-A1) was found to oxidize aryl alcohols and aldehydes. The AaP peroxygenase was purified from *A. aegerita* TM A1 by several steps of ion chromatography and SDS-PAGE, the molecular weight was determined and the N-terminal 14 amino acid sequence was determined after 2-D electrophoresis but the encoding gene was not isolated (Ullrich *et al*., 2004, *Appl. Env. Microbiol*. 70(8): 4575-4581).

WO 2006/034702 discloses methods for the enzymatic hydroxylation of non-activated hydrocarbons, such as, naphtalene, toluol and cyclohexane, using the AaP peroxygenase enzyme of *Agrocybe aegerita* TM A1. This is also described in Ullrich and Hofrichter, 2005, *FEBS Letter*s 579: 6247-6250.

WO 2008/119780 discloses eight different peroxygenases from *Agrocybe aegerita*, *Coprinopsis cinerea*, *Laccaria bicolor* and *Coprinus radians*; also shown as SEQ ID NOs: 1-8 in the present application.

DE 103 32 065 A1 discloses methods for the enzymatic preparation of acids from alcohols through the intermediary formation of aldehydes by using the AaP peroxygenase enzyme of *Agrocybe aegerita* TM A1.

A method was reported for the rapid and selective spectrophotometric direct detection of aromatic hydroxylation by the AaP peroxygenase (Kiuge *et al*., 2007, *Appl Microbiol Biotechnol* 75: 1473-1478).

It is well-known that a direct regioselective introduction of oxygen functions (oxygenation) into organic molecules constitutes a problem in chemical synthesis. It is particularly difficult to catalyse the selective hydroxylation of aliphatic hydrocarbons. The products may be used as important intermediates in a wide variety of different syntheses.

In particular the chemical hydroxylation of alkanes is relatively complex, requires aggressive/toxic chemicals/catalysts and leads to a series of undesired by-products.

It is known that an intracellular enzyme, methane monooxygenase (MMO, EC 14.13.25), oxygenates/hydroxylates the terminal carbon of some hydrocarbons. The MMO enzyme consists of several protein components and is formed by methylotrophic bacteria (*e.g., Methylococcus capsulatus*); it requires complex electron donors such as NADH or NADPH, auxiliary proteins (flavin reductases, regulator protein) and molecular oxygen (O_2). The natural substrate of MMO is methane, which is oxidized to methanol. As a particularly unspecific biocatalyst, MMO oxygenates/hydroxylates, as well as methane, a series of further substrates such as *n*-alkanes and their derivatives, cycloalkanes, aromatics, carbon monoxide and heterocycles. Utilization of the enzyme in biotechnology is currently not possible, since it is difficult to isolate, like most intracellular enzymes, it is of low stability, and the cosubstrates required are relatively expensive.

SUMMARY OF THE INVENTION

In a first aspect, the inventors of the present invention have provided an enzymatic method for introducing a hydroxy or an oxo group, at the second or third carbon of at least two ends of a substituted or unsubstituted, linear or branched, aliphatic hydrocarbon having at least five carbons and having a hydrogen attached to said second or third carbon, comprising contacting the aliphatic hydrocarbon with hydrogen peroxide and a polypeptide having peroxygenase activity; wherein the polypeptide comprises:

a) an amino acid sequence which has at least 30% identity to SEQ ID NO: 1, 2, 3, 4, 5, 6, 7, 8, 16, 17, 18, 19, 20, 21, 22, 23, 24, 25, 26, 27, 28 or 29; and

b) an amino acid sequence represented by one or more of the following motifs:

Motif I:	[FL]XX[YF]S[AN]X[FHY]G[GN]GX[YF]N	(SEQ ID NO: 9);
Motif II:	G[GN]GX[YF]NXX[VA]AX[EH][LF]R	(SEQ ID NO: 10);
Motif III:	RXXRI[QE][DEQ]S[IM]ATN	(SEQ ID NO: 11);
Motif IV:	S[IM]ATN[PG][EQN][FM][SDN][FL]	(SEQ ID NO: 12);
Motif V:	P[PDK][DG]F[HFW]R[AP]	(SEQ ID NO: 13);
Motif VI:	[TI]XXXLYPNP[TK][GV]	(SEQ ID NO: 14);
Motif VII:	E[HG]DXSX[ST]RXD	(SEQ ID NO: 15).

In further aspects, the invention provides uses of polypeptides having peroxygenase activity for removal of lipid containing stains from laundry; and for reducing unpleasant odor from laundry.

Brief Description of the Figures

Figure 1 shows a chromatographic profile of tetradecane incubated with *C. cinerea* peroxygenase (0.5 mM H_2O_2); from Example 3.

Figure 2 shows a chromatographic profile of tetradecane incubated with *A. aegerita* peroxygenase (2.5 mM H_2O_2); from Example 3.

Figure 3 shows a chromatographic profile of tetradecanol incubated with *C. cinerea* peroxygenase (0.5 mM H_2O_2); from Example 4.

Figure 4 shows a chromatographic profile of tetradecanol incubated with *A. aegerita* peroxygenase (2.5 mM H_2O_2); from Example 4.

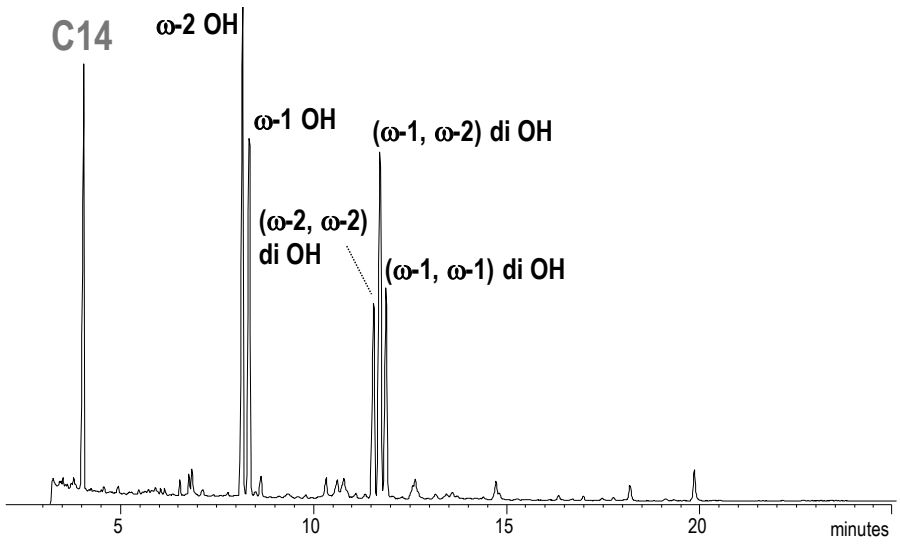

Fig 1. Chromatographic profile of tetradecane incubated with *C. cinerea* peroxigenase (0.5 mM H_2O_2).

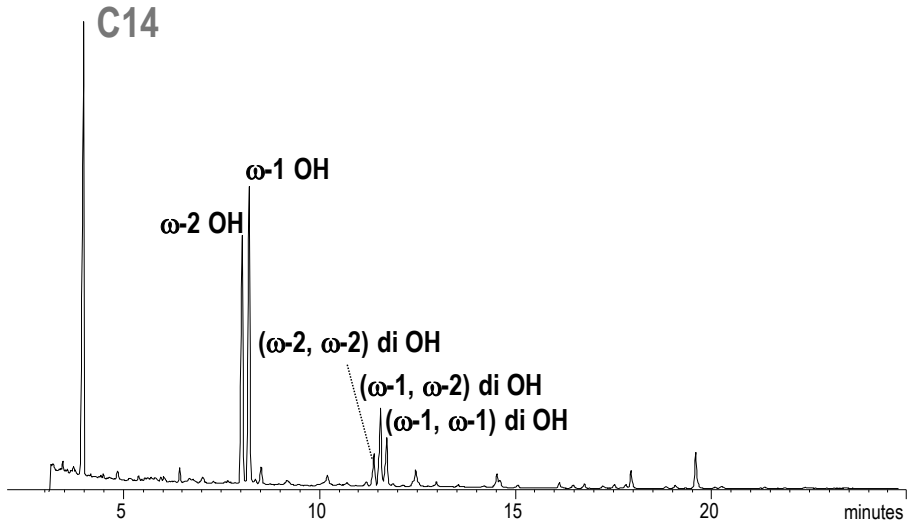

Fig 2. Chromatographic profile of tetradecane incubated with *A. aegerita* peroxigenase (2.5 mM H_2O_2).

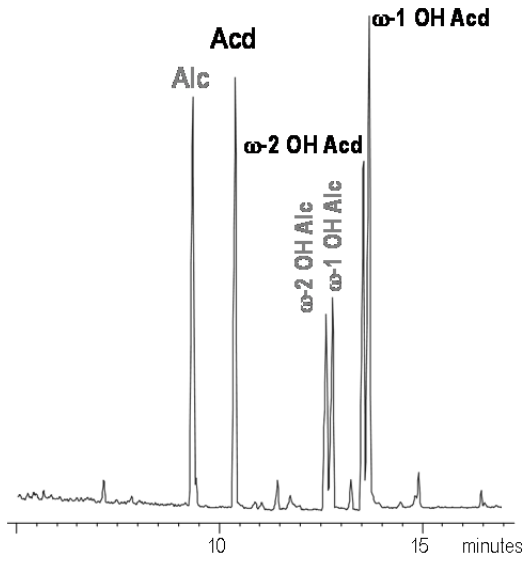

Fig 3. Chromatographic profile of tetradecanol incubated with *C. cinerea* peroxigenase (0.5 mM H_2O_2).

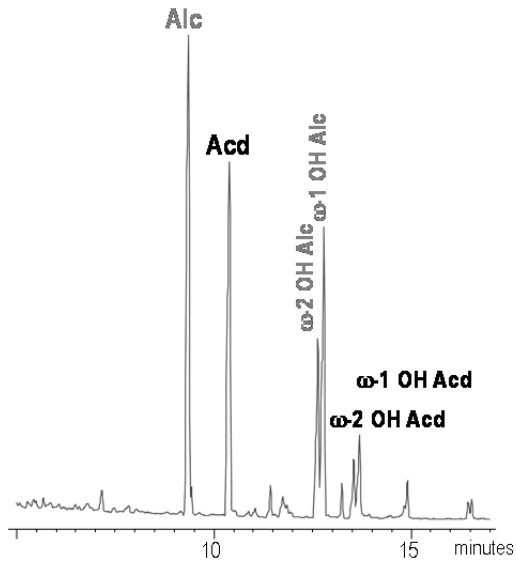

Fig 4. Chromatographic profile of tetradecanol incubated with *A. aegerita* peroxigenase (2.5 mM H_2O_2).

DEFINITIONS

Peroxygenase activity: The term "peroxygenase activity" is defined herein as "unspecific peroxygenase" according to EC 1.11.2.1. This is a heme-thiolate protein. Enzymes of this type include glycoproteins secreted by agaric basidiomycetes. They catalyse the insertion of an oxygen atom from H_2O_2 into a wide variety of substrates, such as naphthalene, 4-nitrobenzodioxole; and alkanes such as propane, hexane and cyclohexane. They have little or no activity toward chloride.

For purposes of the present invention, peroxygenase activity is determined according to the spectrophotometric procedure described by Kluge *et al.* (2007, *Appl Microbiol Biotechnol* 75:1473-1478).

Isolated polypeptide: The term "isolated polypeptide" as used herein refers to a polypeptide that is isolated from a source. In a preferred aspect, the polypeptide is at least 1% pure, preferably at least 5% pure, more preferably at least 10% pure, more preferably at least 20% pure, more preferably at least 40% pure, more preferably at least 60% pure, even more preferably at least 80% pure, and most preferably at least 90% pure, as determined by SDS- PAGE.

Substantially pure polypeptide: The term "substantially pure polypeptide" denotes herein a polypeptide preparation that contains at most 10%, preferably at most 8%, more preferably at most 6%, more preferably at most 5%, more preferably at most 4%, more preferably at most 3%, even more preferably at most 2%, most preferably at most 1%, and even most preferably at most 0.5% by weight of other polypeptide material with which it is natively or recombinantly associated. It is, therefore, preferred that the substantially pure polypeptide is at least 92% pure, preferably at least 94% pure, more preferably at least 95% pure, more preferably at least 96% pure, more preferably at least 96% pure, more preferably at least 97% pure, more preferably at least 98% pure, even more preferably at least 99%, most preferably at least 99.5% pure, and even most preferably 100% pure by weight of the total polypeptide material present in the preparation. The polypeptides of the present invention are preferably in a substantially pure form, *i.e.*, that the polypeptide preparation is essentially free of other polypeptide material with which it is natively or recombinantly associated.

This can be accomplished, for example, by preparing the polypeptide by well-known recombinant methods or by classical purification methods.

Mature polypeptide: The term "mature polypeptide" is defined herein as a polypeptide having peroxygenase activity that is in its final form following translation and any post-translational modifications, such as N-terminal processing, C-terminal truncation, glycosylation, phosphorylation, etc. In a preferred aspect, the mature polypeptide has the amino acid sequence shown in positions 1 to 330 of SEQ ID NO: 1 based on the N-terminal peptide sequencing data (Ullrich *et al.*, 2004, *Appl. Env. Microbiol.* 70(8): 4575-4581), elucidating the start of the mature protein of AaP peroxygenase enzyme. In another preferred aspect, the mature polypeptide has the amino acid sequence shown in positions 1 to 328 of SEQ ID NO: 2.

Identity: The relatedness between two amino acid sequences or between two nucleotide sequences is described by the parameter "identity".

For purposes of the present invention, the degree of identity between two amino acid sequences is determined using the Needleman-Wunsch algorithm (Needleman and Wunsch, 1970, *J. Mol. Biol.* 48: 443-453) as implemented in the Needle program of the EMBOSS package (EMBOSS: The European Molecular Biology Open Software Suite, Rice *et al.*, 2000, *Trends in Genetics* 16: 276-277; http://emboss.org), preferably version 3.0.0 or later. The optional parameters used are gap open penalty of 10, gap extension penalty of 0.5, and the EBLOSUM62 (EMBOSS version of BLOSUM62) substitution matrix. The output of Needle labeled "longest identity" (obtained using the -nobrief option) is used as the percent identity and is calculated as follows:

(Identical Residues x 100)/(Length of Alignment - Total Number of Gaps in Alignment).

For purposes of the present invention, the degree of identity between two deoxyribonucleotide sequences is determined using the Needleman-Wunsch algorithm (Needleman and Wunsch, 1970, *supra*) as implemented in the Needle

program of the EMBOSS package (EMBOSS: The European Molecular Biology Open Software Suite, Rice *et al.*, 2000, *supr*a; http://emboss.org), preferably version 3.0.0 or later. The optional parameters used are gap open penalty of 10, gap extension penalty of 0.5, and the EDNAFULL (EMBOSS version of NCBI NUC4.4) substitution matrix. The output of Needle labeled "longest identity" (obtained using the -nobrief option) is used as the percent identity and is calculated as follows:

(Identical Deoxyribonucleotides x 100)/(Length of Alignment - Total Number of Gaps in Alignment).

Modification: The term "modification" means herein any chemical modification of the polypeptide consisting of the mature polypeptide of SEQ ID NO: 1, 2, 3, 4, 5, 6, 7, 8, 16, 17, 18, 19, 20, 21, 22, 23, 24, 25, 26, 27, 28 or 29; or a homologous sequence thereof; as well as genetic manipulation of the DNA encoding such a polypeptide. The modification can be a substitution, a deletion and/or an insertion of one or more (several) amino acids as well as replacements of one or more (several) amino acid side chains.

DETAILED DESCRIPTION OF THE INVENTION

Polypeptides having peroxygenase activity (peroxygenases)

The present invention relates to uses of an isolated polypeptide, which is preferably recombinantly produced, having peroxygenase activity, which comprises an amino acid sequence having at least 30% identity, preferably at least 35%, 40%, 45%, 50%, 55%, 60%, 65%, 70%, 75%, 80%, 85%, 90%, 95%, 97%, or 98% identity to the polypeptide of SEQ ID NO: 1, 2, 3, 4, 5, 6, 7, 8, 16, 17, 18, 19, 20, 21, 22, 23, 24, 25, 26, 27, 28 or 29; preferably SEQ ID NO: 2 or SEQ ID NO: 4.

In a preferred embodiment, the polypeptide comprises an amino acid sequence represented by one or more of the following motifs, preferably comprising two or more, three or more, four or more, five or six of the following motifs:

Motif I:	[FL]XX[YF]S[AN]X[FHY]G[GN]GX[YF]N	(SEQ ID NO: 9);
Motif II:	G[GN]GX[YF]NXX[VA]AX[EH][LF]R	(SEQ ID NO: 10);
Motif III:	RXXRI[QE][DEQ]S[IM]ATN	(SEQ ID NO: 11);
Motif IV:	S[IM]ATN[PG][EQN][FM][SDN][FL]	(SEQ ID NO: 12);
Motif V:	P[PDK][DG]F[HFW]R[AP]	(SEQ ID NO: 13);
Motif VI:	[TI]XXXLYPNP[TK][GV]	(SEQ ID NO: 14);
Motif VII:	E[HG]DXSX[ST]RXD	(SEQ ID NO: 15).

In a more preferred embodiment, the peroxygenase comprises an amino acid sequence represented by the motif: E[HG]DXSX[ST]RXD.

In another embodiment, the polypeptide comprises an amino acid sequence having a substitution, deletion, and/or insertion of one or several amino acids of the mature polypeptide of SEQ ID NO: 1, 2, 3, 4, 5, 6, 7, 8, 16, 17, 18, 19, 20, 21, 22, 23, 24, 25, 26, 27, 28 or 29; preferably SEQ ID NO: 2 or SEQ ID NO: 4.

In yet another embodiment, the polypeptide of the first aspect comprises or consists of the amino acid sequence of SEQ ID NO: 1, 2, 3, 4, 5, 6, 7, 8, 16, 17, 18, 19, 20, 21, 22, 23, 24, 25, 26, 27, 28 or 29; preferably SEQ ID NO: 2 or SEQ ID NO: 4; or a fragment thereof having peroxygenase activity; preferably the polypeptide comprises or consists of the mature polypeptide of SEQ ID NO: 1, 2, 3, 4, 5, 6, 7, 8, 16, 17, 18, 19, 20, 21, 22, 23, 24, 25, 26, 27, 28 or 29; preferably SEQ ID NO: 2 or SEQ ID NO: 4.

Preferably, amino acid changes are of a minor nature, that is conservative amino acid substitutions or insertions that do not significantly affect the folding and/or activity of the protein; small deletions, typically of one to about 30 amino acids; small amino- or carboxyl-terminal extensions, such as an amino-terminal methionine residue; a small linker peptide of up to about 20-25 residues; or a small extension that facilitates purification by changing net charge or another function, such as a poly-histidine tract, an antigenic epitope or a binding domain.

Examples of conservative substitutions are within the group of basic amino acids (arginine, lysine and histidine), acidic amino acids (glutamic acid and aspartic acid), polar amino acids (glutamine and asparagine), hydrophobic amino acids (leucine, isoleucine and valine), aromatic amino acids (phenylalanine, tryptophan and tyrosine), and small amino acids (glycine, alanine, serine, threonine and methionine). Amino acid substitutions that do not generally alter specific activity are known in the art and are described, for example, by H. Neurath and R.L. Hill, 1979, *In, The Proteins*, Academic Press, New York. The most commonly occurring exchanges are Ala/Ser, Val/Ile, Asp/Glu, Thr/Ser, Ala/Gly, Ala/Thr, Ser/Asn, Ala/Val, Ser/Gly, Tyr/Phe, Ala/Pro, Lys/Arg, Asp/Asn, Leu/Ile, Leu/Val, Ala/Glu, and Asp/Gly.

In addition to the 20 standard amino acids, non-standard amino acids (such as 4-hydroxyproline, 6-*N*-methyl lysine, 2-aminoisobutyric acid, isovaline, and alpha-methyl serine) may be substituted for amino acid residues of a wild-type polypeptide. A limited number of non-conservative amino acids, amino acids that are not encoded by the genetic code, and unnatural amino acids may be substituted for amino acid residues. "Unnatural amino acids" have been modified after protein synthesis, and/or have a chemical structure in their side chain(s) different from that of the standard amino acids. Unnatural amino acids can be chemically synthesized, and preferably, are commercially available, and include pipecolic acid, thiazolidine carboxylic acid, dehydroproline, 3- and 4-methylproline, and 3,3-dimethylproline.

Alternatively, the amino acid changes are of such a nature that the physico-chemical properties of the polypeptides are altered. For example, amino acid changes may improve the thermal stability of the polypeptide, alter the substrate specificity, change the pH optimum, and the like.

Essential amino acids in the parent polypeptide can be identified according to procedures known in the art, such as site-directed mutagenesis or alanine-scanning mutagenesis (Cunningham and Wells, 1989, *Science* 244: 1081-1085). In the latter technique, single alanine mutations are introduced at every residue in the molecule, and the resultant mutant molecules are tested for biological activity (*i.e.*, peroxygenase activity) to identify amino acid residues that are critical to the activity of the molecule. See also, Hilton *et al.*, 1996, *J. Biol. Chem.* 271:4699-4708. The active site of the enzyme or other biological interaction can also be determined by physical analysis of structure, as determined by such

techniques as nuclear magnetic resonance, crystallography, electron diffraction, or photoaffinity labeling, in conjunction with mutation of putative contact site amino acids. See, for example, de Vos *et al.*, 1992, *Science* 255: 306-312; Smith *et al.*, 1992, *J. Mol. Biol.* 224: 899-904; Wlodaver *et al.*, 1992, *FEBS Lett.* 309: 59-64. The identities of essential amino acids can also be inferred from analysis of identities with polypeptides that are related to a polypeptide according to the invention.

Single or multiple amino acid substitutions, deletions, and/or insertions can be made and tested using known methods of mutagenesis, recombination, and/or shuffling, followed by a relevant screening procedure, such as those disclosed by Reidhaar-Oison and Sauer, 1988, *Science* 241: 53-57; Bowie and Sauer, 1989, *Proc. Natl. Acad. Sci. USA* 86: 2152-2156; WO 95/17413; or WO 95/22625. Other methods that can be used include error-prone PCR, phage display (*e.g.*, Lowman *et al.*, 1991, *Biochem.* 30: 10832-10837; U.S. Patent No. 5,223,409; WO 92/06204), and region-directed mutagenesis (Derbyshire *et al.*, 1986, *Gene* 46: 145; Ner *et al.*, 1988, *DNA* 7: 127).

Mutagenesis/shuffling methods can be combined with high-throughput, automated screening methods to detect activity of cloned, mutagenized polypeptides expressed by host cells (Ness *et al.*, 1999, *Nature Biotechnology* 17: 893-896). Mutagenized DNA molecules that encode active polypeptides can be recovered from the host cells and rapidly sequenced using standard methods in the art. These methods allow the rapid determination of the importance of individual amino acid residues in a polypeptide of interest, and can be applied to polypeptides of unknown structure.

The total number of amino acid substitutions, deletions and/or insertions of the mature polypeptide of SEQ ID NO: 1, 2, 3, 4, 5, 6, 7, 8, 16, 17, 18, 19, 20, 21, 22, 23, 24, 25, 26, 27, 28 or 29; preferably SEQ ID NO: 2 or SEQ ID NO: 4; is 10, preferably 9, more preferably 8, more preferably 7, more preferably at most 6, more preferably 5, more preferably 4, even more preferably 3, most preferably 2, and even most preferably 1.

Another preferred embodiment relates to the polypeptide having peroxygenase activity of the first aspect of the invention, wherein the mature polypeptide is amino acids 1 to 330 of SEQ ID NO: 1.

Yet another preferred embodiment relates to the polypeptide having peroxygenase activity of the first aspect of the invention, wherein the mature polypeptide is amino acids 1 to 328 of SEQ ID NO: 2.

Yet another preferred embodiment relates to the polypeptide having peroxygenase activity of the first aspect of the invention, wherein the mature polypeptide is amino acids 1 to 344 of SEQ ID NO: 4.

Yet another preferred embodiment relates to the polypeptide having peroxygenase activity of the first aspect of the invention, wherein the mature polypeptide is amino acids 1 to 261 of SEQ ID NO: 23.

Hydrogen peroxide

The hydrogen peroxide required by the peroxygenase may be provided as an aqueous solution of hydrogen peroxide or a hydrogen peroxide precursor for in situ production of hydrogen peroxide. Any solid entity which liberates upon dissolution a peroxide which is useable by peroxygenase can serve as a source of hydrogen peroxide. Compounds which yield hydrogen peroxide upon dissolution in water or an appropriate aqueous based medium include but are not limited to metal peroxides, percarbonates, persulphates, perphosphates, peroxyacids, alkyperoxides, acylperoxides, peroxyesters, urea peroxide, perborates and peroxycarboxylic acids or salts thereof.

Another source of hydrogen peroxide is a hydrogen peroxide generating enzyme system, such as an oxidase together with a substrate for the oxidase. Examples of combinations of oxidase and substrate comprise, but are not limited to, amino acid oxidase (see *e.g.*, US 6,248,575) and a suitable amino acid, glucose oxidase (see *e.g.*, WO 95/29996) and glucose, lactate oxidase and lactate, galactose oxidase (see *e.g.,* WO 00/50606) and galactose, and aldose oxidase (see *e.g.*, WO 99/31990) and a suitable aldose.

By studying EC 1.1.3._, EC 1.2.3._, EC 1.4.3._, and EC 1.5.3._ or similar classes (under the International Union of Biochemistry), other examples of such combinations of oxidases and substrates are easily recognized by one skilled in the art.

Hydrogen peroxide or a source of hydrogen peroxide may be added at the beginning of or during the method of the invention, *e.g.*, as one or more separate additions of hydrogen peroxide; or continously as fed-batch addition. Typical

amounts of hydrogen peroxide correspond to levels of from 0.001 mM to 25 mM, preferably to levels of from 0.005 mM to 5 mM, and particularly to levels of from 0.01 to 1 mM hydrogen peroxide. Hydrogen peroxide may also be used in an amount corresponding to levels of from 0.1 mM to 25 mM, preferably to levels of from 0.5 mM to 15 mM, more preferably to levels of from 1 mM to 10 mM, and most preferably to levels of from 2 mM to 8 mM hydrogen peroxide.

Surfactants

The method of the invention may include application of a surfactant (for example, as part of a detergent formulation or as a wetting agent). Surfactants suitable for being applied may be non-ionic (including semi-polar), anionic, cationic and/or zwitterionic; preferably the surfactant is anionic (such as linear alkylbenzenesulfonate, alpha-olefinsulfonate, alkyl sulfate (fatty alcohol sulfate), alcohol ethoxysulfate, secondary alkanesulfonate, alpha-sulfo fatty acid methyl ester, alkyl- or alkenylsuccinic acid or soap or non-ionic such as alcohol ethoxylate, nonylphenol ethoxylate, alkylpolyglycoside, alkyldimethylamineoxide, ethoxylated fatty acid monoethanolamide, fatty acid monoethanolamide, polyhydroxy alkyl fatty acid amide, or *N*-acyl *N*-alkyl derivatives of glucosamine ("glucamides"), or a mixture thereof.

When included in the method of the invention, the concentration of the surfactant will usually be from about 0.01% to about 10%, preferably about 0.05% to about 5%, and more preferably about 0.1% to about 1% by weight.

Aliphatic Hydrocarbons

The hydrocarbons, which are oxidized in the method of the invention, are aliphatic hydrocarbons having a chain of at least five carbons. Preferably, the aliphatic hydrocarbon is an alkane or an alkene; more preferably, the aliphatic hydrocarbon is an alkane, such as pentane, hexane, heptane, octane, nonane, decane, undecane, dodecane, tridecane, tetradecane, pentadecane or hexadecane, or isomers thereof. Even more preferably, the aliphatic hydrocarbon is undecane, dodecane, tridecane, tetradecane, pentadecane or hexadecane, or isomers thereof.

In an embodiment, the aliphatic hydrocarbon is not *n*-hexane or *n*-decane.

The aliphatic hydrocarbons are linear or branched, but not cyclic, as site specific oxidation is not possible with cyclic hydrocarbons. Branched hydrocarbons correspond to isomers of linear hydrocarbons.

The aliphatic hydrocarbons are substituted or unsubstituted. Preferably, the aliphatic hydrocarbons are unsubstituted, such as non-activated hydrocarbons.

When the aliphatic hydrocarbons are substituted (functional groups attached), the preferred substituents are halogen, hydroxyl, carboxyl, amino, nitro, cyano, thiol, sulphonyl, formyl, acetyl, methoxy, ethoxy, phenyl, benzyl, xylyl, carbamoyl and sulfamoyl; more preferred substituents are chloro, hydroxyl, carboxyl and sulphonyl; and most preferred substituents are chloro and carboxyl.

The aliphatic hydrocarbons may be substituted by up to 10 substituents, up to 8 substituents, up to 6 substituents, up to 4 substituents, up to 2 substituents, or by up to one substituent.

Methods and Uses

The present invention provides a method for site specific introduction of a hydroxy and/or an oxo (keto) group at the second or third carbon of at least two ends of an aliphatic hydrocarbon, using a peroxygenase and hydrogen peroxide.

The aliphatic hydrocarbon must include a chain of at least five carbons. The second and third carbons are determined by counting the carbon atoms from any end of the aliphatic hydrocarbon.

The aliphatic hydrocarbon must have at least one hydrogen attached to a carbon which is hydroxylated by attachment of a hydroxy group; and at least two hydrogens attached to a carbon when an oxo group is introduced. In a preferred embodiment, the second or third carbon is unsubstituted befare being contacted with the peroxygenase.

According to the method of the invention, the hydroxy and/or oxo groups are introduced independently of each other at the (at least) two ends of the aliphatic hydrocarbon. Thus, a hydroxy group can be introduced at one end, at the same time as an oxo group is introduced at another (the other) end - and

vice versa. Two hydroxy groups, or two oxo groups, or one hydroxy group and one oxo group, cannot be introduced at the same end of the aliphatic hydrocarbon. Some examples of combinations are shown in Example 1.

In the context of the present invention, "oxidation" means introduction of a hydroxy and/or an oxo group.

Accordingly, in a first aspect, the present invention provides a method for introducing a hydroxy and/or an oxo (keto) group at the second or third carbon of (at least) two ends of a substituted or unsubstituted, linear or branched, aliphatic hydrocarbon having at least five carbons and having at least one hydrogen attached to said second or third carbon, comprising contacting the aliphatic hydrocarbon with hydrogen peroxide and a polypeptide having peroxygenase activity; wherein the polypeptide comprises:

c) an amino acid sequence which has at least 30% identity to SEQ ID NO: 1, 2, 3, 4, 5, 6, 7, 8, 16, 17, 18, 19, 20, 21, 22, 23, 24, 25, 26, 27, 28 or 29; preferably SEQ ID NO: 2 or SEQ ID NO: 4; and
d) an amino acid sequence represented by one or more of the following motifs:

Motif I	[FL]XX[YF]S[AN]X[FHY]G[GN]GX[YF]N	(SEQ ID NO: 9);
Motif II:	G[GN]GX[YF]NXX[VA]AX[EH][LF] R	(SEQ ID NO: 10)
Motif III:	RXXRI[QE][DEQ]S[IM]ATN	(SEQ ID NO: 11)
Motif IV:	S[IM]ATN[PG][EQN][FM][SDN][FL]	(SEQ ID NO: 12);
Motif V:	P[PDK][DG]F[HFW]R[AP]	(SEQ ID NO: 13);
Motif VI:	[TI]XXXLYPNP[TK][GV]	(SEQ ID NO: 14);
Motif VII:	E[HG]DXSX[ST]RXD	(SEQ ID NO: 15);

preferably, Motif VII: E[HG]DXSX[ST]RXD.

In an embodiment, the aliphatic hydrocarbon is not *n*-hexane or *n*-decane.

In a preferred embodiment, the aliphatic hydrocarbon is oxidized to (converted to) a diol, by introduction of two hydroxy groups. More preferably, the two hydroxy groups are located at each end of a linear aliphatic hydrocarbon.

The method of the invention may be used for a variety of purposes, like bulk chemical synthesis (biocatalysis), increasing aqueous solubility of aliphatic hydrocarbons, bioremediation, and modification of the characteristics of food products.

The method of the invention may also be used for a number of industrial processes in which said oxidation reactions are beneficial. An example of such use is in the manufacture of pulp and paper products where alkanes and other relevant aliphatic hydrocarbons that are present in the wood (resin) can result in depositioning problems in the pulp and paper manufacturing process. These hydrophobic compounds are the precursors of the so-called pitch deposits within the pulp and paper manufacturing processes. Pitch deposition results in low quality pulp, and can cause the shutdown of pulp mill operations. Specific issues related to pulps with high extractives content include runnability problems, spots and holes in the paper, and sheet breaks. Treatment with peroxygenase can increase the solubility of said compounds and thereby mitigate problems.

Yet another use of the method of the invention is in, for example, oil or coal refineries where the peroxygenase catalyzed oxidation can be used to modify the solubility, viscosity and/or combustion characteristics of hydrocarbons. Specifically the treatment can lead to changes in the smoke point, the kindling point, the fire point and the boiling point of the hydrocarbons subjected to the treatment.

In the synthesis of bulk chemicals, agro chemicals (incl. pesticides), specialty chemicals and pharmaceuticals the method of the invention may obviously be relevant in terms of selectively introducing hydroxy groups in the substrates thereby affecting the solubility of the modified compound. Furthermore, the selective oxidation provides a site for further modification by methods known in the art of organic chemical synthesis and chemo-enzymatic synthesis.

Natural gas is extensively processed to remove higher alkanes. Oxidation of such higher alkanes may be used to improve water solubility, and thus

facilitate removal of the higher alkanes by washing the natural gas stream. Removal may be performed at the well or during refining.

Oxidation, according to the invention, of oil waste will significantly improve biodegradability and will be applicable both in connection with waste water treatment from refineries and bioremediation of contaminated ground or water.

The methods of the invention may be carried out with an immobilized polypeptide having peroxygenase activity (peroxygenase).

The methods of the invention may be carried out in an aqueous solvent (reaction medium), various alcohols, ethers, other polar or non-polar solvents, or mixtures thereof. By studying the characteristics of the aliphatic hydrocarbon used in the methods of the invention, suitable examples of solvents are easily recognized by one skilled in the art. By raising or lowering the pressure at which the oxidation is carried out, the solvent (reaction medium) and the aliphatic hydrocarbon can be maintained in a liquid phase at the reaction temperature.

The methods according to the invention may be carried out at a temperature between 0 and 90 degrees Celsius, preferably between 5 and 80 degrees Celsius, more preferably between 10 and 70 degrees Celsius, even more preferably between 15 and 60 degrees Celsius, most preferably between 20 and 50 degrees Celsius, and in particular between 20 and 40 degrees Celsius.

The methods of the invention may employ a treatment time of from 10 seconds to (at least) 24 hours, preferably from 1 minute to (at least) 12 hours, more preferably from 5 minutes to (at least) 6 hours, most preferably from 5 minutes to (at least) 3 hours, and in particular from 5 minutes to (at least) 1 hour.

Diols (di-hydroxy aliphatic hydrocarbons) produced by the method of the invention may be used for producing polyurethan. Polyurethane is a polymer composed of a chain of organic units joined by carbamate (urethane) links. Polyurethane polymers are formed through step-growth polymerization, by reacting a monomer (with at least two isocyanate functional groups) with another monomer (with at least two hydroxyl groups) in the presence of a catalyst.

In another aspect, the present invention provides a method for introducing an oxo (keto) group at the second or third carbon of a substituted or unsubstituted, linear or branched, aliphatic hydrocarbon having at least five carbons and having at least two hydrogens attached to said second or third carbon, comprising contacting the aliphatic hydrocarbon with hydrogen peroxide and a polypeptide having peroxygenase activity; wherein the polypeptide comprises:

e) an amino acid sequence which has at least 30% identity to SEQ ID NO: 1, 2, 3, 4, 5, 6, 7, 8, 16, 17, 18, 19, 20, 21, 22, 23, 24, 25, 26, 27, 28 or 29; preferably SEQ ID NO: 2 or SEQ ID NO: 4; and
f) an amino acid sequence represented by one or more of the following motifs:

Motif I:	[FL]XX[YF]S[AN]X[FHY]G[GN]GX[YF]N	(SEQ ID NO: 9)
Motif II:	G[GN]GX[YF]NXX[VA]AX[EH][LF]R	(SEQ ID NO: 10);
Motif III:	RXXRI[QE][DEQ]S[IM]ATN	(SEQ ID NO: 11);
Motif IV:	S[IM]ATN[PG][EQN][FM][SDN][FL]	(SEQ ID NO: 12);
Motif V:	P[PDK][DG]F[HFW]R[AP]	(SEQ ID NO: 13);
Motif VI:	[TI]XXXLYPNP[TK][GV]	(SEQ ID NO: 14);
Motif VII:	E[HG]DXSX[ST]RXD	(SEQ ID NO: 15)

preferably, Motif VII: E[HG]DXSX[ST]RXD.

In an embodiment, the aliphatic hydrocarbon is not *n*-hexane or *n*-decane.

In yet another aspect, the present invention also provides a method for introducing a hydroxyl or an oxo group at a terminal carbon of a linear or branched aliphatic hydrocarbon having at least five carbons, which is substituted with a carboxy group, comprising contacting the aliphatic

hydrocarbon with hydrogen peroxide and a polypeptide having peroxygenase activity; wherein the polypeptide comprises:

g) an amino acid sequence which has at least 30% identity to SEQ ID NO: 1, 2, 3, 4, 5, 6, 7, 8, 16, 17, 18, 19, 20, 21, 22, 23, 24, 25, 26, 27, 28 or 29; preferably SEQ ID NO: 2 or SEQ ID NO: 4; and
h) an amino acid sequence represented by one or more of the following motifs:

Motif I:	[FL]XX[YF]S[AN]X[FHY]G[GN]GX[YF]N	(SEQ ID NO: 9);
Motif II:	G[GN]GX[YF]NXX[VA]AX[EH][LF]R	(SEQ ID NO: 10);
Motif III:	RXXRI[QE][DEQ]S[IM]ATN	(SEQ ID NO: 11);
Motif IV:	S[IM]ATN[PG][EQN][FM][SDN][FL]	(SEQ ID NO: 12);
Motif V:	P[PDK][DG]F[HFW]R[AP]	(SEQ ID NO: 13);
Motif VI:	[TI]XXXLYPNP[TK][GV]	(SEQ ID NO: 14);
Motif VII:	E[HG]DXSX[ST]RXD	(SEQ ID NO: 15);

preferably, Motif VII: E[HG]DXSX[ST]RXD.

In an embodiment, the aliphatic hydrocarbon which is substituted with a carboxy group is a fatty acid; preferably butanoic acid (butyric acid), pentanoic acid (valeric acid), hexanoic acid (caproic acid), heptanoic acid (enanthic acid), octanoic acid (caprylic acid), nonanoic acid (pelargonic acid), decanoic acid (capric acid), dodecanoic acid (lauric acid), tetradecanoic acid (myristic acid), hexadecanoic acid (palmitic acid), octadecanoic acid (stearic acid), eicosanoic acid (arachidic acid), linoleic acid, linolenic acid, arachidonic acid, eicosapentaenoic acid, or docosahexaenoic acid.

In an embodiment, the aliphatic hydrocarbon which is substituted with a carboxy group, is not lauric acid or palmitic acid.

In yet another aspect, the present invention also provides a method for changing (oxidizing) a primary alcohol of a linear or branched aliphatic

hydrocarbon having at least five carbons to the corresponding acid, comprising contacting the alcohol of an aliphatic hydrocarbon with hydrogen peroxide and a polypeptide having peroxygenase activity; wherein the polypeptide comprises:

i) an amino acid sequence which has at least 30% identity to SEQ ID NO: 1, 2, 3, 4, 5, 6, 7, 8, 16, 17, 18, 19, 20, 21, 22, 23, 24, 25, 26, 27, 28 or 29; preferably SEQ ID NO: 2 or SEQ ID NO: 4; and
j) an amino acid sequence represented by one or more of the following motifs:

Motif I:	[FL]XX[YF]S[AN]X[FHY]G[GN]GX[YF]N	(SEQ ID NO: 9);
Motif II:	G[GN]GX[YF]NXX[VA]AX[EH][LF]R	(SEQ ID NO: 10);
Motif III:	RXXRI[QE][DEQ]S[IM]ATN	(SEQ ID NO: 11);
Motif IV:	S[IM]ATN[PG][EQN][FM][SDN][FL]	(SEQ ID NO: 12);
Motif V:	P[PDK][DG]F[HFW]R[AP]	(SEQ ID NO: 13);
Motif VI:	[TI]XXXLYPNP[TK][GV]	(SEQ ID NO: 14);
Motif VII:	E[HG]DXSX[ST]RXD	(SEQ ID NO: 15);

preferably, Motif VII: E[HG]DXSX[ST]RXD.

For example, pentanol may be changed (oxidized) to pentanoic acid (valeric acid), hexanol may be changed to hexanoic acid (caproic acid), heptanol may be changed to heptanoic acid (enanthic acid), octanol may be changed to octanoic acid (caprylic acid), nonanol may be changed to nonanoic acid (pelargonic acid), decanol may be changed to decanoic acid (capric acid), dodecanol may be changed to dodecanoic acid (lauric acid), tetradecanol may be changed to tetradecanoic acid (myristic acid), hexadecanol may be changed to hexadecanoic acid (palmitic acid), octadecanol may be changed to octadecanoic acid (stearic acid), and eicosanol may be changed to eicosanoic acid (arachidic acid).

The present invention is further described by the following examples that should not be construed as limiting the scope of the invention.

EXAMPLES

The amino acid sequence of the peroxygenase from *Agrocybe aegerita* is shown as SEQ_ID NO: 2; and the amino acid sequence of the peroxygenase from *Coprinopsis cinerea* is shown as SEQ_ID NO: 4.

EXAMPLE 1

Enzymatic oxidation of dodecane, tetradecane and hexadecane

The extracellular peroxygenase of *A. aegerita* (isoform II, 44 kDa, SEQU ID NO: 2) was used. The enzyme preparation was homogeneous by sodium dodecylsulfate-polyacrylamide gel electrophoresis, an exhibited and A_{418}/A_{280} ratio of 1.75. Its specific activity was 117 units·mg^{-1}, where 1 unit represents the oxidation of 1 μmol of veratryl alcohol to veratraldehyde (ε_{310} 9300 $M^{-1}\cdot cm^{-1}$) in 1 minute at 23 ºC and pH 7, in the presence of 2.5 mM H_2O_2.

Three alkanes: dodecane (C_{12}), tetradecane (C_{14}) and hexadecane (C_{16}) were obtained from Sigma-Aldrich. Five mL reactions of the above model substrates (1 mM) with the *A. aegerita* peroxygenase (1 U) were performed in 50 mM sodium phosphate buffer (pH 7) at 25 ºC for 2 h, in the presence of 2.5 mM H_2O_2. The substrates were previously dissolved in acetone and added to the buffer (the acetone concentration in the reaction was 15%). In control experiments, substrates were treated under the same conditions but without enzyme. After the enzymatic reactions, water was immediately removed in a rotary evaporator, and the products recovered with chloroform, dried under nitrogen, and redissolved in chloroform for GC-MS analyses. Bis(trimethylsilyl)-trifluoroacetamide (Supelco) in the presence of pyridine was used to prepare trimethylsilyl derivatives.

The GC-MS analyses were performed with a Varian 3800 chromatograph coupled to an ion-trap detector (Varian 4000) using a medium-length fused-silica DB-5HT capillary column (12 m x 0.25 mm internal diameter, 0.1 μm film thickness) from J&W Scientific, enabling simultaneous elution of the different compound classes. The oven was heated from 120 ºC (1 minute) to

380 ºC at 10 ºC per minute, and held for 5 minutes. Other temperature program, from 50 ºC to 110 ºC (at 30 ºC per minute) and then to 320 ºC (at 6 ºC per minute), was used when necessary. In all GC-MS analyses, the transfer line was kept at 300 ºC, the injector was.

Compounds were identified by mass fragmentography, and by comparing their mass spectra with those of the Wiley and NIST libraries and standards, and quantification was obtained from total-ion peak area, using response factors of the same or similar compounds. Single-ion chromatographic profiles (of base or other specific ions) were used to estimate compound abundances when two peaks partially overlapped.

Results

Three saturated alkanes (dodecane, tetradecane and hexadecane) were tested as *A. aegerita* peroxygenase substrates.

The reactions with dodecane, gave monohydroxylated derivatives at positions 2 and 3. In addition to the monohydroxylated derivatives, dihydroxylations at the positions 2 and 3 from both ends of the molecule *(i.e.*, α+1 and ω-1/ω-2, or α+2 and ω-1/ω-2) were identified as the predominant compounds.

Table 1

GC-MS peak areas for the peroxygenase reactions.

Substrate	(ω-1) OH	(ω-2) OH	2,(ω-1) di OH	2,(ω-2) di OH	3,(ω-2) di OH	ω-1-OH (2+3 keto)	ω-2-OH (2+3 keto)
dodecane	90,000	80,000	$2.4x10^6$	$4.3x10^6$	$2.1x10^6$	$1.3x10^6$	$1.1x10^6$
tetradecane	120,000	140,000	260,000	420,000	350,000	520,000	740,000
hexadecane	90,000	70,000	60,000	150,000	100,000	100,000	120,000

EXAMPLE 2

Enzymatic oxidation of saturated and unsaturated fatty acids

The extracellular peroxygenase of *A. aegerita* (isoform II, 44 kDa, SEQ_ID NO: 2) was used. The enzyme preparation was homogeneous by sodium dodecylsulfate-polyacrylamide gel electrophoresis, an exhibited and A_{418}/A_{280} ratio of 1.75. Its specific activity was 117 units·mg^{-1}, where 1 unit represents the oxidation of 1 μmol of veratryl alcohol to veratraldehyde (ε_{310} 9300 M^{-1}. cm^{-1}) in 1 minute at 23 ºC and pH 7, in the presence of 2.5 mM H_2O_2.

Saturated and unsaturated acids were obtained from Sigma-Aldrich: Lauric (dodecanoic, C_{12}), myristic (tetradecanoic, C_{14}), palmitic (hexadecanoic, C_{16}), stearic (octadecanoic, C_{18}), arachidic (eicosanoic, C_{20}), lauroleic (*cis*-9-dodecenoic, $C_{12:1}$), myristoleic (*cis*-9-tetradecenoic, $C_{14:1}$), palmitoleic (*cis*-9-hexadecenoic, $C_{16:1}$), oleic (*cis*-9-octadecenoic, $C_{18:1}$), linoleic *(cis,cis*-9,12-octadecadienoic, $C_{18:2}$) and eicosenoic ($C_{20:1}$) acids. Five mL reactions of the above model substrates (1 mM) with the *A. aegerita* peroxygenase (1 U) were performed in 50 mM sodium phosphate buffer (pH 7) at 25 ºC for 2 hours, in the presence of 2.5 mM H_2O_2. The substrates were previously dissolved in acetone and added to the buffer (the acetone concentration in the reaction was 15%). In control experiments, substrates were treated under the same conditions but without enzyme. After the enzymatic reactions, water was immediately removed in a rotary evaporator, and the products recovered with chloroform, dried under nitrogen, and redissolved in chloroform for GC-MS analyses. Bis(trimethylsilyl)trifluoroacetamide (Supelco) in the presence of pyridine was used to prepare trimethylsilyl derivatives.

The GC-MS analyses were performed with a Varian 3800 chromatograph coupled to an ion-trap detector (Varian 4000) using a medium-length fused-silica DB-5HT capillary column (12 m x 0.25 mm internal diameter, 0.1 μm film thickness) from J&W Scientific, enabling simultaneous elution of the different compound classes. The oven was heated from 120 ºC (1 minute) to 380 ºC at 10 ºC per minute, and held for 5 minutes. Other temperature program, from 50 ºC to 110 ºC (at 30 ºC per minute) and then to 320 ºC (at 6 ºC per minute), was used when necessary. In all GC-MS analyses, the transfer line was kept at 300 ºC, the injector was programmed from 120 ºC (0.1 minute) to 380 ºC at 200 ºC·per minute and held until the end of the analysis, and helium was used as carrier gas at a rate of 2 ml per minute.

Compounds were identified by mass fragmentography, and by comparing their mass spectra with those of the Wiley and NIST libraries and standards, and quantification was obtained from total-ion peak area, using response factors of the same or similar compounds. Single-ion chromatographic profiles (of base or other specific ions) were used to estimate compound abundances when two peaks partially overlapped.

Results

Eleven saturated and unsaturated fatty acids were tested as substrates of the *A. aegerita* peroxygenase and all fatty acids showed reactivity towards the enzyme. The abundance (relative percentage) of different mono-hydroxylated, keto, dihydroxylated, keto-hydroxy and dicarboxylic derivatives identified by GC-MS in the reactions of saturated and unsaturated fatty acids are listed in **Table 2**.

Oxidation of the terminal methyl group (ω-OH) was observed for all tested free fatty acids, in some cases this was further oxidized leading to formation of dicarboxylic acids (di-COOH).

EXAMPLE 3

Enzymatic oxidation of tetradecane in 40% acetone

The extracellular peroxygenase of *A. aegerita* (isoform II, 44 kDa, SEQ ID NO: 2) and the recombinant peroxygenase of *Coprinopsis cinerea* (WT392, SEQ ID NO: 4) were used. The activity of the preparations was determined by oxidation of veratryl alcohol. 1 unit represents the oxidation of 1 μmol of veratryl alcohol to veratraldehyde (ε_{310} 9300 $M^{-1}.cm^{-1}$) in 1 minute at 23ºC and pH 7, in the presence of 2.5 mM H_2O_2.

Tetradecane (C_{14}) was obtained from Sigma-Aldrich. Five mL reactions of the above model substrate (0.3 mM) with 1 U of peroxygenase were performed in 50 mM sodium phosphate buffer (pH 7) at 40 ºC for 2 h, in the presence of H_2O_2. The concentration of H_2O_2 was 2.5 mM when *A. aegerita* peroxygenase was applied and 0.5 mM when using *C. cinerea* peroxygenase. The substrate was previously dissolved in acetone and added to the buffer (the acetone concentration in the reaction was 40%). In control experiments,

substrates were treated under the same conditions but without enzyme. After the enzymatic reactions, water was immediately removed in a rotary evaporator, and the products recovered with chloroform, dried under nitrogen, and redissolved in chloroform for GC-MS analyses. Bis(trimethylsilyl)-trifluoroacetamide (Supelco) in the presence of pyridine was used to prepare trimethylsilyl derivatives.

Table 2

Relative abundance of reaction products.

Fatty acid	ω-OH	ω-1 OH	ω-2 OH	ω-3 OH	ω-1 Keto	ω-2 Keto	di-OH	OH-Keto	di-COOH
C_{12}	1.3	39.7	32.0	0.2	5.8	1.0	4.4	15.5	0.3
$C_{12:1}$	3.3	37.4	59.2	0	<0.1	<0.1	0	0	0
C_{14}	3.5	34.4	30.5	0.3	20.8	3.3	0.5	6.2	0.6
$C_{14:1}$	1.8	0	94.6	0	0	3.6	0	0	0
C_{16}	1.4	23.6	23.6	0.3	34.5	16.3	0	0	0.3
$C_{16:1}$	2.5	35.7	47.0	0.1	10.4	4.4	0	0	0
C_{18}	<0.1	22.7	27.0	0.1	32.8	17.0	0	0	0.5
$C_{18:1}$	1.6	40.8	39.0	0.2	13.0	5.3	0	0	0
$C_{18:2}$	1.0	50.2	33.5	2.5	10.0	2.9	0	0	0
C_{20}	<0.1	16.0	28.1	0	38.7	17.3	0	0	0
$C_{20:1}$	1.2	35.0	38.7	0.4	18.8	6.0	0	0	0

The GC-MS analyses were performed with a Varian 3800 chromatograph coupled to an ion-trap detector (Varian 4000) using a medium-length fused-silica DB-5HT capillary column (12 m x 0.25 mm internal diameter, 0.1μm film thickness) from J&W Scientific, enabling simultaneous elution of the different compound classes. The oven was heated from 120ºC (1 minute) to 380 ºC at 10 ºC per minute, and held for 5 minutes. Other temperature program, from 50 ºC to 110 ºC (at 30 ºC per minute) and then to 320 ºC (at

6 ºC per minute), was used when necessary. In all GC-MS analyses, the transfer line was kept at 300 ºC, the injector was programmed from 120 ºC (0.1 minute) to 380 ºC at 200 ºC per minute and held until the end of the analysis, and helium was used as carrier gas at a rate of 2 ml per minute.

Compounds were identified by mass fragmentography, and by comparing their mass spectra with those of the Wiley and NIST libraries and standards, and quantification was obtained from total-ion peak area, using response factors of the same or similar compounds. Single-ion chromatographic profiles (of base or other specific ions) were used to estimate compound abundances when two peaks partially overlapped.

Results

Chromatographic profiles resulting from hydroxylation of the saturated alkane tetradecane (C_{14}) are shown in Figure 1 for *C. cinerea* peroxygenase and Figure 2 for *A. aegerita* peroxygenase.

The reactions with tetradecane, resulted in monohydroxylated derivatives at positions 2 and 3 (ω-1 and ω-2 OH) and dihydroxylations at the positions 2 and 3 from both ends of the molecule *(i.e.,* ω-1/ω-1, ω-2/ω-2 or ω-1/ω-2 di OH).

EXAMPLE 4

Enzymatic oxidation of 1-tetradecanol in 20% acetone

The extracellular peroxygenase of *A. aegerita* (isoform II, 44 kDa, SEQ ID NO: 2) and recombinant peroxygenase of *Coprinopsis cinerea* (WT392, SEQ ID NO: 4) were used. The activity of the preparations was determinated by oxidations of veratryl alcohol. 1 unit represents the oxidation of 1 μmol of veratryl alcohol to veratraldehyde (ε_{310} 9300 $M^{-1}.cm^{-1}$ in 1 minute at 23 ºC and pH 7, in the presence of 2.5 mM H_2O_2.

1-Tetradecanol (C_{14}) was obtained from Sigma-Aldrich. Five mL reactions of the above model substrate (0.1 mM) with 1 U of peroxygenase were performed in 50 mM sodium phosphate buffer (pH 7) at 30 ºC for 1 minute, in the presence of H_2O_2. The concentration of H_2O_2 was 2.5 mM when *A. aegerita* peroxygenase was applied and 0.5 mM when using *C. cinerea*

peroxygenase. The substrate was previously dissolved in acetone and added to the buffer (the acetone concentration in the reaction was 20%). In control experiments, substrates were treated under the same conditions but without enzyme. After the enzymatic reactions, water was immediately removed in a rotary evaporator, and the products recovered with chloroform, dried under nitrogen, and redissolved in chloroform for GC-MS analyses. Bis(trimethylsilyl)-trifluoroacetamide (Supelco) in the presence of pyridine was used to prepare trimethylsilyl derivatives.

The GC-MS analyses were performed with a Varian 3800 chromatograph coupled to an ion-trap detector (Varian 4000) using a medium-length fused-silica DB-5HT capillary column (12 m x 0.25 mm internal diameter, 0.1 μm film thickness) from J&W Scientific, enabling simultaneous elution of the different compound classes. The oven was heated from 120 ºC (1 minute) to 380 ºC at 10 ºC per minute, and held for 5 minutes. Other temperature program, from 50 ºC to 110 ºC (at 30 ºC per minute) and then to 320 ºC (at 6 ºC per minute), was used when necessary. In all GC-MS analyses, the transfer line was kept at 300 ºC, the injector was programmed from 120 ºC (0.1 minute) to 380 ºC at 200 ºC per minute and held until the end of the analysis, and helium was used as carrier gas at a rate of 2 ml per minute.

Compounds were identified by mass fragmentography, and by comparing their mass spectra with those of the Wiley and NIST libraries and standards, and quantification was obtained from total-ion peak area, using response factors of the same or similar compounds. Single-ion chromatographic profiles (of base or other specific ions) were used to estimate compound abundances when two peaks partially overlapped.

Results

Chromatographic profiles resulting from oxidation of 1-tetradecanol (Alc) are shown in Figure 3 for *C. cinerea* peroxygenase and Figure 4 for *A. aegerita* peroxygenase.

The reactions with 1-tetradecanol, resulted in formation of 1-tetradecanoic acid (Acd) and hydroxylated decanoic acid (ω-1 OH Acd and ω-2 OH Acd) and two dihydroxylated products (ω-1 OH Alc and ω-2 OH Alc).

CLAIMS

1. A method for introducing a hydroxy or a keto group at the second or third carbon of at least two ends of a substituted or unsubstituted, linear or branched, aliphatic hydrocarbon having at least five carbons and having at least one hydrogen attached to said second or third carbon, comprising contacting the aliphatic hydrocarbon with hydrogen peroxide and a polypeptide having peroxygenase activity; wherein the polypeptide comprises:

k) an amino acid sequence which has at least 30% identity to SEQ ID NO: 1, 2, 3, 4, 5, 6, 7, 8, 16, 17, 18, 19, 20, 21, 22, 23, 24, 25, 26, 27, 28, or 29; and

l) an amino acid sequence represented by one or more of the following motifs:

Motif I:	[FL]XX[YF]S[AN]X[FHY]G[GN]GX[YF]N	(SEQ ID NO: 9);
Motif II:	G[GN]GX[YF]NXX[VA]AX[EH][LF]R	(SEQ ID NO: 10);
Motif III:	RXXRI[QE][DEQ]S[IM]ATN	(SEQ ID NO: 11);
Motif IV:	S[IM]ATN[PG][EQN][FM][SDN][FL]	(SEQ ID NO: 12);
Motif V:	P[PDK][DG]F[HFW]R[AP]	(SEQ ID NO: 13);
Motif VI:	[TI]XXXLYPNP[TK][GV]	(SEQ ID NO: 14);
Motif VII:	E[HG]DXSX[ST]RXD	(SEQ ID NO: 15).

2. The method of claim 1, wherein the second or third carbon is unsubstituted until contacted with the peroxygenase.
3. The method of claims 1 or 2, wherein the polypeptide comprises or consists of an amino acid sequence having at least 35% identity, preferably at least 40% identity, more preferably at least 45% identity, more preferably at least 50% identity, more preferably at least 55% identity, more preferably at least 60% identity, more preferably at least 65% identity, more preferably at least

70% identity, more preferably at least 75% identity, more preferably at least 80% identity, more preferably at least 85% identity, most preferably at least 90% identity, and in particular at least 95% identity to the mature polypeptide of SEQ ID NO: 1, 2, 3, 4, 5, 6, 7, 8, 16, 17, 18, 19, 20, 21, 22, 23, 24, 25, 26, 27, 28 or 29; preferably SEQ ID NO: 2 or 4.

4. The method of any of claims 1-3, wherein the polypeptide comprises or consists of the amino acid sequence of SEQ ID NO: 1, 2, 3, 4, 5, 6, 7, 8, 16, 17, 18, 19, 20, 21, 22, 23, 24, 25, 26, 27, 28 or 29; preferably SEQ ID NO: 2 or 4; or a fragment thereof having peroxygenase activity.
5. The method of any of claims 1-4, wherein the substituents of the aliphatic hydrocarbon are selected from the group consisting of halogen, hydroxyl, carboxyl, amino, nitro, cyano, thiol, sulphonyl, formyl, acetyl, methoxy, ethoxy, phenyl, benzyl, xylyl, carbamoyl and sulfamoyl.

6. The method of any of claims 1-5, wherein the substituents are selected from the group consisting of chloro, hydroxyl, carboxyl and sulphonyl; in particular chloro and carboxyl.
7. The method of any of claims 1-6, wherein the aliphatic hydrocarbon is an alkane.
8. The method of claim 7, wherein the alkane is pentane, hexane, heptane, octane, nonane, decane, undecane, dodecane, tridecane, tetradecane, pentadecane or hexadecane, or isomers thereof.
9. The method of claim 7, wherein the alkane is undecane, dodecane, tridecane, tetradecane, pentadecane or hexadecane, or isomers thereof.
10. The method of any of claims 1-9, wherein the aliphatic hydrocarbon is unsubstituted.
11. The method of any of claims 1-10, wherein the aliphatic hydrocarbon is linear.
12. The method of any of claims 1-11, wherein the aliphatic hydrocarbon is converted to a diol, by introduction of two hydroxy groups.
13. An enzymatic method for producing polyurethane, comprising converting an aliphatic hydrocarbon to a diol, according to the method of claim 12, and using the diol for producing polyurethane.
14. Use of a diol produced according to claim 12, for producing polyurethane.
15. Use of a peroxygenase for introducing a hydroxyl or a keto group at the second or third carbon of two or more ends of an aliphatic hydrocarbon.

7. Conclusiones

Agrocybe aegerita

7. CONCLUSIONES

En la presente Tesis se ha llevado a cabo el estudio de la oxifuncionalización enzimática de diferentes compuestos alifáticos catalizada por tres peroxigenasas fúngicas, las peroxigenasas salvajes de *Agrocybe aegerita* (*Aae*UPO) y de *Marasmius rotula* (*Mro*UPO) y la peroxigenasa recombinante de *Coprinopsis cinerea* (r*Cci*UPO), en presencia de H_2O_2 como co-sustrato único. Además, se ha estudiado el mecanismo de la oxigenación selectiva de los sustratos por estas enzimas (utilizando $H_2{}^{18}O_2$) así como diferentes aspectos de las relaciones estructura-función de las peroxigenasas mediante estudios computacionales. Las principales conclusiones obtenidas se citan a continuación:

1. El estudio de las reacciones enzimáticas de las peroxigenasas *Aae*UPO, *Mro*UPO y r*Cci*UPO mediante el análisis de los productos de reacción por GC-MS demostró, por primera vez, que estas enzimas son capaces de oxifuncionalizar una gran variedad de compuestos alifáticos lineales (ácidos grasos libres y esterificados, alcoholes grasos y alcanos) y cíclicos (esteroides y secosteroides).

2. Los ácidos grasos (saturados e insaturados) se hidroxilaron selectivamente por la acción de las peroxigenasas *Aae*UPO y r*Cci*UPO dando lugar a derivados monohidroxilados en las posiciones ω-1 y ω-2, a excepción del ácido miristoleico que sólo se hidroxiló en la posición ω-2.

3. Las reacciones enzimáticas de los alcoholes grasos con *Aae*UPO y r*Cci*UPO dieron como producto principal el correspondiente ácido graso, además de los derivados hidroxilados (en las posiciones ω-1 y ω-2) tanto del alcohol como del ácido.

4. En las reacciones enzimáticas de *Aae*UPO y r*Cci*UPO con alcanos se obtuvieron mayoritariamente derivados monohidroxilados y dihidroxilados. Se observó que la predominancia de los derivados mono- o dihidroxilados depende de la mayor o menor proporción de acetona en el medio de reacción.

5. El estudio de las reacciones de compuestos esteroidales con *Aae*UPO, *Mro*UPO y r*Cci*UPO puso de manifiesto que la conversión del sustrato y la regioselectividad de la reacción dependen de la presencia y longitud de la cadena lateral en el C-17 así como de la presencia de grupos oxigenados y/o dobles enlaces conjugados en el anillo esteroidal.

6. Las reacciones de los diferentes compuestos esteroidales (esteroles libres y esterificados, y cetonas e hidrocarburos esteroidales) con *Aae*UPO, *Mro*UPO y r*Cci*UPO dieron lugar en la mayoría de los casos, a la hidroxilación en la cadena lateral (posición C-25) y en algunos casos también se observaron derivados hidroxilados en las posiciones C-24, C-26 (o C-27) y C-28. Además, se observó la formación de derivados hidroxilados en el anillo esteroidal en aquellos esteroides en los que la posición C-3 no contiene grupos oxigenados, y posee dobles enlaces conjugados en las posiciones C-3 y C-5.

7. Las peroxigenasas r*Cci*UPO y *Aae*UPO mostraron una gran regioselectividad (100% en el primer caso) en la hidroxilación de secosteroides (vitamina D_3, colecalciferol) en la posición C-25. La peroxigenasa *Aae*UPO hidroxiló también, aunque en menor proporción, las posiciones C-24 y C26/27 de la vitamina D_3. Ambas peroxigenasas (r*Cci*UPO y *Aae*UPO) mostraron una regioselectividad del 100% en la hidroxilación de la vitamina D_2 en la posición C-25.

8. El análisis de los espectros de masas de los productos de reacción obtenidos en las reacciones enzimáticas de *Aae*UPO y r*Cci*UPO y varios sustratos utilizando $H_2{}^{18}O_2$, reveló que estas enzimas introducen el átomo de oxígeno en el sustrato a partir del H_2O_2 (y no del O_2) demostrando de este modo su actividad peroxigenasa. Asimismo, las reacciones con $H_2{}^{18}O_2$ en las que se utilizó un alcohol graso como sustrato evidenciaron que la formación del ácido carboxílico a partir del alcohol transcurre mediante reacciones sucesivas de hidroxilación/deshidratación con la formación de un *gem*-diol (y probablemente un *gem*-triol).

9. Los estudios computacionales realizados con el objeto de comprender la interacción entre la enzima y los diferentes sustratos estudiados, permitieron establecer una correlación directa entre el grado de conversión obtenido en las reacciones enzimáticas y la entrada del sustrato en el sitio activo de la enzima. En el caso particular de los compuestos esteroidales los factores más determinantes fueron el carácter polar/apolar de los grupos sustituyentes en las posiciones C-3/C-7 del anillo, la presencia/ausencia de dobles enlaces en el anillo esteroidal, y la longitud y características de la cadena lateral que afectan a la entrada del sustrato en el sitio activo de la enzima por la posición C-25.

En conclusión, las peroxigenasas fúngicas estudiadas en esta Tesis (*Aae*UPO, r*Cci*UPO y *Mro*UPO) representan una alternativa sostenible a la síntesis química ya que catalizan la oxifuncionalización selectiva de diferentes compuestos alifáticos (tanto lineales como cíclicos) de interés en la industria química y farmacéutica, en presencia de H_2O_2 como único co-sustrato.